Title
Does reptile body size track climate change over millions of years?

Author
ElShafie, Sara J

Publication Date
2022

Peer reviewed|Thesis/dissertation

Does reptile body size track climate change over millions of years?

By

Sara J ElShafie

A dissertation submitted in partial satisfaction of the

requirements for the degree of

Doctor of Philosophy

in

Integrative Biology

in the

Graduate Division

of the

University of California, Berkeley

Committee in charge:

Professor Kevin Padian, Chair
Professor Anthony D. Barnosky
Professor Jimmy A. McGuire
Professor Ian Wang

Spring 2022

Abstract

Does reptile body size track climate change over millions of years?

by

Sara J ElShafie

Doctor of Philosophy in Integrative Biology

University of California, Berkeley

Professor Kevin Padian, Chair

Climate change particularly affects ectothermic reptiles that cannot regulate their internal temperature metabolically. But it is difficult to anticipate how the unprecedented pace of current climate change will affect these animals based only on recent data. We need a larger temporal context based on historical data spanning deeper time scales and past episodes of rapid climate change. Body size is a suitable response variable to test in such investigations because data from extant taxa can predict body size for fossil specimens from the same lineages. We can also reconstruct past climate parameters from terrestrial and marine proxies. Metabolic theory for ectothermic vertebrates predicts that maximum body size should correlate with environmental temperature over ecological time scales. Here, I test this theory on an evolutionary time scale, using both paleotemperature and paleoprecipitation, for two different higher order reptile groups occupying different habitats. I hypothesize that maximum snout-vent length (SVL) in terrestrial lizards and semiaquatic crocodyliforms tracks temperature and precipitation over geologic time intervals, and that these patterns emerge across both regional and local geographic scales.

I measured 283 lizard and 280 crocodyliform fossil specimens from intermontane basins across the Western Interior of North America through the Paleogene (66-23 million years ago), which spans several warming and cooling events. Most of the fossil record of these animals consists of individual cranial or limb bones. I therefore collected an additional extensive dataset of measurements from extant specimens to develop regression equations for estimating SVL from isolated anatomical elements. I applied these methods to reconstruct lizard body sizes through the Paleogene using the available fossil record (Chapter 1). I then used similar methods to investigate whether deep time body size evolution patterns in terrestrial lizards compared to those of contemporaneous amphibious crocodyliforms, and to see how those patterns compared at regional vs. local geographic scales (Chapter 2). Finally, I collected over 100 estimates each for mean annual paleotemperature (MAPT) and paleoprecipitation (MAPP) and tested for correlation between these variables and maximum body size in lizards or crocodyliforms (Chapter 3).

My results indicated that during the warmest interval in the early Eocene, maximum lizard body size increased to almost one meter, even rivaling some co-occurring crocodyliforms in body size. Maximum lizard SVL demonstrated a positive linear relationship with local terrestrial

temperature within basin assemblages over geologic time scales but did not correlate as strongly with temperatures averaged across the Western Interior. In contrast to the lizards, maximum crocodyliform SVL (about 2 meters) was consistently high across the intermontane basins through the Paleogene and indicated a strong relationship to paleoprecipitation rather than paleotemperature. Large-bodied crocodyliforms were most abundant in localities that hosted large bodies of water at the time of deposition. Maximum body size and diversity decreased for both lizards and crocodyliforms in the early Oligocene, when the Western Interior experienced cooling and aridification. Neontological studies of lizard and crocodylian ecology and physiology corroborate these paleontological observations. These results offer new evidence that climate variables affect body size in ectothermic reptiles on evolutionary time scales, which deepens our understanding of these dynamics on ecological time scales. Studies that integrate data across time scales and biological hierarchies and can inform conservation efforts under current rapid climate change.

To my parents, who always believed in me and supported me through my journey.

To my advisor, Kevin Padian, who encouraged all my aspirations with equal insight, critical thought, and high standards.

I also dedicate this work to the late William A. Clemens, Jr. (1932 – 2020), who mentored many who came through the University of California, Berkeley, and the UC Museum of Paleontology for over 50 years. I feel privileged to have known him and am grateful for his assistance with this research.

TABLE OF CONTENTS

ACKNOWLEDGMENTS

I sincerely thank my doctoral advisor K. Padian for his tireless support and mentorship. I also thank my dissertation committee, J. McGuire, A. Barnosky, and I. Wang, for their mentorship and helpful comments on this work, and my Masters advisor J. Head who mentored the research that started this project.

Thank you to the following individuals for museum collections access and assistance: M. Norell, C. Mehling, J. Meng, D. Kizirian, L. Vonnahme, M. Arnold (AMNH); J. Vindum, L. Scheinberg, E. Ely (CAS); M. Lamanna, J. Padial, A. Henrici, S. Rogers (CM); T. Lyson, L. Ivy, K. MacKenzie (DMNH); J. Bloch, R. Hulbert, J. Bourque (FLMNH); P. Makovicky, L. Grande, A. Resetar, W. Simpson, A. Stroupe, J. Mata (FMNH); A. Aase (FOBU); N. Smith, S. McLeod, V. Rhue (LACM); J.Rosado (MCZ); J. McGuire, C. Spencer (MVZ); T. Williamson (NMMNH); A. Farke, G. Santos (RAM); A. Hastings, E. Whiting (SMM); C. Bell, M. Brown (TMM); T. Culver, N. Ridgwell (UCM); P. Holroyd, C. Marshall (UCMP); J. Wilson, A. Rountrey (UMMP); R. Hunt, Jr., P. Freeman, G. Corner, T. Labedz (UNSM); H. Dieter-Sues, M. Carrano, M. Brett-Surman, A. Millhouse (USNM); L. Vietti (UW); C. Sidor, R. Eng, M. Rivin (UWBM); J. Gauthier, C. Norris, D. Brinkman (YPM). (Institutional Abbreviations are listed on pg. x.)

For helpful discussions, I thank the following: C. Badgley, C. Bell, B-A. Bhullar, J. Bloch, W. Clemens†, C. Crumly, J. Gauthier, W. Gearty, P. Gingerich, L. Grande, A. Gunderson, P. Holroyd, E. Holt, R. Huey, R. Hunt, Jr., M. Kemp, D. Meyer, D. Miles, J. McGuire, J. Parham, H. Petermann, S. Scarpetta, R. Secord, M. Stocker, R. Sullivan, D. Watkins, L. Weaver, S. Werning, E. Whiting, the MVZ Herp Group, the entire UCMP community, and C. Williams who also served on my Qualifying Exam Committee.

C. Bell also provided access to obscure literature. D. Meyer provided measurements of an unpublished specimen. G. Brown (UNSM) prepared a new *Peltosaurus* specimen (UNSM 12102) containing critical limb material. F. Vasconcellos provided the photo in Fig 1.2E. Special thanks to B. Chelemedos and C. Wong for assistance with data collection; to J. Farlow for providing additional measurements of extant crocodylian material; to C. Brochu for extensive help with crocodyliform phylogenetics and nomenclature; to E. Whiting for teaching me how to use QGIS to make the maps; and to J. Lipps for helping me design a visually accessible color palette for my figures.

Finally, thank you to my parents, my partner, my friends, and my family for all their support.

INSTITUTIONAL ABBREVIATIONS

AMNH, American Museum of Natural History, New York, NY
CAS, California Academy of Sciences, San Francisco, CA
CJB, Christopher J. Bell, University of Texas at Austin, Austin, TX
CM, Carnegie Museum of Natural History, Pittsburgh, PA
DMNH, Denver Museum of Natural History (Denver Museum of Nature and Science), Denver, CO
FLMNH, Florida Museum of Natural History, Gainesville, FL
FMNH, Field Museum of Natural History, Chicago, IL
FOBU, Fossil Butte National Monument, Kemmerer, WY
*GCVP, Georgia College Vertebrate Paleontology, Milledgeville, GA
LACM, Natural History Museum of Los Angeles County, Los Angeles, CA
MCZ, Museum of Comparative Zoology, Cambridge, MA
*MSU, Michigan State University, Lansing, MI
MVZ, Museum of Vertebrate Zoology, Berkeley, CA
NMMNH, New Mexico Museum of Natural History, Albuquerque, NM
*PTRM, Pioneer Trails Regional Museum, Bowman, ND
RAM, Raymond M. Alfe Museum of Paleontology, Claremont, CA
SMM, Science Museum of Minnesota, Saint Paul, MN
TMM, Texas Memorial Museum, Austin, TX
UCM, University of Colorado Museum, Boulder, CO
UCMP, University of California Museum of Paleontology, Berkeley, CA
UMMP, University of Michigan Museum of Paleontology, Ann Arbor, MI
UNSM, University of Nebraska State Museum, Lincoln, NE
USNM, United States National Museum (Smithsonian National Museum of Natural History), Washington, DC
UW, University of Wyoming Geological Museum, Laramie, WY
UWBM, University of Washington Burke Museum, Seattle, WA
YPM, Yale Peabody Museum, New Haven, CT

*Museums that I did not contact personally, but from which I obtained specimen measurements from papers or loans to other researchers.

CHAPTER 1

Body size estimation from isolated fossil bones reveals deep time evolutionary trends for lizards

ABSTRACT

Lizards play vital roles in extant ecosystems. However, their roles in extinct ecosystems are poorly understood because the fossil record of lizards consists mostly of isolated bones. This makes it difficult to document changes in morphology and body size over time, which is essential for studies of paleoecology and evolution. It is also difficult to compare available fossil lizard data with existing extant lizard datasets because extant studies rarely measure individual bones. Furthermore, no previous study has regressed measurements of individual bones to body length across crown lizard groups, nor tested those regressions on fossil skeletons. Here I provide an extensive dataset of extant lizard measurements, including individual bones, across crown taxonomic groups, and derive methods for estimating lizard body size from isolated fossil elements. I apply these methods to a large dataset of fossil lizard specimens from the robust Paleogene record (66-23 Ma) of the Western Interior of North America. I test the hypothesis that anatomical proportions have been conserved within higher-level crown lizard groups since the Paleogene and can therefore be used to reconstruct snout-vent length (SVL) for fossil specimens referred to the same groups.

I regressed individual bones to SVL in each extant lizard group and tested the regressions using measurements from complete extant specimens as well as a handful of rare fossil skeletons. The regressions predicted actual SVL for both the extant and fossil test specimens with comparable accuracy. The resulting body size estimates for the entire fossil dataset reveal that lizards reached greatest maximum body size in the early Paleogene, with the largest size class dominated by heavily armored anguid lizards that exceeded 1 meter in SVL. Maximum body size decreased to under 400 mm in the late Paleogene. This is the first study to investigate body size evolution across lizard clades over a deep time interval and across a large geographic region. The proposed methods can provide reasonable estimates of SVL for fossil lizards referred to any crown group.

INTRODUCTION

Body size influences every aspect of a vertebrate's physiology and life history (Peters 1983; Schmidt-Nielsen 1984; Meiri 2008, 2018). It is therefore essential to estimate body size for fossil vertebrate taxa in order to understand the ecological and evolutionary context of any vertebrate group (Damuth 1990; Figueirido et al. 2011; Campione and Evans 2012; Thomas Goodwin and Bullock 2012; Head et al. 2013; Godoy et al. 2019). Lizards are a particularly important group of vertebrates to understand in both extant and extinct ecosystems because they occupy diverse and vital ecological roles. For example, lizards regulate populations of insects, rodents, and other prey on which they feed, and they are an important food source for many animals (Pianka and Vitt 2003; Vitt E.R. Pianka, W.E. Cooper, Jr., and K. Schwenk 2003; Pianka et al. 2017; Meiri 2018). Unfortunately, complete fossil lizard skeletons are rare; most commonly found are isolated elements that can be difficult to identify with taxonomic precision. Therefore, body size for fossil lizards must be inferred primarily from isolated bones (Herrera-Flores et al. 2021). To further complicate matters, anatomical datasets of extant lizards rarely include measurements of individual cranial or limb bones for comparison. Hence, no prior study has reconstructed body size in lizards on evolutionary time scales across higher-level taxonomic groups.

I address this need by presenting detailed methods for estimating body size in fossil lizards from isolated anatomical elements. I use those methods to reconstruct body size in lizard lineages over a deep time interval and across a continental interior.

The first question to consider here is which variable would be best to use as a measure of body size. Some previous studies of fossil reptiles estimated mass as a proxy for body size using scaling relationships between measurements of individual bones and body mass in extant taxa (Farlow et al. 2005; O'Brien et al. 2019). However, body mass can be difficult to estimate in this way for fossil vertebrates because body mass is only weakly correlated with most individual bones (Figueirido et al. 2011). Body length is often more feasible to estimate for fossil reptiles because body length correlates tightly with other anatomical measurements including head length (e.g., $R^2 \geq 0.97$ for extant crocodylians (Sereno et al. 2001)), head width (e.g., $R^2 \geq 0.85$ for extant crocodylians (O'Brien et al. 2019)), lengths of individual cranial elements (e.g., $R^2 = 0.89$ for dentary length in acrodontan lizards (Head et al. 2013); $R^2 \geq 0.78$ for various cranial elements in the lizard genera *Anolis* and *Pholidoscelis* (Bochaton and Kemp 2017)), femur length (e.g., $R^2 \geq 0.99$ for extant crocodylians (Farlow et al. 2005)), or vertebral element width (e.g., $R^2 \geq 0.81$ for extant boine snakes (Head et al. 2009)). Snout-vent length (SVL), measured from the tip of the snout to the cloacal opening at the base of the tail, is often the preferred measure of body length in extant lizard studies (Metzger and Herrel 2005; Bochaton and Kemp 2017). This is because many lizards can autotomize and even regenerate their tails (Arnold 1984; Zani 1996; Bateman and Fleming 2009; Sanggaard et al. 2012; Gilbert et al. 2013), thus lizard tail measurements are highly variable. Total body length is also difficult to reconstruct in lizards because the tail is rarely complete in any extant specimen and is often disarticulated in dry skeletonized specimens. Measurements of SVL are more feasible to obtain from live, wet preserved, or dry skeletonized extant lizard specimens. Maximum SVL strongly correlates with mean adult SVL and SVL at sexual maturity in extant lizards (Greer 2001; Meiri 2008), so maximum SVL is a good metric of mean adult body size for a population of lizards sampled from the fossil record. Furthermore, once SVL is estimated, body mass can be calculated from a general lizard mass-SVL equation (Pough 1980).

Researchers commonly use bivariate linear regressions to estimate SVL for fossil vertebrates using anatomical measurements from specimens of the most inclusive phylogenetic group (Smith 2002). Regressions are more robust than ratios for this purpose because simple ratios do not capture allometric effects. Head length is known to correlate strongly with SVL within extant lizard taxa (e.g., R^2 ~0.79 (Pianka et al. 2017)). Thus, several studies have regressed head length and other anatomical elements to SVL in extant lizard groups in order to estimate SVL for specific fossil congeners (Hecht 1975; Head et al. 2013; Bochaton and Kemp 2017). But these studies focused on specific fossil taxa; no previous study has estimated SVL across higher taxonomic groups of fossil lizards.

Estimating body size across fossil lizard groups would require an extensive reference dataset of individual anatomical element measurements taken across crown group lizard lineages. Many previous studies have recorded measurements of head length and SVL across extant lizard groups (Metzger and Herrel 2005; Olalla-Tárraga et al. 2006a; Meiri 2008, 2010, 2018; Pianka et al. 2017; Roll et al. 2017a; Slavenko et al. 2019; Vidan et al. 2019; Villa and Delfino 2019). However, no previous study has documented measurements of individual cranial and limb elements in addition to head length and SVL from specimens representing higher-level extant lizard groups, nor has any previous study regressed measurements of individual bones to SVL across those groups. Here I fulfill this need by compiling a comprehensive dataset of individual cranial and limb elements as well as SVL across extant lizard lineages.

For this study, I sample lizards from the Paleogene record (23-66 million years ago (Ma)) in the Western Interior of North America, specifically, from localities concentrated in the United States (Fig 1.1). I use this geotemporal system as a paleontological framework because it has a prolonged and robust fossil record preserving many lizards referred to crown groups. This fossil record is extensively sampled and well represented in U.S. natural history museum collections.

I test the hypothesis that proportions of individual bone lengths to SVL have been conserved within higher-level crown group lizard lineages since the Paleogene and can therefore be used to predict SVLs for fossil lizard specimens identified to those same groups. For each extant group represented, I generate regressions of individual cranial and limb bones to SVL and validate these regressions using both extant and fossil lizard skeletons as test specimens. I then use these regressions to reconstruct body size for crown group lizards sampled from across the U.S. Western Interior through the Paleogene. This is the first study to reconstruct lizard body size evolution in different crown groups over a prolonged geologic interval and across a continental interior. The results have broad implications for modes of body size evolution and resource zone partitioning in lizards. In addition to applications for fossil research, the extensive dataset and body size estimation methods presented here can be of great use to functional morphologists and herpetologists.

MATERIALS & METHODS

Data Collection

I collected anatomical measurements from 283 fossil lizard specimens from the Paleogene record of the U.S. Western Interior (Table 1.1, S1.1 Dataset). I only sampled specimens that included complete cranial or limb elements (e.g., Fig 1.2). A few specimens included complete skulls (Fig 1.2) or even skeletons (Figs 1.3-1.4). I grouped the fossil

specimens by North American Land Mammal Age (NALMA), which is the conventional time bin used to divide the Paleogene based on taxonomic turnover in the mammal fossil record (Woodburne 2004). Age ranges for these intervals are listed in Table 1.2 based on Barnosky et al. (Barnosky et al. 2014).

I also measured a total of 332 extant specimens from the crown lizard lineages represented in the fossil dataset (S1.2 Dataset). This included seven extant families (Anguidae, Varanidae, Xenosauridae, Shinisauridae, Xantusiidae, Teiidae, Scincidae). I omitted legless anguids and scincids because proportions of cranial elements to SVL differ between limbed taxa and serpentiform taxa in extant squamate groups (Herrera-Flores et al. 2021) and because all the fossil taxa in my dataset are inferred to have had limbs based on associated limb material or assignment to extant groups with limbs. I had several pleurodont iguanian families represented in my dataset and I treated these as a collective group, "Iguania" (see Special Considerations for Other Lizard Groups). Phylogenetic relationships among iguanian families are poorly resolved, but the group "Iguania" is supported by both morphological and molecular analyses (Estes et al. 1988; Frost and Etheridge 1989; Gauthier et al. 2012; Wiens et al. 2012). I also measured specimens of extant Helodermatidae because they bore closer morphological resemblance and anatomical proportion to large fossil anguids in my paleontological study system than did extant anguids (Fig 1.2; see Special Considerations for Fossil Anguids). I amassed all these data from 26 different natural history museum collections across the United States (see Institutional Abbreviations, pg. x).

Most diagnostic characters for lizards are found in cranial bones (Woolley et al. 2020, 2022) and cranial bones account for most of the lizard fossil record. Therefore, we can be confident in taxonomic assignments for fossil lizard cranial bones based on extant phylogenetic morphological characters. I referred fossil specimens to crown groups based on specimen label identifications as well as taxonomic information from the Paleobiology Database ("The Paleobiology Database" n.d.) and current literature. For fossil taxa whose exact placement within or around an extant lizard group remains unresolved, I assigned the taxon to the closest crown group for the purpose of this study. For example, Smith and Gauthier asserted that the fossil genus *Provaranosaurus* is closely related to extant *Shinisaurus* and placed it within a group called "*Pan-Shinisaurus*" (Smith and Gauthier 2013), so I referred *Provaranosaurus* to Shinisauridae. I indicated any such considerations for specific taxa in the "Notes" column in S1.1 Dataset.

I focused my extant data collection on dry skeletonized specimens to obtain measurements of individual bones as well as SVL from the same specimens. I measured SVL in dry skeletonized specimens from the tip of the snout to the posterior centrum of the second caudal vertebra, which corresponds to the location of the cloaca (vent). I only measured SVL for dry specimens that included a complete articulated vertebral series. Whenever a dried skin was included with a skeletonized specimen, I used it to verify my SVL measurement from the vertebral series. When possible, I included wet specimens of Xenosauridae to increase the sample size for that group because dry skeletonized xenosaurid specimens were less common in museum collections (Table 1.1, S1.2 Dataset). I also included wet specimens of Helodermatidae because I only needed measurements of head length and SVL for that family (see Special Considerations for Fossil Anguids).

All measurements were taken with digital calipers (Mitutoyo 150 mm) to the nearest 0.1 mm for individual bones and the nearest 1 mm for SVL. For specimens with an SVL measuring > 150 mm, or for specimens that were preserved in a curved position, I used a tape measure to

measure SVL to the nearest 1 mm. When I could not access a specimen in person, I took measurements from digital photographs with a scale bar in standard orientation using the open access software ImageJ (available online at: https://imagej.nih.gov/ij/download.html). Measurements taken from photographs are indicated in bold font in S1.2 Dataset.

Georeferencing Localities

I georeferenced locality data for each fossil lizard specimen (S1.1 Dataset) using collections data, literature, and GEOLocate (www.geo-locate.org). When specific locality data were not available, I used the centroid of the county from which the specimen was collected, which is a common practice for specimen data (Zizka et al. 2019). I obtained coordinates for some localities from collections notes included with specimens. These coordinates are listed as approximations within 1º of the actual coordinates and indicated accordingly in S1.1 Dataset to protect sensitive fossil localities. Interested researchers should contact the corresponding collections managers to request exact coordinates for these localities.

I plotted all original locality coordinates onto a map (Fig 1.2) using QGIS-LTR 3.22.6 (download.qgis.org). The map shows localities that occur at least once in S1.1 Dataset, marked according to each taxonomic group occurring in that locality. Only the specimens with locality information that I could georeference are represented in the map. The map does not indicate the total number of specimens that came from any given locality, but occurrences of $n > 1$ have darker shading. Some specimens from different taxonomic groups come from the same locality within a given NALMA time bin; these data points might be stacked and not fully visible in the map.

Generating Regressions from Extant Data

I generated regressions of head length, individual cranial bone length (dentary, mandible, maxilla, frontal, parietal), and limb bone length (humerus, femur, tibia) to SVL for the extant lizard groups in my dataset. I only generated regressions for the anatomical elements represented in my fossil dataset for each specific lizard group (S1.1-S1.7 Tables). For example, I did not find any isolated fossil varanid femora, so I did not generate a regression for varanid femur length to SVL (S1.2 Table). I performed all regression analyses using PAST v.4.03 (Hammer et al. 2001). I used reduced major axis (RMA) linear regressions because RMA accommodates error in both the dependent and independent variable measurements.

Testing and Applying Regressions to Estimate Body Length for Fossil Taxa

I tested each regression for homoskedasticity, or homogenous scatter of residuals around the regression line (Smith 2002). Greater homoskedasticity (closer to 1.00) corresponds to greater precision in regression estimates. To be considered acceptable, a regression had to have a statistically significant probability of homoskedasticity ($p(\text{homosked}) \geq 0.05$). If a regression passed the homoskedasticity test, I then tested it for normal distribution of residuals ($p(\text{norm}) \geq 0.05$, a requirement for RMA regressions). The R^2 values of the resulting regressions that passed both tests ranged from 0.69 to 0.98 ($p(\text{uncorr.}) << 0.01$). I performed these tests also using PAST v.4.03 (Hammer et al. 2001).

For each extant lizard group, I selected one specimen with a head length and SVL close to the average in my extant dataset for that group and removed it from the dataset prior to calculating the regressions. I then used that removed specimen to test the accuracy of each regression that I generated from the sample of that extant lizard group (S1.1-S1.7 Tables). The subsets of extant specimens encompassed the range of body size for most of the crown groups that I sampled, with the exception of Anguidae and Varanidae. The largest taxa in these families were outliers (*Diploglossus millepunctatus* (Anguidae); *Varanus komodoensis* (Varanidae)) and I therefore omitted them from the subsets used to generate regressions. However, I applied specimens of these outliers to their respective family regressions as an additional test. The resulting SVL differences were comparable (see Varanidae, S1.2 Table) or lower (see Anguidae, S1.1 Table) than the first test specimen, indicating that both sets of regressions can reliably predict SVL for large outliers in these families.

To test the assumption that anatomical proportions are conserved between extant and fossil members of the lizard lineages represented in my dataset, I tested my regressions using three of the few available complete fossil lizard skeletons that I measured: a large-bodied varanid (*Saniwa ensidens,* FMNH PR 2378, Fig 1.3A), a small-bodied anguid (*Parophisaurus pawneensis*, YPM VP 060609, which is not yet published at the time of this publication and thus not pictured here), and a very small-bodied polychrotid iguanian (*Afairiguana avius,* FMNH PR 2379, Fig 1.4B; see Special Considerations for Other Lizard Groups). I also measured the only known complete skeleton of a fossil shinisaurid, *Bahndwivici ammoskius* (FMNH PR 2260, Fig 1.4A) and used it to estimate SVL for the other fossil shinisaurid specimens (see Special Considerations for Other Lizard Groups).

I calculated minimum and maximum estimates of SVL for each test specimen by subtracting or adding the standard error, respectively. Confidence intervals are the most useful way to account for uncertainty in a point estimate (Smith 2002). PAST calculates the standard error as the standard deviation of the residuals corrected for the number of degrees of freedom (Hammer et al. 2001). When the residuals of a given regression had a normal distribution, the range of error was more likely to encompass the actual SVL of the test specimen.

For each anatomical element, I tested regressions using both untransformed and natural log transformed measurements. Natural log is commonly used in analyses of fossil vertebrate body size (Alroy 1998, 2000; Egi 2001; Head et al. 2013; Lovegrove and Mowoe 2013). If both the untransformed and transformed regressions passed the tests for homoskedasticity and normal distribution of residuals, I chose the regression with the lowest range of error that included or nearly included the actual SVL of the test specimens. The untransformed regression always had a lower range of error but did not always include the actual SVL of a test specimen within the range of error (e.g., the untransformed anguid regressions for frontal length vs. SVL and humerus length vs. SVL; see S1.1 Table). I chose the transformed regression if the untransformed regression did not meet these criteria (Table 1.1).

If both the untransformed and transformed regressions for a needed element failed the test for normal distribution of residuals, I tried removing outliers from the dataset for that extant lizard group (Smith 2002). I then estimated SVL for the test specimen with and without the outliers removed. If the predicted values for SVL barely changed, I proceeded to generate regressions for that group with the outliers removed. This was the case for groups such as Anguidae and Iguania. However, if the new SVL estimate was very different, or if removing clear outliers still did not result in either regression passing the tests for both homoskedasticity and normal distribution of residuals, then I did not proceed with that regression. This resulted in

the removal of a handful of fossil specimens known from a single element for which a suitable regression could not be generated. For example, I had to omit a few fossil varanid specimens known only from a frontal or parietal (see S1.2 Table).

When a complete skull or mandible was available, I used the regression for head or mandible length to SVL because head length and mandible length are known to correlate with SVL widely among extant lizards (Metzger and Herrel 2005; Pianka et al. 2017; Herrera-Flores et al. 2021) and because the SVL estimates obtained from complete skulls or mandibles were slightly more conservative than estimates taken from other bones. When a complete skull was not available, I used regressions from individual elements.

If a particular fossil specimen included more than one complete element, I used the regression that offered the lowest percentage difference between the actual and estimated SVLs for the extant test specimens. For example, one fossil varanid specimen, FMNH PR 2380, included a complete dentary, maxilla, frontal, and parietal (S1.1 Dataset). My extant varanid dataset did not yield viable regressions for SVL based on frontal or parietal length (S1.2 Table), so I could not use either of those elements to estimate SVL for this specimen. The varanid regression for maxilla length vs. SVL yielded a slightly lower percentage difference than that of dentary length to SVL (S1.2 Table), so I used the maxilla length regression to estimate SVL for this specimen (S1.1 Dataset).

I did not generate separate regressions for males and females because most extant specimens that I measured did not have a sex indicated. Although female lizards often have shorter SVLs than males (Meiri 2018), there is no reliable way to tell the sex of an individual fossil lizard specimen based on isolated bones, so any fossil lizard dataset must be treated as an averaged sample across sexes. The same is largely true for fossils when it comes to determining the ontogeny of a specimen. Unless there are many specimens of differing sizes that are all referred to the same taxon, it can be difficult to determine whether a particular specimen represents a juvenile, subadult, or adult of the fossil taxon to which it is referred. Thus, I only included juvenile specimens in the extant dataset for a particular lizard group if doing so strengthened the regressions generated (this was only the case for Helodermatidae; see S1.8 Table, S1.2 Dataset). Note that we can reasonably identify adult members of a fossil taxon if we have a large sample of referred individuals that reach a consistent maximum size range (e.g., large fossil anguids; S1.1 Dataset) or if some specimens include long bones with fused or unfused epiphyses.

Special Considerations for Fossil Anguids

The family Anguidae is the most abundant lizard group in the Paleogene fossil record of the Western Interior (Gilmore 1928; Meszoely 1970; ElShafie 2014) and the most widely represented group in this fossil dataset (S1.1 Dataset). Estimating body sizes for this group required special consideration because its fossil members exhibit a wide range of morphologies and sizes that fall into two general categories: small to medium-sized with thin osteoderms (e.g., Fig 1.2A) and large with chunky osteoderms (e.g., Fig 1.2G). I used different approaches to estimate SVL for each of these categories.

Body length estimation for small to medium fossil anguids: The small to medium anguids did not exceed 55 mm in skull length (*Peltosaurus*, Fig 1.2A, S1.1 Dataset), which was the same upper limit that I observed in extant limbed anguids (57 mm max skull length for *Diploglossus*

millepunctatus). Anatomical ratios for any individual cranial element to head length were the same or similar for the small to medium fossil anguids as for the entire extant anguid dataset (S1.9 Table). Ratios of cranial bones to SVL were also comparable between the only available complete fossil anguid skeleton, *Parophisaurus pawneensis* (YPM VP 060609, S1.1 Table, S1.1 Dataset) and averages for extant anguids (S1.9 Table). This was true for ratios of long bones to head length as well for Anguidae. The only specimen of a medium-sized fossil anguid that included both a complete skull and a complete long bone (*Peltosaurus granulosus,* AMNH 42913, Fig 1.2A and B) had a humerus : head length ratio equal to the average for the extant limbed anguids in my dataset (0.46 vs. 0.47, S1.9 Table). These comparisons indicate that fossil anguids ranging in comparable size from *Parophisaurus* to *Peltosaurus* probably had anatomical proportions similar to extant limbed anguid lizards. This justifies the use of extant anguid regressions to estimate SVL from individual elements for all small to medium-bodied fossil anguids. The small to medium anguids accounted for most of the fossil anguids in this dataset (S1.1 Dataset), including 28 of the 39 complete skulls measured.

For every extant anguid regression to pass the tests for homoskedasticity and normal distribution of residuals (see Testing and Applying Regressions), I had to omit neonate specimens as well as several outlier taxa. Among the taxa for which I found dry skeletonized specimens, the omitted outliers include *Barisia, Comptus (Celestus) crusculus, Siderolamprus (Celestus) enneagrammus, Sauresia,* and *Diploglossus millepunctatus*. I also omitted legless taxa (see Data Collection).

Diploglossus millepunctatus is an island endemic and the largest extant limbed anguid species (López-Victoria et al. 2011). Because it was comparable in head length to medium-bodied fossil anguids (e.g., *Peltosaurus,* Fig 1.2A), I used a skeleton of *D. millepunctatus* as a test specimen even though I removed that species from the extant anguid dataset (S1.1 Table). Half of the regressions accurately predicted the SVL of the *D. millepunctatus* test specimen to within 1-3% of actual SVL (LN(Head Length), LN(Mandible Length), LN(Dentary Length), and LN(Femur Length) vs. LN(SVL)). The rest had a range of error of up to 36% (LN(Frontal Length) vs. LN(SVL), S1.1 Table), a suboptimal but not unreasonable margin for estimates of fossil body size. These results indicate that the extant anguid regressions calculated in this study can generate reasonable estimates of SVL for the medium-bodied fossil anguid specimens (skull length $\leq$ 55 mm), but clearly some anatomical elements will provide more accurate estimates than others.

In addition to *D. millepunctatus*, I used a test specimen that represented the average measurements for the taxa in the extant anguid dataset (*Gerrhonotus liocephalus*, S1.1 Table). I also used the only available and fortuitously complete fossil anguid skeleton (*Parophisaurus pawneensis,* YPM VP 060609) as a fossil test specimen. I averaged the SVL percentage differences across all three test specimens to rank the anguid regressions. For regressions that had similar accuracy, I prioritized regressions that yielded more conservative SVL estimates and lower ranges of error.

Body length estimation for large fossil anguids: The largest anguid specimens in the fossil dataset (e.g., skull length $\geq$ 55 mm) were large and robust, with thick osteoderms covering the dorsal cranial elements and postcranial regions (e.g., Fig 1.2G). These specimens belonged to an extinct subgroup within Anguidae called Glyptosaurinae (Marsh 1871, 1872). Large glyptosaurines did not mirror the anatomical proportions of extant anguids (S1.9 Table). The mandible : humerus length ratio of *Helodermoides* (1.69, UNSM 4511, Fig 1.2H and I), differed

from the mean ratio for extant limbed anguids (2.07, n = 49, Fig 1.2C and D). Therefore, I could not use the extant anguid regressions to estimate SVL for large glyptosaurines.

However, large glyptosaurines did compare in anatomical proportion to the extant monogeneric family Helodermatidae (S1.9 Table). The mean mandible : humerus length ratio of extant *Heloderma* (1.64, n = 24, Fig 1.2E and F) was nearly equal to the aforementioned ratio for *Helodermoides* (1.69 (ElShafie 2014)). Large glyptosaurines also approached or exceeded the maximum skull length of *Heloderma* (84 mm, S1.1 and S1.2 Datasets) and resembled the cranial and osteoderm morphology of Helodermatidae (Fig 1.2G vs. E; in fact, *Helodermoides* was initially thought to be a fossil helodermatid on this basis (Douglass 1903)). I therefore assumed that large glyptosaurines and helodermatids also had comparable cranium : SVL proportions because those proportions correlate in most extant limbed lizards (Metzger and Herrel 2005; Pianka et al. 2017; Herrera-Flores et al. 2021). Furthermore, when I applied a test specimen of *Heloderma* to the extant anguid regressions, the SVL estimates for *Heloderma* were off by about 70%. These lines of evidence indicate that large glyptosaurines such as *Helodermoides* had anatomical proportions dissimilar to extant limbed anguids but comparable to extant *Heloderma.* Helodermatidae is placed close to Anguidae within the group Anguimorpha in both morphological and molecular phylogenetic analyses (Estes et al. 1988; Frost and Etheridge 1989; Gauthier et al. 2012; Wiens et al. 2012), so it is reasonable to consider Helodermatidae as an extant morphological and close phylogenetic analogue to large glyptosaurines. This approach is sometimes necessary when a fossil taxon deviates morphologically from the extant members of its direct phylogenetic lineage (Figueirido et al. 2011).

Given these considerations, I used a regression for head length to SVL derived from extant helodermatids to estimate SVL for large glyptosaurines (S1.8 Table, S1.1 Dataset). I applied this regression directly to the few complete large glyptosaurine skulls in my dataset (e.g., Fig 1.2G). I used a combined dataset of both dry skeletonized and wet preserved helodermatid specimens to maximize the sample size for the head length to SVL regression (S1.2 Dataset). Otherwise, the sample size of dry specimens with both head length and SVL measured would have been very small (n = 8 vs. n = 35 with wet specimens included). To minimize bias, I calibrated my measurements of head length and SVL between dry skeletonized and wet preserved specimens to make sure that I was taking measurements from the same points on both.

Even with this solution, a major problem remained: the ratios of individual cranial bones to mandible length in extant *Heloderma* were very different from those of large glyptosaurines. For example, the dentary length of *Heloderma* was unusually short relative to the mandible length (mean dentary length : mandible length = 0.42 for *Heloderma* vs. 0.62 for *Helodermoides,* S1.9 Table). The values were significantly different for every cranial bone : head length ratio that I tested for extant helodermatids compared to the average for all large glyptosaurines. Cranial element morphology often varies between closely related lizard groups (Evans 2008), more so than proportions of head or limb length to SVL. Thus, I could not use helodermatid regressions of individual cranial bones like dentary length to SVL to reconstruct body length for large glyptosaurines. To work around this problem, I estimated head lengths for large glyptosaurine specimens using anatomical ratios from complete fossil skulls of the same or closely related glyptosaurine genera (S1.10 Table). I then applied the fossil skull length estimates to the helodermatid regression for head length to SVL (S1.8 Table).

Using ratios to estimate head length in this way cannot account for allometric differences. However, large fossil glyptosaurines seem to have consistent maximum sizes within genera. For instance, I found eight frontals of *Glyptosaurus* from two different NALMA intervals

(Wasatchian and Bridgerian, Early Eocene) all measuring in the upper range of 38-45 mm and two frontals of *Paraglyptosaurus* from the same NALMAs measuring 40-45 mm (S1.1 Dataset). I selected reference specimens representing the largest skull length for each large glyptosaurine genus to estimate head length for referable specimens of comparable size. This method may slightly overestimate head length for large-bodied individuals that are slightly smaller than the reference specimen used, but that would not significantly change the overall anguid body size distribution for any given time bin.

When several specimens referred to the same genus exhibited a range of sizes for a particular anatomical element, I assumed that the smaller elements from that genus represented subadult individuals. I also assumed that observed proportions in any fossil genus in my dataset did not change ontogenetically. While these may have been false assumptions in some cases, they likely presented less bias than the alternative of using different genera as anatomical references for different ontogenetic stages of a single genus. For example, the largest *Melanosaurus* elements were comparable to corresponding elements of *Glyptosaurus*: I therefore assumed that *Melanosaurus* reached the same adult size as *Glyptosaurus* and I used *Glyptosaurus* as the only reference genus for *Melanosaurus*. The smaller *Melanosaurus* elements likely came from subadult individuals, but for consistency, I still used the same reference taxon (*Glyptosaurus,* UCMP 126000, S1.10 Table) for every specimen of *Melanosaurus.* Even though this approach might have overestimated the size of the subadults somewhat, this would not affect the overall observed patterns of body size evolution in anguid lizards because the largest SVL estimates for other anguids in the same NALMA intervals were much larger.

Special Considerations for Other Lizard Groups

Iguania: Within extant Iguania, I sampled a representative range of the body size, morphology, and taxonomic diversity within pleurodont iguanians because all the fossil iguanian specimens I measured had pleurodont dentition but not all were identified to a specific iguanian family. I measured specimens from several large-bodied genera within Iguanidae (*Conolophus, Ctenosaura, Dipsosaurus, Iguana, Sauromalus*) to capture the upper range of iguanian body size. I also included some members of Phrynosomatidae (*Sceloporus, Urosaurus*) and Liolaemidae (*Liolaemus*) to account for small-bodied iguanians, and Corytophanidae (*Basiliscus*) to add morphological variety for mid-sized iguanians. I did not include *Amblyrhynchus* or *Crotaphytus* because they were outliers with respect to head length : SVL ratio compared to the rest of the extant iguanian dataset.

I tested the iguanian regression for LN(Head Length) vs. LN(SVL) using both a large-bodied extant iguanid (*Ctenosaura*) and a complete fossil skeleton of a small-bodied polychrotid (*Afairiguana avius,* FMNH PR 2379, Fig 1.4B). The SVL estimates for both the large extant and small fossil test specimens were accurate within 22% (S1.7 Table). This indicates that the regressions I generated for Iguania can provide reasonable and reliable estimates of SVL for both small and large-bodied fossil pleurodont iguanians.

Shinisauridae: I did not find any complete dry skeletonized specimens of extant *Shinisaurus* to measure. I only found one dry skull and four wet preserved specimens of this monotypic family. But I was able to measure the holotype and only known complete skeleton of a fossil shinisaurid, *Bahndwivici ammoskius* (FMNH PR 2260, Fig 1.4A), which is included within the crown group (Conrad 2006). The *B. ammoskius* holotype skeleton had the same head length : SVL ratio as the

average that I measured for extant *Shinisaurus* based on wet preserved specimens (0.23 vs. 0.22, n = 4). Therefore, I used ratios of individual cranial elements to SVL from the *Bahndwivici* skeleton to estimate SVL for the handful of fossil specimens referred to Shinisauridae in my dataset (S1.1 Dataset), following the method I used for the large fossil anguids (see Special Considerations for Fossil Anguids).

Estimating Body Mass for Fossil Taxa

Body mass scales linearly with SVL in extant lizards with limbs (Meiri 2010). Pough developed a general lizard mass-SVL equation (Body Mass = $(0.031*SVL)^{2.98}$) based on measurements of extant taxa (Pough 1980). This equation has been used to estimate body mass for other fossil lizard taxa (Head et al. 2013), so I applied the equation to my SVL estimates to calculate body mass for each fossil specimen in my dataset (S1.1 Dataset).

RESULTS

Protocol for Estimating Fossil Lizard Body Size

For any researcher who wishes to estimate body length for fossil lizard specimens, here is the final protocol that I recommend:

1. Measure specimens representing the crown group or closest crown group to which the fossil specimens in question belong. Be sure to measure all cranial and limb element lengths in addition to SVL. An ideal sample size will include 20 or more individuals, but even $n \geq 10$ can be useful.
2. Choose one or more test specimens that represent the average and/or extreme proportions of the dataset. Ideally, the test specimen(s) will represent species for which you have multiple individuals sampled. Make sure the test specimen(s) has all measurements available, including limb measurements if any of your fossil specimens from that taxonomic group include limb elements. Remove the test specimen(s) from the dataset.
3. Generate regressions for cranial and/or limb elements to SVL, depending on what type of fossil material you have available. Generate both untransformed and natural log transformed equations for each regression.
4. Test each regression:
    a. Test for homoskedasticity first ($p(\text{homoskedastic}) \geq 0.05$).
    b. If the regression passes the first test, test the residuals of the regression for normal distribution ($p(\text{normal}) \geq 0.05$).
        i. If a regression fails one or both tests, it is often for dentary, frontal, or parietal length to SVL. These cranial elements tend to have the greatest variation within lizard groups. The limb measurements usually have strongest correlation with SVL across a given group (e.g., $R^2 \geq 0.90$, S1.1 and S1.2 Tables).
    c. Check the regression for outliers and remove them as needed for the regression to pass both tests.
        i. If removing outliers does not work, the regression cannot be used.

ii. If you have a complete fossil skeleton available, you can instead use ratios to estimate body length for incomplete specimens from the same taxonomic group. Otherwise, you may wish to omit fossil specimens for which a suitable regression could not be generated.

5. Use the regression to calculate SVL for the test specimen(s) that you removed from the dataset. If both the transformed and untransformed regressions passed all tests, and the equations have comparably strong R^2 values, choose the equation that gives the most accurate estimate with the lowest range of error.

The regressions provided here can generate SVL estimates for any fossil lizard specimen referred to the crown groups represented in this dataset if the fossil includes a complete cranial or limb bone. These methods can also be used to generate regressions for any extant lizard group not included in this study.

Fossil Lizard Body Size Evolution

Maximum lizard SVL remained below 300 mm through the early and middle Paleocene (Puercan – Tiffanian, Figs 1.5-1.6). This upper limit increased to 500 mm around the Paleocene-Eocene transition (Clarkforkian). Body mass estimates showed that the largest lizards exceeded 1 kg in body weight by that time (Fig 1.7). In the Wasatchian, maximum SVL surpassed 1 meter. The SVL estimate for the largest individual from this NALMA (*Paraglyptosaurus princeps,* USNM 6004, Table 1.3) exceeded the rest of the Wasatchian sample by over 200 mm (Fig 1.6). However, the maximum SVL remained around 1 meter through the late early Eocene (Bridgerian), which produced several specimens with estimated SVL exceeding 750 mm (Fig 1.5, S1.1 Dataset).

The pattern for the middle Eocene (Uintan – Duchesnean) was dubious. The observed maximum SVL for the middle Eocene was much lower than the early or late Eocene (542 mm, *Saniwa ensidens,* Fig 1.5, Table 1.3). Fewer outcrops are available from this interval in the U.S. Western Interior, so this result was likely an artifact of poor sampling (n = 4 for the Uintan, n = 1 for the Duchesnean, Figs 1.5-1.6). The rarefaction analysis in Fig 1.8 showed that the number of expected size groups recovered in a sample from this fossil dataset peaked and leveled off around n = 50, supporting the assumption that the NALMAs with small sample sizes in this study did not capture the full range of lizard body size that was likely present during those intervals.

The sample size was higher for the late Eocene (n = 24 for the Chadronian, Figs 1.5-1.6). The Chadronian record included several large individuals, but the maximum SVL (769 mm, *Helodermoides sp.*, Table 1.3) was slightly lower than that observed for the early Eocene. By the early Oligocene (Orellan), maximum SVL dropped to 360 mm (*Peltosaurus sp.*) and remained below that limit through the late Paleogene. The Orellan was very well sampled (n = 64) compared to other NALMAs. Rarefaction analysis (Fig 1.8) indicated that this observed decrease in maximum SVL was likely valid.

Taxonomic Turnover

The results of this study indicate that taxonomic diversity was greatest in the early Eocene and then decreased along with maximum body size range in the early Oligocene (Fig 1.5, Table 1.2). Rarefaction analysis indicates that the number of crown groups recovered within a

given NALMA peaked above a sample size of 50 specimens (Fig 1.9). I sampled 64 specimens from the Orellan (Fig 1.5, S1.1 Dataset) and yet recovered only three crown groups (Table 1.2, Fig 1.9), supporting the interpretation of a decline in diversity in the late Paleogene.

Among the eight lizard crown groups sampled, only two reached SVLs over 200 mm: Anguidae and Varanidae (Fig 1.5). Interestingly, body size in the largest extant limbed anguid, *Diploglossus millepunctatus* (maximum SVL 280 mm, mass ~630 g (Pough 1980; Meiri 2010, 2018)), does not approach the upper limit exhibited by large Eocene anguids, nor do the largest lizards occurring in North America today (*Heloderma horridum,* maximum SVL 520 mm (Beck 2005); *Iguana iguana,* maximum SVL 580 mm (Meiri 2018)). Conversely, Varanidae includes the largest extant lizard, *Varanus komodoensis*, which exceeds the adult size of the largest Eocene anguid at around 1.5 m (Pianka 1995; Meiri 2018), but this clade is now restricted to the Eastern Hemisphere (Pianka and Vitt 2003).

Anguids were the most abundant lizards in the Western Interior throughout the Paleogene (Fig 1.5, Table 1.2, S1.1 Dataset). The largest fossil anguids (head length ≥ 55 mm) all belonged to the extinct subgroup Glyptosaurinae. Only six genera fell into this category, dominated by *Glyptosaurus* and *Melanosaurus*. By the late Eocene (Chadronian), only one large glyptosaurine genus was present, *Helodermoides* (Fig 1.2G, S1.1 Dataset).

Most of the lizards in this geotemporal system did not experience an increase in body size range. Small-bodied lizards, including smaller anguid taxa, dominate the North American Paleogene lizard record. For example, 75% of the most common isolated bone in this dataset, the dentary, are < 26 mm in length with an estimated SVL of < 210 mm (S1.1 Dataset). This likely reflects a preservation bias (e.g., see the censuses of microvertebrate localities in this system by Smith (Smith 2006, 2009, 2011a, 2011b; Smith and Gauthier 2013)), but it could also reflect an ecological hierarchy in these paleocommunities. Large-bodied lizards are less abundant than smaller ones in extant ecosystems (Meiri 2008).

No more than two distinct species were documented for any given fossil genus in this study (S1.1 Dataset). In general, it is much more difficult to discern diagnostic species within a fossil genus than it is to parse fossil genera within a clade. However, this is unlikely to affect the observed patterns of taxonomic richness. Even in extant lizards, elevated richness usually reflects a high number of genera with a low number of species per genus, possibly because genera within families are more ecologically distinct from each other than are species within genera (Meiri 2008). Thus, tracking richness at the level of genera and higher taxonomic groups (Fig 1.9) likely captured a sufficient view of taxonomic diversity for fossil lizards in this study.

The only diagnostic record of large glyptosaurines occurring outside the U.S. Western Interior was a Uintan skeleton from San Diego County, California, that was referred to *Glyptosaurus* (Moscato 2013). Some small osteoderms from the Clarkforkian of South Carolina were also referred to Glyptosaurinae (Cicimurri et al. 2016), but it was impossible to estimate the size of the animal that produced them. The largest Paleogene varanid from the Western Interior, *Saniwa ensidens* (Fig 1.3A), was also previously reported from Eocene deposits in California ("The Paleobiology Database" n.d.). Thus, it appeared that these large Eocene lizards were restricted to the Western half of the present-day United States.

Among the eight lizard groups documented in this study from the Paleogene record of this region, only Anguidae, Scincidae, and Teiidae still occur in the area. Xenosaurids, xantusiids, and iguanians have since been extirpated from the Western Interior; varanids and shinisaurids no longer occur anywhere in North America (Pianka 1995; Pianka and Vitt 2003; Meiri 2018; Vidan et al. 2019).

DISCUSSION

Mechanisms of Body Size Evolution in Paleogene Lizards

Diet and competition: The most common lizard clade in the Western Interior through the Paleogene was an extinct subgroup of anguid lizards, Glyptosaurinae (Marsh 1871, 1872; Gilmore 1928; Meszoely 1970; Sullivan 1979; Gauthier 1982; ElShafie 2014). In fact, Glyptosaurinae has the most complete fossil record of any lizard group (Gauthier 1982). Glyptosaurines ranged widely in body size and include the largest Paleogene lizards documented in this study (> 12 kg, Fig 1.5, Table 1.3, S1.1 Dataset). Several glyptosaurine taxa exceeded 1 kg in body weight during the Eocene (Fig 1.7, Table 1.3), which makes their body masses comparable to those of medium-sized mammals (> 1 kg and < 50 kg (Rose 1981)).

Evolution of large body size in a lizard can lead to direct competition with mammals occupying the same ecological resource space (Pough 1973). Head et al. made this observation for a large-bodied mid-Eocene agamid lizard, *Barbaturex* (Head et al. 2013). *Barbaturex* occurred in Myanmar, which was a closed tropical forest system in the middle Eocene similar to the environment in the Western Interior of North America during the early Eocene (Wing 1987; Wing et al. 1991; Wing and Greenwood 1993; Fricke and Wing 2004). Head et al. inferred that *Barbaturex* competed with mid-sized co-occurring mammalian herbivores and omnivores (Head et al. 2013). This brings up two questions for the large glyptosaurines of the Western Interior of North America: what kind of diet enabled these lizards to get so large, and were they competing with any mammals for those resources?

To address the question of diet, we must first examine the dentition of glyptosaurines. Dentition is linked to diet in all toothed vertebrates, including squamates (Hotton III 1955; Melstrom 2017; Herrera-Flores et al. 2021). Dental morphology varied considerably among taxa within Glyptosaurinae, exhibiting a gradation between peg-like teeth with weakly pointed cusps (e.g., *Proxestops,* Fig 1.10A) and round teeth with blunt cusps (e.g., *Glyptosaurus,* Fig 1.10D), all with striated crowns. The latter were especially common among the large-bodied early Eocene glyptosaurines. The dentition in any glyptosaurine genus was typically homodont. However, Sullivan characterized the teeth in some specimens of *Paraglyptosaurus princeps,* which had the maximum estimated SVL for the Wasatchian in this study (1012 mm, Table 1.3), as heterodont (Sullivan 1979).

Researchers have interpreted the blunt, round teeth of large-bodied early Eocene glyptosaurines like *Glyptosaurus* (Fig 1.10D) as representing an omnivorous diet (Gauthier 1982) or a durophagous diet of gastropods and mollusks (Sullivan 1979). Herrera-Flores et al. also inferred a durophagous diet for "large, robust and round teeth" in a survey of fossil squamates (Herrera-Flores et al. 2021). The dentition of *Glyptosaurus* and similar forms was comparable to the teeth of the extant island endemic anguid *Diploglossus millepunctatus* (Fig 1.10G), the largest extant limbed anguid (maximum SVL 280 mm, mass ~630 g (Pough 1980; Meiri 2010, 2018)). *Diplogossus millepunctatus* is an opportunistic scavenger-predator that preys on crabs, bird carcasses, bird eggs and hatchlings, smaller lizards, and occasional insects (López-Victoria et al. 2011; Meiri 2018). Large glyptosaurine dentition also resembled the rearmost teeth of some large extant teiids such as *Tupinambis teguixin* (Fig 1.10H, maximum SVL 500 mm, mass ~3.5 kg (Pough 1980; Meiri 2010, 2018)) that are carnivorous but also

opportunistically durophagous and omnivorous (Hotton III 1955; Pianka and Vitt 2003; Meiri 2018).

Other aspects of large-bodied glyptosaurine morphology may point to a primarily durophagous diet. Like extant anguids, glyptosaurines were covered in osteoderms, and the largest glyptosaurines were heavily armored. Previous studies suggested that the dermal armor and robust mandibles of large glyptosaurines were additional adaptations for crushing hard shells or carapaces (Sullivan 1979; Gauthier 1982). Snails would have been a source of meat that was easy to capture and abundant throughout the Eocene and Oligocene of North America (Sullivan 1979; Evanoff et al. 1992). Gastropods could also have provided a source of calcium and phosphorous to assist adult glyptosaurines with osteoderm growth (J. Gauthier, pers. comm.). Based on these observations, it would be reasonable to conclude that large glyptosaurines of the early Eocene were primarily durophagous and likely opportunistic omnivores or carnivores.

The only large-bodied glyptosaurine in the late Eocene, *Helodermoides,* was also heavily armored but had more conical teeth with slightly pointed cusps (Fig 1.2G and H, Fig 1.10E). Sullivan proposed that *Helodermoides* was likely eating small mammals and possibly carrion (Sullivan 1979). *Heloderma*, the best extant morphological analogue for *Helodermoides* (Fig 1.2E-I), feeds on eggs and juvenile animals (Pough 1973; Beck 2005). However, *Helodermoides* lacked the sharp, recurved teeth of extant *Heloderma*, so it does not appear to have been an obligate carnivore (Gauthier 1982). Gauthier inferred an omnivorous diet for *Helodermoides* based on the stout teeth and blunt crowns of the extant armored omnivorous scincid genus *Tiliqua* (Fig 1.10I; (Gauthier 1982; Meiri 2010, 2018)).

Regardless of exact dietary composition, the consensus is that large glyptosaurines must have subsisted through some mix of omnivory, carnivory, and even durophagy (Sullivan 1979; Gauthier 1982). This is consistent with current observations of lizard diets. Extant lizards with SVL > 150 mm rely on carnivory, omnivory, herbivory, or some mix to achieve large body size as adults (Pough 1973). Most extant lizards that exceed 300 g as adults are herbivorous (Pough 1973; Meiri 2008, 2018), but no glyptosaurine had the characteristic three-pronged dentition of herbivorous lizards (for example, see the teeth of the iguanid *Conolophus subcristatus*, Fig 1.10L; (Hotton III 1955; Herrera-Flores et al. 2021)).

As durophagous carnivores or omnivores in the Western Interior, large Eocene glyptosaurines would have shared ecological resource space with mid-sized terrestrial carnivorous mammalian taxa that also exploited a mixed diet. These included miacids as well as oxyaenid and hyaenodontid creodontans (Rose 1981; Stucky 1992; Chester et al. 2010; Tomiya et al. 2021). Large glyptosaurines may have faced less competition with a primarily durophagous diet because blunt-cusped teeth are uncommon among carnivorous mammals. At least one oxyaenid, *Palaeonictis wingi,* and one miacid, *Uintacyon gingerichi,* both from the Paleogene of Western Interior, have been interpreted as durophagous or at least omnivorous (Chester et al. 2010), and durophagy was inferred for some Paleogene hyaenodontids in Africa (Borths and Stevens 2017). Some studies suggested a durophagous diet for mid-sized Paleogene pantolestids from the Western Interior (Rose and Von Koenigswald 2005; Rose et al. 2014), but other analyses favor a general carnivorous/piscivorous diet for this group (Boyer and Georgi 2007). In any case, pantolestids were likely semiaquatic (Boyer and Georgi 2007) and therefore an unlikely competitor for large glyptosaurines.

Most glyptosaurine genera in the early Eocene reached a maximum mass of 1 to about 5 kg (Fig 1.7, S1.1 Dataset). The dentition of these medium-sized glyptosaurines was quite varied. For example, *Melanosaurus* (maximum mass 5.1 kg, Fig 1.10C) had round teeth with blunt cusps

similar to its larger congeners (e.g., *Glyptosaurus,* Fig 1.10D), whereas *Xestops* (maximum mass 1.4 kg, Fig 1.10B) had the characteristic conical teeth with small cusps of extant generalist insectivorous lizards (e.g., *Xenosaurus*, Fig 1.10K; (Ballinger et al. 1995; Meiri 2010, 2018; Melstrom 2017; Herrera-Flores et al. 2021)). If any of these mid-sized glyptosaurines were primarily insectivorous, they would have faced little competition from co-occurring mammals. The only mid-sized, terrestrial, strictly insectivorous mammals in the Western Interior at the time were the pangolin-like palaeanodonts in the early and middle Eocene (Rose 1981, 2008; Rose et al. 1991; Stucky 1992; Gunnell and Gingerich 1993) and a single genus, *Patriomanis*, of the stem-pangolin group Pholidota in the late Eocene (Rose 2008). Meanwhile, any mid-sized glyptosaurines consuming mostly snails or small vertebrates would have occupied the same ecological resource space as the putatively durophagous miacids, oxyaenids and hyaenodontids (Rose 1981; Chester et al. 2010; Borths and Stevens 2017; Tomiya et al. 2021).

The mid-sized glyptosaurine *Peltosaurus* (Fig 1.2A, Fig 1.10F), the only Oligocene glyptosaurine that reached body sizes above 1 kg (Table 1.3, S1.1 Dataset), had homodont peg-like dentition but with cusps that were anteroposteriorly widened and laterally compressed (Fig 1.10F). The teeth of *Peltosaurus* resembled those of the extant durophagous carnivore *D. millepunctatus* (Fig 1.10G) as well as extant omnivorous species like the large armored scincid genus *Tiliqua* (e.g., *Tiliqua scincoides,* maximum mass ~1.6 kg (Pough 1980; Meiri 2010, 2018); Fig 1.10I). *Peltosaurus* teeth were also comparable to the conical dentition of primarily insectivorous extant lizards (Hotton III 1955; Melstrom 2017; Herrera-Flores et al. 2021) that are also armored and reach a similar size, such as the cordylid *Smaug giganteus* (maximum 1 kg (Pough 1980; Meiri 2010, 2018), Fig 1.10J). *Diploglossus millepunctatus, Tiliqua*, and *Smaug* all opportunistically prey on small vertebrates in addition to their primary food sources, as do many other extant lizards that are predominantly insectivorous or durophagous (Hotton III 1955; Losos and Greene 1988; Meiri 2010, 2018; López-Victoria et al. 2011; Melstrom 2017). These comparisons indicate that *Peltosaurus* was likely an opportunistic carnivore-omnivore that may also have eaten snails and insects. This may have led the genus to compete with mid-sized carnivorous-insectivorous mammals like creodontans (Rose 1981; Stucky 1992), but having a varied diet would certainly have given *Peltosaurus* an ecological advantage. This lability may account for the abundance of *Peltosaurus* specimens in the early Oligocene and the persistence of *Peltosaurus* through the Oligocene above all other glyptosaurines (Table 1.3, S1.1 Dataset; (Scarpetta 2019; Sullivan 2019)).

For the smallest glyptosaurines and other small-bodied lizards, the primary food source would likely have been insects. Among extant lizards, many small-bodied taxa (< 300 g) as well as juveniles of large-bodied species are insectivores (Pough 1973; Meiri 2008). The small-bodied glyptosaurines *Proxestops* (Fig 1.10A) and *Odaxosaurus* (maximum mass ~160 g and ~430 g, respectively, S1.7 Table) had dentition that is most comparable to that of extant insectivorous lizards like *Xenosaurus* (Fig 1.10K)*,* which reaches comparable size and has osteoderms in its skin (Pough 1980; Ballinger et al. 1995; Meiri 2010, 2018; Melstrom 2017; Herrera-Flores et al. 2021). Small insectivorous lizards in the Western Interior would have shared ecological resource space with many small insectivorous mammals through the Paleogene (Rose 1981; Morgan et al. 1995). They also would have been likely prey items for medium to large carnivorous or omnivorous mammals or even larger lizards (Hotton III 1955; Pough 1973; López-Victoria et al. 2011; Meiri 2018). At least one coprolite specimen has been found containing *in situ* osteoderms from a small glyptosaurine (CM 42242, Wasatchian, Wind River Basin).

Glyptosaurine anguids were not the only Paleogene lizards that reached large body sizes. The varanid genus *Saniwa* (Fig 1.3) also exceeded 1 kg during the Eocene (Fig 1.7, Table 1.3). *Saniwa* was likely carnivorous: it had sharp, recurved, widely spaced teeth (Fig 1.3B) analogous to extant carnivorous lizards (e.g., *Heloderma,* Fig 1.2E; (Losos and Greene 1988; Grande 2013; Melstrom 2017; Herrera-Flores et al. 2021)). However, *Saniwa* may also have fed opportunistically on insects, mollusks, and eggs, as many extant primarily carnivorous varanids do (Losos and Greene 1988). Extant varanids can also increase their aerobic metabolism and thus occupy a resource zone similar to those of carnivorous mammals of comparable size (Pough 1973). It is possible that Eocene varanids had a similar capacity. As a terrestrial carnivore in the early to middle Eocene in the Western Interior, *Saniwa* would have inhabited the same ecological resource zone as mid-sized, terrestrial carnivorous mammals such as carnivorans, mesonychids, viverravids, and arctocyonids (Gingerich 1978; Rose 1981; Stucky 1992; Bertrand et al. 2020; Tomiya et al. 2021). If *Saniwa* was also arboreal or semi-aquatic, as many extant varanids are (Pianka 1995; Meiri 2018; Vidan et al. 2019), it may have also competed with primates (Rose 1981; Morgan et al. 1995; Grande 2013) or mid-sized crocodyliforms (Hutchison 1982; Brochu 2010; Stout 2012; Grande 2013), respectively.

The Eocene varanids did not reach the size of their extant congener *Varanus komodoensis*, the largest living lizard (Pianka 1995; Pianka and Vitt 2003). However, the largest glyptosaurines did reach the minimum length of *V. komodoensis,* over 1 m in SVL (Table 1.3; (Pianka 1995; Meiri 2018)). *Varanus komodoensis* does not have any natural predators (Pianka 1995; Meiri 2018), which can release size constraints on extant lizards (Meiri 2008). This was not the case for the large Eocene lizards in the Western Interior, which lived with many contemporaneous medium- and large-sized mammalian carnivores that could have preyed on lizards. But unlike extant *V. komodoensis*, large glyptosaurines were heavily armored (Fig 1.2G). It is possible that gigantism together with robust body armor protected large glyptosaurines from predation.

Biotic interactions should at least partially drive body sizes in reptiles (Zimmerman and Tracy 1989; Hutchison 1992; Head et al. 2013). Early in the Paleogene, lizards may have been constrained to small body sizes due to competition, predation, or specializations related to resource zones of small taxa (Angilletta et al. 2004; Kingsolver and Huey 2008). Changes in faunal composition between the late Eocene and early Oligocene could similarly explain the loss of large lizards in the Western Interior and the eventual extinction of glyptosaurines.

Climate: It is also possible that climate played a role in the evolution of large body size in Paleogene lizards. Metabolic rate scales with body size in all poikilothermic vertebrates (Peters 1983; Makarieva et al. 2005a, 2005b), including lizards (Pough 1973, 1980). Increased temperatures around the Paleocene-Eocene Thermal Maximum (PETM, 56 Ma; (Wing et al. 2005; Zachos et al. 2008)) could have elevated metabolism and released a physiological constraint on maximum size for some squamate taxa (Head et al. 2009, 2013). But the body size evolution patterns observed here could also reflect indirect effects of climate (Sinervo et al. 2010). Temperatures were warmer during both the summer and winter months around the PETM, and most precipitation came during the summer (Gregory and McIntosh 1996; Snell 2011; Snell et al. 2013). This would have allowed lizards to be active and growing during a longer portion of the year (Huey and Slatkin 1976; Sinervo et al. 2010) and could also have led to greater food availability from increased productivity, especially in the summer months (Wing 1987; Wing et al. 1991; Stucky 1992). Previous studies found elevated growth rates in tropical

lizards occupying areas that received greater precipitation (Stamps 1977). Attaining large body size in a closed tropical forest system with an equable climate, like that present in the Western Interior in the early Eocene (Wing 1987; Wing et al. 1991; Wing and Greenwood 1993; Fricke and Wing 2004), would also have allowed lizards to spend less time and energy on active thermoregulation (Huey 1974; Peters 1983). Large body size sometimes corresponds with thermoconforming behavior and nocturnal activity in extant lizards (Huey and Slatkin 1976; Meiri 2008; Pianka et al. 2017), and these strategies could have reduced competition with diurnal mammals for large Eocene glyptosaurines.

Regardless of the mechanisms that influenced the evolution of large-bodied lizards in North America during the middle Paleogene, the late Paleogene reductions in maximum body size represent the extinction of larger taxa (Scarpetta 2019; Sullivan 2019). Even in extant lizards, extinction risk increases with body size (Meiri 2008). Anguid lizards still occur in the Western Interior today, but varanids are extirpated from the region (Pianka 1995; Pianka and Vitt 2003; Meiri 2018; Vidan et al. 2019).

Considerations

This study only presents body size estimates for fossil lizard specimens that included a complete cranial or limb element (or in rare cases, a complete skeleton). There were many other specimens available that contained only fragmentary material. This dataset does not reflect the full diversity or geographic distribution of that diversity within this geotemporal system, but it is a representative sample. For a thorough census of Paleogene lizard diversity in the U.S. Western Interior, see the work of Krister Smith (Smith 2006, 2009, 2011a, 2011b; Smith and Gauthier 2013).

This study does not encompass all extant lizard groups. I only focused on those that are represented in the fossil dataset presented here. Furthermore, I was not able to sample every known species of every group represented in the fossil dataset. I only included the extant species for which I was able to find reasonably complete dry skeletonized specimens to measure. In a few cases (Helodermatidae and Xenosauridae), I supplemented the dataset with measurements from wet preserved specimens to increase the sample size (S1.2 Dataset).

When collecting extant data, I aimed for a sample size of at least n = 20 for each taxonomic group whenever possible because this is considered acceptable for simple bivariate equations when *x* and *y* are highly correlated (Smith 2002). The only group for which I could not reach that sample size was Xenosauridae because there were not enough dry skeletonized specimens available. For that family, I had a usable sample size of only 12 (S1.3 Table), so body size estimates for fossil xenosaurids in this study may be less reliable than for other taxa. However, the fossil specimens I sampled from that family were all relatively small (estimated SVL < 175 mm, S1.1 Dataset). Any inaccuracies for the fossil xenosaurid specimens within the margin of error would not change the observed patterns of body size evolution for Paleogene lizards in the Western Interior.

I did not generate regressions for every cranial or limb element for every taxonomic group sampled. I only generated the regressions that I needed to estimate SVL from the elements that I had in my fossil dataset (S1.1-S1.8 Tables). If you wish to estimate SVL for a fossil lizard specimen referred to a family included in this study, but the anatomical element in question is not represented by the regressions offered here, you can generate the necessary regressions from the included extant dataset (S1.2 Dataset) following the methods outlined in this paper. I do not

recommend combining measurements from different lizard groups to create “generic” lizard regressions to generate SVL estimates for unidentified lizard elements because anatomical proportions vary between crown groups. These methods only work for fossil lizard elements that can be referred to a specific crown group.

CONCLUSIONS

This study offers the first survey and reconstruction of body size across crown lizard groups through a prolonged geologic interval and across a large continental interior region. The findings indicate that lizard body size peaked in the early Eocene. Only two lizard groups, Anguidae and Varanidae, reached large body sizes, while body size range remained unchanged for other groups. Most large-bodied lizards in the Eocene were heavily armored glyptosaurine anguids, which appear to have achieved gigantism through omnivorous or carnivorous and possibly durophagous diets. Both maximum body size and taxonomic diversity decreased for lizards across the Western Interior in the early Oligocene. The methods presented here can be applied to other lizard clades to generate reasonably accurate body size estimates for fossil taxa and to study patterns of body size evolution across higher taxonomic groups.

CHAPTER 2

Body size changes in reptile assemblages across the Western Interior of North America through the Paleogene

ABSTRACT

In Chapter 1, I found that maximum lizard body size across the Western Interior of North America peaked in the early Eocene and decreased in the early Oligocene. But how do these deep time evolutionary patterns in terrestrial lizards compare to those of contemporaneous higher reptile groups with semiaquatic life histories? And are these patterns consistent between local community assemblages with varying local climates, or do the patterns only emerge across a larger geographic region? Here, I test the hypotheses that 1) Paleogene crocodyliforms exhibit the same body size evolution patterns as co-occurring lizards across this region, and 2) patterns of body size evolution in Paleogene lizards and crocodyliforms are ubiquitous within the intermontane basins of the Western Interior and congruent with the pattern observed across the entire region. I reconstruct body size for 280 fossil crocodyliforms across this geotemporal system and compare the results to body sizes estimated for 283 fossil lizards from Chapter 1. My results indicate that, in contrast to the lizards, maximum crocodyliform snout-vent length (SVL) was consistently large at or above two meters across the Western Interior from the early Paleocene through the middle Eocene. Individual basin subsamples reveal the same pattern. Lizards also show consistent body size evolution patterns across contemporaneous assemblages: maximum SVL in the large-bodied lizard families Anguidae and Varanidae peak in the Eocene in all well sampled basins. Interestingly, the largest lizards in the early Eocene (SVL > 0.7 meters) outsize some co-occurring crocodyliforms. These findings indicate that body size evolution trajectories differ between higher level reptile groups with terrestrial vs. amphibious ecologies but observed body size evolution patterns among those groups emerge both within assemblages and across continental interiors over geologic time.

INTRODUCTION

Reconstructing body size for a group of animals over geologic time offers insights into the evolutionary biology and ecology of its extant members (Damuth 1990; Figueirido et al. 2011; Campione and Evans 2012; Thomas Goodwin and Bullock 2012; Head et al. 2013; Godoy et al. 2019). But we cannot fully comprehend past ecosystems or evolutionary processes by investigating taxonomic groups in isolation. We must examine patterns of evolution across co-occurring groups with different ecologies over deep time intervals to understand how they affect each other and how abiotic factors similarly or differentially affect them. In Chapter 1, I examined body size evolution patterns in terrestrial lizards across the Western Interior of North America through the Paleogene (66-23 million years ago (Ma)). Here, I aim to 1) determine whether the same patterns of body size evolution are evident in a co-occurring higher taxonomic group of semiaquatic reptiles, Crocodyliformes, and 2) observe whether regional patterns of body size evolution in terrestrial lizards and amphibious crocodyliforms also emerge within local assemblages through the Paleogene.

I chose crocodyliforms (crown group crocodylians and their extinct relatives) over other reptile groups to compare with lizards not only for their semiaquatic ecology, but because complete cranial elements of fossil crocodyliforms are much more abundant in this study system than are those of fossil turtles or snakes. In addition, body size estimation relies on measurements of vertebrae for fossil snakes (Head et al. 2009) and carapaces for fossil turtles (Hutchison 1982; Cadena et al. 2012, 2020; Angielczyk et al. 2015), whereas researchers commonly use cranial and limb bones to estimate body size for fossil crocodyliforms (Sereno et al. 2001; Farlow et al. 2005; Young et al. 2011; Aureliano et al. 2015; O'Brien et al. 2019). Therefore, I could apply the same methods I developed in Chapter 1 for body size estimation in fossil lizards to the fossil crocodyliform specimens examined in this study.

Cranial and femoral dimensions strongly correlate with body size in extant crocodylians (Greer 1974; Webb et al. 1978; Woodward et al. 1995; Verdade 2000; Sereno et al. 2001; Farlow et al. 2005; Young et al. 2011; Erickson et al. 2012; Fukuda et al. 2013; Aureliano et al. 2015; Godoy et al. 2019; O'Brien et al. 2019; Lakin et al. 2020). For example, femur length predicts total body length (TBL) and body mass in *Alligator mississippiensis* ($R^2 \geq 0.99$ (Farlow et al. 2005)); head length scales with TBL in *A. mississippiensis* ($R^2 > 0.98$ (Woodward et al. 1995)) and in *Crocodylus porosus* ($R^2 \geq 0.96$ (Fukuda et al. 2013)); head length and body mass correlate with snout-vent length (SVL) in *Caiman latirostris* ($R^2 \geq 0.97$ (Verdade 2000)); and head width corresponds to SVL, TBL, and body mass across extant crocodylians ($R^2 \geq 0.85$ (O'Brien et al. 2019)). Several studies previously used regressions from extant measurements to estimate body size for fossil crocodyliforms (Sereno et al. 2001; Farlow et al. 2005; Young et al. 2011; Aureliano et al. 2015; O'Brien et al. 2019). However, as was the case with the Paleogene lizard record from the Western Interior in Chapter 1, the crocodyliform record from this geotemporal system mostly consists of individual bones. Complete fossil skulls are more common for crocodyliforms than for lizards (compare S1.1 Dataset to S2.1 Dataset), but isolated elements still dominate. And here again, I did not find published data with comprehensive measurements of individual cranial elements for extant crocodylians. Thus, I compiled an extensive dataset of cranial and limb measurements from extant crocodylian taxa for this study.

The Paleogene record of the Western Interior in North America comes from a series of intermontane basins (Fig 2.1) that formed as the Rocky Mountains arose during that interval (Carlson and Anderson 1965; Cherven and Jacob 1985; Swinehart et al. 1985; Dickinson et al.

1988; Elder and Kirkland 1994; Janecke 1994; Robson and Banta 1995; Wilf, Beard, et al. 1998; Johnson et al. 2003; Townsend et al. 2010; Peppe 2010; Rothfuss et al. 2012; Foreman et al. 2012; Rasmussen and Foreman 2017). Local climates and environments varied between contemporaneous basins across this region. For example, during the earliest Paleocene, the Denver Basin contained a hot and humid rainforest (Johnson and Ellis 2002; Johnson et al. 2003), while the Raton Basin to the south and the Williston Basin farther north were both about 5ºC cooler (Fig 2.1 (Davies-Vollum 1997; Peppe et al. 2011)).

Paleontologists have thoroughly sampled these basins over the last 150 years and the fossils are easily accessible in natural history museum collections across the United States. Some previous studies thoroughly described the fossil communities of particular basins (e.g., Denver Basin (Johnson et al. 2003); Bighorn Basin (Gingerich 1980; Bloch et al. 2004; Wing et al. 2009); Williston Basin (Peppe 2010)) or localities within basins (e.g., Wannagan Creek, Williston Basin (Erickson 1999); Castle Rock, Denver Basin (Johnson and Ellis 2002)) in this geotemporal system. Others examined a specific group across the intermontane basins (e.g., mammals (Rose 1981; Stucky 1992); flora (Wing 1987, 1998; Wing and Greenwood 1993); lizards (Smith 2009, 2011a; Smith and Gauthier 2013)). Here, I treat continuous horizons within these basins as community assemblages because the organisms preserved in them probably occurred together, and I compare contemporaneous reptile assemblages between basins to see if body size evolution patterns aligned or diverged among them.

This is the first study to reconstruct and compare body size evolution in terrestrial and amphibious higher reptile groups across this or any other continental region and to compare the results at both regional and local geographic scales. I hypothesize that 1) body size evolution followed a similar trajectory in terrestrial lizards and semiaquatic crocodyliforms across the Western Interior of North America through the Paleogene, and 2) this trajectory emerges both within local communities and across the entire region through this interval.

MATERIALS & METHODS

Data Collection

I sampled 280 fossil crocodyliform specimens from the Paleogene record of the Western Interior (S2.1 Dataset). I only measured specimens that contained complete cranial or limb elements. Many specimens included a complete skull and a few even had a complete skeleton (Fig 2.2). I also measured complete elements from an equally large dataset of fossil lizard specimens (n = 283) from the same geotemporal system (S1.1 Dataset). I grouped all these fossil specimens by North American Land Mammal Age (NALMA), the conventional system used to divide the Paleogene into shorter intervals of time based on taxonomic turnover in the mammal fossil record (Woodburne 2004). Age ranges for these NALMA intervals are given in Table 2.1 (Barnosky et al. 2014).

I assigned each fossil crocodyliform specimen to the most specific taxonomic group possible based on literature on crocodyliform evolution and phylogenetics (Wassersug and Hecht 1967; Brochu 1997, 1999, 2000, 2003, 2004, 2010, 2013; Markwick 1998c; Hill and Lucas 2006; Stout 2012; Grande 2013; Cossette and Brochu 2020). Many Paleogene crocodyliform taxa cannot be confidently assigned to a crown family (Alligatoridae, Crocodylidae, or Gavialidae). In these cases, I labeled the taxon with the next most precise higher taxonomic designation. The

hierarchy of the five taxonomic groups used (in increasing order of hierarchy: Alligatoridae and Crocodylidae, Crocodyloidea, Crocodylia, Eusuchia) is illustrated in the cladogram in Fig 2.3. It is important to note that these five groups do not represent five separate clades but, rather, the most specific taxonomic assignment possible for each crocodyliform taxon represented in the fossil dataset (S2.1 Dataset). For example, the extinct taxon *Borealosuchus* consistently falls within Eusuchia, but researchers debate its inclusion within Crocodylia (Brochu 1997, 2003; Stout 2012; Cossette and Brochu 2020), so I labeled it as "Eusuchia" in this study (Fig 2.3, S2.1 Dataset). I did not include specimens of the gavialid-like group Choristodera, although I found many suitable specimens of choristoderes in collections, because its phylogenetic placement is dubious and likely falls outside of Crocodyliformes (Ezcurra 2016; Dudgeon et al. 2020).

I also measured 73 dry skeletonized specimens of extant crocodylians, representing about half of extant diversity within Crocodylidae and Alligatoridae (at least 13 out of 27 currently recognized species (Uetz and Hallermann n.d.); S2.2 Dataset). I did not include Gavialidae in my extant dataset because my fossil dataset does not include longirostrine (long snouted) crocodyliforms. For the lizards, I needed a larger and more diverse dataset of extant taxa to generate regressions for the eight crown lizard clades represented in the fossil dataset (n = 332 extant specimens, S1.2 Dataset; see Chapter 1: Data Collection). I collected all these extant and fossil data from 26 different natural history museum collections across the United States (see Institutional Abbreviations, pg. x).

All measurements were taken with digital calipers (Mitutoyo 150 mm) to the nearest 0.1 mm for individual bones and the nearest 1 mm for SVL. I measured SVL in fossilized and dry skeletonized specimens from the tip of the snout to the posterior centrum of the second caudal vertebra, which corresponds to the location of the cloaca (vent). For crocodyliforms and large lizard specimens with an SVL measuring > 150 mm, and for specimens that were preserved in a curved position, I used a tape measure to measure SVL to the nearest 1 mm.

Generating Regressions from Extant Data

In Chapter 1, I outlined methods I developed for generating regressions from extant measurements to estimate SVL for fossil lizards from isolated bones (see Chapter 1: Materials & Methods). I applied the same protocol here to estimate SVL for fossil crocodyliforms. I again used reduced major axis (RMA) linear regressions to accommodate error in both the dependent and independent variable measurements. I transformed all values using natural log, which is commonly used in analyses of fossil vertebrate body size (Alroy 1998, 2000; Egi 2001; Head et al. 2013; Lovegrove and Mowoe 2013). I tested both natural log transformed and untransformed regressions for homoskedasticity ($p(\text{homosked}) \geq 0.05$) and normal distribution of residuals ($p(\text{norm}) \geq 0.05$, a requirement for RMA regressions). I performed all regression analyses using PAST v.4.03 (Hammer et al. 2001).

In contrast to Chapter 1, it was not necessary here to generate separate sets of regressions for different taxonomic groups. Extant alligatorids and crocodylids, as well as crown-group fossil crocodyliforms, share common proportions that are strongly correlated (Farlow et al. 2005; O'Brien et al. 2019). Furthermore, when I tried calculating regressions specifically for Alligatoridae (n = 22 that included both SVL and other cranial elements, S2.2 Dataset), the regressions did not pass the tests for homoskedasticity or normal distribution of residuals. Regressions for Crocodylidae did pass both tests, but the sample size that included measurements of SVL was very low (n = 6, S2.2 Dataset). Therefore, I combined measurements from extant

alligatorids and crocodylids and calculated regressions for both families combined. This approach produced viable regressions for every anatomical element that I measured ($n \geq 26$, $R^2 \geq 0.77$, S2.1 Table).

For regressions based on femur length and femur circumference, I added femoral measurements from 33 additional extant specimens of *Alligator mississippiensis* provided by J. Farlow from a previous study (Farlow et al. 2005). These additional data included measurements of both "anterior SVL" (aSVL, measured to the anterior edge of the cloaca) and "posterior SVL" (pSVL, to the posterior edge of the cloaca). I took my own measurements of SVL to the approximate midpoint of the cloaca, so I calculated the mean value of aSVL and pSVL as the measurement of SVL for these added specimens (S2.2 Dataset). The resulting regressions were very strong ($n = 59$, $R^2 = 0.99$ for Femur Length vs. SVL; $n = 47$, $R^2 = 0.98$ for LN(Femur Circumference) vs. LN(SVL); S2.1 Table).

In addition to the regressions I generated, I used a published equation from O'Brien et al. to estimate SVL for fossil crocodyliforms based on head width (O'Brien et al. 2019). The authors derived this equation (LN(SVL) = (0.768 * (LN(Head Width))) + 2.525, $R^2 = 0.86$; see Fig 5 in (O'Brien et al. 2019)) from a large dataset of extant alligatorids, crocodylids, and gavialids ($n = 76$), encompassing most of the known extant crocodylian species ($n = 22$ out of 27 taxa). Thus, I did not feel the need to add my own data to get a sufficiently comprehensive regression equation for estimating SVL from head width. O'Brien et al. successfully applied their equations to estimate body size for several fossil crocodyliform taxa (O'Brien et al. 2019). They also pointed out that differences in posture and habitat can present some limitations to using femoral dimensions to estimate body size. For these reasons, I used the O'Brien et al. equation for all fossil crocodyliform specimens in my dataset that had a measurement for head width available. For all others, I used the regressions I generated for Alligatoridae + Crocodylidae (S2.1 Table).

Testing and Applying Regressions to Estimate Body Length for Fossil Taxa

Following the protocol from Chapter 1 (Chapter 1: Materials & Methods), I selected two extant test specimens, one alligatorid and one crocodylid, removed them from the extant dataset prior to generating regressions, and then used those specimens to test the predictive power of the regressions (S2.1 Table). Accuracy ranged from 1-3% (Femur Length vs. SVL) to 18-20% (LN(Maxilla Length) vs. LN(SVL)) within actual SVL for the extant test specimens. I also used four complete fossil crocodyliform skeletons, one small-bodied (SVL < 0.5 m, e.g., Fig 2.2A) and three large-bodied (SVL > 1 m, e.g., Fig 2.2B), to test the assumption that anatomical proportions are conserved between extant and fossil crocodyliform taxa within my dataset. The regressions delivered similar accuracy for the fossil skeletons compared to the extant test skeletons (within 1-19% of actual SVL), validating my approach. The only exception was the parietal regression (Parietal Length vs. SVL, 21-36%). This equation may have been less accurate for the fossil skeletons due to measurement error because it was sometimes difficult to see the frontoparietal suture on fossil specimens.

Some specimens in the fossil crocodyliform dataset include more than one complete element (S2.1 Dataset). To determine which regression to prioritize when more than one element is available for a given specimen, I ranked the regression equations (S2.1 Table) according to the following criteria:

1. Lowest mean difference between estimated and actual SVL across all extant and fossil test specimens (5-16%).
2. Regression sample size, i.e., the number of extant specimens for which measurements of both the given anatomical element and SVL were obtained and use to generate the regression equation (n = 26-59).
3. Test sample size, i.e., the number of extant and fossil test specimens for which measurements of both the given anatomical element and SVL were available to test the regression (n = 1-6).

The best viable equations for estimating SVL proved to be the untransformed equation for femur length and the natural log transformed equations for femur circumference, tibia length, and dentary length. The untransformed equation for parietal length and the transformed equation for maxilla length were the least reliable, so I only used them when no other measurements were available for a given specimen. The full list of equation rankings and justifications are given in S2.1 Table.

Estimating Body Mass for Fossil Crocodyliforms

I used regression equations from O'Brien et al. for estimating body mass from head width (LN(Mass) = (2.953 * (LN(Head Width))) – 5.072, R^2 = 0.93; 25% reduction in mass is factored in to account for the mass discrepancy between extant captive and wild crocodylians; see Fig 3C in (O'Brien et al. 2019)) and for estimating SVL from head width (LN(SVL) = (0.768 * (LN(Head Width))) + 2.525, R^2 = 0.86; see Fig 5 in (O'Brien et al. 2019)) to derive an equation for estimating body mass from SVL for fossil crocodyliforms (Mass = EXP(((2.953 * (LN(SVL))) / 2.268) – 8.359). I applied this new equation to all SVL estimates for fossil crocodyliforms in my dataset (S2.1 Dataset).

Georeferencing Localities

I georeferenced locality data for each fossil specimen (S1.1 Dataset, S2.1 Dataset) using collections data, literature, and GEOLocate (www.geo-locate.org). When specific locality data were not available, I used the centroid of the county from which the specimen was collected. This is a common practice for natural history collections (Zizka et al. 2019). The basins I sampled generally encompass the counties they include, so using a county centroid would not change the basin assignment for a given locality. I obtained coordinates for some localities from collections notes included with specimens. To protect sensitive fossil localities, these coordinates are listed as approximations within 1º of the actual coordinates and indicated accordingly in S1.1 and S2.1 Datasets. Interested researchers may contact the corresponding collections managers to request exact coordinates for these localities.

I plotted all original locality coordinates onto maps using QGIS-LTR 3.22.6 (download.qgis.org). The maps show localities that occur at least once in the datasets, marked according to each taxonomic group occurring in that locality (Figs 2.4-2.16). Only the specimens with locality information that I could georeference are represented on the maps. The maps do not indicate the total number of specimens that came from any given locality, but occurrences of n > 1 have darker shading. Some specimens from different taxonomic groups come from the same locality within a given NALMA time bin; these data points might be stacked and not fully visible in the maps.

I added the intermontane basins of the Western Interior of North America to the maps (Figs 2.1, 2.4-2.16) based on literature (Carlson and Anderson 1965; Cherven and Jacob 1985; Swinehart et al. 1985; Dickinson et al. 1988; Elder and Kirkland 1994; Janecke 1994; Robson and Banta 1995; Wilf, Beard, et al. 1998; Johnson et al. 2003; Townsend et al. 2010; Peppe 2010; Rothfuss et al. 2012; Foreman et al. 2012; Rasmussen and Foreman 2017). I regard the Western Great Plains as a basin in this study (see the dashed outline in Fig 2.4), even though the area is not surrounded completely by mountains, because a continental divide runs east-west through the Black Hills just to the north and the whole area was a unified drainage basin when its Paleogene deposits formed in the late Eocene through the Oligocene (Swinehart et al. 1985; Dickinson et al. 1988). After mapping the basins, I subsampled data points from individual basins in QGIS to examine body size evolution patterns and taxonomic turnover within each basin and compare the results to the regional pattern across the Western Interior for both lizards and crocodyliforms.

RESULTS

Crocodyliform Body Size Evolution

Crocodyliforms in this study system consistently reached maximum SVLs above 1.6 meters from the early Paleocene through the middle Eocene (Figs 2.17-2.18). The maximum SVL estimated in this study was 2.36 meters, occurring in the Tiffanian (*Borealosuchus formidabilis,* SMM P82.12.700, Table 2.1). The rarefaction analysis in Fig 2.19 shows that the number of expected size groups recovered in a sample from the fossil crocodyliform dataset leveled off around n = 65. Therefore, the maximum size observed in the Tiffanian, with n = 62, likely represented the upper limit for crocodyliform body size in this study system. These results contrasted with the regional pattern observed in co-occurring lizards, for which maximum SVL doubled between the late Paleocene and early Eocene (Fig 1.5, Table 1.3).

However, not all these crocodyliforms were large: smaller individuals were always present (Figs 2.17-2.18). Some of the smaller specimens could represent juvenile individuals, with SVLs as low as 129 mm (Crocodylidae indet., UCM 45655, Bridgerian, S2.1 Dataset). The NALMA with the largest sample of crocodyliforms, the Bridgerian (n = 108), showed a continuous spread of SVLs between that minimum and a maximum of 2.24 meters (*"Crocodylus" sp.,* UW 3155, Table 2.1, S2.1 Dataset) for that interval (Fig 2.17). The largest Paleogene crocodyliforms ubiquitously fell outside of crown groups Crocodylidae and Alligatoridae (Figs 2.3, 2.17). SVL for those families did not exceed 1.3 meters throughout this study system (Fig 2.17, Table 2.2, S2.1 Dataset).

In the late Eocene, maximum SVL, diversity, and abundance all dropped for crocodyliforms (Figs 2.17-2.18, Table 2.1). This drop appeared to precede the early Oligocene decrease in maximum SVL observed in lizards (Fig 1.5, Table 1.3). The Duchesnean was poorly sampled for both lizards and crocodyliforms (n = 1 for each group), and the Chadronian was decently represented for lizards but not for crocodyliforms (n = 25 Chadronian lizards vs. 5 Chadronian crocodyliforms; Figs 1.5, 2.17). The rarefaction curve in Fig 2.19 shows that the late Eocene crocodyliform samples I obtained were statistically likely to under sample the body size range that was present for crocodyliforms at the time. However, the rarefaction curve in Fig 1.8 demonstrates that large samples of lizards in the Chadronian and Orellan did not recover any

large-bodied taxa either. Taken together, these results support the interpretation that there were indeed fewer and smaller crocodyliforms (maximum SVL < 1 meter, Fig 2.17) present in the Western Interior by the late Eocene. I only recovered two comparably small crocodyliform specimens from the early Oligocene, and I did not find any past the Orellan (Figs 2.17-2.18). Thus, it appears that crocodyliforms were extirpated from this region by the Whitneyan. Crocodyliforms continued to occur in North America south of the Western Interior after the Orellan and later returned to the area in the Miocene (23-5.3 Ma; (Markwick 1998c; Brochu 1999; Whiting and Hastings 2015; Miller-camp 2016)). Today, extant crocodylians do not occur in the Western Interior, and alligatorids do not occur north of North Carolina (Lang 2008).

Body Size Evolution in Crocodyliforms Compared to Lizards Within and Across Basins

Examining results within basin assemblages allowed for comparison of body size evolution patterns within local communities to regional patterns across the Western Interior (Figs 1.5, 2.17, 2.20-2.27; for Figs 2.20-2.27, note that SVL distributions were only charted for basins with n > 10 and more than one NALMA represented)). For example, the Bighorn Basin, which preserves the best record available in North America for the Paleocene and the Paleocene-Eocene transition (Rose 1981), indicated that maximum crocodyliform SVL increased in the early Eocene (Fig 2.20). However, the Williston Basin showed that large-bodied crocodyliforms were abundant in that location through the Paleocene (Fig 2.21). The mid-Paleocene (Tiffanian) Wannagan Creek locality within the Williston Basin produced over 60 complete crocodyliform skulls, with an average estimated SVL of 1.7 meters (S2.1 Dataset). This average was comparable to the range of SVLs found in later crocodyliforms of the Green River Basin (Fig 2.22) on the other side of the rising Rockies in the early to middle Eocene (Figs 2.5-2.10). Thus, maximum crocodyliform body size seems to have been comparably high across most intermontane basins in the Western Interior through the early and middle Paleogene, reflecting the pattern observed across the entire region (Figs 2.17-2.18).

The best snapshot of a Paleogene community in this system came from early Eocene deposits in the Green River Basin (Figs 2.9-2.10, 2.22). This basin has been thoroughly sampled from several rich localities in and around Fossil Butte National Monument (Grande 2013). In this study, the Bridgerian of the Green River Basin alone yielded the largest total sample of lizard and crocodyliform specimens from any basin for any NALMA interval (n = 103, 81 of which were crocodyliforms, Fig 2.22). The Lagerstätten deposits in this basin are well known for producing spectacular fossil skeletons (e.g., Figs 1.3-1.4, 2.2), including nine out of only ten complete fossil skeletons represented in this collective dataset (three lizards and six crocodyliforms, S1.1, S2.1 Datasets).

Lizards also demonstrated intrabasinal patterns of body size evolution that mirrored the regional pattern observed across the Western Interior (Fig 1.5). The Bighorn Basin showed maximum lizard SVL increasing through the Paleocene-Eocene transition (Fig 2.20). This pattern was consistent among contemporaneous lizard data across other well sampled basins (Figs 2.22-2.24), with maximum SVL peaking around one meter in the Wasatchian (Fig 2.25). By the early Eocene, the largest lizards in the Bighorn Basin and Green River Basin even rivaled some co-occurring crocodyliforms in body size (Figs 2.20, 2.22-2.25).

The basins that preserved the late Paleogene show that maximum body size and diversity decreased for both lizards and crocodyliforms in the early Oligocene (Figs 2.14, 2.21, 2.24, 2.26-2.27). By that time, maximum SVL among the lizard faunas dropped by about 50% and

remained below 400 mm through the late Paleogene, as demonstrated across the Western Interior in Chapter 1 (Fig 1.5). These lizards were now smaller than the persisting crocodyliforms, but the latter had also diminished in both size and abundance. Even by the late Eocene, maximum crocodyliform SVL was less than half of that observed in the Green River Basin in the middle Eocene (about 900 mm vs. 2.2 meters, Figs 2.22, 2.26). Early Oligocene localities were concentrated in the Western Great Plains, from which Orellan deposits produced 50 lizard specimens (all but one of them anguids) and only two crocodyliform specimens, both alligatorids (Figs 2.14, 2.26). Alligatoridae is still the only crocodylian family that extends its range north of the Gulf of Mexico in North America today (Lang 2008).

Overall, the body size evolution patterns observed at local scales within basins reflect the patterns observed across the entire Western Interior through the Paleogene for both crocodyliforms and lizards.

DISCUSSION

Potential Drivers of Body Size Evolution in Crocodyliforms and Lizards

Climatic and environmental change: Crocodyliforms and lizards clearly followed different body size evolution trajectories, even within contemporaneous assemblages in each basin. This could have resulted from differences in habitat, diet, physiology, or experienced microclimate. The largest lizards in this geotemporal system exhibit morphologies characteristic of extant terrestrial and arboreal lizards, which must respond behaviorally or physiologically to changes in ambient temperature (Huey 1974; Huey and Slatkin 1976; Huey et al. 2003; Muñoz et al. 2014; Muñoz and Losos 2018; Muñoz and Bodensteiner 2019). Extant crocodylians seem to be less impacted by ambient temperatures overall if they remain above freezing (Hutchison 1982; Markwick 1998b; Godoy et al. 2019; Gearty and Payne 2020). Water, rather than air temperature, may be the limiting factor for crocodyliforms. Extant crocodylians spend much of their time in water and only occur where large bodies of water are plentiful (Lang 2008). The greatest concentrations of large crocodyliform specimens in this study came from two areas known to have had especially large bodies of water at the time of deposition. The Wannagan Creek locality in North Dakota, located within the Williston Basin (Fig 2.21), was a swamp in the Tiffanian (Erickson 1999). The Fossil Lake deposits preserved across the Green River (Fig 2.22), Washakie (Fig 2.23), and Uinta Basins represent a system of giant lakes (Grande 2013) that formed during an interval of high temperatures and prolonged humid warm seasons in the early and middle Eocene (Gregory and McIntosh 1996; Snell 2011; Snell et al. 2013). Recent studies also link large body size in fossil crocodyliforms to the evolution of aquatic or semiaquatic habits (Godoy et al. 2019; Gearty and Payne 2020) and changes in deep time crocodyliform diversity to changes in precipitation (Brochu et al. 2020).

In the late Bridgerian and Uintan, subtropical and paratropical forests were replaced by open forests across the region (Wing 1987; Stucky 1992; Townsend et al. 2010). By the late Eocene, deciduous forests and more open grasslands had taken over the Western Interior (Wing 1987; Stucky 1992). Subsequent cooling and aridification across the Eocene-Oligocene transition (Zanazzi et al. 2007; Boardman and Secord 2013) coincided with the decrease in maximum SVL and diversity observed in both lizards and crocodyliforms across the Western Interior (Figs 1.5, 2.17), as well as the extirpation of crocodyliforms from the region (Figs 2.14-2.15, 2.17). Colder

temperatures and the disappearance of large bodies of water may have driven extirpation of large-bodied lizards and crocodyliforms (Eronen et al. 2015). For further discussion, see Chapter 3, which tests for correlation between temperature, precipitation, and gigantism in these reptile groups.

Faunal communities in the Western Interior also experienced changes in local climate due to changes in elevation during the ongoing Laramide Orogeny from the early Paleocene into the late Eocene (Meyer 1986; Dickinson et al. 1988; Wing and Greenwood 1993; Rasmussen 2003; Snell 2011; Rothfuss et al. 2012; Eronen et al. 2015; Rasmussen and Foreman 2017). Rocky Mountain uplift peaked in the late Paleocene and early Eocene, during which the present intermontane basins began to take shape (Stucky 1992). The Rocky Mountain ranges would have exhibited high relief during that time (e.g., 1000-3000 m; (Norris et al. 1996; Dettman and Lohmann 2000; Fricke 2003)). However, the intermontane basins still had a lower elevation than at present, about 700 meters or less above sea level, because the region had not yet been uplifted (Dickinson et al. 1988; Snoke et al. 1993; Snell et al. 2013; Allen 2017b). Elevation increased later through the late Eocene and early Oligocene, contributing to cooling and aridification in the region (Dickinson et al. 1988).

There did not appear to be any latitudinal gradient for maximum body size among the Paleogene reptile faunas examined in this system. Almost all lizard data from the early and early mid-Eocene, when large-bodied lizards were most abundant, came from localities in Wyoming and Colorado with no clear latitudinal gradient among them (Figs 2.9-2.10). One could possibly interpret a latitudinal gradient for the lizards of the late Eocene since all the largest Chadronian lizards come from latitudes south of Montana (Fig 2.13, S1.1 Dataset). However, the sample size is too small to draw a strong conclusion. Interestingly, researchers recently observed the opposite pattern in *Microlophus* iguanian lizards in South America (Toyama and Boccia 2022). That study found that larger species corresponded to colder and more arid environments, consistent with "Bergmann's rule" (Bergmann 1847; Angilletta and Dunham 2003; Angilletta, Jr. et al. 2004; Brandt and Navas 2013; Zamora-Camacho et al. 2014; Toyama and Boccia 2022). Among extant lizards worldwide, anoles and geckos also exhibit distinct latitudinal gradients (Whiting and Fox 2021), but neither of those clades were represented in this fossil dataset. One recent study found evidence for a global latitudinal pattern in adult female body mass among extant crocodylians (Lakin et al. 2020), but there is no evidence of a latitudinal gradient among the Paleogene crocodyliforms sampled in this study. For example, there were large crocodyliforms in both New Mexico and Montana in the early Paleocene (Figs 2.5-2.6, S2.1 Dataset).

Competition: Alligatorids and crocodylids remained about half the maximum size of the largest non-crocodylian crocodyliforms throughout the Paleogene (Figs 2.3, 2.17, Table 2.1). Interestingly, the largest extant alligatorids and crocodylids worldwide now reach SVLs comparable to the largest Paleogene crocodyliforms from the Western Interior of North America. (Table 2.2; (Woodward et al. 1995; Fukuda et al. 2013)). These results indicate that crown group alligatorids and crocodylids in North America may have been unable to reach their largest possible sizes during the early and middle Paleogene because the ecological resource space for large-bodied crocodyliforms was already filled, rather than due to some phylogenetic constraint. Larger alligatoroids had previously occurred in North America during the Cretaceous (*Deinosuchus* (Cossette and Brochu 2020)) and later occurred in South America during the Miocene (*Purussaurus* (Aureliano et al. 2015)). The largest Paleogene crocodyliforms may have used different growth strategies to get large (e.g., growing faster, growing for more years, or

growing for longer parts of the year), but testing those mechanisms would require histological sampling of many diagnostic femora from this study system (S. Werning, pers. comm.).

Among the lizards, only anguids and varanids increased their body size range during the Eocene (Fig 1.5, Table 1.3). In several basins, the maximum size of the largest Eocene anguid lizards even exceeded that of some co-occurring crocodyliforms (Figs 2.20, 2.22-2.25). Large-bodied Eocene anguids as well as some contemporaneous small-medium Eocene crocodyliforms (e.g., *Allognathosuchus* (Wasatchian – Uintan) and *Procaimanoidea* (Bridgerian – Uintan), S2.1 Dataset) are thought to have been durophagous based on their blunt-crowned dentition (Sullivan 1979; Estes and Hutchison 1980; Brochu 2004; Miller-camp 2016; Herrera-Flores et al. 2021). These groups may have utilized the same food resources and possibly competed with mid-sized durophagous mammals (Rose and Von Koenigswald 2005; Chester et al. 2010; Rose et al. 2014; Borths and Stevens 2017). However, these animals also occupied different habitats, which may have limited their interactions. Researchers have also interpreted the large-bodied Eocene anguids as omnivorous based on comparable dentition in extant lizards ((Hotton III 1955; Gauthier 1982; Meiri 2018); see Chapter 1: Mechanisms of Body Size Evolution in Paleogene Lizards for further discussion). Perhaps a varied diet allowed these animals of similar size to co-exist and even share some food sources.

Preservation bias: Both crocodyliforms and lizards displayed body size evolution patterns within basin communities that were congruent with their respective patterns observed across the Western Interior region. Given the consistencies in the cumulative Paleogene record across these intermontane basins (Figs 2.20-2.27), deviations from the overall regional patterns (Figs 1.5, 2.17) seem best attributed to preservation and sampling bias in the records of individual basins (e.g., the paucity of data from the early and middle Eocene in the Williston Basin, Fig 2.21). Any fossil assemblage will only capture a portion of the community it preserves due to differential preservation, time-averaging, and collecting bias (Hoffman 1979; Rose 1981).

CONCLUSIONS

Large-bodied crocodyliforms (SVL > 1.5 meters) were present across the Western Interior of North America from the early Paleocene through the middle Eocene. In contrast, large-bodied lizards (SVL > 600 mm) were only present during the Eocene across this region. The largest taxa in each reptile group were restricted to certain clades; not every clade increased its body size range during the Paleogene. Body size and diversity decreased for both lizards and crocodyliforms by the early Oligocene. These patterns surfaced both within individual basin assemblages and across the entire Western Interior through the Paleogene. The differences in body size evolution patterns between lizards and crocodyliforms may have resulted from their different ecologies. Terrestrial lizards may have been more affected by changes in ambient temperature, whereas the determining factors for semiaquatic crocodyliforms were likely precipitation and availability of large bodies of water. Future investigations can build on this study by using the new regressions presented here, which expand the suite of tools available to estimate crocodyliform body size from individual bones. This is the first study to investigate body size evolution in several higher taxonomic groups of reptiles with different ecologies on an evolutionarily meaningful time scale and across both local and regional geographic scales.

CHAPTER 3

Does gigantism track climate in lizards or crocodyliforms over deep time?

ABSTRACT

Metabolic theory for ectothermic vertebrates predicts that maximum body size should correspond to environmental temperature. But studies of this relationship in extant reptiles have not revealed consistent patterns among higher order taxonomic groups. Could there be a relationship between these variables over millions of years? Here, I test the hypothesis that maximum body size in assemblages of terrestrial lizards and semiaquatic crocodyliforms correlates with transitions in environmental temperature or precipitation over geologic time intervals. I estimated snout-vent length (SVL) using regressions from extant specimens for 283 lizard and 280 crocodyliform fossil specimens from the Western Interior of North America through the Paleogene (66-23 Ma). This interval spans several warming events followed by cooling and aridification evidenced by terrestrial and marine climate proxies. My results indicate that maximum lizard SVL strongly correlated with local terrestrial temperature and weakly correlated with regional temperature across this geotemporal system. Lizard SVL showed no relationship to precipitation. In contrast, maximum crocodyliform SVL did not track environmental temperature but did indicate a positive linear relationship with precipitation. These results agree with some recent studies of relationships between these climate variables and extant lizards and crocodylians, indicating that climate constrains gigantism in these groups on both ecological and evolutionary time scales. This is the first study to examine body size evolution in the context of climate change in different higher taxonomic groups of reptiles with different ecologies through a deep time interval and across a continental interior. Investigations that connect these data from different time scales in a meaningful way can enhance predictive models of current climate change effects on biodiversity and inform conservation efforts.

INTRODUCTION

Global average temperatures have increased significantly over the last few decades (Ripple et al. 2021). Among its many effects, climate change induced by human activity is contributing to a substantial loss in biodiversity (Barnosky et al. 2011; Barnosky 2015). Ectothermic animals such as reptiles and amphibians are of particular concern because they regulate their body temperature less effectively than do mammals and birds, and are generally more susceptible to changes in environmental temperature (Huey et al. 2012). Lizards are especially vulnerable (Huey et al. 2010). Sinervo et al. predicted that approximately 40% of global lizard populations will be extirpated by 2080 (Sinervo et al. 2010). They concluded that these losses would result not just from overheating, but also from indirect effects of having reduced time for activities such as foraging for food and finding mates. Significant losses in reptile diversity can trigger a cascade of other negative effects (Sinervo et al. 2010; Roll et al. 2017b; Slavenko et al. 2019).

Many factors can put lizards and other reptiles at risk, so many lines of evidence are needed to inform predictions about how current climate change will affect them. However, the unprecedented rate of current climate change compared to recent history presents an added challenge. If we try to predict outcomes over the next century and beyond based only on data from the last few decades (e.g., (Keeling et al. 2001; Sinervo et al. 2010; Piantoni et al. 2019)) or even the last few centuries to millennia (MacFarling Meure et al. 2006; Lüthi et al. 2008), we may still not have enough information to inform predictive models for the near future.

What if we look at climate change effects on reptiles in the deep past? Can we get information from the fossil record that can help us understand how climate change might affect animals in the near and distant future? Or are the time scales – a few decades or centuries vs. *millions* of years – too different to tell us anything meaningful?

The Paleogene, which lasted from 66 to 23 million years ago (Ma), is an appropriate window in time to investigate this question because it has a robust terrestrial fossil record. We also know from its continuous marine microfossil record (Zachos et al. 2008) that several episodes of significant climate change occurred during this interval. Notably, the Paleocene Eocene Thermal Maximum (PETM, ~56 Ma) saw pronounced warming of about 5ºC within a few thousand years (Wing et al. 2005; Jardine 2011; McInerney and Wing 2011). By comparison, scientists advocate curtailing current warming to just 1.5ºC above pre-industrial levels (Masson-Delmotte et al. 2018). After the PETM, temperatures remained relatively high through the Eocene until cooling occurred across the Eocene-Oligocene Transition (EOT; (Zachos et al. 2008)).

The Paleogene record of the Western Interior of North America, particularly within the United States, preserved many reptile fossils in a series of intermontane basins that formed as the Rocky Mountains arose (Carlson and Anderson 1965; Cherven and Jacob 1985; Swinehart et al. 1985; Dickinson et al. 1988; Elder and Kirkland 1994; Janecke 1994; Robson and Banta 1995; Wilf, Beard, et al. 1998; Johnson et al. 2003; Peppe 2010; Townsend et al. 2010; Foreman et al. 2012; Rothfuss et al. 2012; Rasmussen and Foreman 2017). Paleobotanical and paleosol proxies indicate that the Western Interior had a tropical wet climate during the PETM and a tropical wet-dry climate during the early-mid Eocene, which included the Early Eocene Climatic Optimum (53-50 Ma; (Wing and Greenwood 1993; Wilf, Beard, et al. 1998; Wilf, Wing, et al. 1998; Snell et al. 2013)). From the middle to the late Eocene, the climate began to dry out in the Western Interior. The environment shifted from tropical forest to savannah woodlands, then to shrubland

with a semiarid steppe climate in the late Eocene (Townsend et al. 2010). By the early Oligocene, the region had become an arid grassland (Boardman and Secord 2013). This well-documented history of climatic and environmental change makes this geotemporal system ideal for this study.

Body size is a suitable response variable to test in fossil reptiles because we would expect it to change in response to climate change. Metabolic theory predicts that maximum body size in ectothermic reptiles should correlate with environmental temperature (Makarieva et al. 2005a, 2005b). Indeed, most of the largest extant reptiles occur in the tropics (Halliday and Adler n.d.; Uetz and Hallermann n.d.; Vitt and Caldwell 2009). Interestingly, studies of this relationship in extant reptiles have not found consistent patterns over short time scales of years to decades (Bartholomew and Tucker 1964; Pough 1973; Huey and Slatkin 1976; Ashton and Feldman 2003; Cruz et al. 2005; Olalla-Tárraga et al. 2006b; Pincheira-Donoso et al. 2007; Kingsolver and Huey 2008; Meiri 2008; Pincheira-Donoso et al. 2008; Brandt and Navas 2013; Feldman and Meiri 2014; Slavenko et al. 2019). But a recent study (Slavenko et al. 2019) found evidence for a global correlation between body mass and local temperature among lizards (exclusive of snakes).

Here I test the hypothesis that maximum body size in lizards and crocodyliforms corresponds to environmental temperature or precipitation over millions of years across continental interiors. I focus on lizards and crocodyliforms (crown group crocodylians + extinct relatives, Fig 2.3) to compare these patterns in reptiles with terrestrial vs. amphibious life histories. Complete cranial and limb bones of these reptile groups are also much more abundant in this study system than are those of fossil snakes or turtles, or of any amphibian group. Furthermore, morphology and proportions are largely conserved between extant taxa and their fossil predecessors for both lizards and crocodyliforms (Sereno et al. 2001; Farlow et al. 2005; Young et al. 2011; Head et al. 2013; ElShafie 2014; Aureliano et al. 2015; O'Brien et al. 2019). Previous studies have investigated deep time relationships between body size and climate in specific vertebrate groups, including mammals (Dayan et al. 1991; Alroy 1998; Barnosky et al. 2004; Lovegrove and Mowoe 2013; Saarinen et al. 2014; Eronen et al. 2015; Huang et al. 2017), turtles (Angielczyk et al. 2015), and crocodyliforms (Markwick 1998a; Godoy et al. 2019), and by comparing individual fossil reptile taxa with extant members (e.g., crocodyliforms (Sereno et al. 2001), snakes (Head et al. 2009), lizards (Head et al. 2013), and turtles (Cadena et al. 2012, 2020)). This is the first study to document body size evolution trends in relation to climate change in different higher order reptile groups, over a geologic time scale, across a large geographic region.

MATERIALS & METHODS

Data Collection

I measured 283 lizard and 280 crocodyliform fossil specimens (563 specimens total, S1.1 and S2.1 Datasets). Most of these specimens consisted of isolated bones. To estimate snout-vent length (SVL) from individual bones, I also measured 405 extant specimens of the same or closely related crown groups as the fossil taxa (S1.2 and S2.2 Datasets). I collected all these data from 26 natural history museum collections across the United States (see Institutional Abbreviations, pg. x).

I compiled 147 published estimates for mean annual paleotemperature (MAPT) from across the U.S. Western Interior through the Paleogene from literature (S3.1 Dataset). These estimates came from terrestrial proxies based on oxygen isotopes from bone and enamel (Fricke and Wing 2004; Zanazzi et al. 2007), floral morphology and composition (Meyer 1986; Wing et al. 1991; Wolfe 1992; Wing and Greenwood 1993; Davies-Vollum 1997; Wilf, Beard, et al. 1998; Wilf 2000; Wing et al. 2000; Johnson and Ellis 2002; Johnson et al. 2003; Kowalski and Dilcher 2003; Fricke and Wing 2004; Sandau 2005; Wing et al. 2005; Huber and Caballero 2011; Peppe et al. 2011; Allen 2017a), paleosols (Retallack 2007; Hobbs and Fawcett 2012; Hyland and Sheldon 2013; Hyland et al. 2018; Sheldon 2018; Dzombak et al. 2021; Stein et al. 2021), and land snail distributions (Evanoff et al. 1992). The latter three proxy types also provided 112 estimates for mean annual paleoprecipitation (MAPP; S3.2 Dataset) from the same geotemporal system (floral morphology (Wing and Greenwood 1993; Davies-Vollum 1997; Wilf, Beard, et al. 1998; Wilf, Wing, et al. 1998; Wilf 2000; Johnson and Ellis 2002; Johnson et al. 2003; Peppe et al. 2011; Allen 2017a); paleosols (Retallack 2007; Hobbs and Fawcett 2012; Hyland and Sheldon 2013, 2016; Dzombak et al. 2021; Stein et al. 2021); and land snail distributions (Evanoff et al. 1992)).

I georeferenced locality data for each MAPT and MAPP estimate (S3.1 Dataset, S3.2 Dataset) using literature and GEOLocate (www.geo-locate.org). Researchers have proposed paleocoordinates for Paleogene localities in the Western Interior of the U.S. that are 5-8º north to south of current locations (Roehler 1993; Wolfe et al. 1998; Fricke 2003; Hyland and Sheldon 2013; Fan and Carrapa 2014; Allen 2017a). Either way, the localities were not far from their current positions at the time of deposition. For this reason, and due to lack of available paleocoordinates for most of the localities in this study, I used present-day coordinates to map all localities. When specific locality data were not available, I used the centroid of the county from which the specimen was collected. I then subsampled localities by intermontane basin. (See Chapter 2: Georeferencing Localities for details.) The maps in Figs 2.4-2.16 show these basins and indicate localities for fossil as well as climate proxy data.

I binned climate proxy data points by North American Land Mammal Ages (NALMA), the conventional time bin used to divide the Paleogene based on taxonomic turnover in the mammal fossil record, thereby reflecting major climatic and environmental changes (Woodburne 2004). Averaging climate estimates within each NALMA time bin also helps to alleviate potential discrepancies among proxy methods. The most commonly used proxies, those based on leaf morphology, can especially vary in precision (Huber and Caballero 2011; Peppe et al. 2011; Royer 2012).

Correlation Analysis

I generated regression equations for both lizards and crocodyliforms using the extant measurements I collected and verified the predictive power of the regressions using the few complete skeletons in my fossil dataset (S1.1-1.8 and S2.1 Tables). I performed all regression analyses in PAST v.4.03 (Hammer et al. 2001) using reduced major axis (RMA) linear regressions to accommodate for error in both the dependent and independent variable measurements. I transformed all values using natural log, which is commonly used in analyses of fossil vertebrate body size as well as paleoclimate (Alroy 1998, 2000; Egi 2001; Head et al. 2013; Lovegrove and Mowoe 2013). (See Materials & Methods in Chapter 1 and Chapter 2 for details.)

I correlated maximum SVLs, 90th percentile maximum SVLs, and mean SVLs for each NALMA time bin with regional terrestrial MAPT averaged for each NALMA (Table 3.1, S3.1 Table). I omitted the Duchesnean from all correlations because I only had a single specimen each for both lizards and crocodyliforms for that NALMA, and the corresponding SVL estimates were both low (Table 3.1, S1.1 and S2.1 Datasets). The regional average MAPT for the Puercan was quite high (17.9ºC) due to elevated MAPT estimates from the Castle Rock locality in the Denver Basin (Johnson and Ellis 2002; Johnson et al. 2003), which is interpreted as a warm and humid rainforest with MAPT estimates ranging between 17.8-25.6ºC (S3.1 Dataset). This locality appeared to be an outlier among contemporaneous temperature proxies across the Western Interior: Puercan MAPT estimates from other basins were cooler (9-15.7ºC), as were successive estimates for the middle Paleocene (12.1-12.4ºC; S3.1 Dataset). Therefore, I ran each terrestrial MAPT correlation with and without the Puercan, and with and without the Castle Rock data included.

I also ran correlations for local terrestrial average MAPT and local maximum lizard SVL for basins with $n \geq 4$ for both variables. This was only possible for two basins, the Bighorn Basin and the Western Great Plains (Fig 2.1, S3.1 Table). To test for possible relationship to global temperature, I also correlated SVL values with global marine MAPT data from Zachos et al. (2008). This proxy is based on oxygen isotopes from marine foraminifera, and it represents the most continuous available record of paleotemperature through the Cenozoic (66 Ma to Recent). I used a midpoint value rather than a mean value for each NALMA from this proxy (Table 3.1, S3.1 Table) because the original dataset was not available in ºC. I also tested all major results for autocorrelation by regressing first differences, or the absolute values of the differences between successive data points (Table 3.1, S3.1 Table).

RESULTS

Temperature vs. Lizard Body Size

Lizards stayed relatively small through the Paleocene across this region, with maximum SVL under 400mm. Then in the early Eocene, maximum SVL exceeded one meter, and remained high until it dropped again in the early Oligocene (Fig 1.5; see Chapter 1: Fossil Lizard Body Size Evolution). Plotted against regional terrestrial MAPT across the Western Interior through the Paleogene, maximum lizard SVL increased with temperature through the PETM but did not track environmental temperature closely during successive cooling events (Fig 3.1). The resulting regression was modest ($R^2 = 0.51$, p(uncorr.) = 0.02, n = 10; Fig 3.2A, S3.1 Table). In that regression, I eliminated NALMAs for which $n \leq 3$ for lizards (Puercan and Duchesnean; S1.1 Dataset) because the few available SVL estimates for those NALMAs were very small (SVL ≤ 116 mm) and were therefore unlikely to capture the range of body size for lizards from those intervals. Running the regional MAPT correlation for lizards with only NALMAs that exceeded a sample size of $n \geq 5$ for both SVL and MAPT (which also eliminated the Uintan) gave the same result ($R^2 = 0.51$, p(uncorr.) = 0.04, n = 9). The correlation for regional MAPT and maximum lizard SVL was weaker with the Puercan included, with or without the MAPT estimates for Castle Rock ($R^2 = 0.09$, p(uncorr.) = 0.36, vs. $R^2 = 0.37$, p(uncorr.) = 0.05, n = 11 for both). Correlations with 90th percentile maximum SVLs gave a result similar to that of the full dataset in every instance (S3.1 Table).

Correlating first differences revealed that regional terrestrial MAPT and regional maximum lizard SVL may be autocorrelated (R^2 = 0.02, p(uncorr.) = 0.73, n = 9; S3.1 Table). However, the first differences of mean lizard SVL showed stronger correlation with regional MAPT (R^2 = 0.57, p(uncorr.) = 0.02, n = 9), even though the original correlation seemed weaker (R^2 = 0.25, p(uncorr.) = 0.14, n = 10).

The correlation between maximum lizard SVL and terrestrial MAPT was much stronger within basins. The Bighorn Basin showed a tight relationship between these variables across the PETM (Tiffanian – Bridgerian, R^2 = 0.85, p(uncorr.) = 0.08, n = 4; first differences: R^2 = 0.71, p(uncorr.) = 0.36, n = 3; Figs 3.3-3.4, S3.1 Table). The Western Great Plains showed an equally strong correlation across the EOT (Chadronian – Arikareean, R^2 = 0.87, p(uncorr.) = 0.07, n = 4; first differences: R^2 = 0.69, p(uncorr.) = 0.37, n = 3; Figs 3.5-3.6, S3.1 Table). Even though the sample sizes for these intrabasinal correlations were low (n = 4 for each), it is striking that the two correlations have the same strength while spanning different sets of consecutive NALMAs. I did not have enough paired data (n ≥ 4) to run a correlation between local MAPT and local lizard data for any other basin.

Lizard SVL showed no relationship to global marine temperatures ($R^2 \leq 0.04$, p(uncorr.) ≥ 0.56, n = 11; Fig 3.2B, S3.1 Table). Global marine MAPT data appeared to parallel the regional terrestrial MAPT data (LN(Global Marine MAPT, NALMA Midpoint (ºC)) vs. LN(Regional Terrestrial MAPT, NALMA Average (ºC)): R^2 = 0.60, p(uncorr.) = 0.003 with the Puercan estimates from Castle Rock included; R^2 = 0.55, p(uncorr.) = 0.006 with Castle Rock excluded, n = 12 for both; Fig 3.1, S3.1 Table). However, the terrestrial and marine proxies were likely autocorrelated based on lack of correlation in their first differences (R^2 = 0.01, p(uncorr.) = 0.75; R^2 = 0.14, p(uncorr.) = 0.26, respectively, n = 11; S3.1 Table). This may explain why the lizard data showed very different relationships to terrestrial vs. marine MAPT.

Temperature vs. Crocodyliform Body Size

In contrast to the lizards, large-bodied crocodyliforms were present and abundant throughout the Western Interior through most of the Paleogene. Then body size, diversity, and abundance all dropped for crocodyliforms in the late Eocene. Crocodyliforms were absent from the region by the middle Oligocene (Fig 2.17; see Chapter 2: Crocodyliform Body Size Evolution).

Maximum crocodyliform SVL clearly did not correlate with regional environmental temperature over time ($R^2 \leq 0.25$, p(uncorr.) ≥ 0.18, n = 8; Figs 3.7-3.8A, S3.1 Table). Correlations with 90th percentile maximum SVLs and mean SVLs also showed no relationship to regional temperatures. First differences autocorrelation tests confirmed that these variables were not correlated ($R^2 \leq 0.32$, p(uncorr.) ≥ 0.14, n = 7; S3.1 Table). I did not have enough paired data (n ≥ 4) from any intermontane basin to correlate local MAPT with local crocodyliform data.

Interestingly, maximum crocodyliform SVL appeared to track global marine temperatures (R^2 = 0.78, p(uncorr.) = 0.002, n = 9; Figs 3.7 and 3.8B, S3.1 Table). But a test of first differences indicated that this apparent correlation was artificial (R^2 = 0.08, p(uncorr.) = 0.51, n = 8). Lack of correlation with 90th percentile or mean crocodyliform SVLs corroborated this result ($R^2 \leq 0.15$, p(uncorr.) ≥ 0.29, n = 9; S3.1 Table).

Precipitation vs. Body Size

Maximum lizard SVL showed no correlation with terrestrial MAPP ($R^2 \leq 0.04$, p(uncorr.) ≥ 0.56, n = 11; Figs 3.9-3.10, S3.1 Table). Conversely, maximum crocodyliform SVL showed a strong correlation with MAPP, with or without the inclusion of Puercan data ($R^2 \geq 0.69$, p(uncorr.) ≤ 0.006, n = 9 with the Puercan included; Figs 3.11-3.12, S3.1 Table). The first differences correlations for MAPP vs. crocodyliform SVL were not as strong but still sufficient given the modest sample size ($R^2 \geq 0.38$, p(uncorr.) ≤ 0.11, n = 8 with the Puercan included). The correlation of 90th percentile maximum crocodyliform SVL was weaker ($R^2 = 0.23$, p(uncorr.) = 0.20, n= 9) unless the Clarkforkian (n = 3) was omitted from the regression ($R^2 = 0.78$, p(uncorr.) = 0.004, n = 8; S3.1 Table).

I did not have enough paired data (n $\geq$ 4) from any basin to correlate local MAPP with local crocodyliform or lizard data.

DISCUSSION

Lizard Body Size Evolution During Climate Warming

Lizard body size appeared to track environmental temperature at local scales more than regional scales over deep time. Maximum lizard body size strongly correlated with environmental temperature within basins (Figs 3.3-3.6). The intrabasinal correlations presented here each spanned four successive NALMA intervals that document major climatic transitions: a warming period (the PETM in the Bighorn Basin, Fig 3.3) and a cooling period (the EOT in the Western Great Plains, Fig 3.5). Correlation between these variables across the entire Western Interior was weaker and likely artificial (Figs 3.1-Fig 3.2A, S3.1 Table). Mean lizard SVL showed a lower but more stable correlation with regional MAPT (S3.1 Table). The largest lizard body sizes came from only two families, Anguidae and Varanidae, throughout this geotemporal system regardless of the geographic scale sampled (see Chapter 1: Fossil Lizard Body Size Evolution). These results indicate that body size evolution in some lizard groups strongly tracks local environmental temperature and may coarsely track regional environmental temperature. It makes sense that lizards would respond more directly to the local environmental temperatures they experience compared to temperatures averaged across a larger region. Slavenko et al. recently observed a similar pattern globally in extant lizards (Slavenko et al. 2019).

At both local and regional scales, the relationship between maximum lizard body size and temperature was most pronounced across the Paleocene-Eocene boundary in this study. The largest lizard genera occurred in the early Eocene, just after the PETM (Fig 3.1, Table 3.1). It is possible that increased temperatures around the PETM led to gigantism in these lizards by elevating metabolism, as predicted by metabolic theory for terrestrial poikilotherms (Makarieva et al. 2005a, 2005b). Increased activity within a preferred body temperature range can increase energy uptake and growth in extant lizards (Davis 1967; Ballinger 1983; Sinervo and Adolph 1989; Grant and Dunham 1990; Piantoni et al. 2019). This effect is documented on decadal scales in extant tropical lizards. Piantoni et al. collected specimens of *Tropidurus torquatus* (Iguania: Tropiduridae) at sites in Brazil that warmed 1-2ºC over the last four decades (Piantoni et al. 2019). They also sampled specimens collected from the same sites in the 1960s and found

that the more recent specimens were larger and reached adult size two years earlier than the specimens collected from the same localities over 40 years ago.

The patterns observed in this study could also reflect indirect effects. Temperatures were warmer during both the summer and winter months around the PETM and into the early Eocene (Wing and Greenwood 1993; Greenwood and Wing 1995; Sewall and Sloan 2006; Snell 2011; Snell et al. 2013; Hyland et al. 2018). Rainfall was especially plentiful in the summer during this time (Snell et al. 2013). Paleogene productivity and biomass in the Western Interior were probably greatest in the early-middle Eocene around 51-50 Ma based on a peak in "tropical"-aspect floras (Wing 1987; Wing et al. 1991; Stucky 1992). Thus, lizards could have been actively feeding, growing, and mating during a longer portion of the year throughout this interval.

On the other hand, some lizards actively avoid increased environmental temperatures. Many extant lizards use behavioral thermoregulation to maintain a relatively constant body temperature despite fluctuating diurnal environmental temperatures (Huey 1974; Huey and Slatkin 1976; Muñoz et al. 2014; Muñoz and Bodensteiner 2019). This phenomenon is known as the “Bogert Effect”: organisms can use behavioral thermoregulation to mitigate climate change effects, avoiding or delaying physiological evolution (Bogert 1949; Huey et al. 2003; Muñoz et al. 2014; Muñoz and Losos 2018; Muñoz and Bodensteiner 2019). This might explain why some lizard clades evolved large body size across the PETM while others remained small-bodied. While higher temperatures may have lifted a physiological constraint for some lizard groups (Huey and Stevenson 1979; Bennett 1987; Huey and Kingsolver 1989, 1993), others could have used behavioral thermoregulation to remain within their preferred body temperature range (Huey 1974; Huey and Slatkin 1976; Muñoz et al. 2014).

Taxonomic richness among the fossil lizards sampled here also corresponded to elevated MAPT (Fig 3.1; see also Table 1.2). This finding concurs with recent research indicating that extant squamate species richness in North America correlates with higher warmest month maximum temperature and milder coldest month minimum temperature (Whiting and Fox 2021).

The Puercan-age Castle Rock locality of the Denver Basin indicated high temperatures comparable to those of the PETM (Table 3.1, S3.1 Dataset), but I did not find any large-bodied lizards from those deposits (S1.1 Dataset). It is possible that larger lizards were present in this basin during this interval, but they were not recovered in the small sample (n = 3 Puercan lizards, including two specimens from the Denver Basin; S1.1 Dataset). Alternatively, factors other than temperature may have prevented lizards from reaching large body size in this region during the early Paleocene. Large-bodied squamates disproportionately succumbed to the End-Cretaceous mass extinction event (66 Mya) and it took about 10 Myrs for squamate diversity to recover in North America (Longrich et al. 2012). Kemp and Hadly also documented a Quaternary extinction bias toward large-bodied lizards in Caribbean islands (Kemp and Hadly 2015).

Lizard Body Size Evolution During Climate Cooling

Cooling and aridification resulting from glaciation at the poles (Zachos et al. 2001, 2008) and uplift in the Western Interior during the late Eocene and early Oligocene (Dickinson et al. 1988) likely contributed to extinctions across the EOT (Eronen et al. 2015). The large-bodied lizard genera present in this region in the early Eocene were extinct by the late Eocene. Only one large-bodied genus, *Helodermoides* (Glyptosaurinae: Anguidae), was present in the Chadronian (Table 1.3, S1.1 Dataset).

Patterns of physiological evolution in extant lizards may elucidate this finding as well. Janzen's "climate variability hypothesis" predicts that tropical lizard species will have narrower thermal tolerances than temperate species because they do not experience as much thermal variation (Janzen 1967). Muñoz et al. documented this pattern in extant *Anolis* (Iguania: Dactyloidae) on the Caribbean island of Hispaniola (Muñoz et al. 2014; Muñoz and Bodensteiner 2019). They also found that anoles experiencing colder temperatures had greater cold tolerance, and that cold tolerance in these lizards evolved at a faster rate than other physiological traits such as heat tolerance or preferred temperature range (Muñoz et al. 2014; Muñoz and Bodensteiner 2019). Thus, perhaps *Helodermoides* had a wider thermal tolerance than earlier large-bodied Paleogene lizards in the Western Interior. Other research suggests that a flexible omnivorous diet can buffer lizards from environmental changes at higher latitudes (Bansal and Thaker 2021). Several studies have inferred an omnivorous diet for *Helodermoides* based on its dentition ((Sullivan 1979; Gauthier 1982); see Chapter 1 : Mechanisms of Body Size Evolution in Paleogene Lizards for further discussion). This may help explain the presence of *Helodermoides* in the late Eocene despite initial cooling and aridification.

Helodermoides persisted until MAPT dropped below 15ºC during the EOT (Fig 3.1, Table 3.1). I did not recover any large-bodied lizards from the Western Interior fossil record after the late Eocene (S1.1 Dataset). It is possible that during this transition, diurnal temperatures dropped below a critical thermal minimum needed for *Helodermoides* to maintain large body size. Reduced temperatures lead to reduced metabolism and growth in extant lizards (Castanet and Baez 1991; Andreone and Guarino 2003; Piantoni et al. 2019). Perhaps the smaller lizards that persisted across the EOT successfully used behavioral thermoregulation to stay warm during the day, had a wider thermal tolerance, or more quickly evolved sufficient cold tolerance to survive the cooler nighttime temperatures and increased seasonality.

Crocodyliform Body Size and Climate

The results of this study indicate that precipitation is key to the occurrence of large crocodyliforms (Figs 3.11-3.12). Southwestern Wyoming (Green River Basin, Washakie Basin), northeastern Utah (Uinta Basin), and part of northwestern Colorado (Piceance Creek Basin) were covered by a system of large lakes in the early Eocene (Grande 2013; Stein et al. 2021), and this area produced the greatest abundance of large-bodied fossil crocodyliforms in this dataset (Figs. 2.9-2.11, 2.22-2.23). A recent study similarly proposed precipitation as a deep time driver of past and recent crocodyliform distributions in Africa (Brochu et al. 2020).

Large body size confers an advantage in aquatic habitats by buffering against rapid heat loss (Smith 1979; Gearty and Payne 2020). Beyond inland lakes, shifts to marine habitats have also been linked to increased body size in crocodyliforms throughout their evolutionary history (Godoy et al. 2019; Gearty and Payne 2020). However, the putative correlation found in this study between maximum crocodyliform body size and marine temperature (Figs 3.7 and 3.8B, S3.1 Table) was likely artificial based on the lack of correlation with 90th percentile SVL or mean SVL, and among first differences (S3.1 Table). Interestingly, Godoy et al. found evidence to suggest a global inverse correlation between crown-group crocodylian body size and marine temperature through the Cenozoic (Godoy et al. 2019). But they interpreted this apparent relationship as an artifact of a shrinking geographic range with fewer available habitats over time, creating an extinction bias toward smaller-bodied crocodylians (see also (Slavenko et al. 2016; Solórzano et al. 2020)).

Although MAPT does not appear here to be a driving factor in crocodyliform body size evolution, other evidence indicates that frost is a limiting factor in crocodyliform distribution. Most extant crocodylians only occur in areas with a coldest month mean temperature of no less than 5.5ºC, corresponding to a mean annual temperature of ~14.2ºC (Markwick 1998b). Only the northernmost extant crocodylian, *Alligator mississippiensis,* can tolerate near-freezing conditions amid cold month minimum temperatures as low as 4.4ºC (Hutchison 1982). Correspondingly, paleobotanical evidence indicates that the Paleogene localities in the Western Interior producing the largest and most abundant crocodyliforms did not experience frost at the time of deposition. Southwestern Wyoming was a humid subtropical climate with no seasonal frost or pronounced dry season in the Clarkforkian before the end of the Paleocene (Wilf, Beard, et al. 1998). Fossil tree specimens from the Early-mid Eocene Bridger Formation (49 Ma) of the Blue Rim site in southwestern Wyoming indicate warm conditions and limited seasonality (Allen 2017a, 2017b). Fossils of extant palms that do not tolerate frost are found in Eocene deposits across the Bridger, Green River, and Wind River Formations of Wyoming, indicating that the climate in this region did not experience frost during the early and middle Eocene (Allen 2015), which may have been partly due to high humidity (Wilf, Wing, et al. 1998). Here I found that maximum crocodyliform SVL dropped in the late Eocene (Fig 3.7) before maximum SVL decreased in lizards in the early Oligocene (Fig 3.1); this could reflect an onset of freezing temperatures in this region in the late Eocene prior to an overall drop in MAPT (Table 3.1, S3.1 Dataset). Other studies have also documented declines in crocodyliform body size, diversity, and abundance during past periods of cooling and aridification (Markwick 1998c; Eronen et al. 2015; Mannion et al. 2015; Brochu et al. 2020).

Conservation Implications

Lizard evolution is not keeping pace with current shifts in climate and environment (Quintero and Wiens 2013; Whiting and Fox 2021). Some lizards might benefit from elevated environmental temperatures in the short term (Chamaillé-Jammes et al. 2006; Kubisch et al. 2012; Piantoni et al. 2019), but others face extirpation or extinction as a result (Sinervo et al. 2010; Huey et al. 2012). Many extant North American squamates may already be experiencing or approaching the limits of their thermal safety margins (Whiting and Fox 2021). Increased environmental temperatures can also lead to reduced time suitable for activity and change how much energy is needed for growth and reproduction. These effects can be mitigated by changes in behavior and physiology, which sometimes lead to suboptimal performance (Huey 1991; Adolph and Porter 1993; Miles 1994; Sinervo et al. 2010; Seebacher and Franklin 2012; Piantoni et al. 2019), or by shifting geographic or elevational range, which can introduce interspecific competition (Davis and Shaw 2001; Thuiller 2004; Hampe and Petit 2005; Keith et al. 2008; Lavergne et al. 2010; Lawler et al. 2013; Muñoz and Bodensteiner 2019).

Current biodiversity targets for these and other organisms must factor risks from prolonged and rapid climate change to be realistic (Polly et al. 2011; Arneth et al. 2020). The PETM may be a relevant analog event to current accelerated warming. Although the rapid rate of climate warming during the PETM was slower relative to the present (Jardine 2011; Whiting and Fox 2021), and we should use caution when inferring paleoclimatic parameters for fossil poikilothermic vertebrates based on extant tolerances (Scarpetta 2019), broad patterns observed over millions of years during prolonged climatic and environmental changes can give us a general sense of long-term trends. This study adds a larger temporal scope to existing literature

addressing climate change impacts on reptiles, including the neontological investigations mentioned within (e.g., (Bogert 1949; Janzen 1967; Huey 1974, 1991; Huey and Slatkin 1976; Huey and Stevenson 1979; John-Alder et al. 1983; Bennett 1987; Grant and Dunham 1988, 1990; Huey and Kingsolver 1993; Sinervo and Adolph 1989; Huey and Kingsolver 1989; Adolph and Porter 1993; Miles 1994; Chamaillé-Jammes et al. 2006; Sinervo et al. 2010; Huey et al. 2012; Kubisch et al. 2012; Seebacher and Franklin 2012; Muñoz et al. 2014; Muñoz and Bodensteiner 2019; Piantoni et al. 2019; Bansal and Thaker 2021; Whiting and Fox 2021)). The deep time data presented here can have conservation implications for how current climate change may affect body size, distribution, and related ecological factors in extant lizards and crocodylians. For example, have body size increases already occurred in mainland extant taxa of the lizard groups that exhibited gigantism in this study, Anguidae and Varanidae? If some lizards will get larger as a result of increased temperatures, will that change their dietary preferences? Will changes in temperature or precipitation lead to geographic range shifts for lizards or crocodylians? How will those shifts affect ecological interactions between these and other animals? These types of questions warrant further exploration through integration of neontological and paleontological data to inform conservation plans.

CONCLUSIONS

This study indicates that body size in some lizard groups can track land temperatures over time, particularly within local areas and during rapid temperature increase. Some large-bodied taxa may persist unless temperatures drop below a critical minimum threshold. This pattern is clearly not ubiquitous for all lizards because only two lizard families in this geotemporal system attained large body size during periods of elevated ambient temperature, while body size range for other contemporaneous lizard clades did not change. Crocodyliform maximum body size does not track temperature, but correlates strongly with precipitation. These findings agree with results from both paleontological and neontological studies of evolutionary patterns in these groups. This is the first study to document and compare climate relationships to body size in terrestrial lizards and semiaquatic crocodyliforms over geologic time scales and across a continental interior. Understanding short- and long-term effects on these reptiles during past episodes of accelerated warming can deepen and strengthen investigations of adaptation and resilience in extant reptiles under current rapidly shifting climate regimes.

FIGURES & CAPTIONS

CHAPTER 1 FIGURES

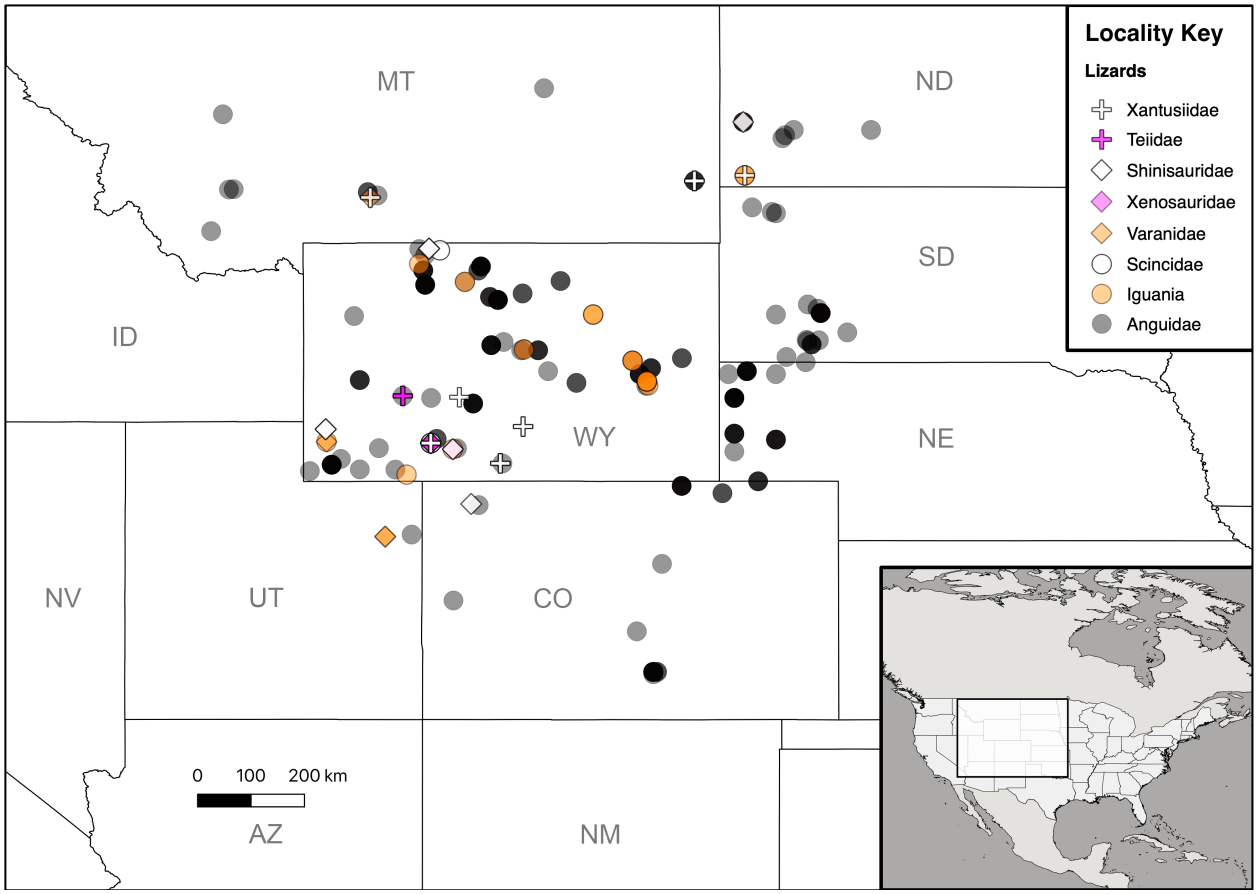

Figure 1.1. Map showing all localities for fossil lizard data across the Western Interior of North America through the Paleogene. Featured area is highlighted in inset map. Data points represent only specimens for which the locality could be georeferenced. Some taxonomic groups occurring with others in a particular locality may not be visible. Base map made with Natural Earth.

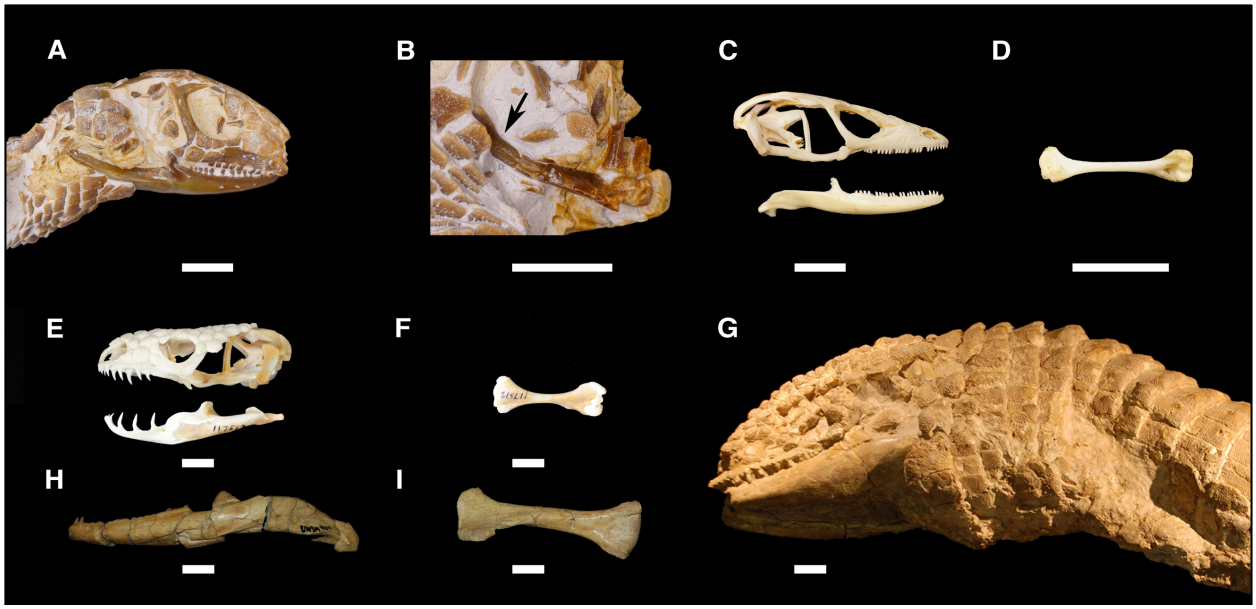

Figure 1.2. Paleogene anguid lizards and extant morphological analogues. (A) *Peltosaurus granulosus*† (Glyptosaurinae; Anguidae) skull in right lateral view, and B) right humerus in medial view (AMNH 42913), Orellan. (C) *Gerrhonotus infernalis* (Anguidae) skull and right mandible in right lateral view and (D) left humerus in medial view (FMNH 22452), extant. A-D are oriented with anterior to the right. (E) *Heloderma suspectum* (Helodermatidae) skull and left mandible in left lateral view, and (F) right humerus in medial view (UCMP 117512), extant. (G) *Helodermoides tuberculatus*† skull, mandibles, and cervical osteoderms in right lateral view, reflected for continuity (USNM V 13869), Chadronian. (H) *Helodermoides tuberculatus*† (Glyptosaurinae; Anguidae) left mandible in lateral view, and (I) right humerus in medial view, reflected for continuity (UNSM 4511), Chadronian. E-I are oriented with anterior to the left. Scale bar = 1 cm. USNM V 13869 (G) image courtesy of the Smithsonian Institution.

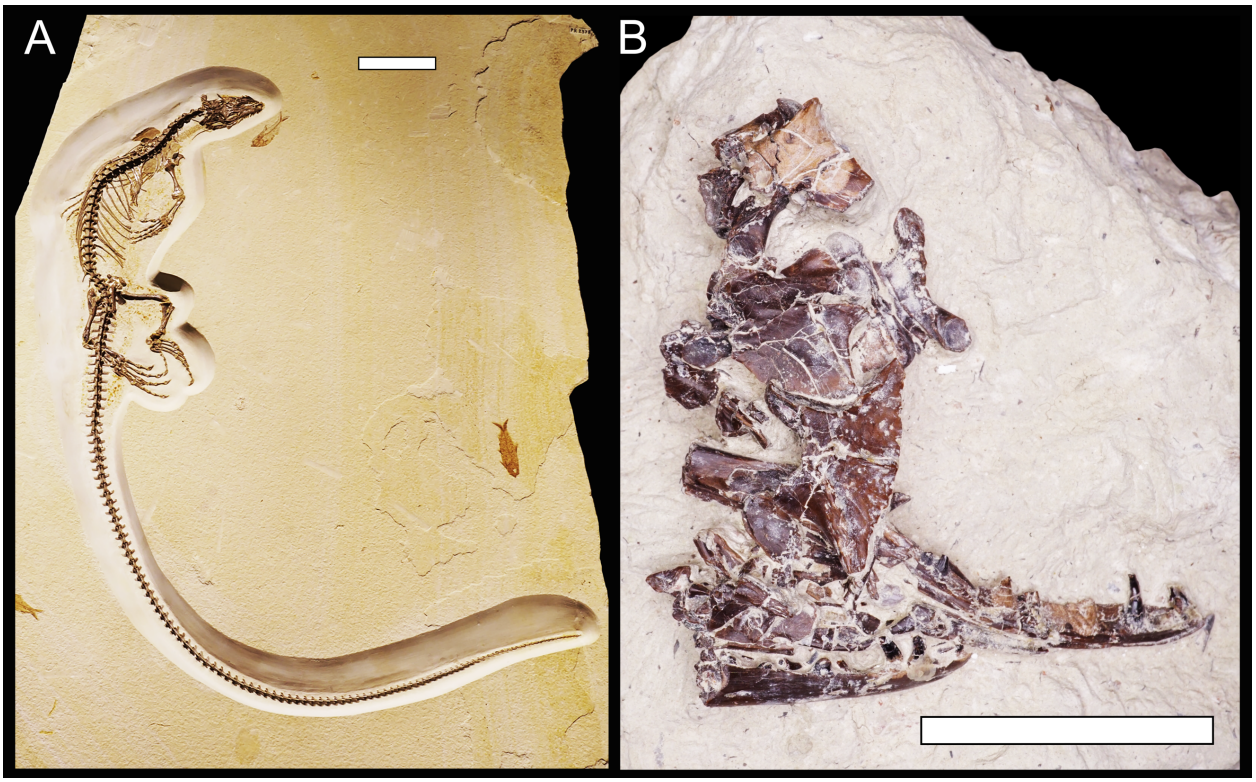

Figure 1.3. Paleogene varanids from the Western Interior of North America. (A) *Saniwa ensidens*† (Varanidae) skeleton (FMNH PR 2378), Wasatchian. Scale bar = 10 cm. (B) *Saniwa sp.*† dentaries, vertebrae, and fragments (DMNH EPV.34588), Bridgerian. Scale bar = 3 cm.

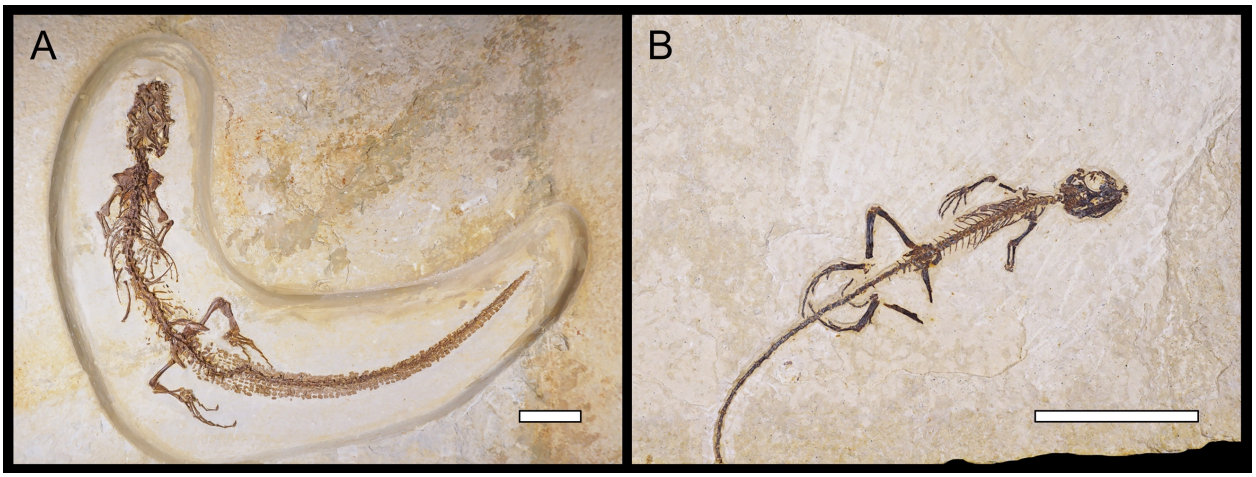

Figure 1.4. Other complete Paleogene lizard skeletons from the Western Interior of North America. (A) *Bahndwivici ammoskius*† (Shinisauridae) skeleton (FMNH PR 2260), Wasatchian. Scale bar = 3 cm. (B) *Afairiguana avius*† (Iguanidae) skeleton (FMNH PR 2379), Wasatchian. Scale bar = 3 cm.

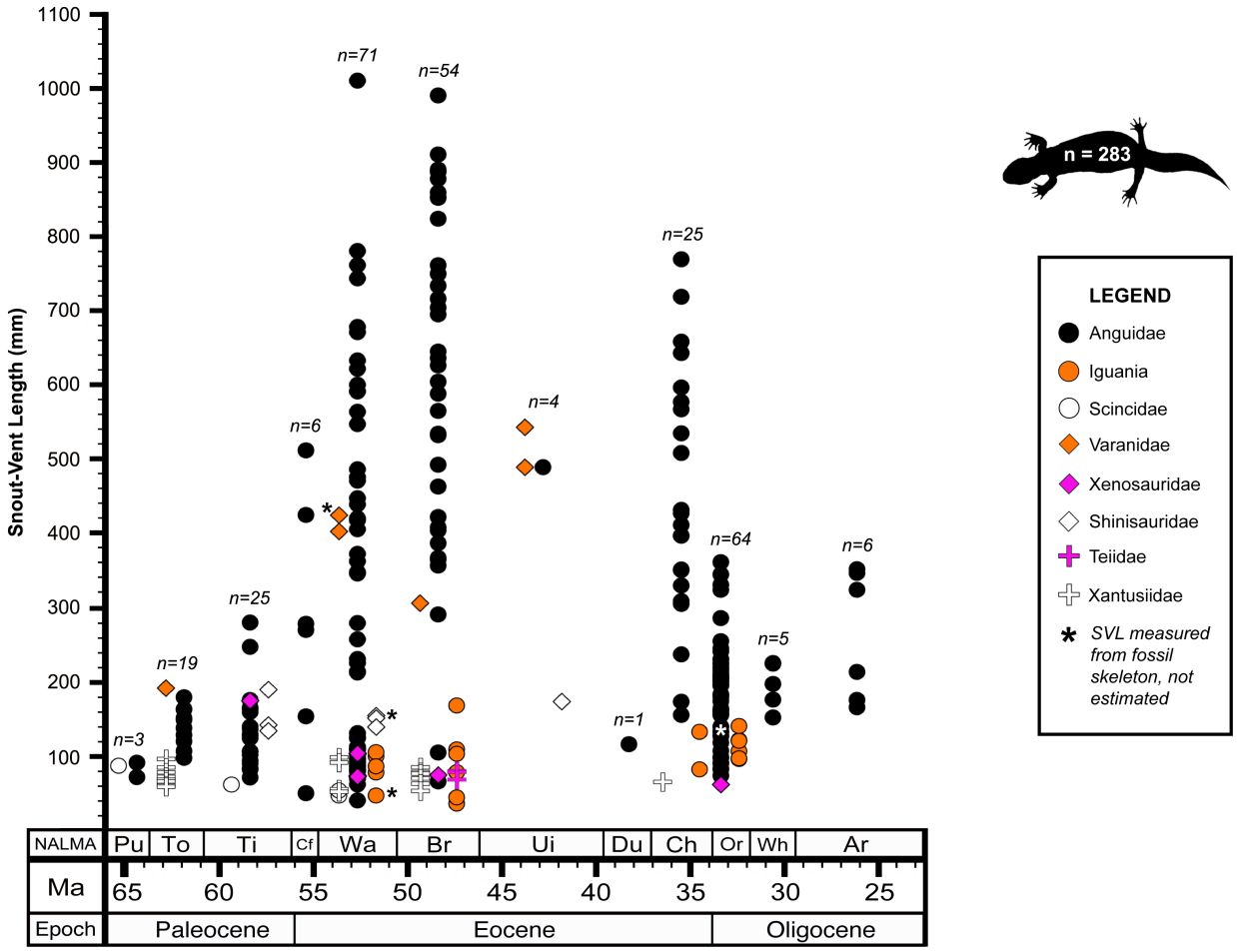

Figure 1.5. Snout-vent length distribution by taxonomic group for fossil lizards in the Western Interior of North America through the Paleogene. Sample sizes are per North American Land Mammal Age (NALMA). Data points are arbitrarily spread within each NALMA for visibility. NALMA abbreviations: Pu = Puercan, To = Torrejonian, Ti = Tiffanian, Cf = Clarkforkian, Wa = Wasatchian, Br = Bridgerian, Ui = Uintan, Du = Duchesnean, Ch = Chadronian, Or = Orellan, Wh = Whitneyan, Ar = Arikareean. Data points marked with an asterisk (*) were measured from complete fossil skeletons. All others were estimated from individual cranial or limb elements using regressions and sometimes ratios (see S1.1-1.10 Tables).

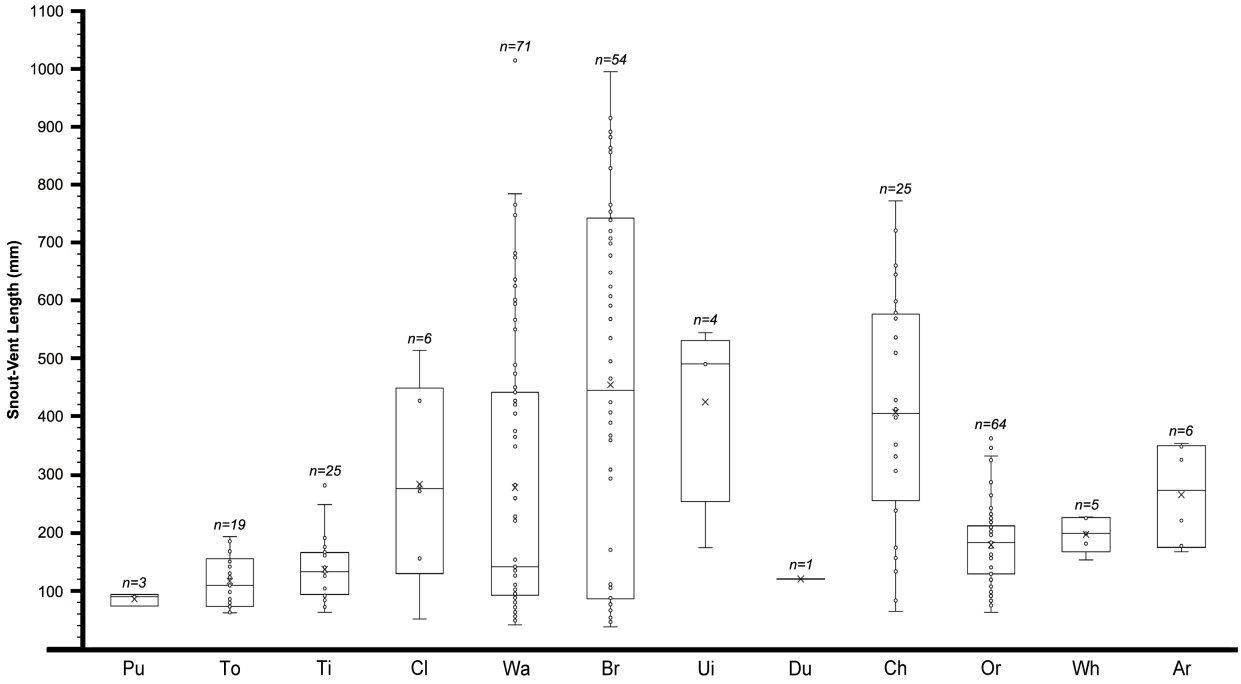

Figure 1.6. Box plots of snout-vent length distribution for fossil lizards in the Western Interior of North America through the Paleogene. Box plots represent samples for each North American Land Mammal Age (NALMA). NALMA abbreviations: Pu = Puercan, To = Torrejonian, Ti = Tiffanian, Cf = Clarkforkian, Wa = Wasatchian, Br = Bridgerian, Ui = Uintan, Du = Duchesnean, Ch = Chadronian, Or = Orellan, Wh = Whitneyan, Ar = Arikareean.

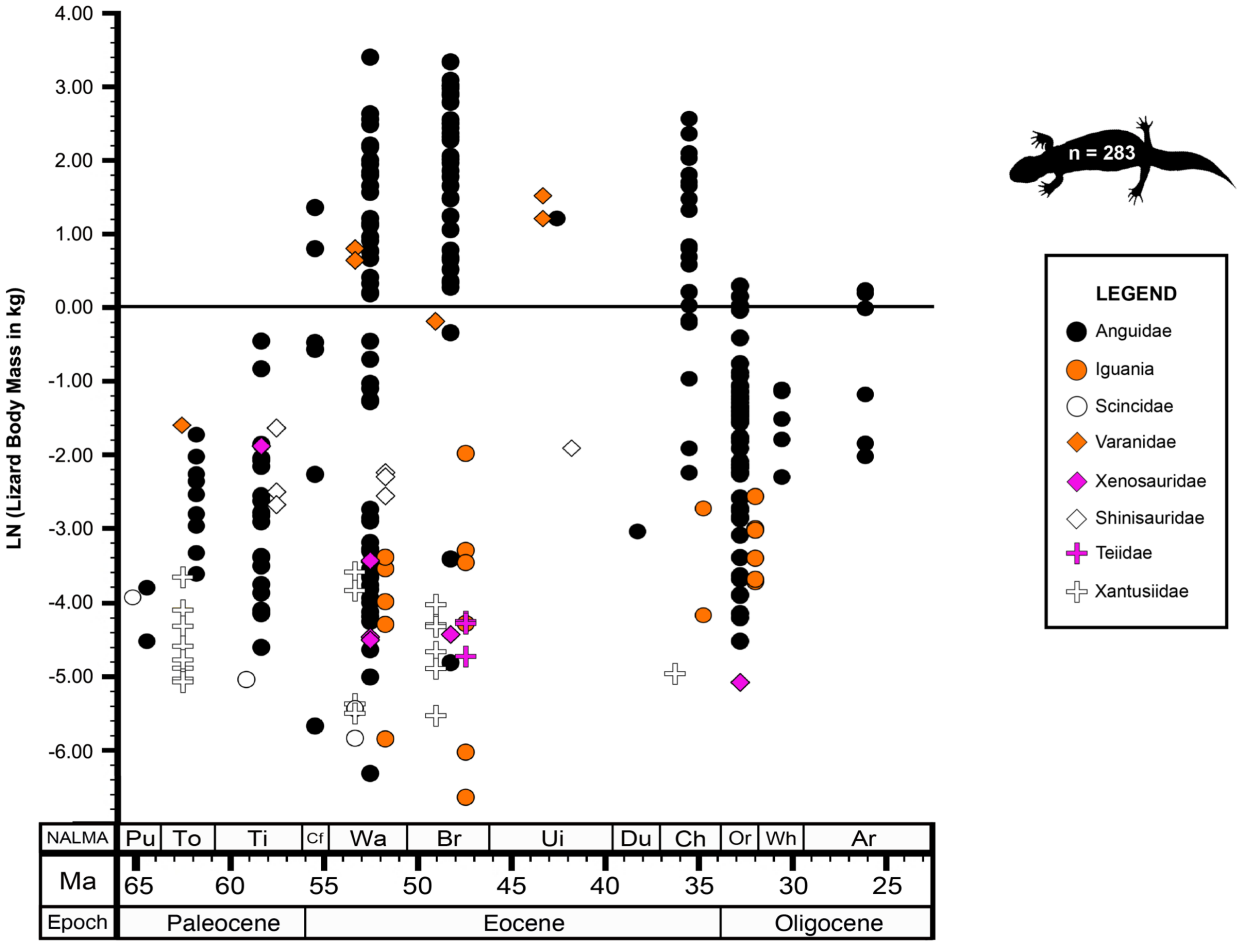

Figure 1.7. Body mass distribution by taxonomic group for fossil lizards in the Western Interior of North America through the Paleogene. Body mass is in kg and natural log transformed. Data points are arbitrarily spread within each North American Land Mammal Age (NALMA) for visibility. NALMA abbreviations: Pu = Puercan, To = Torrejonian, Ti = Tiffanian, Cf = Clarkforkian, Wa = Wasatchian, Br = Bridgerian, Ui = Uintan, Du = Duchesnean, Ch = Chadronian, Or = Orellan, Wh = Whitneyan, Ar = Arikareean.

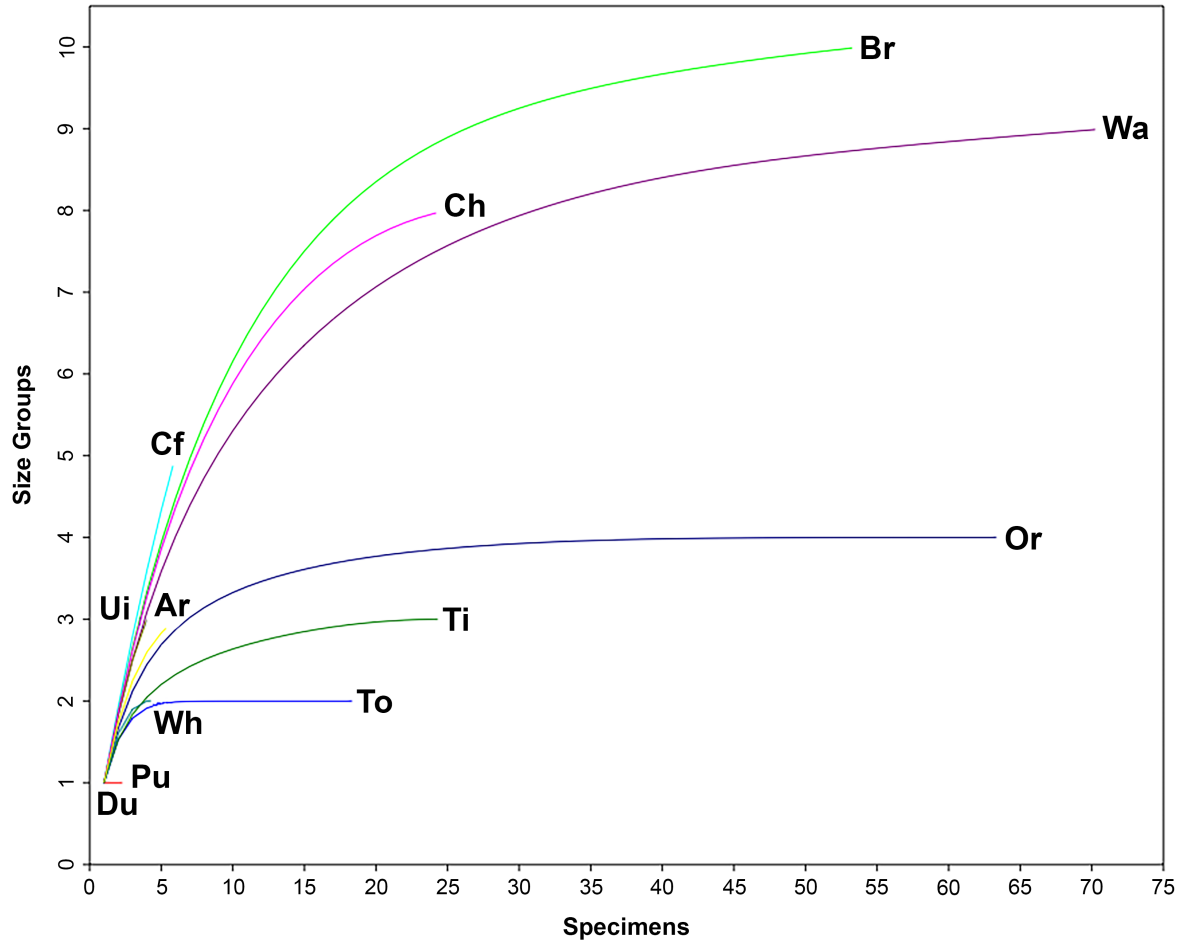

Figure 1.8. Rarefaction curve showing the number of expected size groups for NALMA sample sizes within the fossil lizard dataset. To conduct this analysis, I assigned each fossil specimen in S1.1 Dataset to one of 11 size groups, each group representing a bin of 100 mm (e.g., 100-199 mm, 200-299 mm, etc.; the last group was ≥ 1 m). S1.1 Dataset is subsampled here by North American Land Mammal Age (NALMA) interval. The y-axis in this graph shows the total number of size groups recovered in the sample for each NALMA interval. NALMA abbreviations: Pu = Puercan, To = Torrejonian, Ti = Tiffanian, Cf = Clarkforkian, Wa = Wasatchian, Br = Bridgerian, Ui = Uintan, Du = Duchesnean, Ch = Chadronian, Or = Orellan, Wh = Whitneyan, Ar = Arikareean. Individual rarefaction analysis was performed using PAST v4.03 (Hammer et al. 2001).

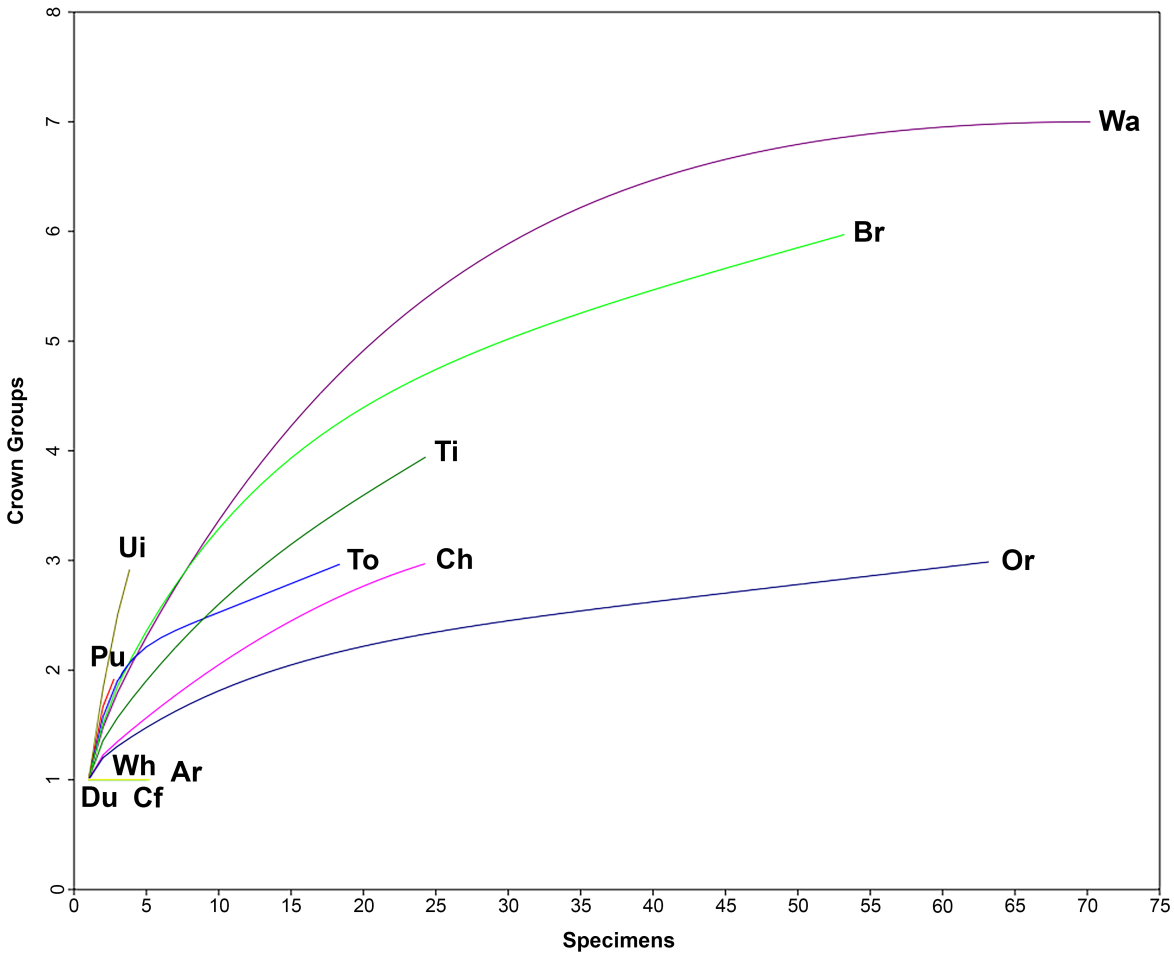

Figure 1.9. Rarefaction curve showing the number of expected crown taxonomic groups for NALMA sample sizes within the fossil lizard dataset. S1.1 Dataset is subsampled here by North American Land Mammal Age (NALMA) interval. NALMA abbreviations: Pu = Puercan, To = Torrejonian, Ti = Tiffanian, Cf = Clarkforkian, Wa = Wasatchian, Br = Bridgerian, Ui = Uintan, Du = Duchesnean, Ch = Chadronian, Or = Orellan, Wh = Whitneyan, Ar = Arikareean. Individual rarefaction analysis was performed using PAST v4.03 (Hammer et al. 2001).

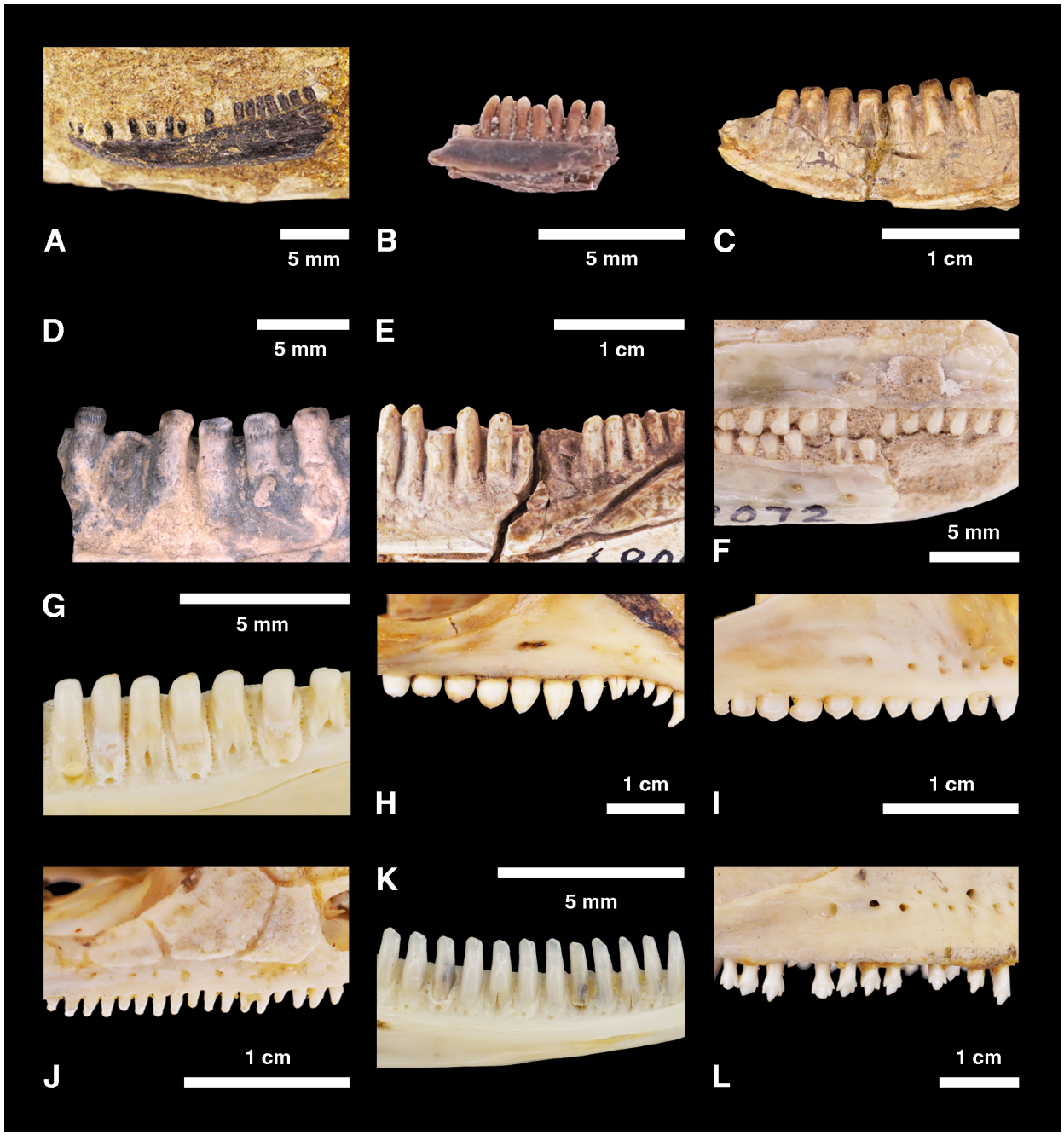

Figure 1.10. Dentition of Paleogene glyptosaurine (Anguidae) lizards and extant morphological analogues. A) *Proxestops silberlingi*† (AMNH 2672), Puercan – Wasatchian. B) *Xestops vagrans*† (USNM 42775), Clarkforkian – Bridgerian. C) *Melanosaurus maximus*† (AMNH 5175), Tiffanian – Bridgerian. D) *cf. Glyptosaurus sylvestris*† (UW 39291), Clarkforkian – Uintan. E) *Helodermoides tuberculatus*† (AMNH 6800), Chadronian. F) *Peltosaurus granulosus*† (FMNH P-27072), Chadronian – Arikareean. G) *Diploglossus millepunctatus* (Anguidae; FMNH 19248). H) *Tupinambis teguixin* (Teiidae; FMNH 98759). I) *Tiliqua scincoides* (Scincidae; FMNH 51702). J) *Smaug giganteus* (Cordylidae; FMNH 31283). K) *Xenosaurus grandis* (Xenosauridae; MVZ 128947). L) *Conolophus subcristatus* (Iguanidae; FMNH 22406), shown here for comparison to a primarily herbivorous lizard.

CHAPTER 2 FIGURES

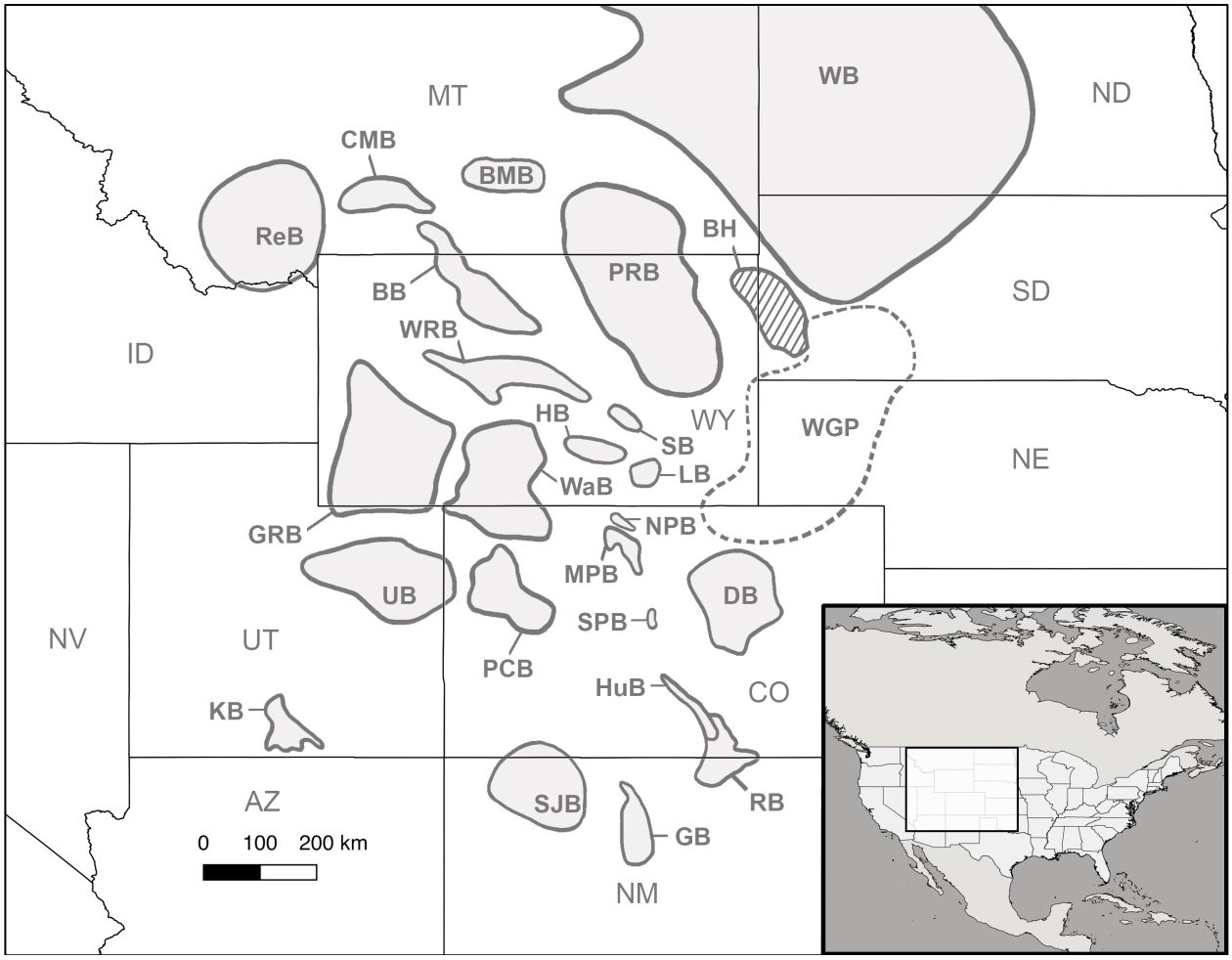

Figure 2.1. Map showing intermontane basins present in the Western Interior of North America. Featured area is highlighted in inset map. Basin acronyms: BB = Bighorn Basin, BH = Black Hills, BMB = Bull Mountains Basin, CMB = Crazy Mountains Basin, DB = Denver Basin, GB = Galisteo Basin, GRB = Green River Basin, HB = Hanna Basin, HuB = Huerfano Basin, KB = Kaiparowits Basin, LB = Laramie Basin, MPB = Middle Park Basin, NPB = North Park Basin, PCB = Piceance Creek Basin, PRB = Powder River Basin, RB = Raton Basin, ReB = Renova Basin, SB = Shirley Basin, SJB = San Juan Basin, SPB = South Park Basin, UB = Uinta Basin, WaB = Washakie Basin, WB = Williston Basin, WGP = Western Great Plains, WRB = Wind River Basin. Base map made with Natural Earth.

Figure 2.2. Paleogene crocodyliforms from the Western Interior of North America. (A) *Tsoabichi greenriverensis*† (Alligatoridae) skeleton (FMNH PR 3050), Wasatchian; (B) *Borealosuchus wilsoni*† (Eusuchia) skeleton (FMNH PR 1674), Wasatchian. Scale bars = 10 cm. Both specimens come from Fossil Lake localities in the Green River Basin, Wyoming. Photo in (B) courtesy of: R. Testa. (c) Field Museum of Natural History. https://mm.fieldmuseum.org/27d04761-dcd6-4801-96d0-7e85b80a*a2b (accessed on 27 Oct 2021)

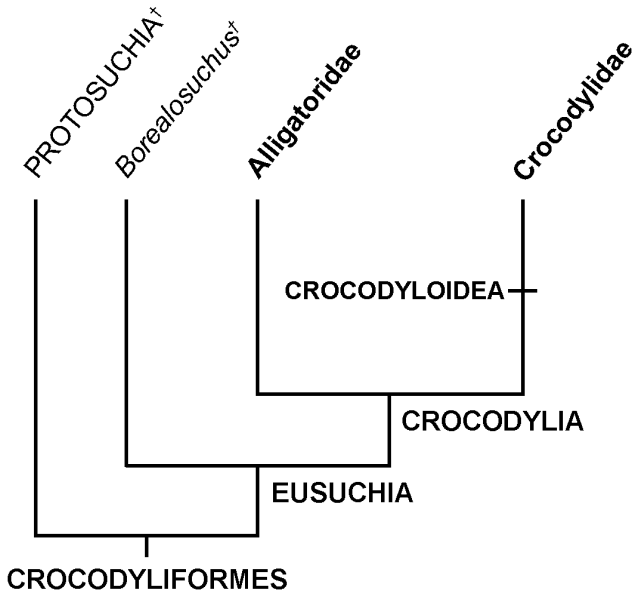

Figure 2.3. Cladogram showing phylogenetic relationships between hierarchical taxonomic groups within Crocodyliformes. Protosuchia† is shown as an outgroup to Eusuchia within Crocodyliformes. The five taxonomic groups within Crocodyliformes used in this study are shown in bold font. Cladogram is based on several sources (Brochu 2003, 2013; Bronzati et al. 2012, 2015; Cossette and Brochu 2020).

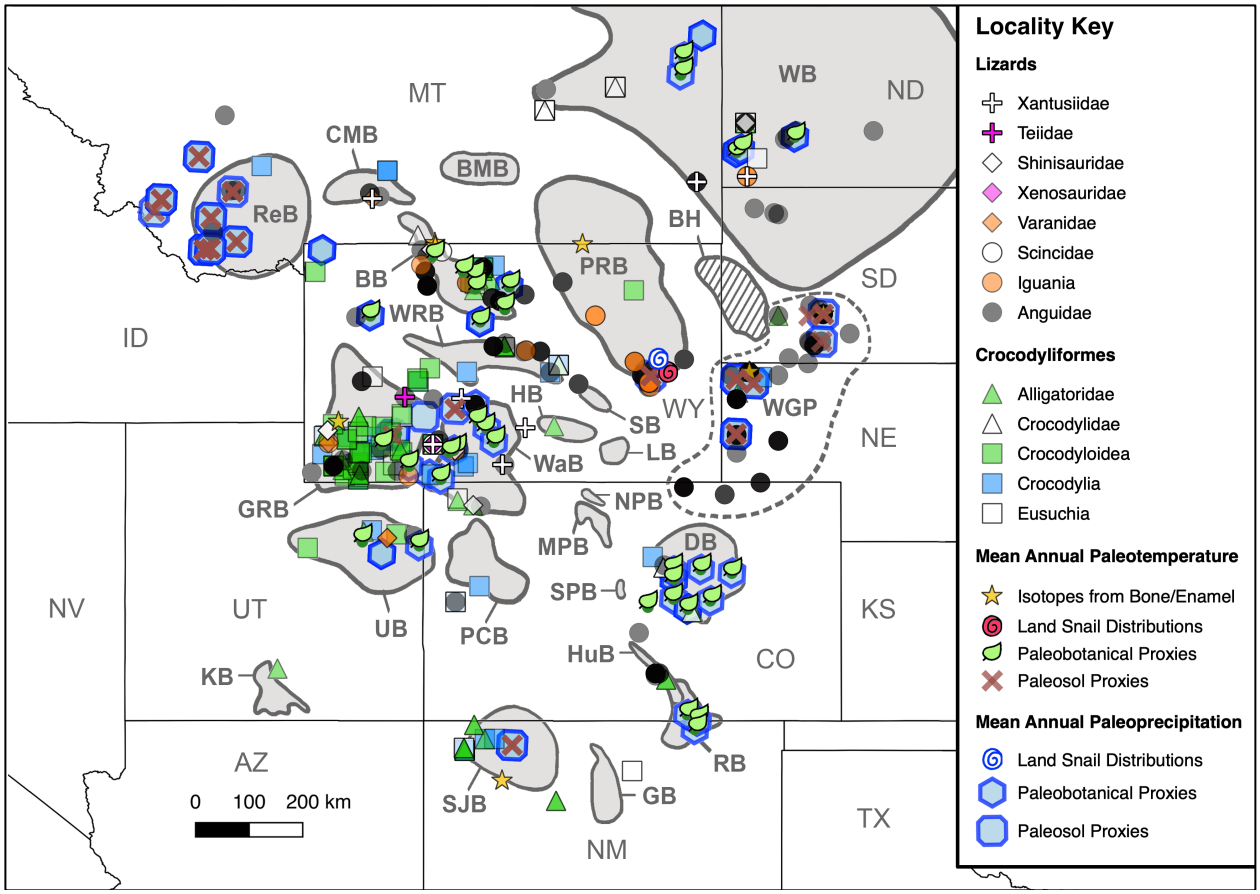

Figure 2.4. Map showing all localities for fossil and paleoclimate data across the Western Interior of North America through the Paleogene. Featured area is highlighted in inset map in Fig 2.1. Basin acronyms are listed in the caption for Fig 2.1. Data points represent only specimens for which the locality could be georeferenced. Some taxonomic groups occurring with others in a particular locality may not be visible. Mean Annual Paleotemperature and Paleoprecipitation Proxy localities are discussed in Chapter 3. Base map made with Natural Earth.

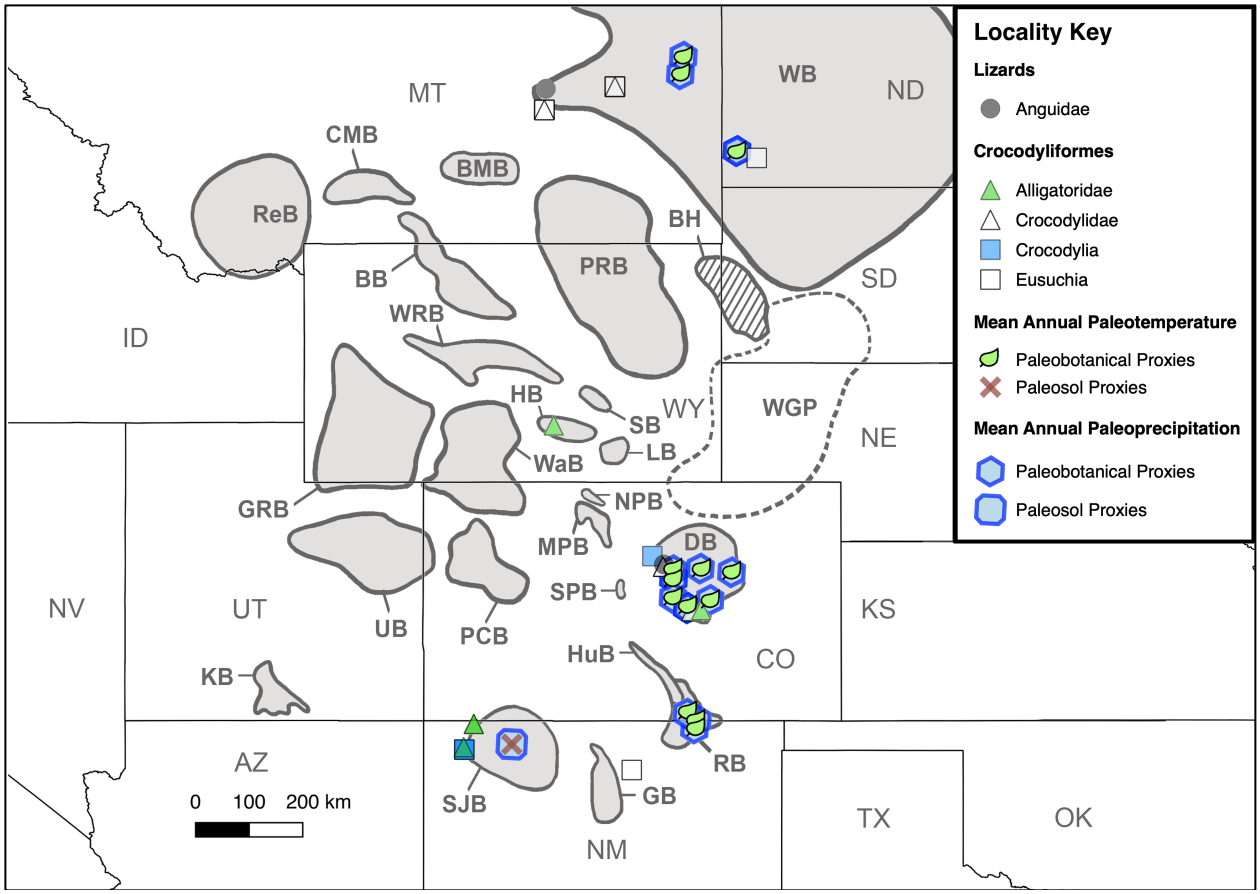

Figure 2.5. Map showing Puercan (early Paleocene) localities for fossil and paleoclimate data across the Western Interior of North America through the Paleogene. Featured area is highlighted in inset map in Fig 2.1. Basin acronyms are listed in the caption for Fig 2.1. Data points represent only specimens for which the locality could be georeferenced. Some taxonomic groups occurring with others in a particular locality may not be visible. Mean Annual Paleotemperature and Paleoprecipitation Proxy localities are discussed in Chapter 3. Base map made with Natural Earth.

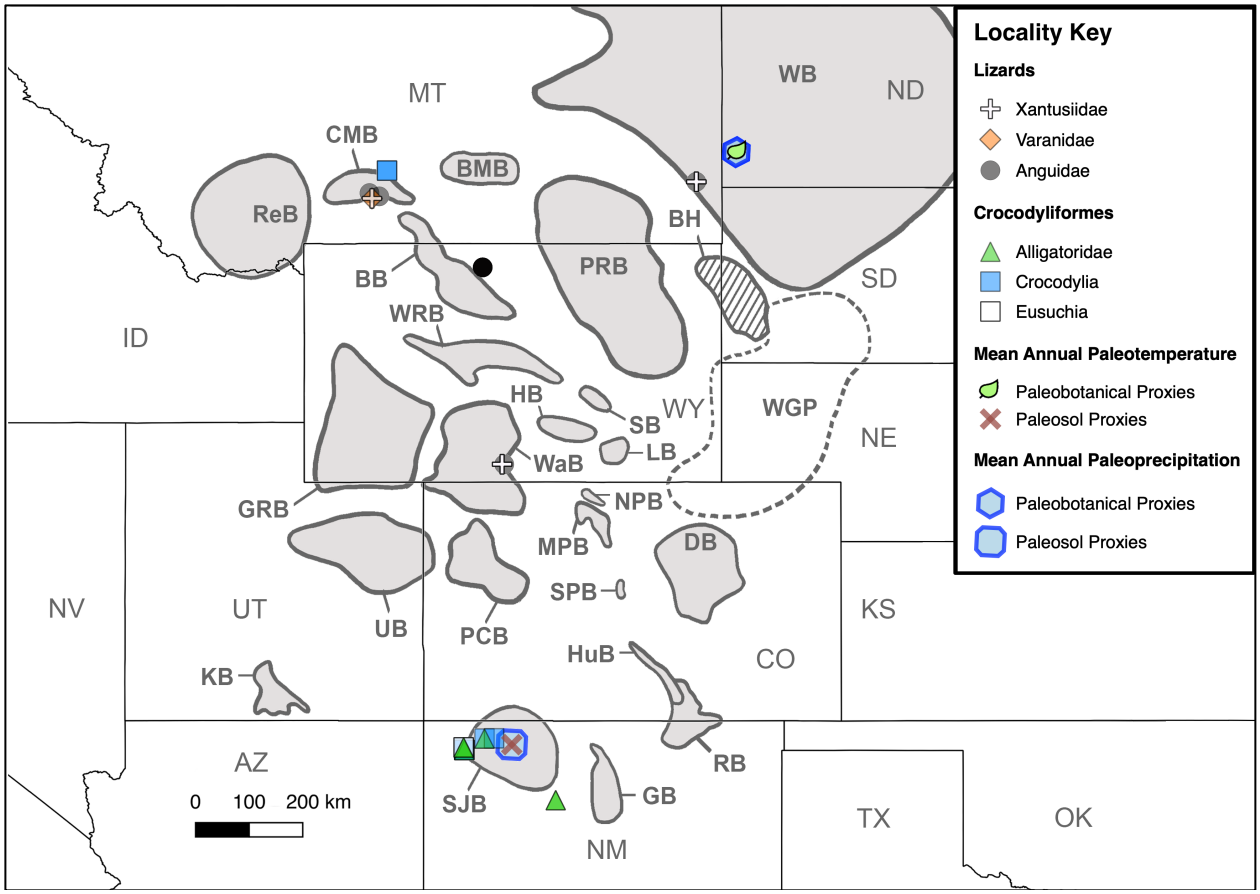

Figure 2.6. Map showing Torrejonian (early Paleocene) localities for fossil and paleoclimate data across the Western Interior of North America through the Paleogene. Featured area is highlighted in inset map in Fig 2.1. Basin acronyms are listed in the caption for Fig 2.1. Data points represent only specimens for which the locality could be georeferenced. Some taxonomic groups occurring with others in a particular locality may not be visible. Mean Annual Paleotemperature and Paleoprecipitation Proxy localities are discussed in Chapter 3. Base map made with Natural Earth.

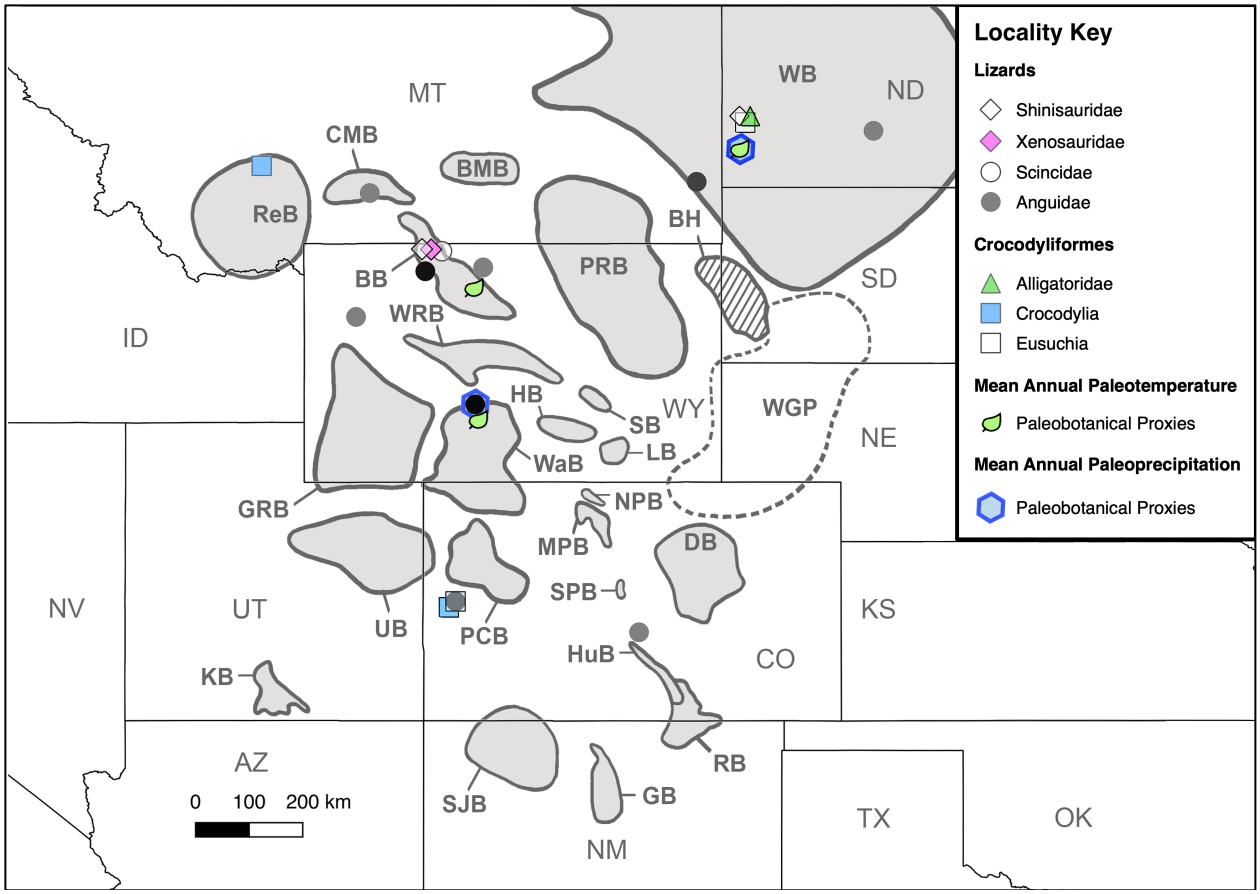

Figure 2.7. Map showing Tiffanian (middle Paleocene) localities for fossil and paleoclimate data across the Western Interior of North America through the Paleogene. Featured area is highlighted in inset map in Fig 2.1. Basin acronyms are listed in the caption for Fig 2.1. Data points represent only specimens for which the locality could be georeferenced. Some taxonomic groups occurring with others in a particular locality may not be visible. Mean Annual Paleotemperature and Paleoprecipitation Proxy localities are discussed in Chapter 3. Base map made with Natural Earth.

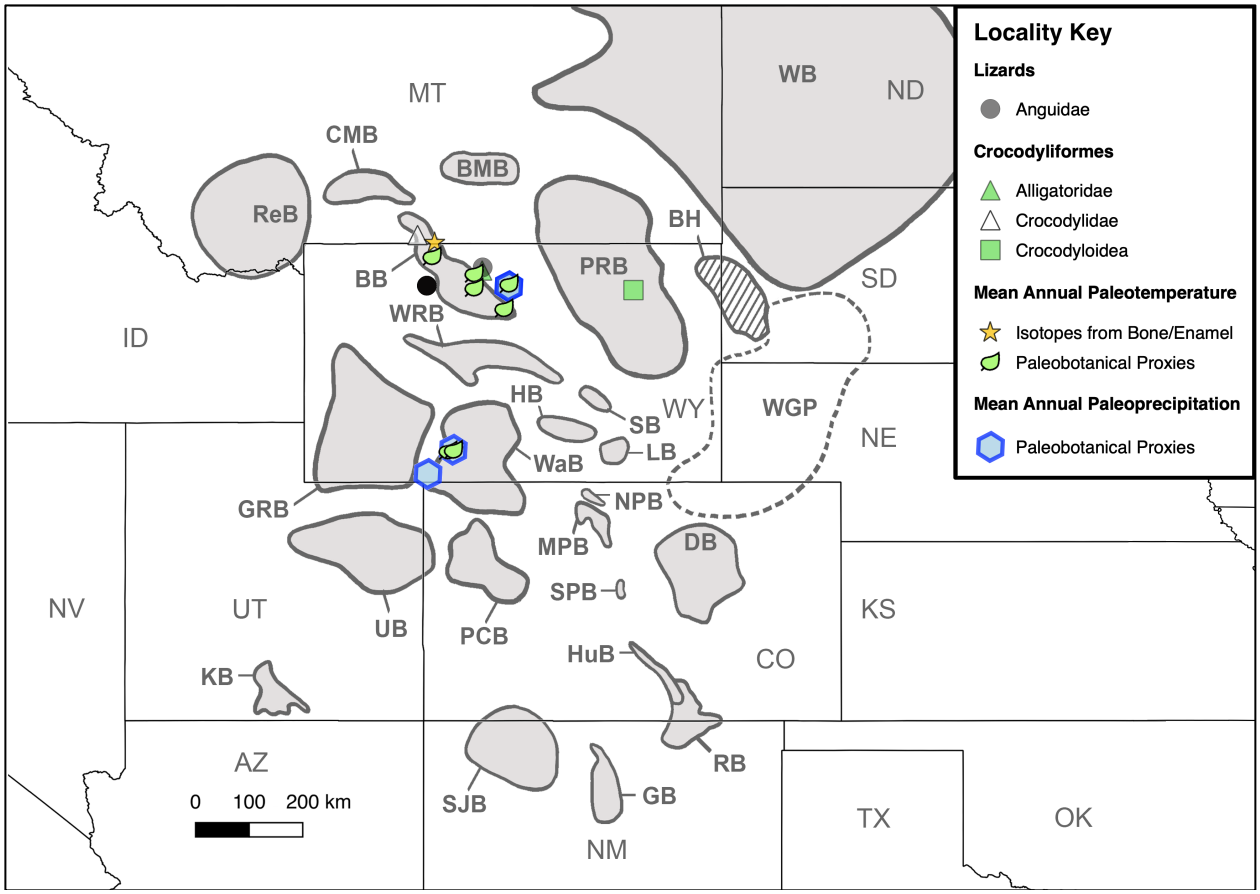

Figure 2.8. Map showing Clarkforkian (late Paleocene – early Eocene) localities for fossil and paleoclimate data across the Western Interior of North America through the Paleogene. Featured area is highlighted in inset map in Fig 2.1. Basin acronyms are listed in the caption for Fig 2.1. Data points represent only specimens for which the locality could be georeferenced. Some taxonomic groups occurring with others in a particular locality may not be visible. Mean Annual Paleotemperature and Paleoprecipitation Proxy localities are discussed in Chapter 3. Base map made with Natural Earth.

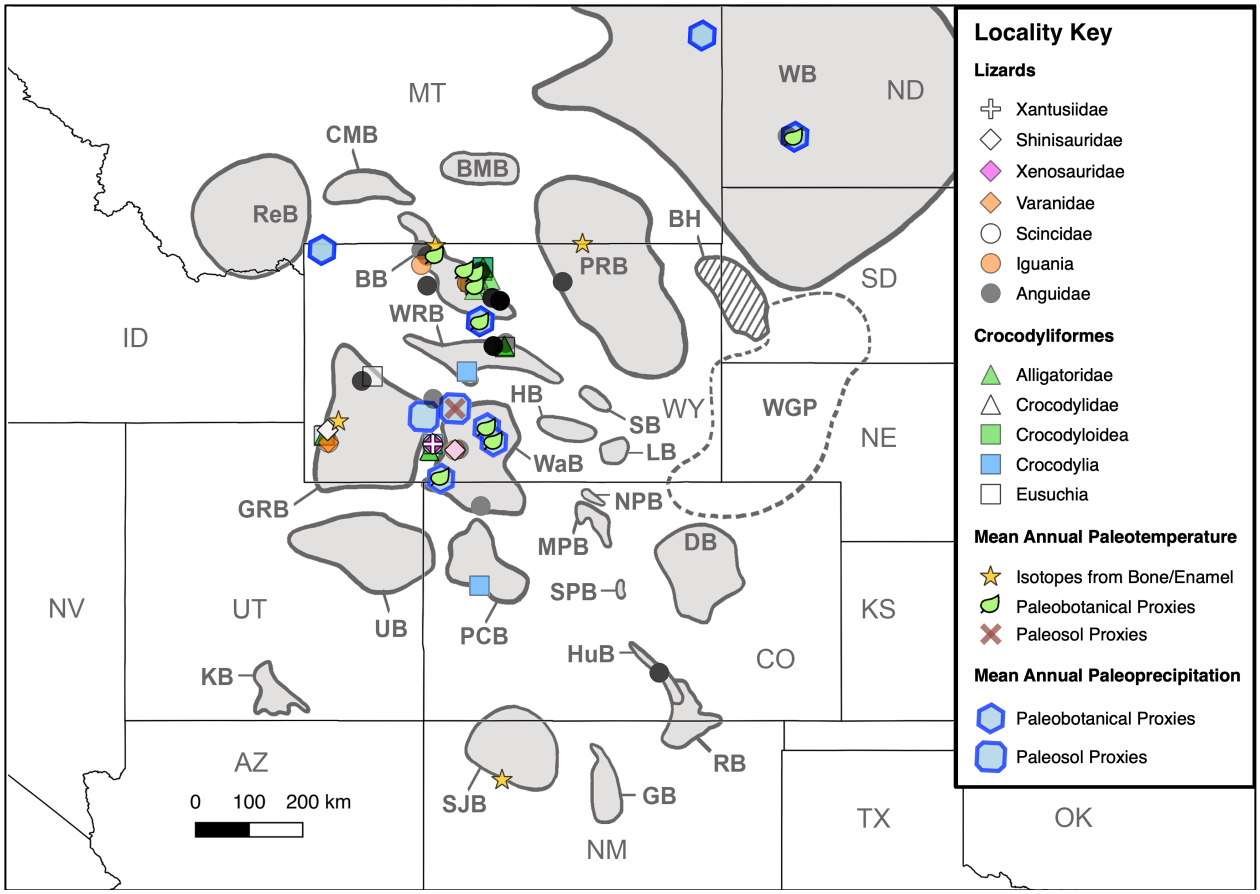

Figure 2.9. Map showing Wasatchian (early Eocene) localities for fossil and paleoclimate data across the Western Interior of North America through the Paleogene. Featured area is highlighted in inset map in Fig 2.1. Basin acronyms are listed in the caption for Fig 2.1. Data points represent only specimens for which the locality could be georeferenced. Some taxonomic groups occurring with others in a particular locality may not be visible. Mean Annual Paleotemperature and Paleoprecipitation Proxy localities are discussed in Chapter 3. Base map made with Natural Earth.

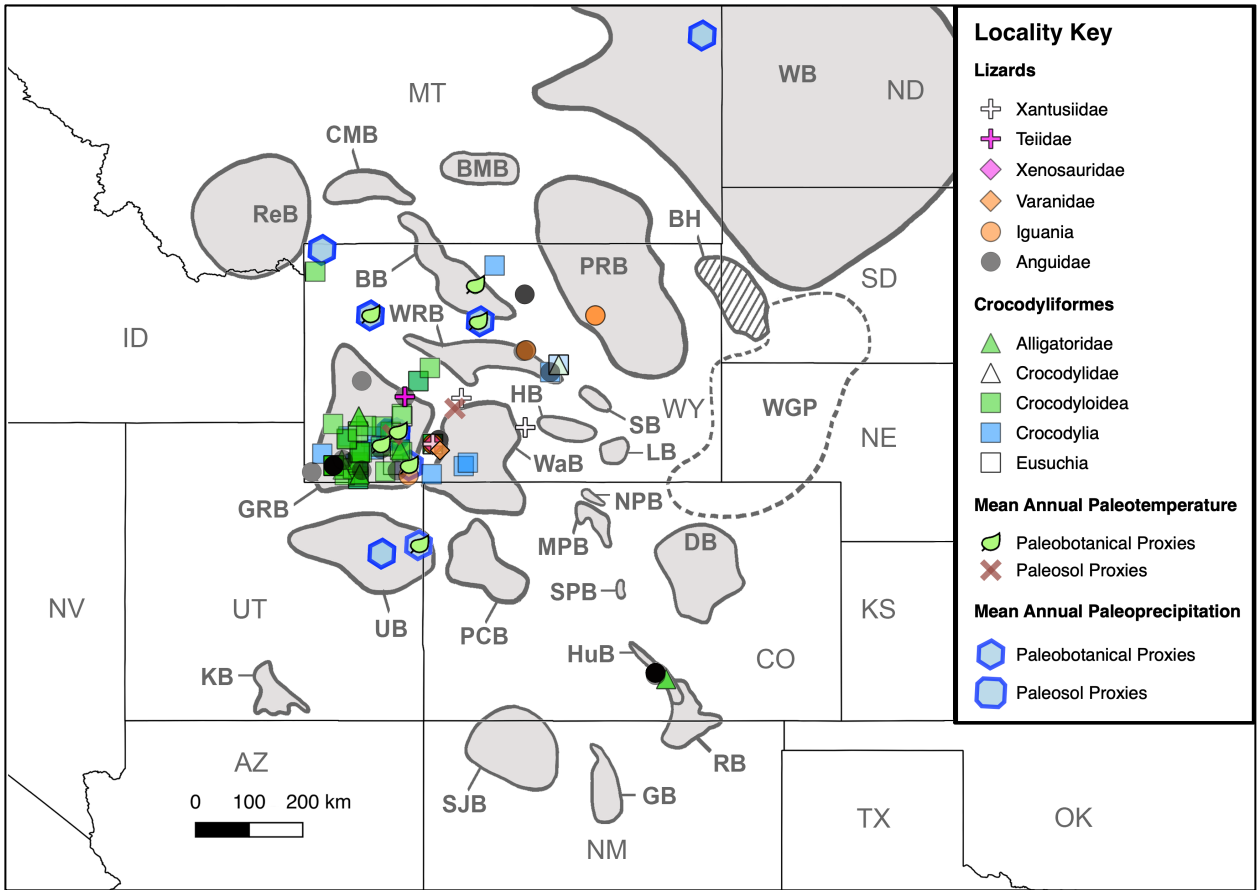

Figure 2.10. Map showing Bridgerian (early Eocene) localities for fossil and paleoclimate data across the Western Interior of North America through the Paleogene. Featured area is highlighted in inset map in Fig 2.1. Basin acronyms are listed in the caption for Fig 2.1. Data points represent only specimens for which the locality could be georeferenced. Some taxonomic groups occurring with others in a particular locality may not be visible. Mean Annual Paleotemperature and Paleoprecipitation Proxy localities are discussed in Chapter 3. Base map made with Natural Earth.

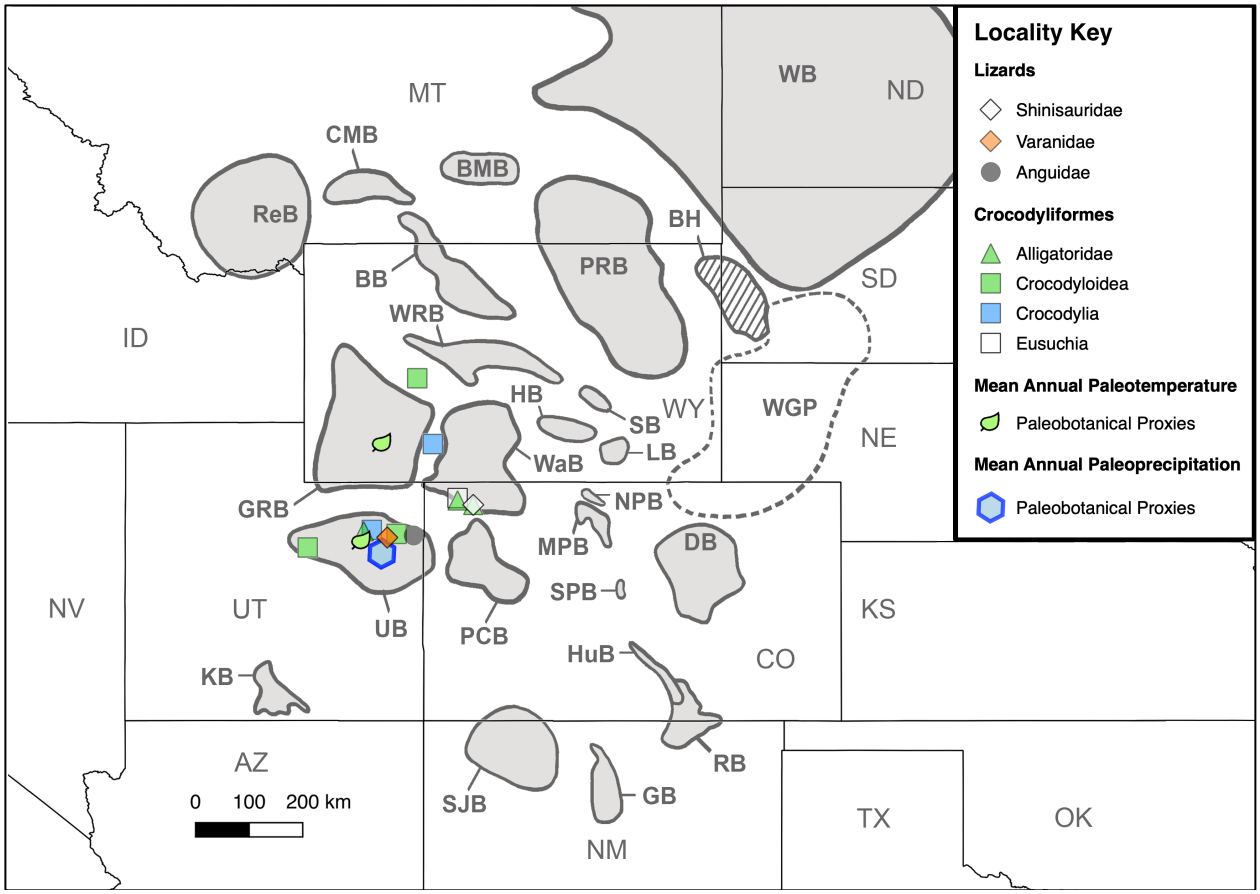

Figure 2.11. Map showing Uintan (middle Eocene) localities for fossil and paleoclimate data across the Western Interior of North America through the Paleogene. Featured area is highlighted in inset map in Fig 2.1. Basin acronyms are listed in the caption for Fig 2.1. Data points represent only specimens for which the locality could be georeferenced. Some taxonomic groups occurring with others in a particular locality may not be visible. Mean Annual Paleotemperature and Paleoprecipitation Proxy localities are discussed in Chapter 3. Base map made with Natural Earth.

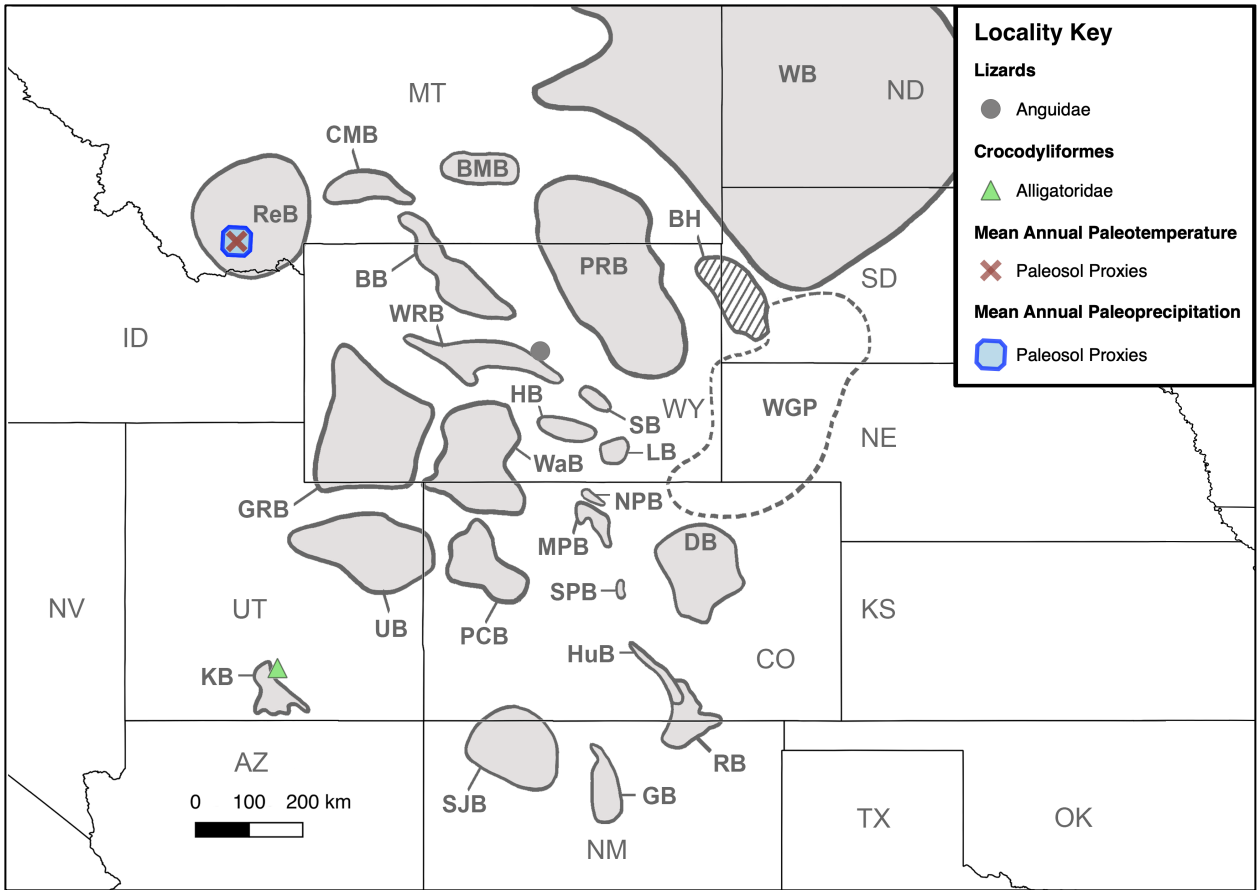

Figure 2.12. Map showing Duchesnean (middle Eocene) localities for fossil and paleoclimate data across the Western Interior of North America through the Paleogene. Featured area is highlighted in inset map in Fig 2.1. Basin acronyms are listed in the caption for Fig 2.1. Data points represent only specimens for which the locality could be georeferenced. Some taxonomic groups occurring with others in a particular locality may not be visible. Mean Annual Paleotemperature and Paleoprecipitation Proxy localities are discussed in Chapter 3. Base map made with Natural Earth.

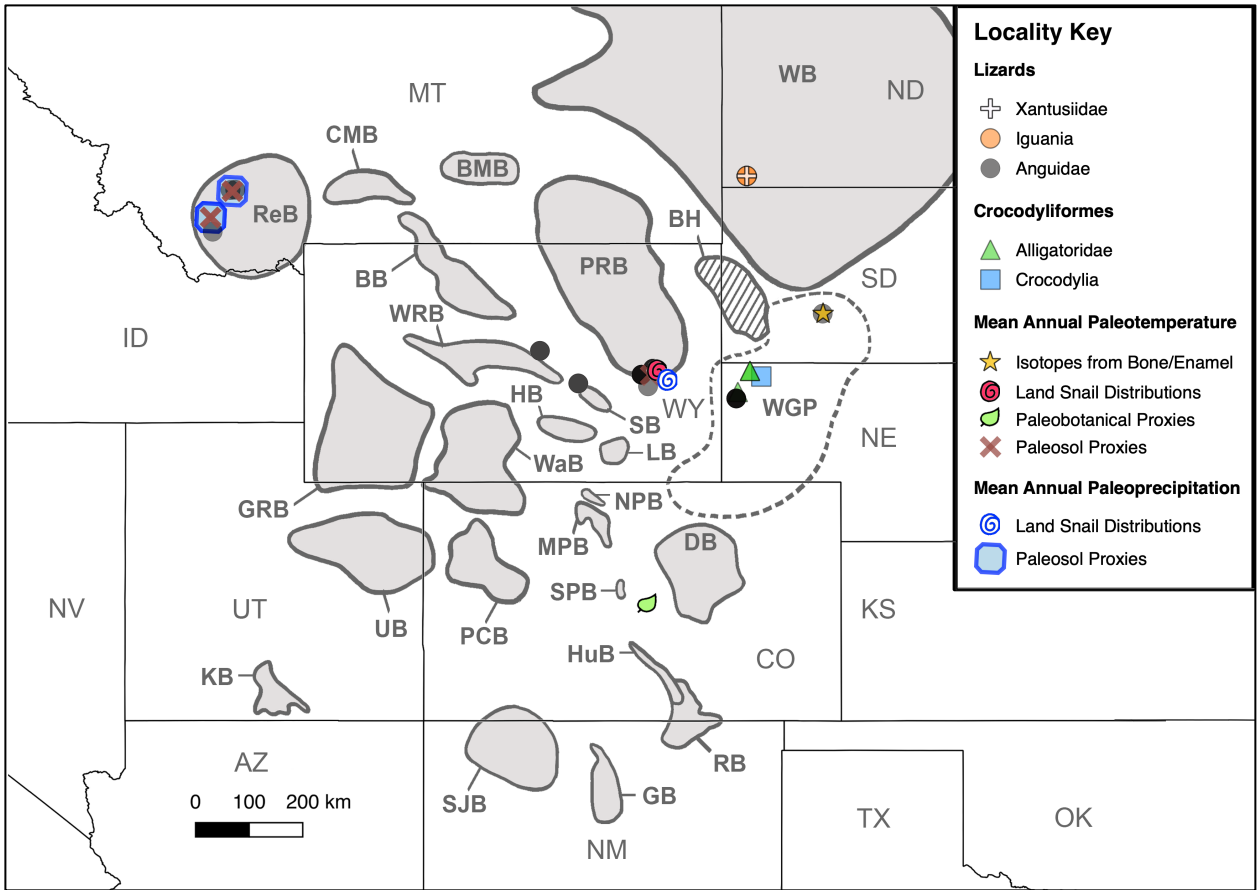

Figure 2.13. Map showing Chadronian (late Eocene) localities for fossil and paleoclimate data across the Western Interior of North America through the Paleogene. Featured area is highlighted in inset map in Fig 2.1. Basin acronyms are listed in the caption for Fig 2.1. Data points represent only specimens for which the locality could be georeferenced. Some taxonomic groups occurring with others in a particular locality may not be visible. Mean Annual Paleotemperature and Paleoprecipitation Proxy localities are discussed in Chapter 3. Base map made with Natural Earth.

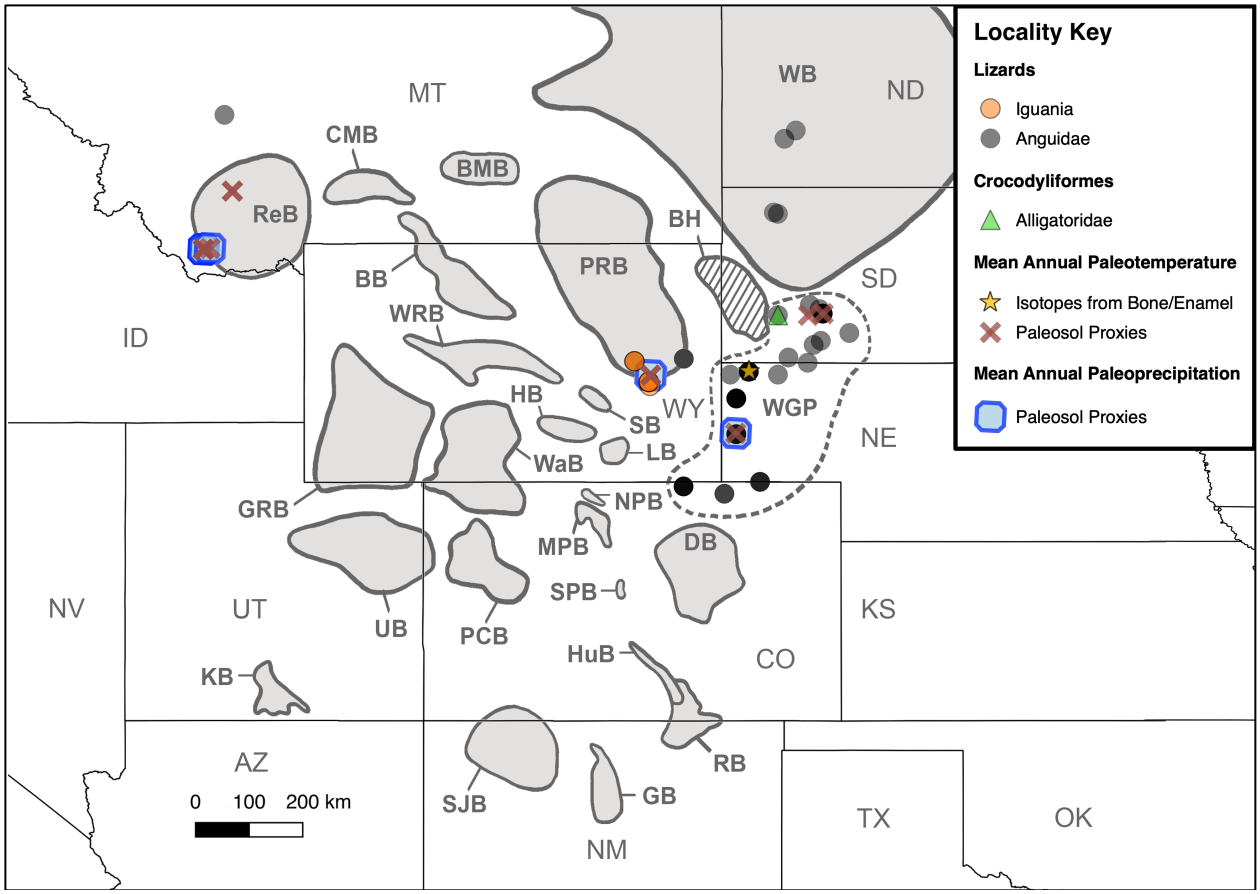

Figure 2.14. Map showing Orellan (early Oligocene) localities for fossil and paleoclimate data across the Western Interior of North America through the Paleogene. Featured area is highlighted in inset map in Fig 2.1. Basin acronyms are listed in the caption for Fig 2.1. Data points represent only specimens for which the locality could be georeferenced. Some taxonomic groups occurring with others in a particular locality may not be visible. Mean Annual Paleotemperature and Paleoprecipitation Proxy localities are discussed in Chapter 3. Base map made with Natural Earth.

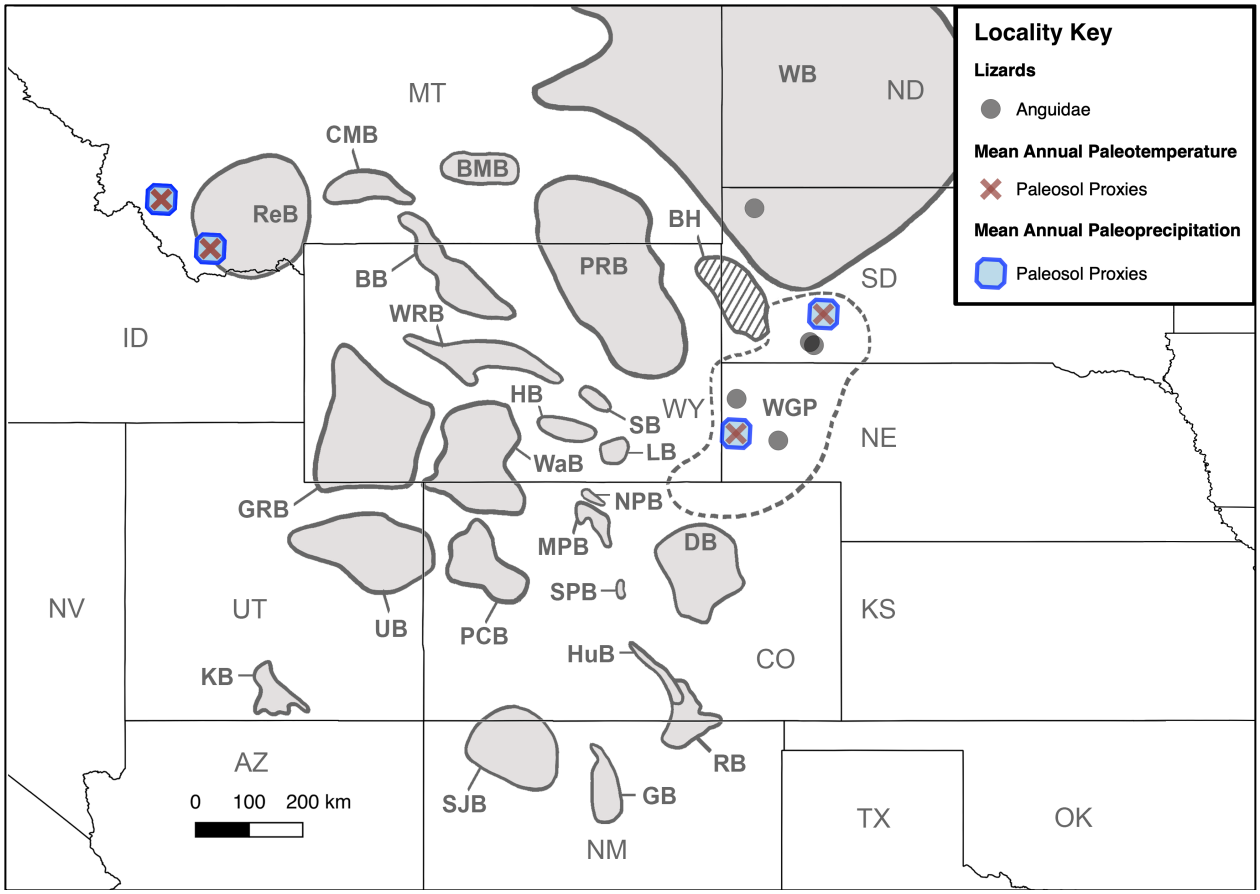

Figure 2.15. Map showing Whitneyan (middle Oligocene) localities for fossil and paleoclimate data across the Western Interior of North America through the Paleogene. Featured area is highlighted in inset map in Fig 2.1. Basin acronyms are listed in the caption for Fig 2.1. Data points represent only specimens for which the locality could be georeferenced. Some taxonomic groups occurring with others in a particular locality may not be visible. Mean Annual Paleotemperature and Paleoprecipitation Proxy localities are discussed in Chapter 3. Base map made with Natural Earth.

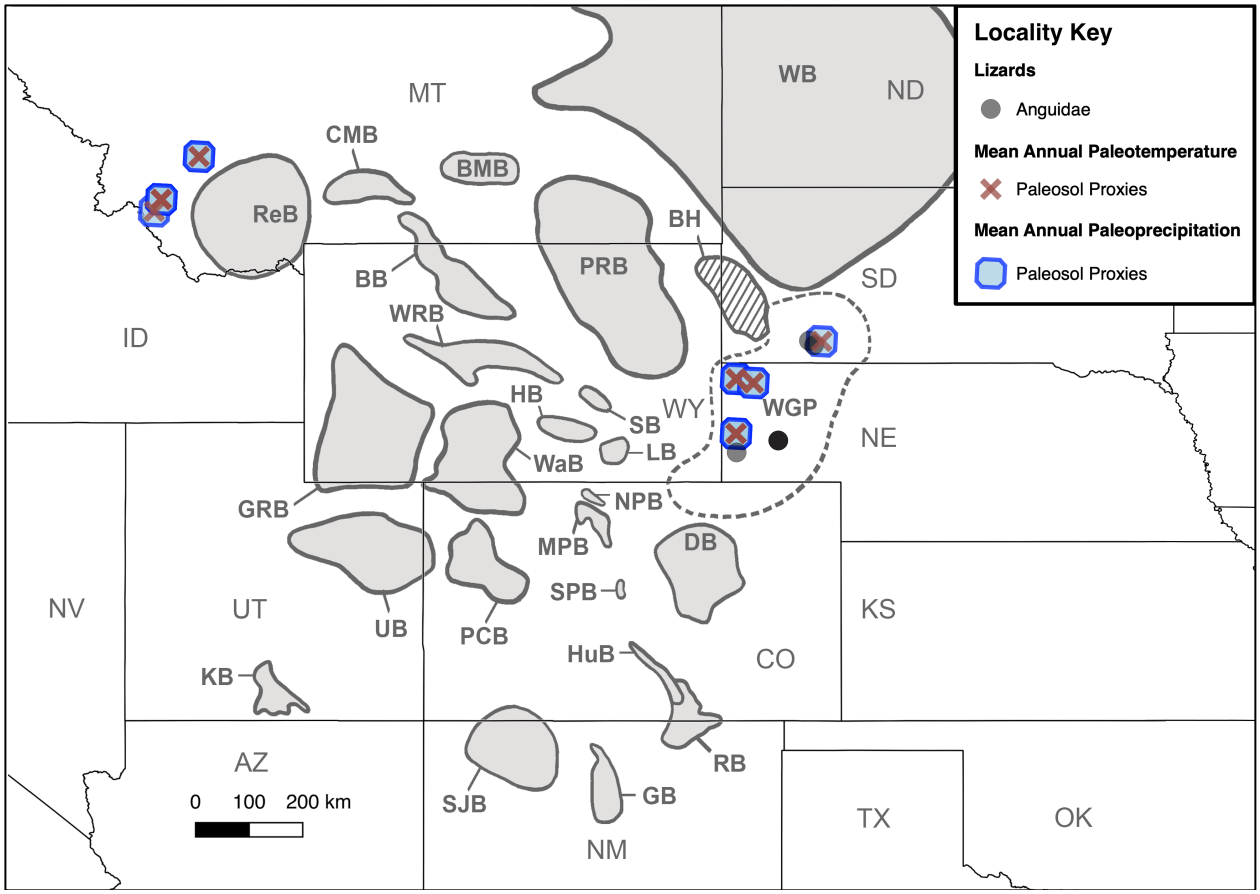

Figure 2.16. Map showing Arikareean (late Oligocene) localities for fossil and paleoclimate data across the Western Interior of North America through the Paleogene. Featured area is highlighted in inset map in Fig 2.1. Basin acronyms are listed in the caption for Fig 2.1. Data points represent only specimens for which the locality could be georeferenced. Some taxonomic groups occurring with others in a particular locality may not be visible. Mean Annual Paleotemperature and Paleoprecipitation Proxy localities are discussed in Chapter 3. Base map made with Natural Earth.

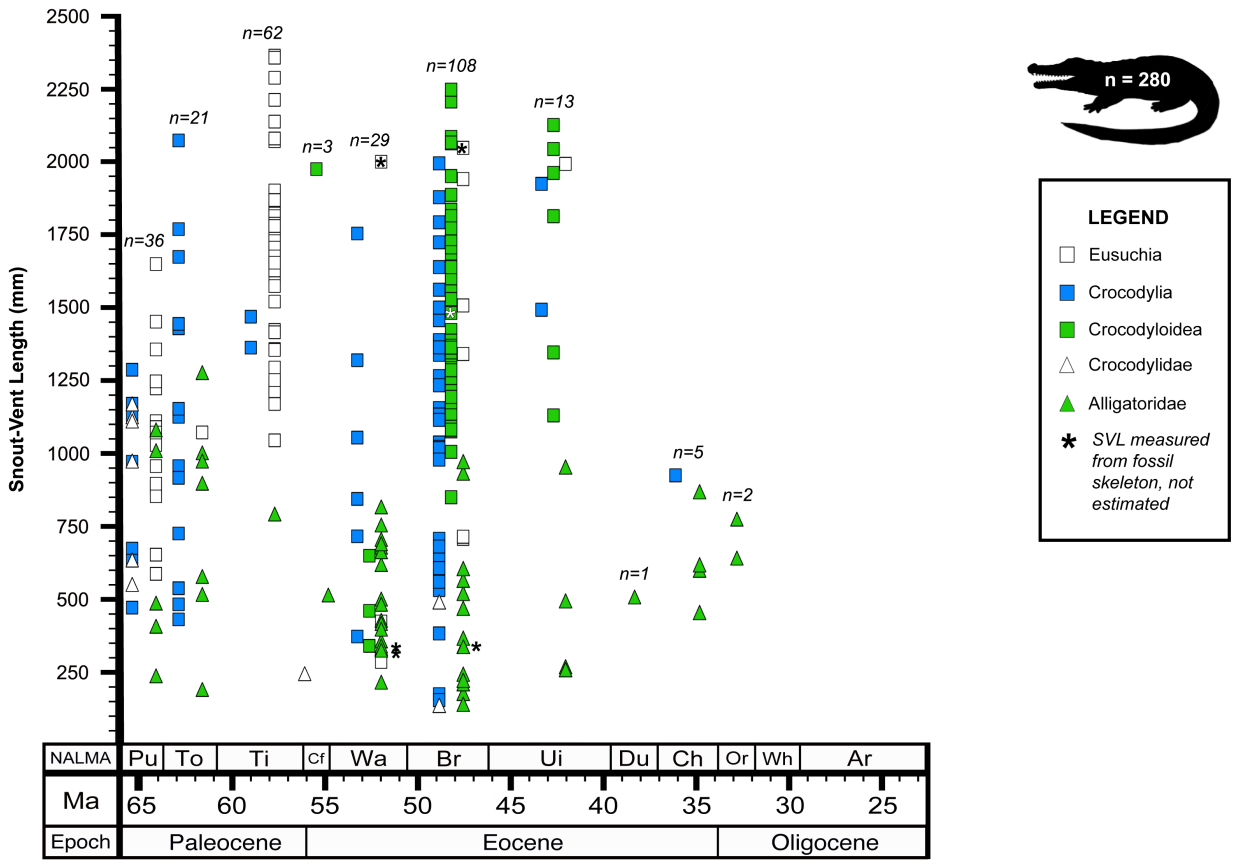

Figure 2.17. Snout-vent length distribution by highest taxonomic group for fossil crocodyliforms in the Western Interior of North America through the Paleogene. Sample sizes are per North American Land Mammal Age (NALMA). Data points are arbitrarily spread within each NALMA for visibility. NALMA abbreviations: Pu = Puercan, To = Torrejonian, Ti = Tiffanian, Cf = Clarkforkian, Wa = Wasatchian, Br = Bridgerian, Ui = Uintan, Du = Duchesnean, Ch = Chadronian, Or = Orellan, Wh = Whitneyan, Ar = Arikareean. Ma = Millions of years ago. Data points marked with an asterisk (*) were measured from complete fossil skeletons. All others were estimated from individual cranial or limb bones using regressions (see S2.1 Table).

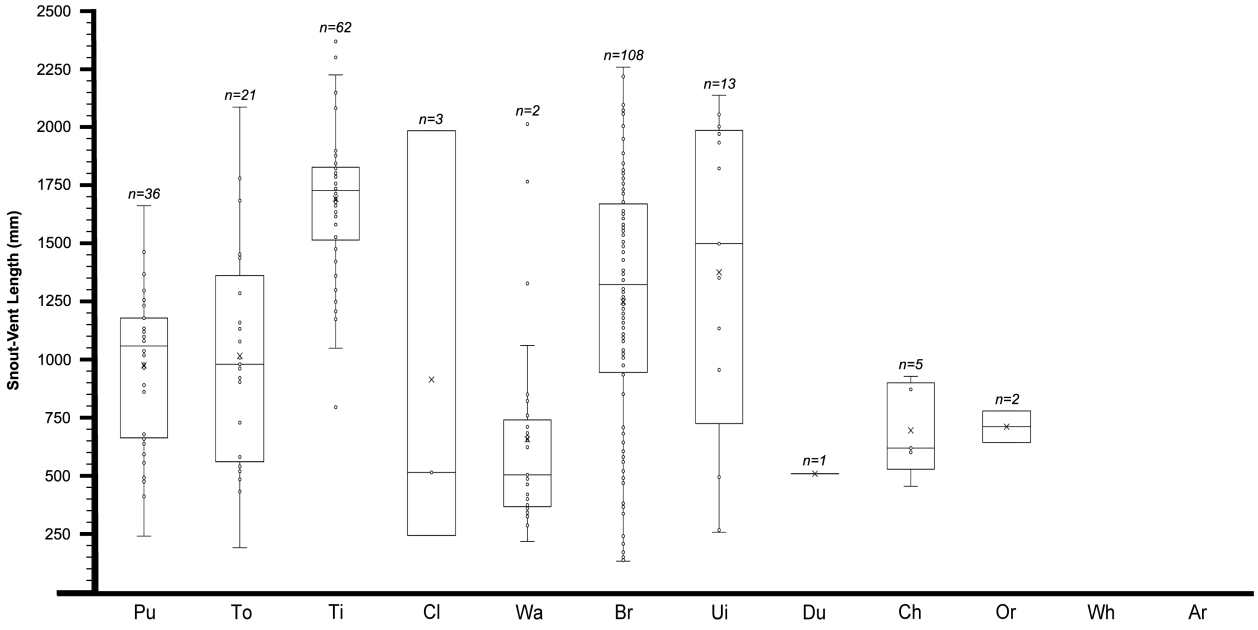

Figure 2.18. Box plots of snout-vent length distribution for fossil crocodyliforms in the Western Interior of North America through the Paleogene. Box plots represent samples for each North American Land Mammal Age (NALMA). NALMA abbreviations: Pu = Puercan, To = Torrejonian, Ti = Tiffanian, Cf = Clarkforkian, Wa = Wasatchian, Br = Bridgerian, Ui = Uintan, Du = Duchesnean, Ch = Chadronian, Or = Orellan, Wh = Whitneyan, Ar = Arikareean.

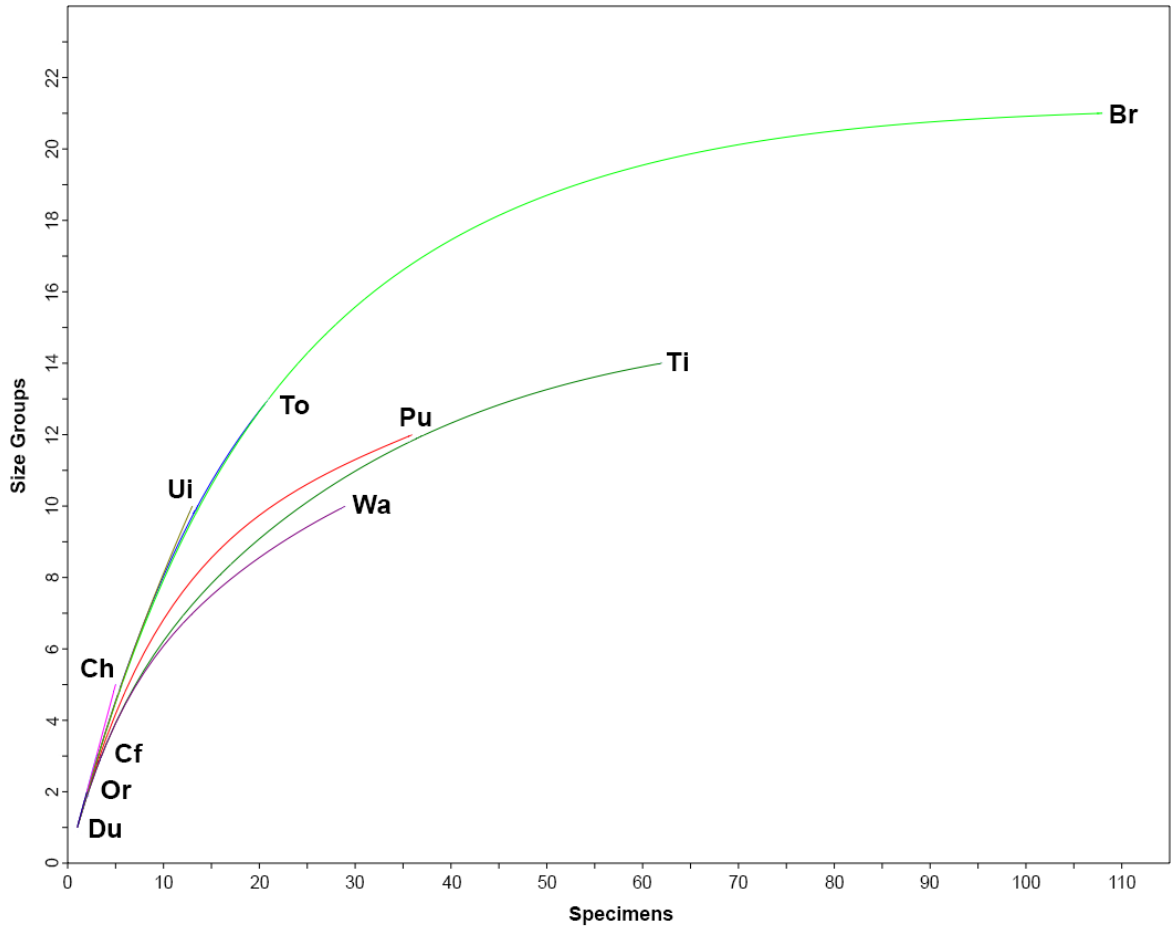

Figure 2.19. Rarefaction curve showing the number of expected size groups for NALMA sample sizes within the fossil crocodyliform dataset. To conduct this analysis, I assigned each fossil specimen in S2.1 Dataset to one of 24 size groups, each group representing a bin of 100 mm (e.g., 100-199 mm, 200-299 mm, etc.; the last group was ≥ 2.3 m). S2.1 Dataset is subsampled here by North American Land Mammal Age (NALMA) interval. The y-axis in this graph shows the total number of size groups recovered in the sample for each NALMA interval. NALMA abbreviations: Pu = Puercan, To = Torrejonian, Ti = Tiffanian, Cf = Clarkforkian, Wa = Wasatchian, Br = Bridgerian, Ui = Uintan, Du = Duchesnean, Ch = Chadronian, Or = Orellan. Individual rarefaction analysis was performed using PAST v4.03 (Hammer et al. 2001).

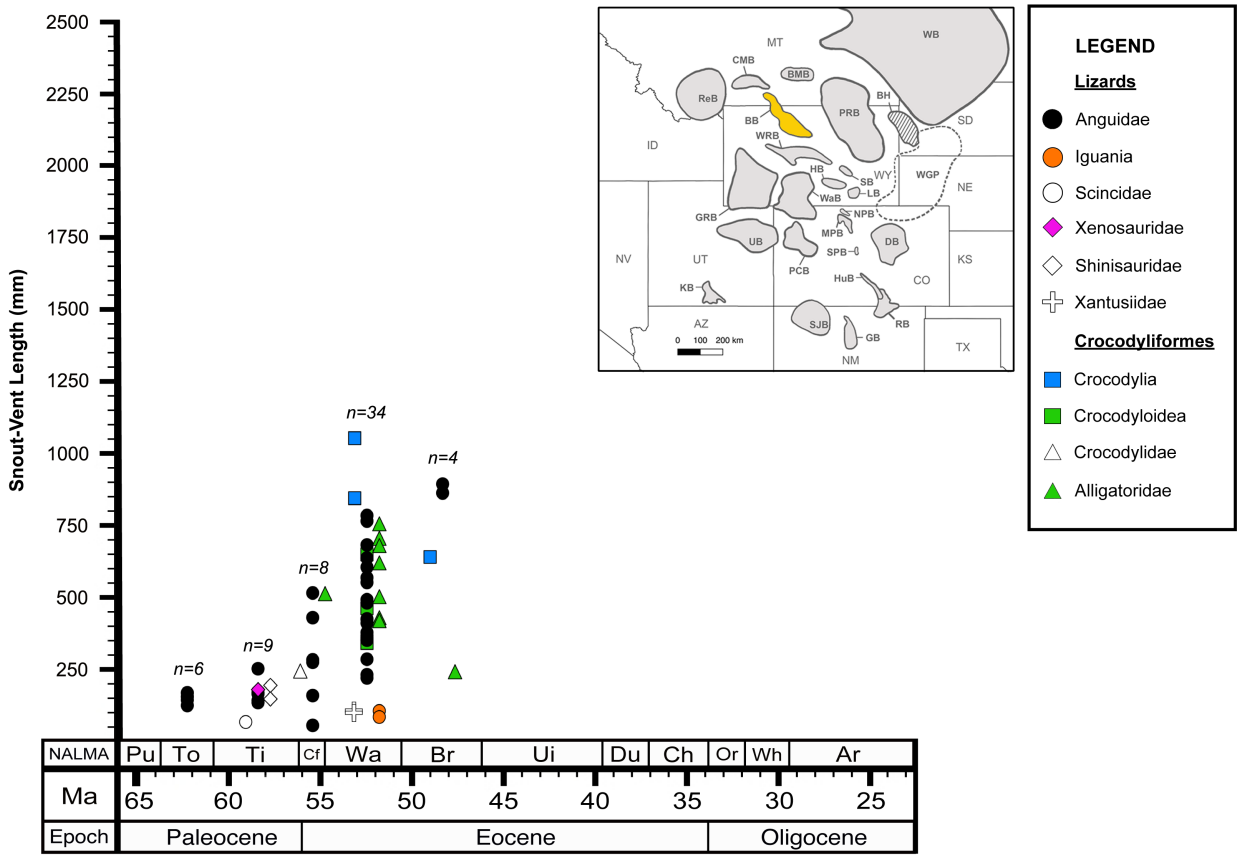

Figure 2.20. Snout-vent length distribution by taxonomic group for fossil lizards and crocodyliforms in the Bighorn Basin through the Paleogene. The Bighorn Basin is highlighted in the inset map (see also Fig 2.1). Sample sizes are per North American Land Mammal Age (NALMA). Data points are arbitrarily spread within each NALMA for visibility. Lizard SVL estimates are from Chapter 1 (Fig 1.5, S1.1 Dataset). NALMA abbreviations: Pu = Puercan, To = Torrejonian, Ti = Tiffanian, Cf = Clarkforkian, Wa = Wasatchian, Br = Bridgerian, Ui = Uintan, Du = Duchesnean, Ch = Chadronian, Or = Orellan, Wh = Whitneyan, Ar = Arikareean.

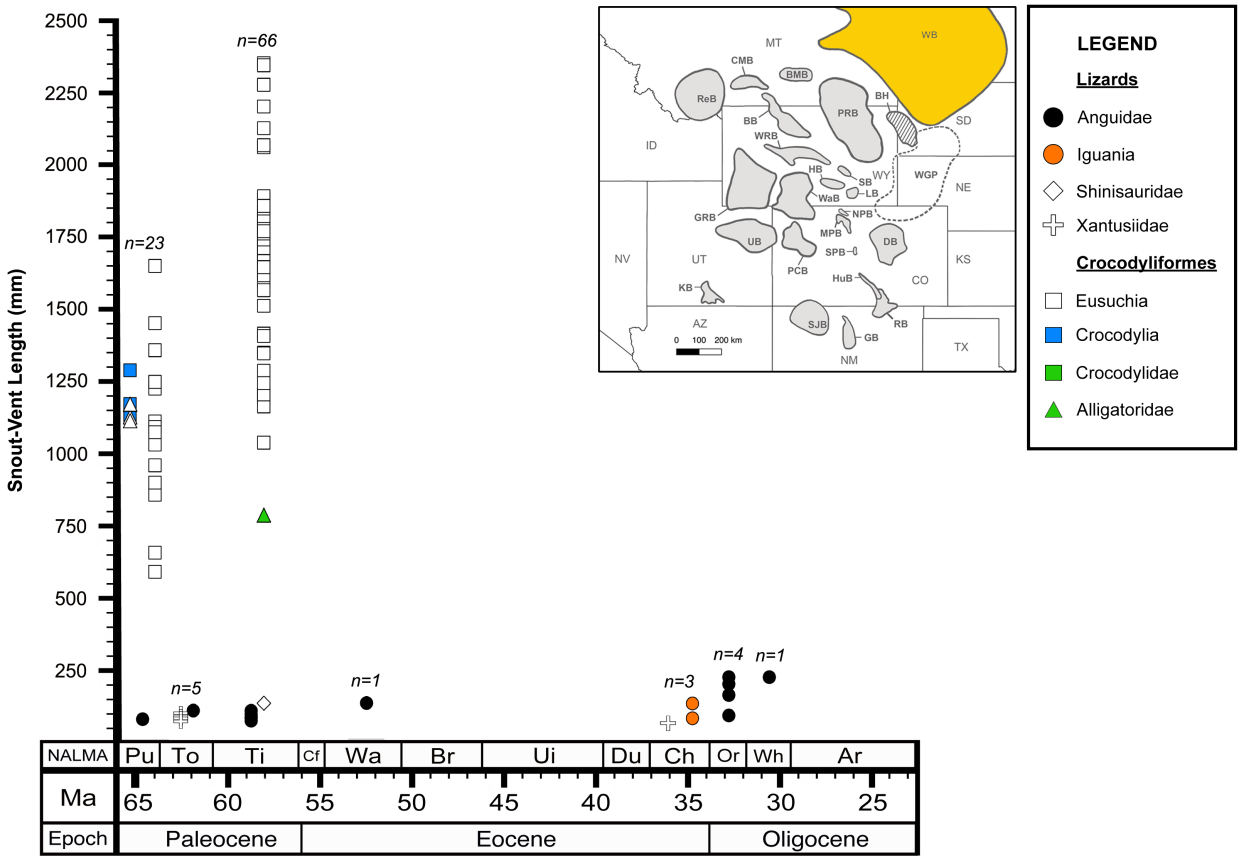

Figure 2.21. Snout-vent length distribution by taxonomic group for fossil lizards and crocodyliforms in the Williston Basin through the Paleogene. The Williston Basin is highlighted in the inset map (see also Fig 2.1). Sample sizes are per North American Land Mammal Age (NALMA). Data points are arbitrarily spread within each NALMA for visibility. Lizard SVL estimates are from Chapter 1 (Fig 1.5, S1.1 Dataset). NALMA abbreviations: Pu = Puercan, To = Torrejonian, Ti = Tiffanian, Cf = Clarkforkian, Wa = Wasatchian, Br = Bridgerian, Ui = Uintan, Du = Duchesnean, Ch = Chadronian, Or = Orellan, Wh = Whitneyan, Ar = Arikareean.

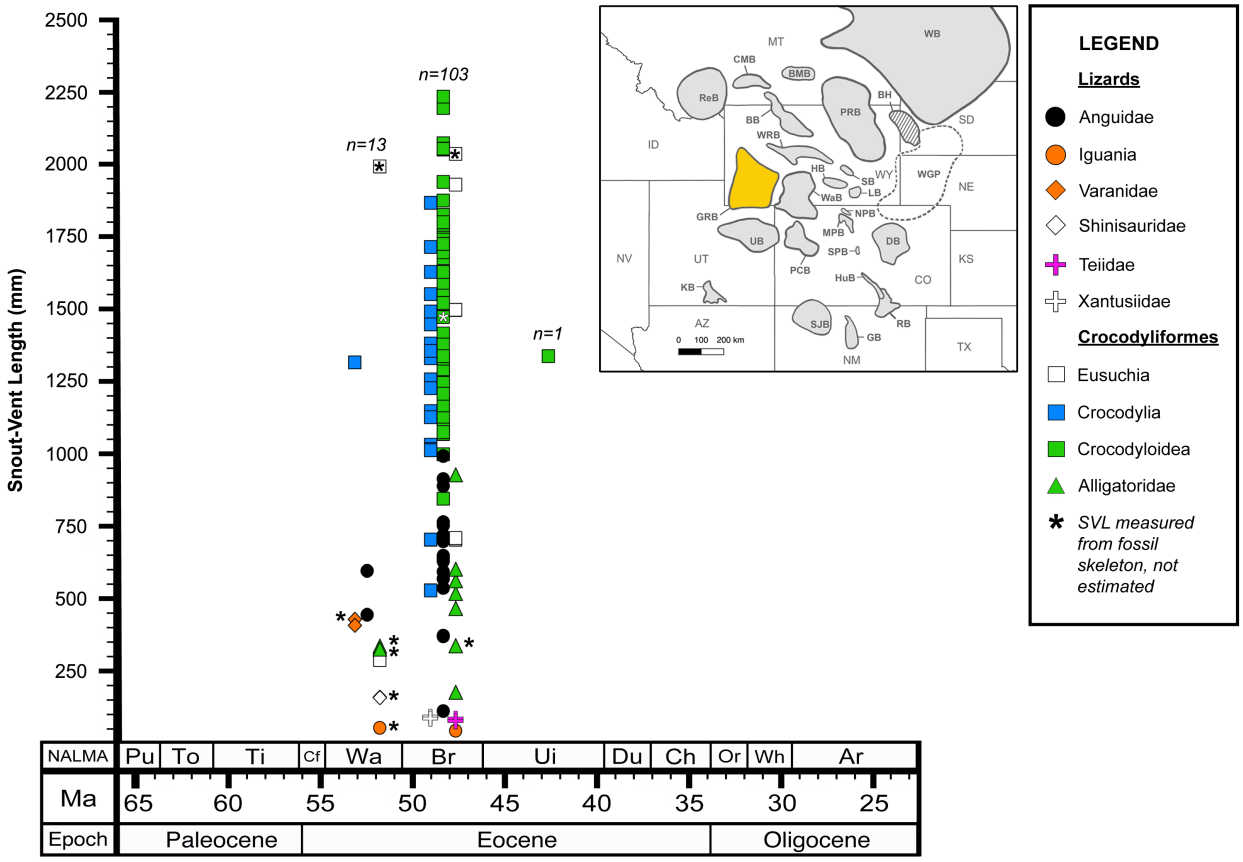

Figure 2.22. Snout-vent length distribution by taxonomic group for fossil lizards and crocodyliforms in the Green River Basin through the Paleogene. The Green River Basin is highlighted in the inset map (see also Fig 2.1). Sample sizes are per North American Land Mammal Age (NALMA). Data points are arbitrarily spread within each NALMA for visibility. Lizard SVL estimates are from Chapter 1 (Fig 1.5, S1.1 Dataset). Data points marked with an asterisk (*) were measured from complete fossil skeletons. NALMA abbreviations: Pu = Puercan, To = Torrejonian, Ti = Tiffanian, Cf = Clarkforkian, Wa = Wasatchian, Br = Bridgerian, Ui = Uintan, Du = Duchesnean, Ch = Chadronian, Or = Orellan, Wh = Whitneyan, Ar = Arikareean.

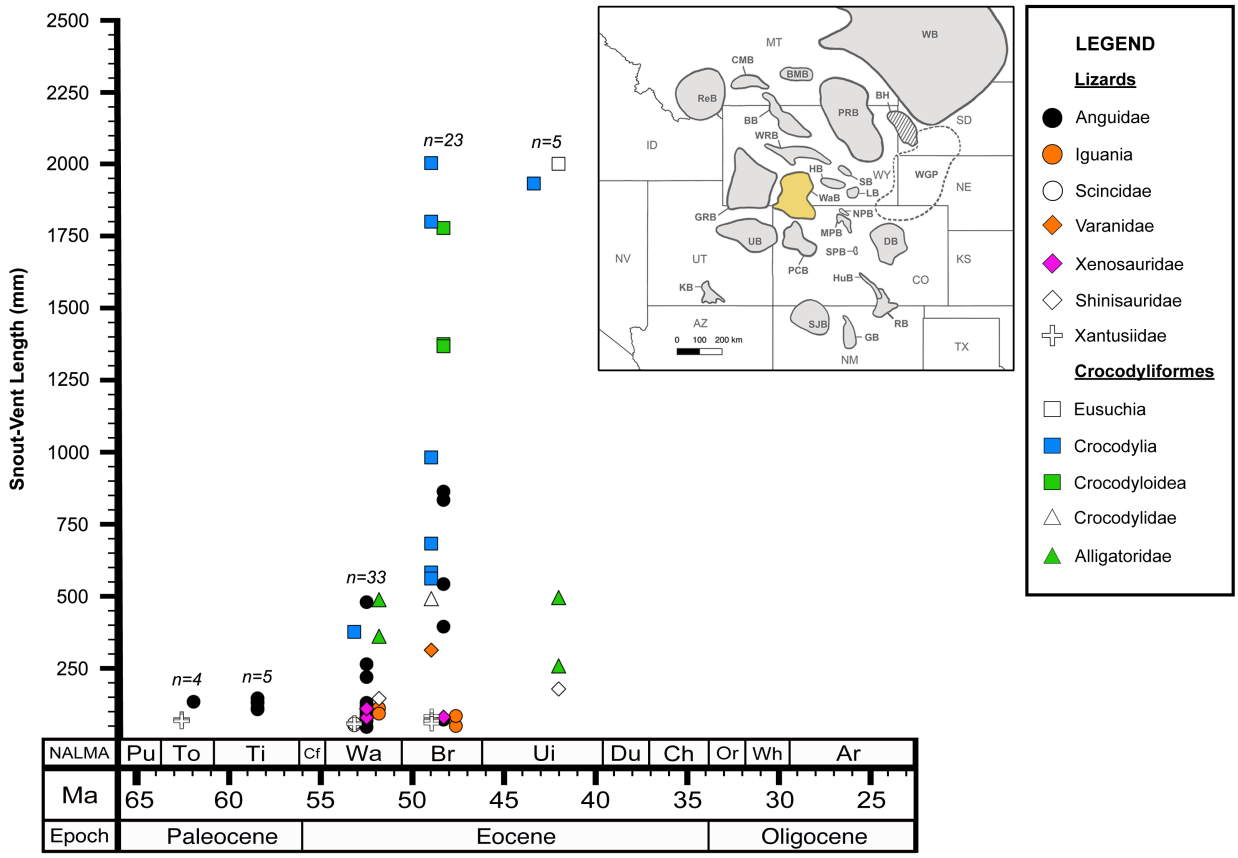

Figure 2.23. Snout-vent length distribution by taxonomic group for fossil lizards and crocodyliforms in the Washakie Basin through the Paleogene. The Washakie Basin is highlighted in the inset map (see also Fig 2.1). Sample sizes are per North American Land Mammal Age (NALMA). Data points are arbitrarily spread within each NALMA for visibility. Lizard SVL estimates are from Chapter 1 (Fig 1.5, S1.1 Dataset). NALMA abbreviations: Pu = Puercan, To = Torrejonian, Ti = Tiffanian, Cf = Clarkforkian, Wa = Wasatchian, Br = Bridgerian, Ui = Uintan, Du = Duchesnean, Ch = Chadronian, Or = Orellan, Wh = Whitneyan, Ar = Arikareean.

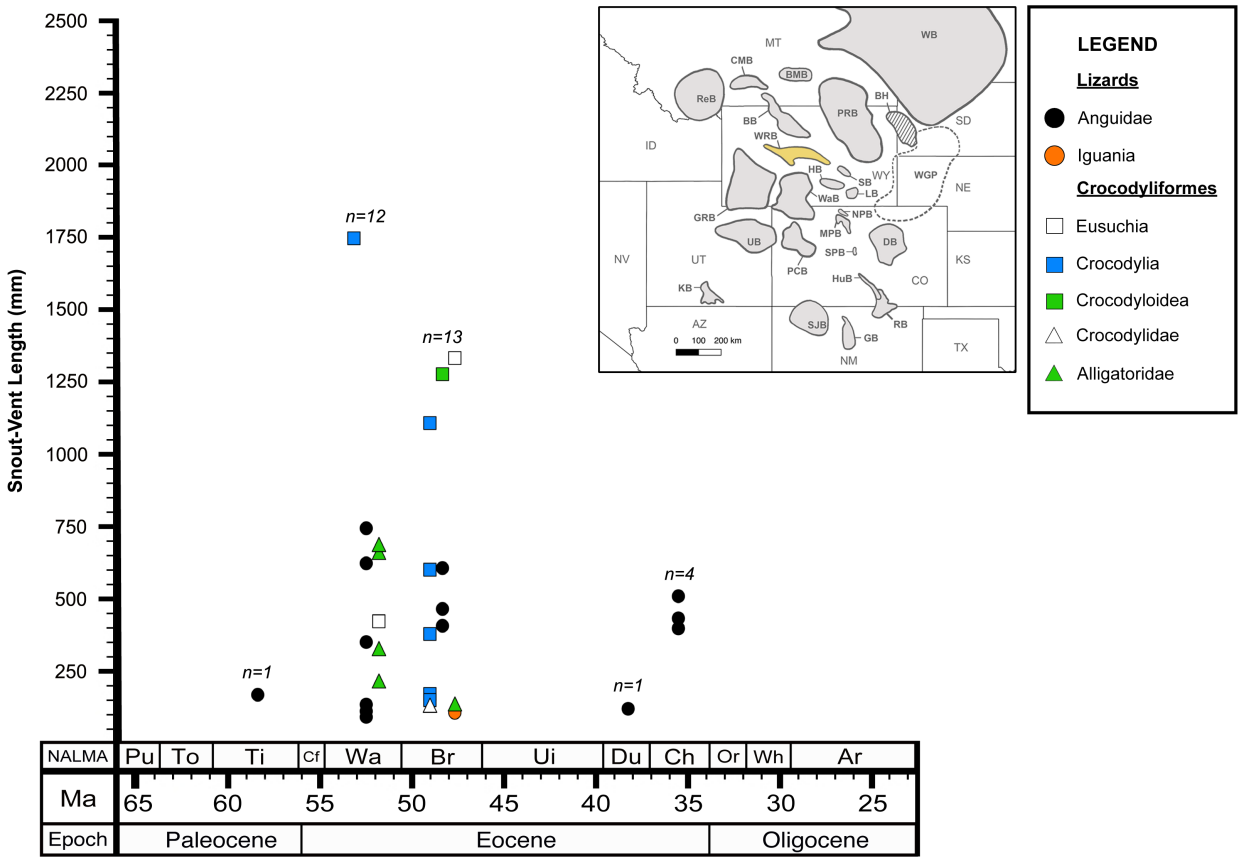

Figure 2.24. Snout-vent length distribution by taxonomic group for fossil lizards and crocodyliforms in the Wind River Basin through the Paleogene. The Wind River Basin is highlighted in the inset map (see also Fig 2.1). Sample sizes are per North American Land Mammal Age (NALMA). Data points are arbitrarily spread within each NALMA for visibility. Lizard SVL estimates are from Chapter 1 (Fig 1.5, S1.1 Dataset). NALMA abbreviations: Pu = Puercan, To = Torrejonian, Ti = Tiffanian, Cf = Clarkforkian, Wa = Wasatchian, Br = Bridgerian, Ui = Uintan, Du = Duchesnean, Ch = Chadronian, Or = Orellan, Wh = Whitneyan, Ar = Arikareean.

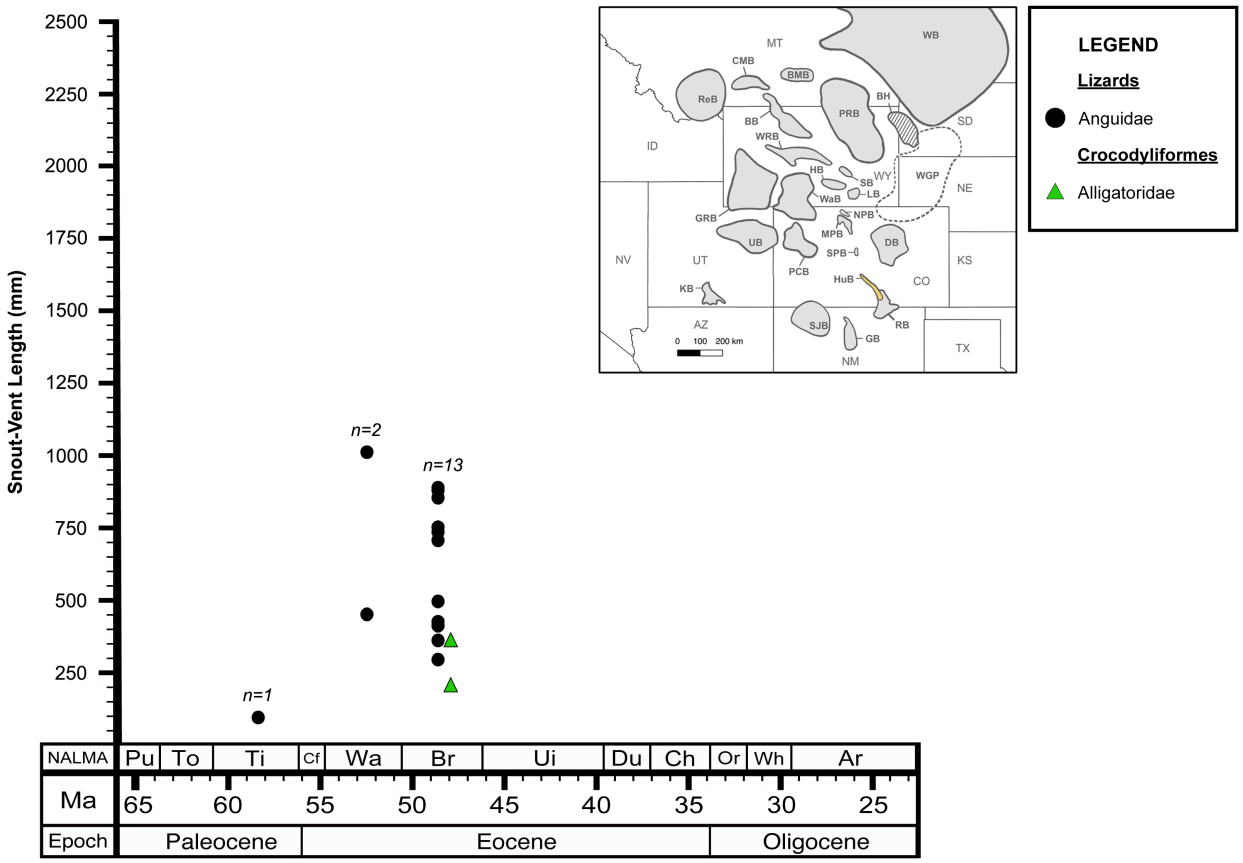

Figure 2.25. Snout-vent length distribution by taxonomic group for fossil lizards and crocodyliforms in the Huerfano Basin through the Paleogene. The Huerfano Basin is highlighted in the inset map (see also Fig 2.1). Sample sizes are per North American Land Mammal Age (NALMA). Data points are arbitrarily spread within each NALMA for visibility. Lizard SVL estimates are from Chapter 1 (Fig 1.5, S1.1 Dataset). NALMA abbreviations: Pu = Puercan, To = Torrejonian, Ti = Tiffanian, Cf = Clarkforkian, Wa = Wasatchian, Br = Bridgerian, Ui = Uintan, Du = Duchesnean, Ch = Chadronian, Or = Orellan, Wh = Whitneyan, Ar = Arikareean.

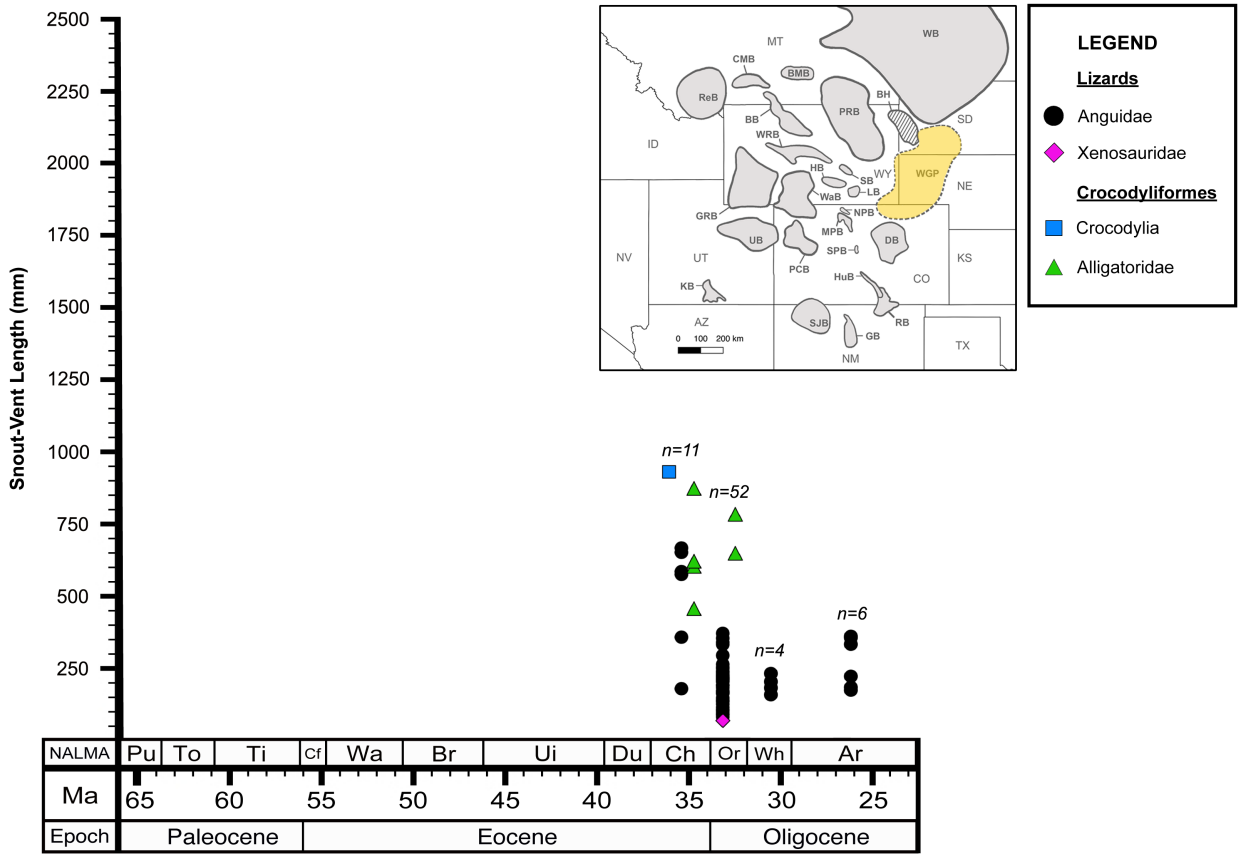

Figure 2.26. Snout-vent length distribution by taxonomic group for fossil lizards and crocodyliforms in the Western Great Plains through the Paleogene. The Western Great Plains area is highlighted in the inset map (see also Fig 2.1). This area is treated as a basin even though it is not surrounded completely by mountains because a continental divide runs east-west through the Black Hills just north of the area highlighted in the dashed line. Sample sizes are per North American Land Mammal Age (NALMA). Data points are arbitrarily spread within each NALMA for visibility. Lizard SVL estimates are from Chapter 1 (Fig 1.5, S1.1 Dataset). NALMA abbreviations: Pu = Puercan, To = Torrejonian, Ti = Tiffanian, Cf = Clarkforkian, Wa = Wasatchian, Br = Bridgerian, Ui = Uintan, Du = Duchesnean, Ch = Chadronian, Or = Orellan, Wh = Whitneyan, Ar = Arikareean.

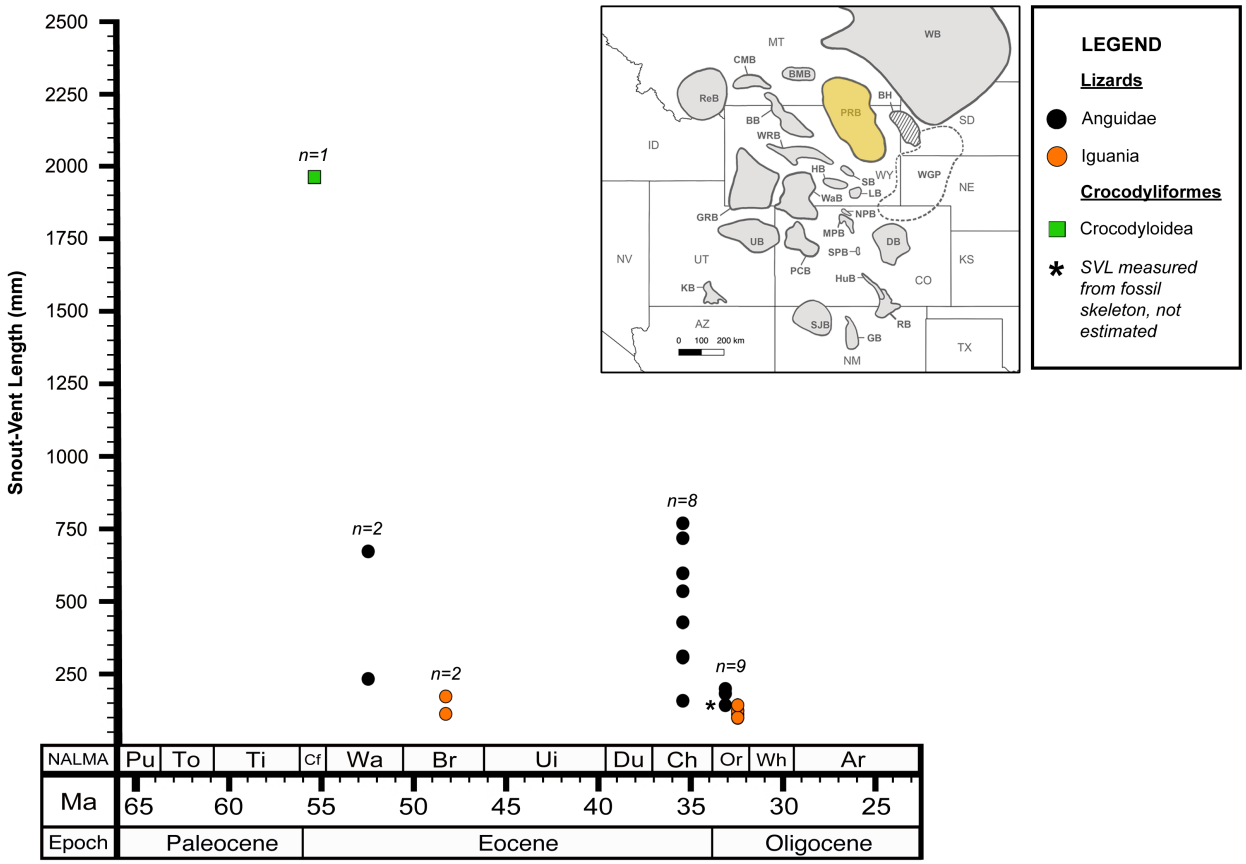

Figure 2.27. Snout-vent length distribution by taxonomic group for fossil lizards and crocodyliforms in the Powder River Basin through the Paleogene. The Powder River Basin is highlighted in the inset map (see also Fig 2.1). Sample sizes are per North American Land Mammal Age (NALMA). Data points are arbitrarily spread within each NALMA for visibility. Lizard SVL estimates are from Chapter 1 (Fig 1.5, S1.1 Dataset). Data points marked with an asterisk (*) were measured from complete fossil skeletons. NALMA abbreviations: Pu = Puercan, To = Torrejonian, Ti = Tiffanian, Cf = Clarkforkian, Wa = Wasatchian, Br = Bridgerian, Ui = Uintan, Du = Duchesnean, Ch = Chadronian, Or = Orellan, Wh = Whitneyan, Ar = Arikareean.

CHAPTER 3 FIGURES

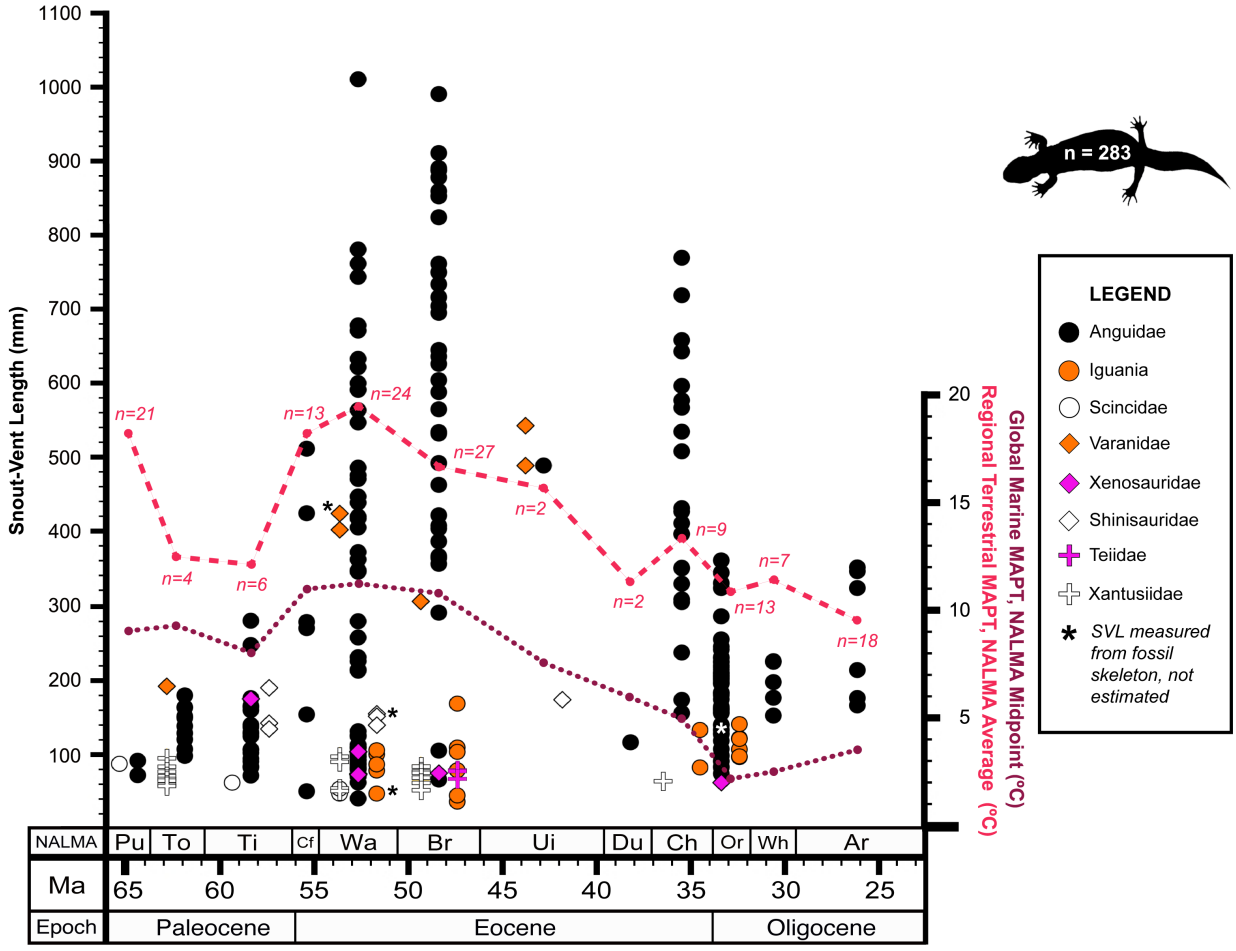

Figure 3.1. Paleogene lizard snout-vent lengths by taxonomic group plotted against regional terrestrial and global marine mean annual paleotemperatures (MAPT). Regional terrestrial MAPT (red dashed line) is averaged by North American Land Mammal Age (NALMA) across the Western Interior of North America. Sample sizes with red dashed line indicate number of MAPT data points sampled from each NALMA interval. References for MAPT data are listed in S3.1 Dataset. Global marine MAPT data (maroon dotted line) come from Zachos et al. (2008) and represent NALMA midpoint values. SVL data points are arbitrarily spread within each NALMA for visibility. Data points marked with an asterisk (*) were measured from complete fossil skeletons. All others were estimated from individual cranial or limb elements using regressions and sometimes ratios (see S1.1-1.10 Tables). NALMA abbreviations: Pu = Puercan, To = Torrejonian, Ti = Tiffanian, Cf = Clarkforkian, Wa = Wasatchian, Br = Bridgerian, Ui = Uintan, Du = Duchesnean, Ch = Chadronian, Or = Orellan, Wh = Whitneyan, Ar = Arikareean.

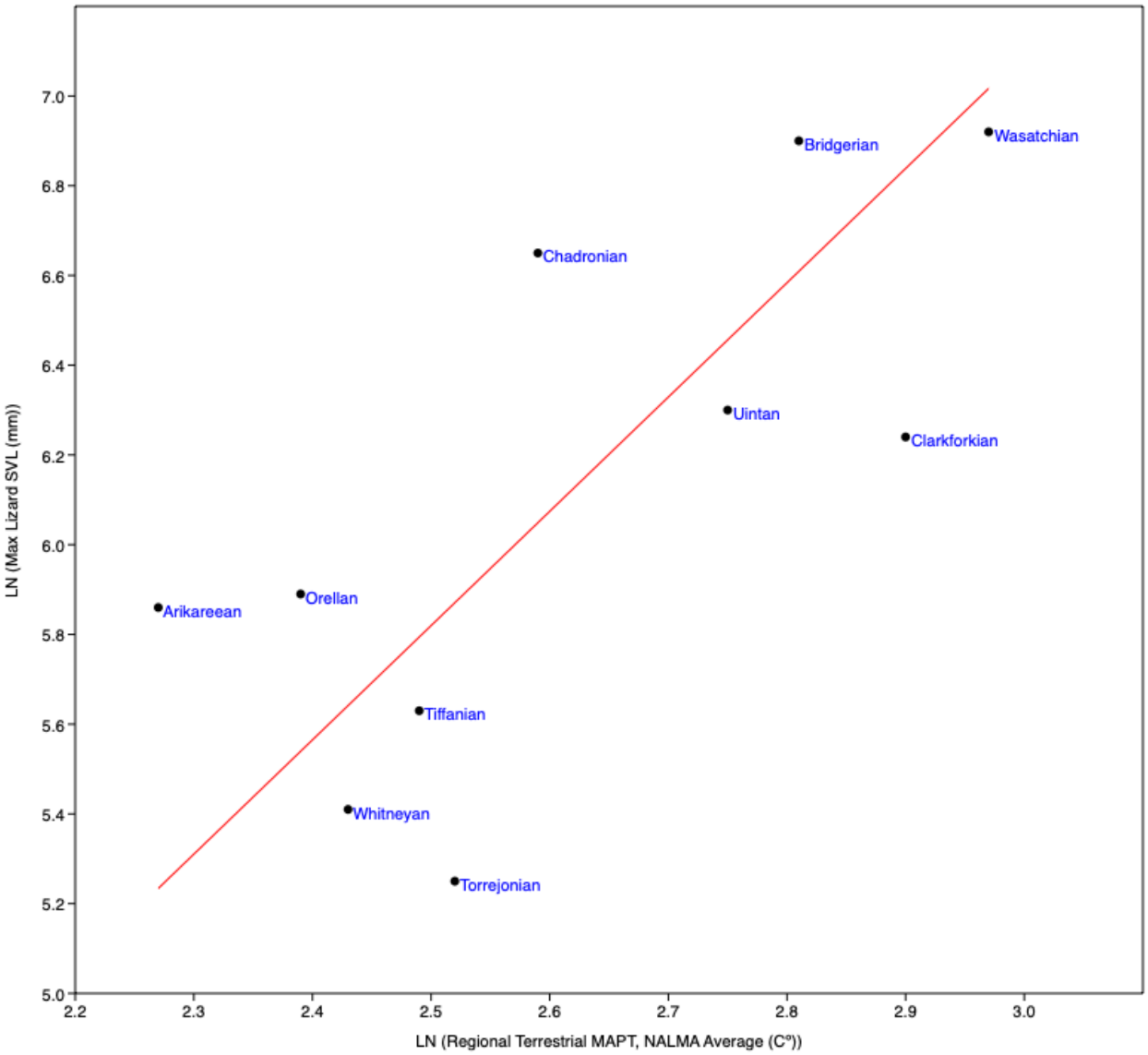

Figure 3.2A. Regional terrestrial mean annual paleotemperature (MAPT) correlated with maximum lizard snout-vent length (SVL) from across the Western Interior of North America through the Paleogene. All values are transformed using natural log. Regional terrestrial MAPT is averaged by North American Land Mammal Age (NALMA) across the Western Interior of North America (see Fig 3.1 for sample sizes). References for MAPT data are listed in S3.1 Dataset. The Puercan and Duchesnean are omitted due to low sample size. Regression equation: LN(Max Lizard SVL) = (2.547 * (LN(Reg. Terr. MAPT)) – 0.548; R^2 = 0.51, p(uncorr.) = 0.02, n = 10.

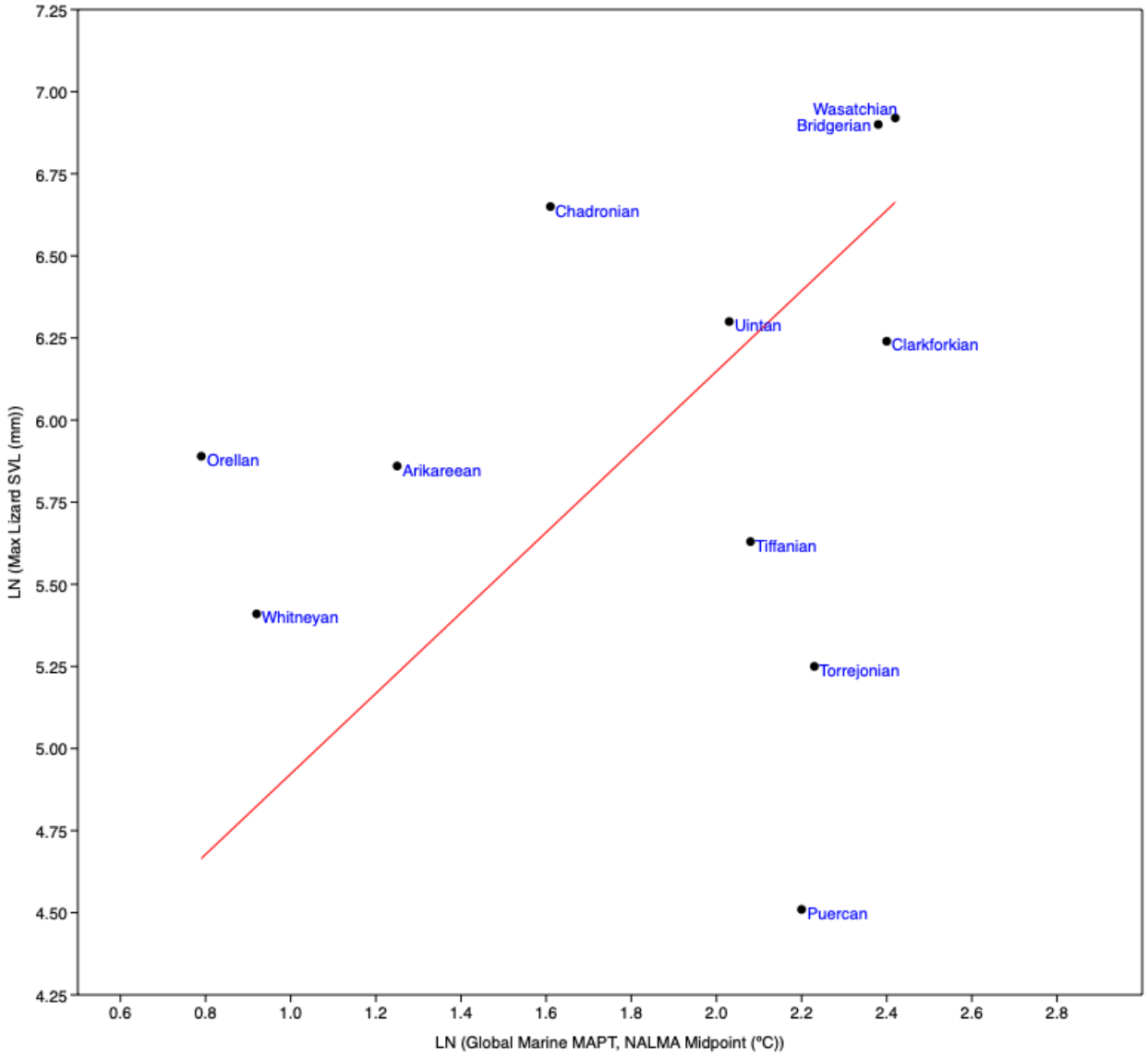

Figure 3.2B. Global marine mean annual paleotemperature (MAPT) correlated with maximum lizard snout-vent length (SVL) from across the Western Interior of North America through the Paleogene. All values are transformed using natural log. Global marine MAPT data come from Zachos et al. (2008) and represent NALMA midpoint values. The Duchesnean is omitted for consistency. Regression equation: LN(Max Lizard SVL) = (1.226 * (LN(Global Marine MAPT)) + 3.697; R^2 = 0.04, p(uncorr.) = 0.56, n = 11.

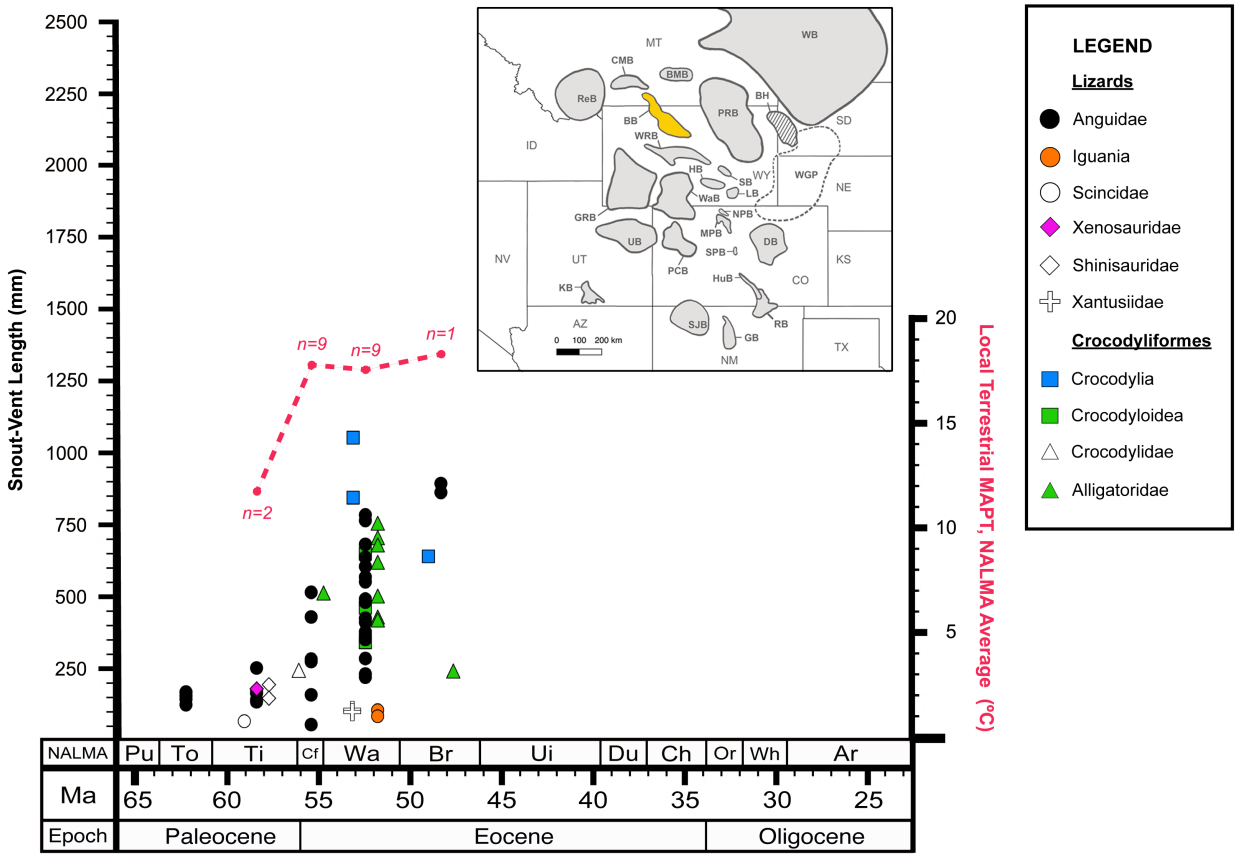

Figure 3.3. Bighorn Basin lizard and crocodyliform snout-vent lengths by taxonomic group plotted against local terrestrial mean annual paleotemperatures (MAPT) through the early and middle Paleogene. Local terrestrial MAPT (red dashed line) is averaged by North American Land Mammal Age (NALMA) across the Bighorn Basin. Sample sizes with red dashed line indicate number of MAPT data points from localities within the Bighorn Basin sampled from each NALMA interval. References for MAPT data are listed in S3.1 Dataset. The Bighorn Basin is highlighted in the inset map (see also Fig 2.1). NALMA abbreviations: Pu = Puercan, To = Torrejonian, Ti = Tiffanian, Cf = Clarkforkian, Wa = Wasatchian, Br = Bridgerian, Ui = Uintan, Du = Duchesnean, Ch = Chadronian, Or = Orellan, Wh = Whitneyan, Ar = Arikareean.

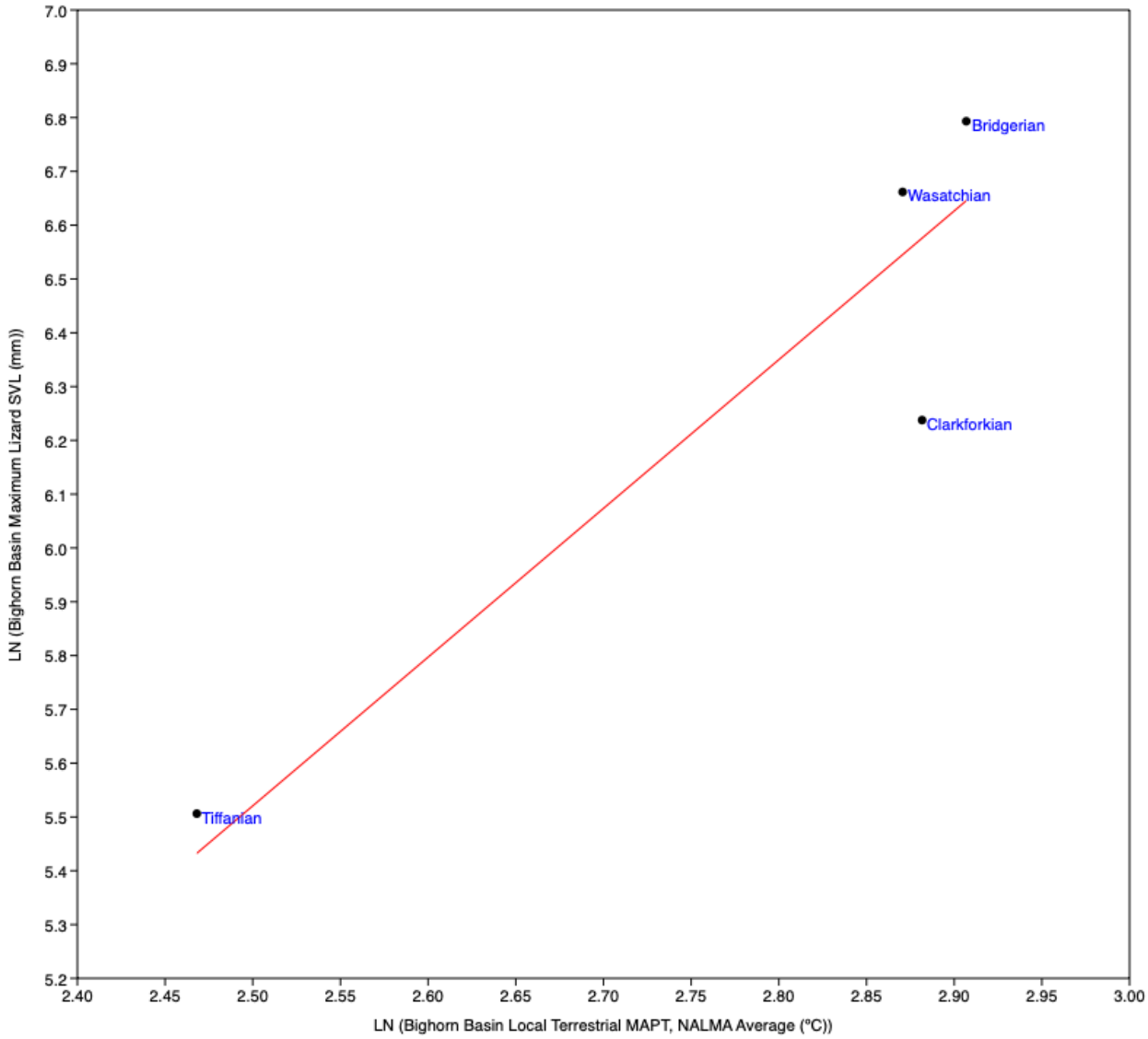

Figure 3.4. Local terrestrial mean annual paleotemperature (MAPT) correlated with maximum lizard snout-vent length (SVL) within the Bighorn Basin. All values are transformed using natural log. Local MAPT is averaged by North American Land Mammal Age (NALMA; see Fig 3.3 for sample sizes). Paired data were only available for the four NALMAs indicated. References for MAPT data are listed in S3.1 Dataset. Regression equation: LN(Bighorn Max Lizard SVL) = (2.764 * (LN(Bighorn MAPT)) – 1.390; R^2 = 0.85, p(uncorr.) = 0.08, n = 4.

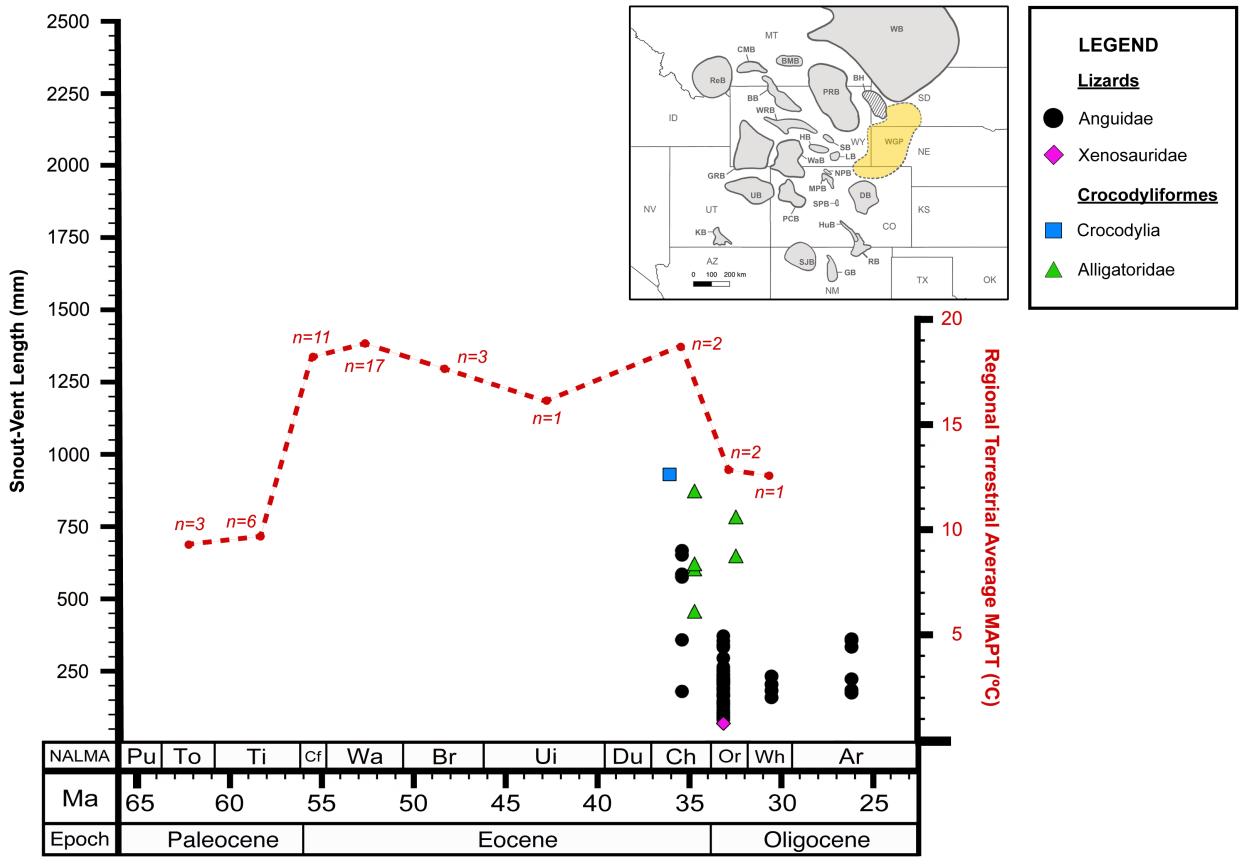

Figure 3.5. Western Great Plains lizard and crocodyliform snout-vent lengths by taxonomic group plotted against local terrestrial mean annual paleotemperatures (MAPT) through the late Paleogene. Local terrestrial MAPT (red dashed line) is averaged by North American Land Mammal Age (NALMA) across the Western Great Plains. Sample sizes with red dashed line indicate number of MAPT data points from localities within the Western Great Plains sampled from each NALMA interval. References for MAPT data are listed in S3.1 Dataset. The Western Great Plains are highlighted in the inset map (see also Fig 2.1). NALMA abbreviations: Pu = Puercan, To = Torrejonian, Ti = Tiffanian, Cf = Clarkforkian, Wa = Wasatchian, Br = Bridgerian, Ui = Uintan, Du = Duchesnean, Ch = Chadronian, Or = Orellan, Wh = Whitneyan, Ar = Arikareean.

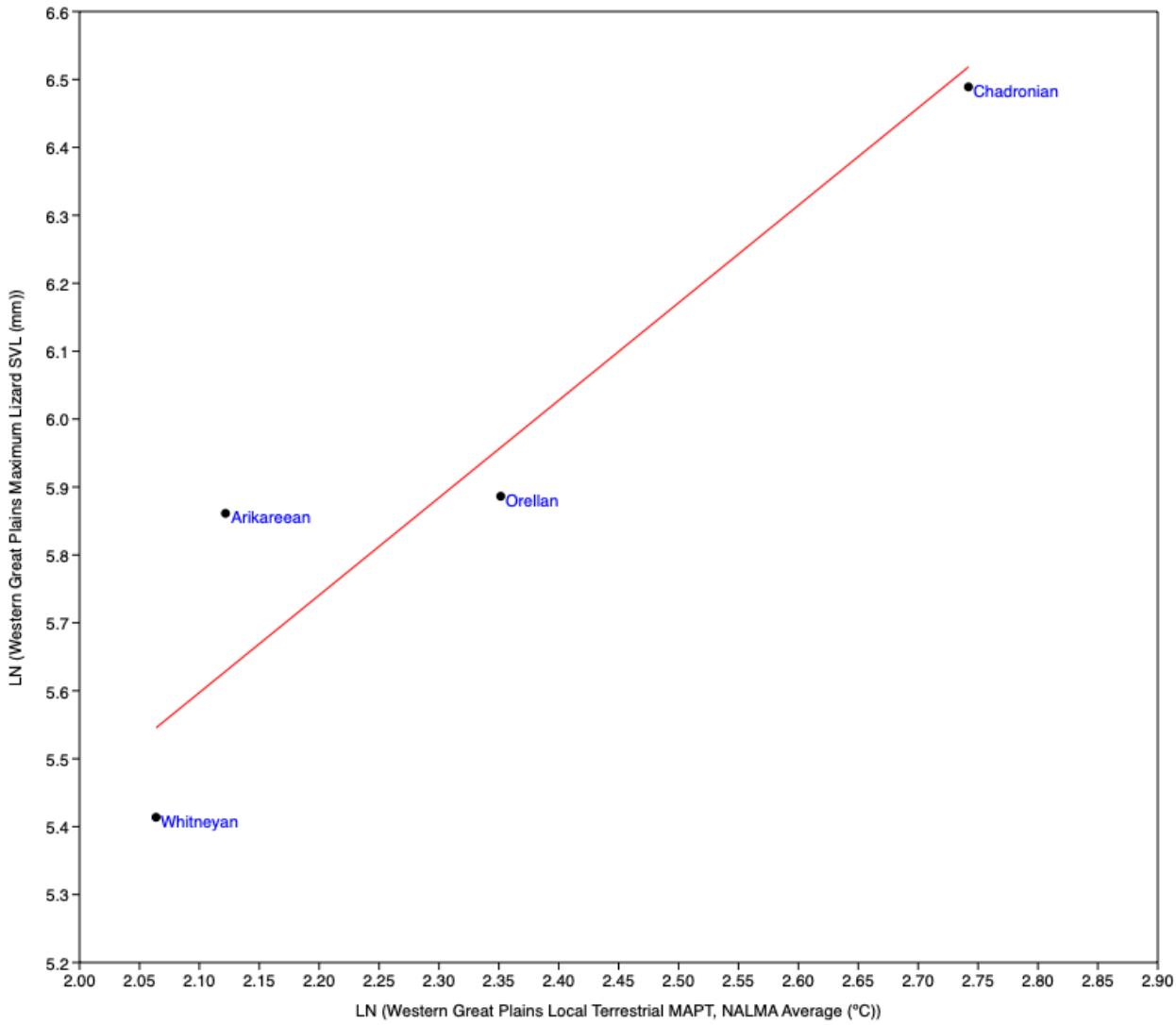

Figure 3.6. Local terrestrial mean annual paleotemperature (MAPT) correlated with maximum lizard snout-vent length (SVL) within the Western Great Plains. All values are transformed using natural log. Local MAPT is averaged by North American Land Mammal Age (NALMA; see Fig 3.5 for sample sizes). Paired data were only available for the four NALMAs indicated. References for MAPT data are listed in S3.1 Dataset. Regression equation: LN(Western Great Plains Max Lizard SVL) = (1.435 * (LN(Western Great Plains MAPT)) + 2.585; R^2 = 0.87, p(uncorr.) = 0.07, n = 4.

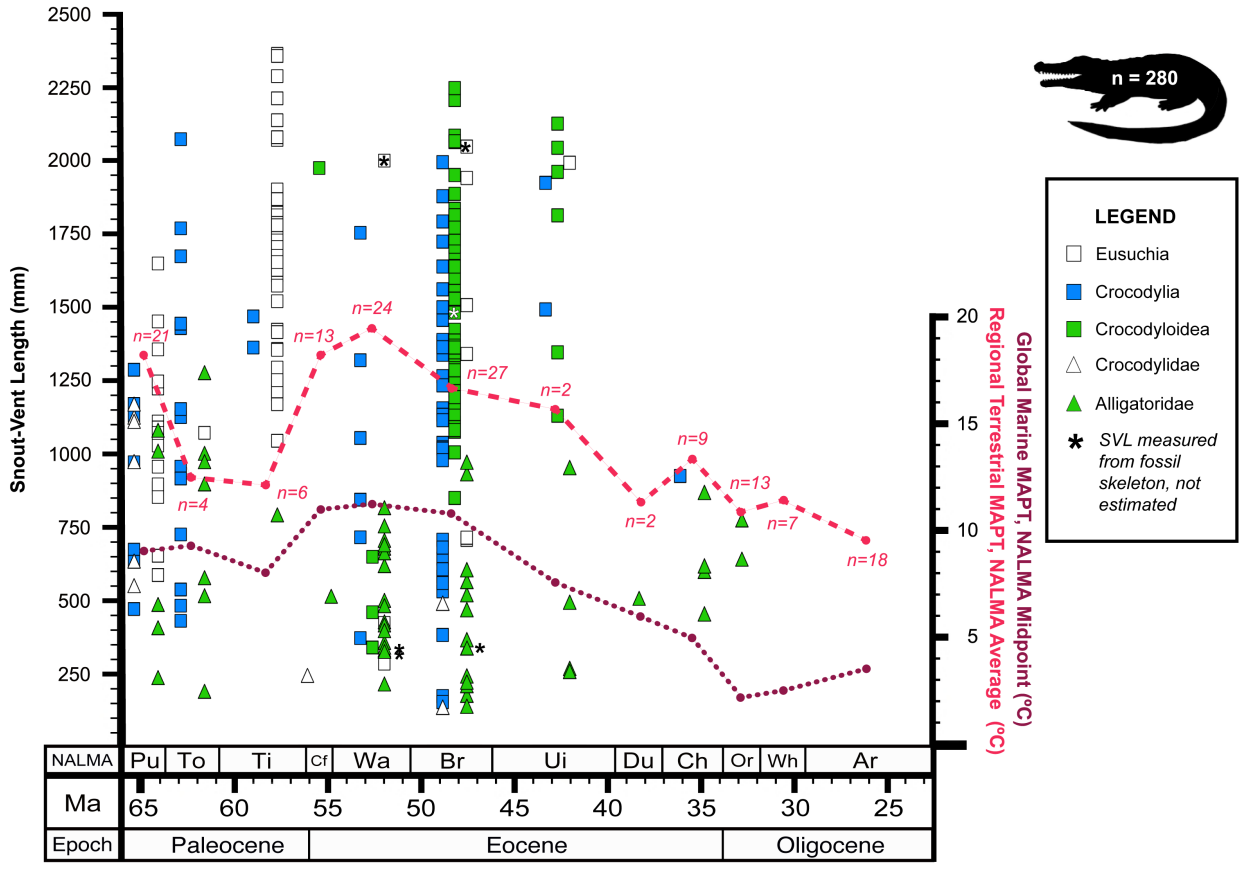

Figure 3.7. Paleogene crocodyliform snout-vent lengths by taxonomic group plotted against regional terrestrial and global marine mean annual paleotemperatures (MAPT). Regional terrestrial MAPT (red dashed line) is averaged by North American Land Mammal Age (NALMA) across the Western Interior of North America. Sample sizes with red dashed line indicate number of MAPT data points sampled from each NALMA interval. References for MAPT data are listed in S3.1 Dataset. Global marine MAPT data (maroon dotted line) come from Zachos et al. (2008) and represent NALMA midpoint values. SVL data points are arbitrarily spread within each NALMA for visibility. Data points marked with an asterisk (*) were measured from complete fossil skeletons. All others were estimated from individual cranial or limb bones using regressions (see S2.1 Table). NALMA abbreviations: Pu = Puercan, To = Torrejonian, Ti = Tiffanian, Cf = Clarkforkian, Wa = Wasatchian, Br = Bridgerian, Ui = Uintan, Du = Duchesnean, Ch = Chadronian, Or = Orellan, Wh = Whitneyan, Ar = Arikareean.

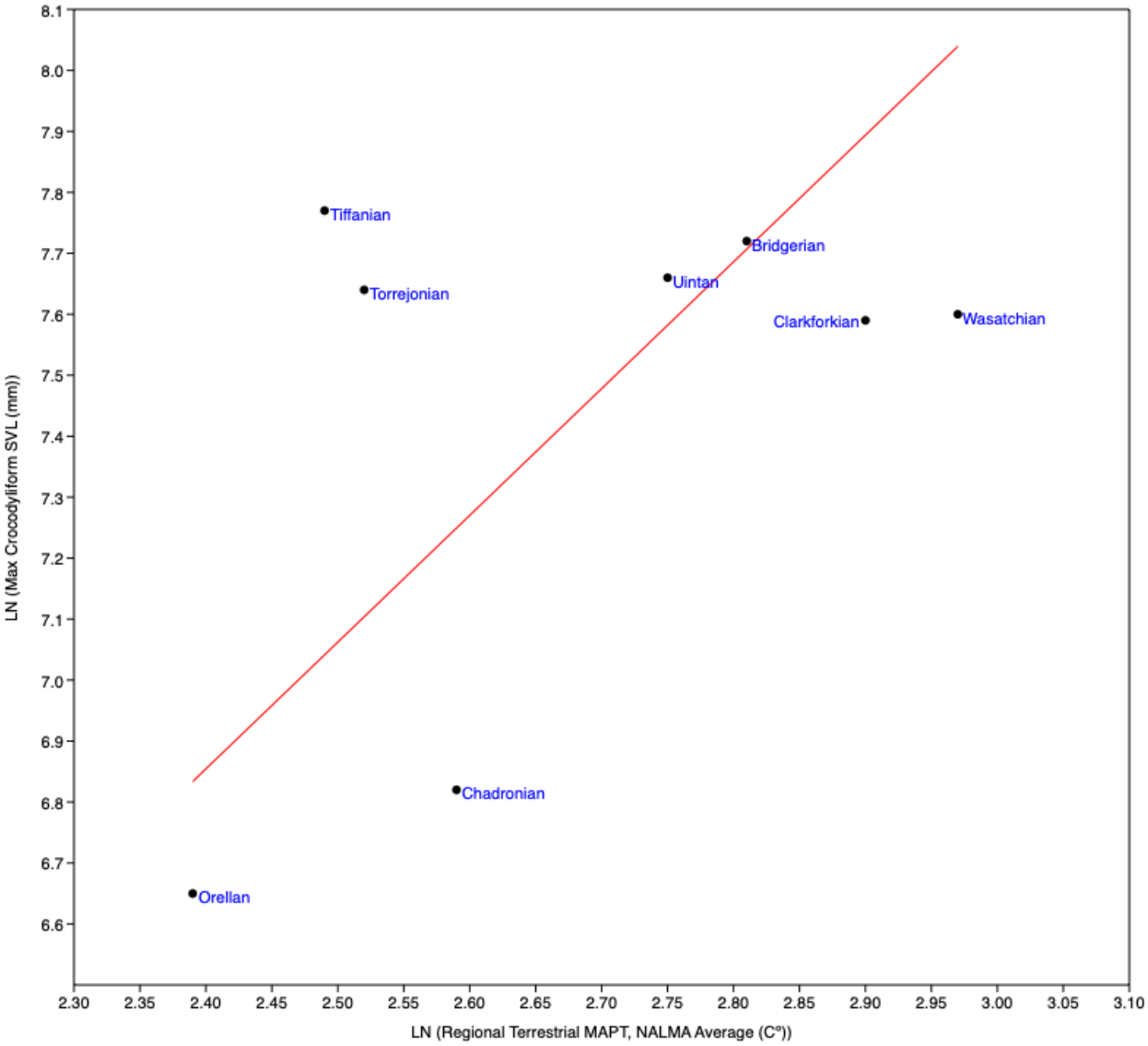

Figure 3.8A. Regional terrestrial mean annual paleotemperature (MAPT) correlated with maximum crocodyliform snout-vent length (SVL) from across the Western Interior of North America through the Paleogene. All values are transformed using natural log. Regional terrestrial MAPT is averaged by North American Land Mammal Age (NALMA) across the Western Interior of North America (see Fig 3.7 for sample sizes). References for MAPT data are listed in S3.1 Dataset. The Puercan and Duchesnean are omitted due to low sample size. Regression equation: LN(Max Croc SVL) = (2.079 * (LN(Reg. Terr. MAPT)) + 1.865; R^2 = 0.25, p(uncorr.) = 0.21, n = 8.

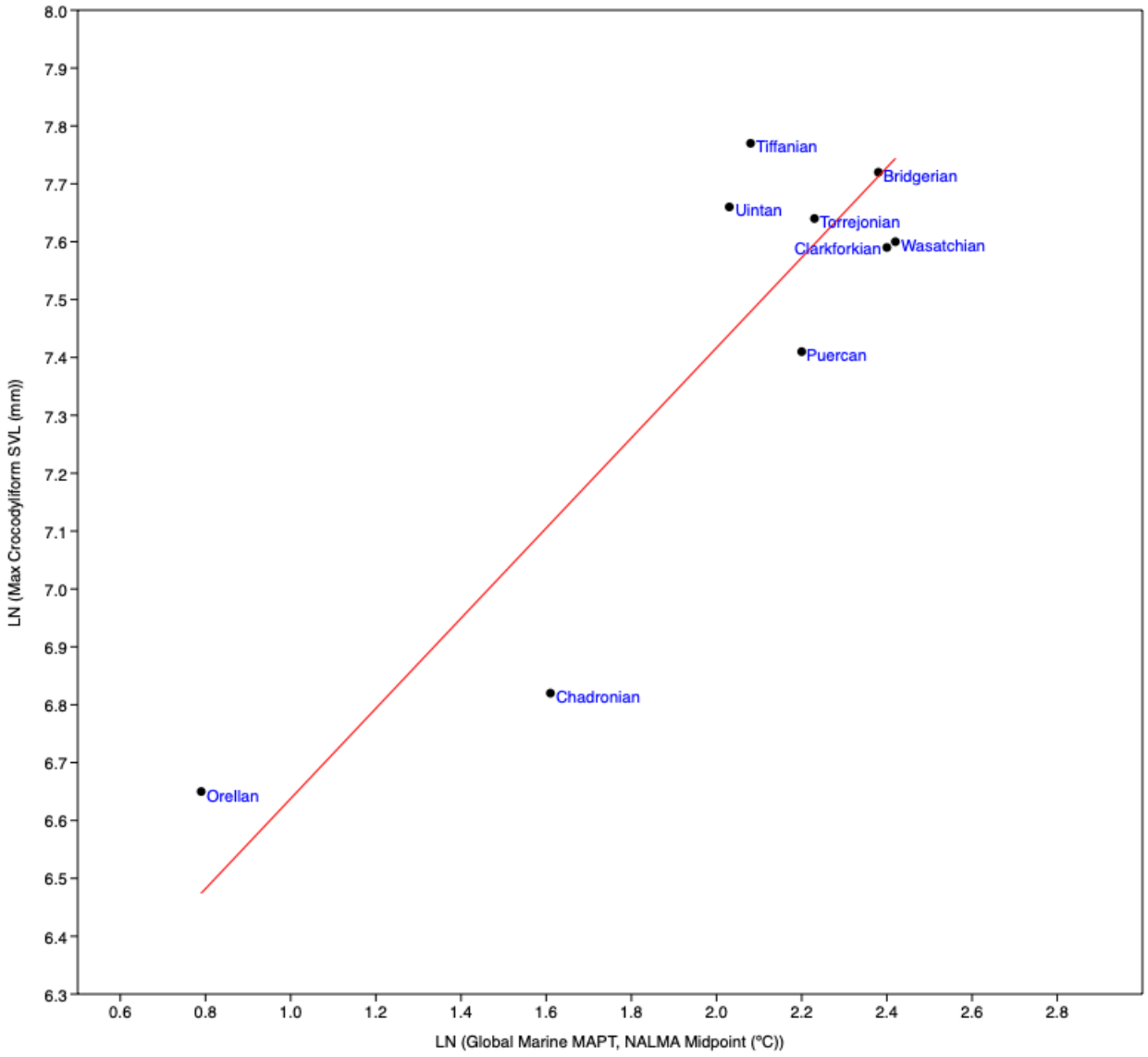

Figure 3.8B. Global marine mean annual paleotemperature (MAPT) correlated with maximum crocodyliform snout-vent length (SVL) from across the Western Interior of North America through the Paleogene. All values are transformed using natural log. Global marine MAPT data come from Zachos et al. (2008) and represent NALMA midpoint values. The Duchesnean is omitted for consistency. Regression equation: LN(Max Croc SVL) = (0.779 * (LN(Global Marine MAPT)) + 5.859; R^2 = 0.78, p(uncorr.) = 0.002, n = 9.

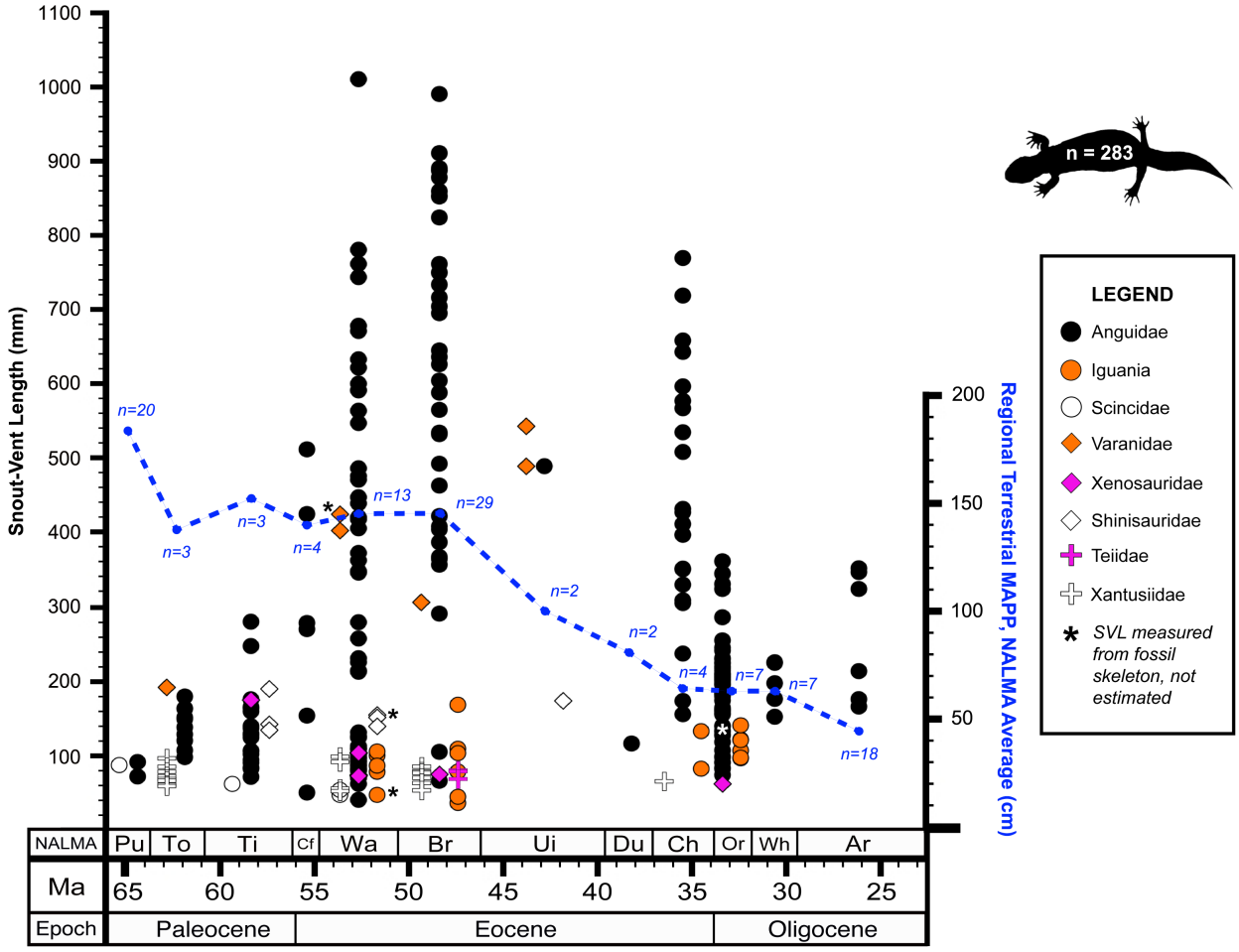

Figure 3.9. Paleogene lizard snout-vent length by taxonomic group plotted against regional terrestrial mean annual paleoprecipitation (MAPP) across the Western Interior of North America. Regional MAPP (blue dashed line) is averaged by North American Land Mammal Age (NALMA). Sample sizes with blue dashed line indicate number of MAPP data points sampled from each NALMA interval. SVL data points are arbitrarily spread within each NALMA for visibility. Data points marked with an asterisk (*) were measured from complete fossil skeletons. All others were estimated from individual cranial or limb bones using regressions and sometimes ratios (see S1.1-1.10 Tables). References for MAPP data are listed in S3.2 Dataset. NALMA abbreviations: Pu = Puercan, To = Torrejonian, Ti = Tiffanian, Cf = Clarkforkian, Wa = Wasatchian, Br = Bridgerian, Ui = Uintan, Du = Duchesnean, Ch = Chadronian, Or = Orellan, Wh = Whitneyan, Ar = Arikareean.

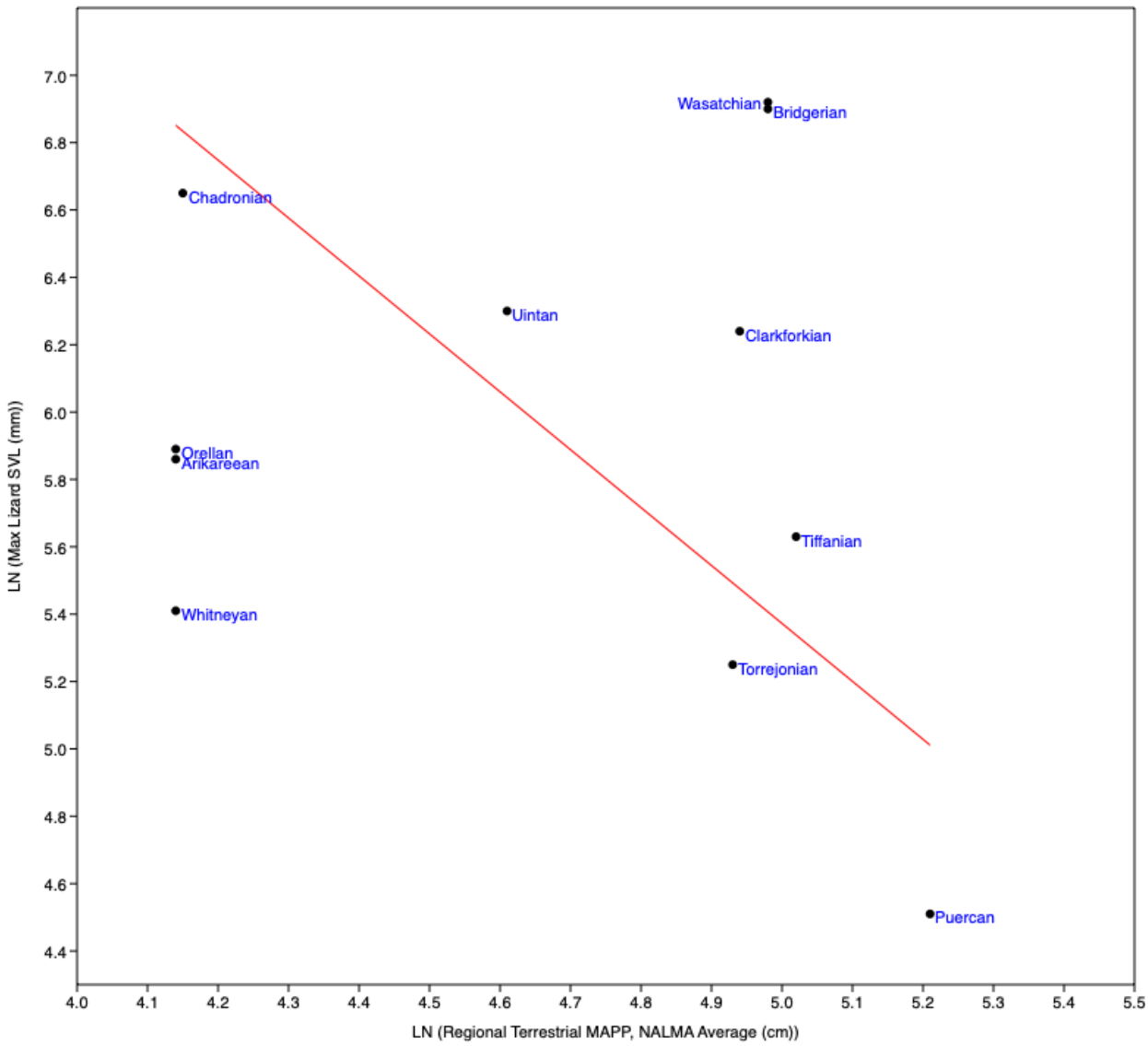

Figure 3.10. Regional terrestrial mean annual paleoprecipitation (MAPP) correlated with maximum lizard snout-vent length (SVL) across the Western Interior of North America through the Paleogene. All values are transformed using natural log. Regional MAPP is averaged by North American Land Mammal Age (NALMA; see Fig 3.9 for sample sizes). Castle Rock data are included in the Puercan value in this graph. The Duchesnean is omitted due to low sample size. References for MAPP data are listed in S3.2 Dataset. Regression equation: LN(Max Lizard SVL) = (-1.72 * (LN(MAPP)) + 13.972; R^2 = 0.02, p(uncorr.) = 0.70, n = 11.

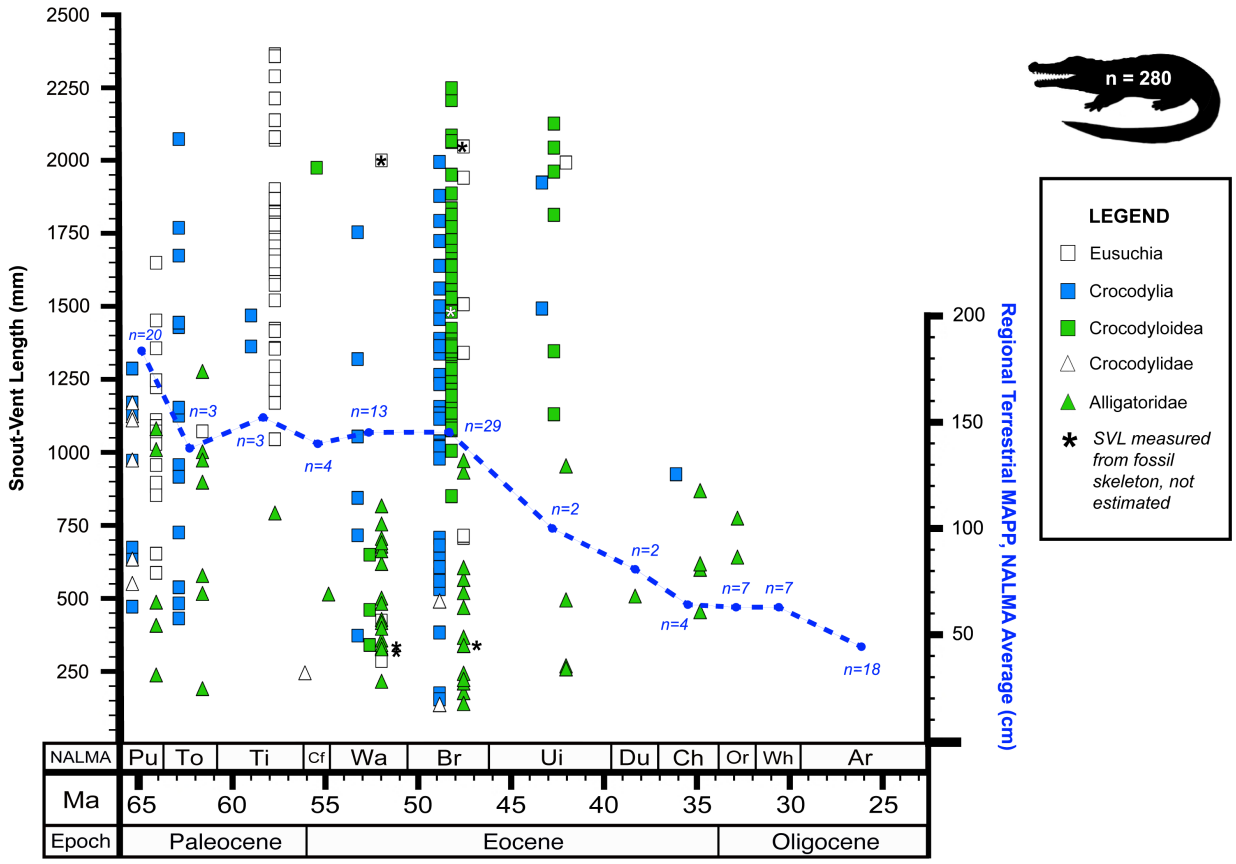

Figure 3.11. Paleogene crocodyliform snout-vent lengths by taxonomic group plotted against regional terrestrial mean annual paleoprecipitation (MAPP). Regional terrestrial MAPP (blue dashed line) is averaged by North American Land Mammal Age (NALMA) across the Western Interior of North America. Sample sizes with blue dashed line indicate number of MAPP data points sampled from each NALMA interval. SVL data points are arbitrarily spread within each NALMA for visibility. Data points marked with an asterisk (*) were measured from complete fossil skeletons. All others were estimated from individual cranial or limb bones using regressions (see S2.1 Table). References for MAPP data are listed in S3.2 Dataset. NALMA abbreviations: Pu = Puercan, To = Torrejonian, Ti = Tiffanian, Cf = Clarkforkian, Wa = Wasatchian, Br = Bridgerian, Ui = Uintan, Du = Duchesnean, Ch = Chadronian, Or = Orellan, Wh = Whitneyan, Ar = Arikareean.

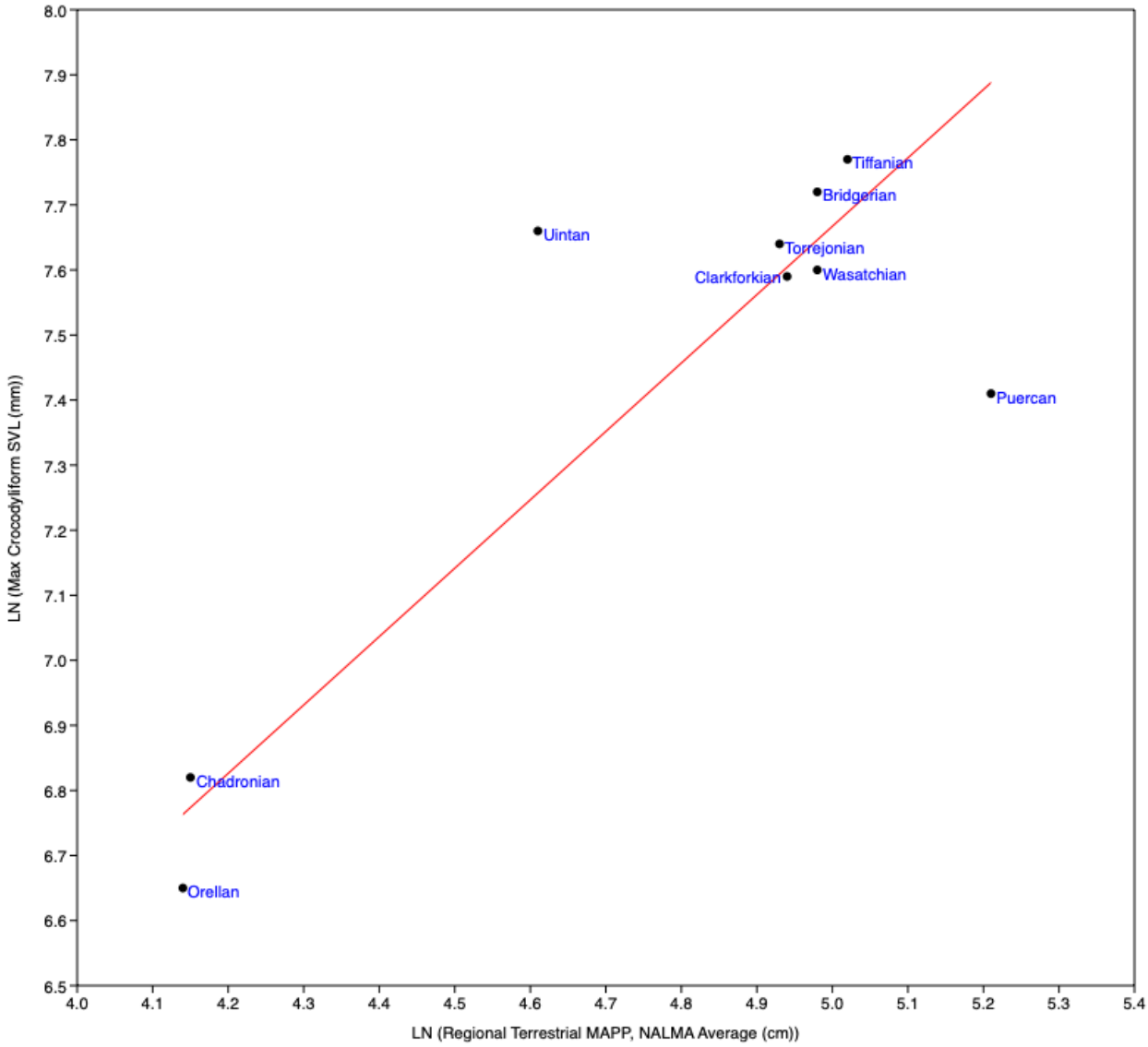

Figure 3.12. Regional terrestrial mean annual paleoprecipitation (MAPP) correlated with maximum crocodyliform snout-vent length (SVL) across the Western Interior of North America through the Paleogene. All values are transformed using natural log. Regional MAPP is averaged by North American Land Mammal Age (NALMA; see Fig 3.11 for sample sizes). Castle Rock data are included in the Puercan value in this graph. The Duchesnean is omitted due to low sample size. References for MAPP data are listed in S3.2 Dataset. Regression equation: LN(Max Croc SVL) = (1.051 * (LN(MAPP)) + 2.411; R^2 = 0.71, p(uncorr.) = 0.004, n = 9.

TABLES & CAPTIONS

CHAPTER 1 TABLES

Table 1.1. Summary of datasets and regressions.

Taxonomic group	# Fossil specimens	# Extant specimens	# Extant species sampled*	Preservation of extant specimens	Anatomical elements regressed to SVL or LN(SVL) (LN = natural log transformed)
Anguidae	218	66	17	Dry only	LN(HL), LN(MnL), LN(DL), LN(MxL), LN(FrL), LN(PaL), LN(HuL), LN(FeL)
Helodermatidae	0	67	2	Dry & Wet	HL
Varanidae	6	47	17	Dry only	DL, MxL, TiL
Teiidae	3	33	11	Dry only	LN(DL)
Scincidae	4	28	19	Dry only	LN(DL), LN(MxL)
Xantusiidae	19	20	3	Dry only	LN(DL), MxL
Xenosauridae	7	17	3	Dry & Wet	DL, FrL, PaL
Iguania	19	55	16	Dry only	LN(HL), LN(DL), LN(MxL)
Shinisauridae	7	N/A	N/A	N/A	N/A
Total	**283**	**333**	**88**	**N/A**	**N/A**

Abbreviations: DL = Dentary Length, FeL = Femur Length, FrL = Frontal Length, HL = Head Length, HuL = Humerus Length, MnL = Mandible Length, MxL = Maxilla Length, PaL = Parietal Length, TiL = Tibia Length. Modes of preservation: Dry = dry skeletonized, Wet = wet preserved in ethanol.

*Subspecies are included in these totals.

Table 1.2. Lizard crown group diversity by NALMA interval.

Epoch	NALMA (Mya)	Lizard Crown Groups Sampled
Paleocene	Puercan (66.0 - 63.8)	Anguidae Scincidae
	Torrejonian (63.8 - 60.9)	Anguidae Varanidae Xantusiidae
	Tiffanian (60.9 - 56.2)	Anguidae Scincidae Shinisauridae Xenosauridae
	Clarkforkian (56.2 - 54.9)	Anguidae
Eocene		
	Wasatchian (54.9 - 50.5)	Anguidae Iguania Scincidae Shinisauridae Varanidae Xantusiidae Xenosauridae
	Bridgerian (50.5 - 46.2)	Anguidae Iguania Teiidae Varanidae Xantusiidae Xenosauridae
	Uintan (46.2 - 39.7)	Anguidae Shinisauridae Varanidae
	Duchesnean (39.7 - 37.0)	Anguidae
	Chadronian (37.0 - 33.9)	Anguidae Iguania Xantusiidae
Oligocene	Orellan (33.9 - 31.8)	Anguidae Iguania Xenosauridae
	Whitneyan (31.8 - 29.5)	Anguidae
	Arikareean (29.5 - 23.0)	Anguidae

This table does not represent the full taxonomic diversity of Paleogene lizards represented in the U.S. Western Interior fossil record; it only represents groups for which I found complete fossil cranial or limb bones. NALMA dates are from Barnosky et al. (2014).

Table 1.3. Maximum lizard body size estimate per NALMA interval.

NALMA	Age Range (Mya)	Crown Group	Binomial	Specimen	Basin	Max SVL Estimate (mm)	Max Mass Estimate (kg)
Puercan	66.0-63.8	Anguidae	*cf. Odaxosaurus piger*	UCM 34991	DB	91	0.022
Torrejonian	63.8-60.9	Varanidae	cf. Varanidae indet.	UCMP 2671	CMB	191	0.20
Tiffanian	60.9-56.2	Anguidae	*Melanosaurus sp.*	UCM 98615	PCB	279	0.62
Clarkforkian	56.2-54.9	Anguidae	*Melanosaurus maximus*	UMMP 74618	BB	512	3.8
Wasatchian	54.9-50.5	Anguidae	*Paraglyptosaurus princeps*	USNM 6004	HuB	1012	28.8
Bridgerian	50.5-46.2	Anguidae	*Glyptosaurus sylvestris*	USNM 12590	GRB	992	27.2
Uintan	46.2-39.7	Varanidae	*Saniwa ensidens*	FMNH UC1719	UB	542	4.5
Duchesnean	39.7-37.0	N/A	N/A	N/A	N/A	N/A	N/A
Chadronian	37.0-33.9	Anguidae	*Helodermoides sp.*	UW 11057	PRB	769	12.7
Orellan	33.9-31.8	Anguidae	*Peltosaurus sp.*	UCM 20877	WGP	360	1.3
Whitneyan	31.8-29.5	Anguidae	*Peltosaurus sp.*	SMM P81.8.71	WGP	224	0.32
Arikareean	29.5-23.0	Anguidae	*Peltosaurus sp.*	UNSM 81001	WGP	351	1.2

The Duchesnean is listed as “N/A" because I only have one specimen from that North American Land Mammal Age (NALMA) and it is very small compared to the maxima before and after it. Basin acronyms: BB = Bighorn Basin, CMB = Crazy Mountains Basin, DB = Denver Basin, GRB = Green River Basin, HuB = Huerfano Basin, PCB = Piceance Creek Basin, PRB = Powder River Basin, UB = Uinta Basin, WGP = Western Great Plains.

CHAPTER 2 TABLES

Table 2.1. Maximum crocodyliform body size estimate per NALMA interval.

NALMA	Age Range (Mya)	Most Specific Taxonomic Group	Binomial	Specimen	Basin	Max SVL Estimate (mm)	Max Mass Estimate (kg)
Puercan	66.0-63.8	Eusuchia	*Borealosuchus sternbergii*	UCMP 138375	WB	1651	3.624
Torrejonian	63.8-60.9	Crocodylia	Crocodylia indet.	NMMNH P-35001	SJB	2073	4.875
Tiffanian	60.9-56.2	Eusuchia	*Borealosuchus formidabilis*	SMM P82.12.700	WB	2361	5.777
Clarkforkian	56.2-54.9	Crocodyloidea	*"Crocodylus" sp.*	UCM 46874	PRB	1972	4.567
Wasatchian	54.9-50.5	Eusuchia	*Borealosuchus wilsoni*	FMNH PR 1674	GRB	2000	4.653
Bridgerian	50.5-46.2	Crocodyloidea	*"Crocodylus" sp.*	UW 3155	GRB	2244	5.407
Uintan	46.2-39.7	Crocodyloidea	*"Crocodylus" affinis*	FMNH P 12202	UB	2123	5.030
Duchesnean	39.7-37.0	N/A	N/A	N/A	N/A	N/A	N/A
Chadronian	37.0-33.9	Crocodylia	Crocodylia indet.	FLMNH UF 209734	WGP	920	1.694
Orellan	33.9-31.8	Alligatoridae	*Alligator prenasalis*	AMNH 4994	WGP	771	1.346

The Duchesnean is listed as "N/A" because I only have one specimen from that North American Land Mammal Age (NALMA) and it is small compared to the maxima before and after it. Basin acronyms: GRB = Green River Basin, PRB = Powder River Basin, SJB = San Juan Basin, UB = Uinta Basin, WB = Williston Basin, WGP = Western Great Plains. Maximum body size estimates per NALMA for lizards are listed in Table 1.3. Age ranges listed here are based on Barnosky et al. (2014).

Table 2.2. Maximum and mean SVLs for Paleogene and extant crocodyliforms.

	PALEOGENE		EXTANT		
Taxonomic Group	**Max SVL**	**Mean SVL**	**Max SVL**	**Mean SVL**	**Extant Data Source**
Alligatoridae	1276	557	1963	1056 – 1784	Upper range of mean SVL based on data from Woodward et al. (1995).
Crocodylidae	1170	713	2928	1260	Maximum SVL from Guinness World Records*; Mean SVL based on data from Fukuda et al. (2013), calculated using equations from O'Brien et al. (2019).
Other Paleogene Crocodyliforms	2361	1397	N/A	N/A	N/A

*guinnessworldrecords.com

The extant values listed for the crown group families are based only on specimens of the largest-bodied species members: *Alligator mississippiensis* for Alligatoridae and *Crocodylus porosus* for Crocodylidae. Data are from this study (S2.1, S2.2 Datasets) unless otherwise noted. All data come from North America except the data for extant *C. porosus.*

CHAPTER 3 TABLES

Table 3.1. Climate and body size correlation data.

Climate Data

NALMA	Regional Terrestrial MAPT (ºC)	LN (Reg. Terr. MAPT (Cº))	Global Marine MAPT** (ºC)	LN (Global Marine MAPT** (ºC))	Regional Terrestrial MAPP (cm)	LN (Reg. Terr. MAPP (cm))	First Differences LN (Reg. Terr. MAPT (Cº))	First Diffs. LN (Global Marine MAPT** (ºC))	First Diffs. LN (Reg. Terr. MAPP (cm))
Puercan	17.9 (*12.6)	2.89 (*2.54)	9.00	2.20	183 (*192)	5.21 (*5.25)	–	–	–
Torrejonian	12.4	2.52	9.30	2.23	138	4.93	0.369 (*0.019)	0.033	0.280 (*0.328)
Tiffanian	12.1	2.49	8.00	2.08	152	5.02	0.024	0.151	0.097
Clarkforkian	18.2	2.90	11.0	2.40	140	4.94	0.410	0.318	0.084
Wasatchian	19.5	2.97	11.3	2.42	146	4.98	0.068	0.027	0.040
Bridgerian	16.7	2.81	10.8	2.38	146	4.98	0.157	0.045	0.002
Uintan	15.7	2.75	7.60	2.03	100	4.61	0.064	0.351	0.377
Duchesnean	11.3	2.43	6.00	1.79	81	4.39	0.322	0.236	0.212
Chadronian	13.3	2.59	5.00	1.61	64	4.15	0.160	0.182	0.239
Orellan	10.9	2.39	2.20	0.790	63	4.14	0.200	0.821	0.015
Whitneyan	11.4	2.43	2.50	0.920	63	4.14	0.043	0.128	0.001
Arikareean	9.70	2.27	3.50	1.25	45	3.80	0.157	0.336	0.341

*With Castle Rock data removed
** NALMA Midpoint

Lizard Snout-Vent Length (SVL) Data

NALMA	Max Lizard SVL (mm)	LN (Max Lizard SVL (mm))	90th Percentile Max Lizard SVL (mm)	LN (90th % Max Lizard SVL (mm))	Mean Lizard SVL (mm)	LN (Mean Lizard SVL (mm))	First Diffs. LN (Max Lizard SVL (mm))	First Diffs. LN (90th % Max Lizard SVL (mm))	First Diffs. LN (Mean Lizard SVL (mm))
Puercan	91	4.51	91	4.51	83	4.42	–	–	–
Torrejonian	191	5.25	191	5.25	113	4.73	0.741	0.741	0.309
Tiffanian	279	5.63	279	5.63	134	4.89	0.381	0.381	0.166
Clarkforkian	512	6.24	512	6.24	281	5.64	0.606	0.606	0.743
Wasatchian	1012	6.92	634	6.92	275	5.62	0.682	0.682	0.021
Bridgerian	992	6.90	627	6.90	452	6.11	0.020	0.020	0.496
Uintan	542	6.30	542	6.30	423	6.05	0.604	0.604	0.066
Duchesnean	116	4.75	116	4.75	116	4.75	–	–	–
Chadronian	769	6.65	596	6.65	404	6.00	0.350	0.350	0.045
Orellan	360	5.89	360	5.89	176	5.17	0.759	0.759	0.832
Whitneyan	224	5.41	224	5.41	194	5.27	0.473	0.473	0.098
Arikareean	351	5.86	351	5.86	262	5.57	0.447	0.447	0.301

Crocodyliform Snout-Vent Length (SVL) Data

NALMA	Max Croc SVL (mm)	LN (Max Croc SVL (mm))	90th Percentile Max Croc SVL (mm)	LN (90th % Max Croc SVL)	Mean Croc SVL (mm)	LN (Mean Croc SVL (mm))	First Differences LN (Max Croc SVL (mm))	First Diffs. LN (90th % Max Croc SVL (mm))	First Diffs. LN (Mean Croc SVL (mm))
Puercan	1651	7.41	1651	7.41	968	6.87	–	–	–
Torrejonian	2073	7.64	1768	7.48	1008	6.92	0.228	0.068	0.041
Tiffanian	2361	7.77	1865	7.53	1681	7.43	0.130	0.053	0.511
Clarkforkian	1972	7.59	509	6.23	906	6.81	0.180	1.299	0.618
Wasatchian	2000	7.60	1754	7.47	650	6.48	0.014	1.237	0.332
Bridgerian	2244	7.72	1875	7.54	1240	7.12	0.115	0.067	0.646
Uintan	2123	7.66	1810	7.50	1365	7.22	0.056	0.035	0.096
Duchesnean	503	6.22	503	6.22	503	6.22	–	–	–
Chadronian	920	6.82	920	6.82	688	6.53	0.836	0.677	0.685
Orellan	771	6.65	771	6.65	704	6.56	0.177	0.177	0.023

Numbers are NALMA averages unless otherwise indicated. See Figs 3.1, 3.7, 3.9, and 3.11 for climate data sample sizes. Puercan data are listed with Castle Rock data included and excluded (*). Global marine MAPT data are from Zachos et al. (2008). References for all other climate data are listed in S3.1 and S3.2 Datasets. I omitted the Duchesnean from all correlations because I only had a single specimen for both lizards and crocodyliforms for that NALMA, and the corresponding SVL estimate was low for each. First differences are not listed for the Duchesnean accordingly.

REFERENCES

Adolph SC, Porter WP. 1993. Temperature, activity, and lizard life histories. Am Nat 142:273–95.

Allen SE. 2015. Fossil palm flowers from the Eocene of the Rocky Mountain Region with affinities to *Phoenix* L. (Arecaceae: Coryphoideae). Int J Plant Sci 176:586–96.

Allen SE. 2017a. The uppermost lower Eocene Blue Rim flora from the Bridger Formation of Southwestern Wyoming: Floristic composition, paleoclimate, and paleoecology.

Allen SE. 2017b. Reconstructing the local vegetation and seasonality of the lower Eocene Blue Rim site of Southwestern Wyoming using fossil wood. Int J Plant Sci 178:689–714.

Alroy J. 1998. Cope's Rule and the Dynamics of Body Mass Evolution in North American Fossil Mammals. Science (80-) 280:731–34.

Alroy J. 2000. New Methods for Quantifying Macroevolutionary Patterns and Processes. Paleobiology 26:707–33.

Andreone F, Guarino FM. 2003. Giant and long-lived? Age structure in *Macroscincus coctei*, an extinct skink from Cape Verde. Amphib Reptil 24:459–70.

Angielczyk KD, Burroughs RW, Feldman CR. 2015. Do turtles follow the rules? Latitudinal gradients in species richness, body size, and geographic range area of the world's turtles. J Exp Zool Part B Mol Dev Evol 324:270–94.

Angilletta, Jr. MJ, Niewiarowski PH, Dunham AE, Leaché AD, Porter WP. 2004. Bergmann's Clines in Ectotherms: Illustrating a Life-History Perspective with Sceloporine Lizards. Am Nat 164:E168–83.

Angilletta MJ, Dunham AE. 2003. The Temperature-Size Rule in Ectotherms: Simple Evolutionary Explanations May Not Be General. Am Nat 162:332–42.

Angilletta MJ, Steury TD, Sears MW. 2004. Temperature, growth rate, and body size in ectotherms: Fitting pieces of a life-history puzzle. Integr Comp Biol 44:498–509.

Arneth A, Shin YJ, Leadley P, Rondinini C, Bukvareva E, Kolb M, Midgley GF, Oberdorff T, Palomo I, Saito O. 2020. Post-2020 biodiversity targets need to embrace climate change. Proc Natl Acad Sci U S A 117:30882–91.

Arnold EN. 1984. Evolutionary aspects of tail shedding in lizards and their relatives. J Nat Hist 18:127–69.

Ashton KG, Feldman CR. 2003. Bergmann's Rule in Nonavian Reptiles : Turtles Follow It, Lizards and Snakes Reverse It. Evolution (N Y) 57:1151–63.

Aureliano T, Ghilardi AM, Guilherme E, Souza-Filho JP, Cavalcanti M, Riff D. 2015. Morphometry, bite-force, and paleobiology of the Late Miocene caiman *Purussaurus brasiliensis*. PLoS One 10:1–14.

Ballinger RE. 1983. Life-history variations. In: RB H, ER P, TW S, editors. Lizard Ecology: Studies of a Model Organism Cambridge and London: Harvard University Press. p. 241–260.

Ballinger RE, Lemos-Espinal J, Sanoja-Sarabia S, Coady NR. 1995. Ecological observations of the Lizard, *Xenosaurus grandis* in Cuautlapan, Veracruz, Mexico. Biotropica 27:128–32.

Bansal U, Thaker M. 2021. Diet influences latitudinal gradients in life-history traits, but not reproductive output, in ectotherms. Glob Ecol Biogeogr 30:2431–41.

Barnosky AD. 2015. Transforming the global energy system is required to avoid the sixth mass extinction. MRS Energy Sustain 2:1–13.

Barnosky AD, Bell CJ, Emslie SD, Goodwin HT, Mead JI, Repenning CA, Scott E, Shabel AB.

2004. Exceptional record of mid-Pleistocene vertebrates helps differentiate climatic from anthropogenic ecosystem perturbations. Proc Natl Acad Sci U S A 101:9297–9302.
Barnosky AD, Holmes M, Kirchholtes R, Lindsey E, Maguire KC, Poust AW, Allison Stegner M, Sunseri J, Swartz B, Swift J, Villavicencio NA, Wogan GOU. 2014. Prelude to the Anthropocene: Two new North American Land Mammal Ages (NALMAs). Anthr Rev 1:225–42.
Barnosky AD, Matzke N, Tomiya S, Wogan GOU, Swartz B, Quental TB, Marshall C, McGuire JL, Lindsey EL, Maguire KC, Mersey B, Ferrer EA. 2011. Has the Earth's sixth mass extinction already arrived? Nature 471:51–57.
Bartholomew GA, Tucker VA. 1964. Size, body temperature, thermal conductance, oxygen consumption, and heart rate in Australian varanid lizards. Physiol Zool 37:341–54.
Bateman PW, Fleming PA. 2009. To cut a long tail short: A review of lizard caudal autotomy studies carried out over the last 20 years. J Zool 277:1–14.
Beck DD. 2005. Biology of Gila Monsters and Beaded Lizards. 9th ed Berkeley: University of California Press.
Bennett AF. 1987. Evolution of the control of body temperature: Is warmer better? In: Dejours P, Bolis L, Taylor CR, Weibel ER, editors. Comparative Physiology: Life in Water and on Land Padova: IX-Liviana Press. p. 421–31.
Bergmann K. 1847. Über die Ver- hältnisse der wärmeokönomie der Thiere zu ihrer Grösse. Göttinger Stud 3:595–708.
Bertrand OC, Shelley SL, Wible JR, Williamson TE, Holbrook LT, Chester SGB, Butler IB, Brusatte SL. 2020. Virtual endocranial and inner ear endocasts of the Paleocene 'condylarth' *Chriacus*: new insight into the neurosensory system and evolution of early placental mammals. J Anat 236:21–49.
Bloch JI, Boyer DM, Strait SG, Wing SL. 2004. New Sections and Fossils From the Southern Bighorn Basin, Wyoming Document Faunal Turnover During the PETM. In: American Geophysical Union, Fall Meeting.
Boardman GS, Secord R. 2013. Stable isotope paleoecology of White River ungulates during the Eocene-Oligocene climate transition in northwestern Nebraska. Palaeogeogr Palaeoclimatol Palaeoecol 375:38–49.
Bochaton C, Kemp ME. 2017. Reconstructing the body sizes of Quaternary lizards using *Pholidoscelis Fitzinger*, 1843, and Anolis Daudin, 1802, as case studies. J Vertebr Paleontol 37:9 pp.
Bogert CM. 1949. Thermoregulation in reptiles, a factor in evolution. Evolution (N Y) 3:195–211.
Borths MR, Stevens NJ. 2017. The first hyaenodont from the late Oligocene Nsungwe Formation of Tanzania: Paleoecological insights into the Paleogene-Neogene carnivore transition. PLoS One 12:1–30.
Boyer DM, Georgi JA. 2007. Cranial morphology of a pantolestid eutherian mammal from the eocene bridger formation, Wyoming, USA: Implications for relationships and habitat. J Mamm Evol 14:239–80.
Brandt R, Navas CA. 2013. Body size variation across climatic gradients and sexual size dimorphism in Tropidurinae lizards. J Zool 290:192–98.
Brochu CA. 1997. A review of "*Leidyosuchus*" (Crocodyliformes, Eusuchia) from the Cretaceous through Eocene of North America. J Vertebr Paleontol 17:679–97.
Brochu CA. 1999. Phylogenetics, taxonomy, and historical biogeography of Alligatoroidea. J

Vertebr Paleontol 19:9–100.
Brochu CA. 2000. Phylogenetic relationships and divergence timing of *Crocodylus* based on morphology and the fossil record. Copeia 2000:657–73.
Brochu CA. 2003. Phylogenetic approaches toward crocodylian history. Annu Rev Earth Planet Sci 31:357–97.
Brochu CA. 2004. Alligatorine phylogeny and the status of *Allognathosuchus mooki*, 1921. J Vertebr Paleontol 24:857–73.
Brochu CA. 2010. A new alligatorid from the lower Eocene Green River Formation of Wyoming and the origin of Caimans. J Vertebr Paleontol 30:1109–26.
Brochu CA. 2013. Phylogenetic relationships of Palaeogene ziphodont eusuchians and the status of *Pristichampsus* Gervais, 1853. Earth Environ Sci Trans R Soc Edinburgh 103:521–50.
Brochu CA, Adams A, Drumheller SK, Miller-Camp J, Rubin M. 2020. The interplay between regional and global climatic trends in crocodyliform faunal change. In: Journal of Vertebrate Paleontology The Society of Vertebrate Paleontology. p. 85–86.
Bronzati M, Montefeltro FC, Langer MC. 2012. A species-level supertree of Crocodyliformes. Hist Biol 24:598–606.
Bronzati M, Montefeltro FC, Langer MC. 2015. Diversification events and the effects of mass extinctions on Crocodyliformes evolutionary history. R Soc Open Sci 2:1–9.
Cadena EA, Ksepka DT, Jaramillo CA, Bloch JI. 2012. New pelomedusoid turtles from the late Palaeocene Cerrejón Formation of Colombia and their implications for phylogeny and body size evolution. J Syst Palaeontol 10:313–31.
Cadena EA, Scheyer TM, Carrillo-Briceño JD, Sánchez R, Aguilera-Socorro OA, Vanegas A, Pardo M, Hansen DM, Sánchez-Villagra MR. 2020. The anatomy, paleobiology, and evolutionary relationships of the largest extinct side-necked turtle. Sci Adv 6:1–13.
Campione NE, Evans DC. 2012. A universal scaling relationship between body mass and proximal limb bone dimensions in quadrupedal terrestrial tetrapods. BMC Biol 10.
Carlson CG, Anderson SB. 1965. Sedimentary and tectonic history of North Dakota part of Williston Basin. Bull Am Assoc Pet Geol 49:1833–46.
Castanet J, Baez M. 1991. Adaptation and evolution in *Gallotia* lizards from the Canary Islands: Age, growth, maturity and longevity. Amphibia-Reptilia 12:81–102.
Chamaillé-Jammes S, Massot M, Aragón P, Clobert J. 2006. Global warming and positive fitness response in mountain populations of common lizards Lacerta vivipara. Glob Chang Biol 12:392–402.
Cherven VB, Jacob AF. 1985. Evolution of Paleogene Depositional Systems, Williston Basin, in Response to Global Sea Level Changes. In: Cenozoic Paleogeography of the West-Central United States AAPG Rocky Mountain Section (SEPM). p. 127–70.
Chester SGB, Bloch JI, Secord R, Boyer DM. 2010. A New Small-Bodied Species of *Palaeonictis* (Creodonta, Oxyaenidae) from the Paleocene-Eocene Thermal Maximum. J Mamm Evol 17:227–43.
Cicimurri DJ, Knight JL, Self-Trail JM, Ebersole SM. 2016. Late Paleocene glyptosaur (Reptilia: Anguidae) osteoderms from South Carolina, USA. J Paleontol 90:147–53.
Conrad JL. 2006. An Eocene shinisaurid (Reptilia, Squamata) from Wyoming, U.S.A. J Vertebr Paleontol 26:113–26.
Cossette AP, Brochu CA. 2020. A systematic review of the giant alligatoroid *Deinosuchus* from the Campanian of North America and its implications for the relationships at the root of Crocodylia. J Vertebr Paleontol 40:e1767638.

Cruz FB, Fitzgerald LA, Espinoza RE, Schulte II JA. 2005. The importance of phylogenetic scale in tests of Bergmann's and Rapoport's rules: lessons from a clade of South American lizards. J Evol Biol 18:1559–74.
Damuth J. 1990. Problems in estimating body masses of archaic ungulates using dental measurements. Body Size Mamm Paleobiol Estim Biol Implic 229:tables 16.9-16.10.
Davies-Vollum KS. 1997. Early Palaeocene palaeoclimatic inferences from fossil floras of the western interior, USA. Palaeogeogr Palaeoclimatol Palaeoecol 136:145–64.
Davis J. 1967. Growth and Size of the Western Fence Lizard (*Sceloporus occidentalis*). Copeia 1967:721–31.
Davis MB, Shaw RG. 2001. Range shifts and adaptive responses to quaternary climate change. Science (80-) 292:673–79.
Dayan T, Simberloff D, Tchernov E, Yom-Tov Y. 1991. Calibrating the paleothermometer: climate, communities, and the evolution of size. Paleobiology 17:189–99.
Dettman DL, Lohmann KC. 2000. Oxygen isotope evidence for high-altitude snow in the Laramide Rocky Mountains of North America during the Late Cretaceous and Paleogene. Geology 28:243–46.
Dickinson WR, Klute MA, Hayes MJ, Janecke SU, Lundin ER, Mckittrick MA, Olivares MD. 1988. Paleogeographic and paleotectonic setting of Laramide sedimentary basins in the central Rocky Mountain region: Reply. Geol Soc Am Bull 100:1023–39.
Douglass E. 1903. New vertebrates from the Montana Tertiary. Ann Carnegie Museum 2:145–99.
Dudgeon TW, Maddin HC, Evans DC, Mallon JC. 2020. The internal cranial anatomy of *Champsosaurus* (Choristodera: Champsosauridae): Implications for neurosensory function. Sci Rep 10:1–20.
Dzombak RM, Midttun NC, Stein RA, Sheldon ND. 2021. Incorporating lateral variability and extent of paleosols into proxy uncertainty. Palaeogeogr Palaeoclimatol Palaeoecol 582:110641.
Egi N. 2001. Body mass estimates in extinct mammals from limb bone dimensions: The case of North American Hyaenodontids. Palaeontology 44:497–528.
Elder WP, Kirkland JI. 1994. Cretaceous paleogeography of the southern western interior region, Mesozoic Systems of the Rocky Mountain Region, USA.
ElShafie SJ. 2014. Body size and species richness changes in Glyptosaurinae (Squamata: Anguidae) through climatic transitions of the North American Cenozoic. Master's Thesis. Department of Earth & Atmospheric Sciences: University of Nebraska, Lincoln.
Erickson BR. 1999. Fossil Lake Wannagan (Paleocene: Tiffanian) – Billings County, North Dakota. North Dakota Geol Surv MS:1–14.
Erickson GM, Gignac PM, Steppan SJ, Lappin AK, Vliet KA, Brueggen JD, Inouye BD, Kledzik D, Webb GJW. 2012. Insights into the ecology and evolutionary success of crocodilians revealed through bite-force and tooth-pressure experimentation. PLoS One 7:e31781.
Eronen JT, Janis CM, Chamberlain CP, Mulch A. 2015. Mountain uplift explains differences in palaeogene patterns of mammalian evolution and extinction between North America and Europe. Proc R Soc B Biol Sci 282:1–8.
Estes R, De Queiroz K, Gauthier J. 1988. Phylogenetic Relationships within Squamata. In: Estes R, Pregill G, editors. Phylogenetic Relationships of the Lizard Families Palo Alto, CA: Stanford University Press. p. 119–281.
Estes RA, Hutchison JH. 1980. Eocene lower vertebrates from Ellesmere Island, Canadian Arctic

Archipelago. Palaeogeogr Palaeoclimatol Palaeoecol 30:325–47.
Evanoff E, Prothero DR, Lander RH. 1992. Eocene-Oligocene climatic change in North America: The White River Formation near Douglas, east-central Wyoming. In: Eocene-Oligocene Climatic and Biotic Evolution p. 116–30.
Evans SE. 2008. The Skull of Lizards and Tuatara. In: Gans C, Gaunt AS, Adler K, editors. The Skull of Lepidosauria. Volume 20,. ed Ithaca, NY: Society for the Study of Amphibians and Reptiles. p. 1–348.
Ezcurra MD. 2016. The phylogenetic relationships of basal archosauromorphs, with an emphasis on the systematics of proterosuchian archosauriforms. PeerJ 2016:e1778.
Fan M, Carrapa B. 2014. Late Cretaceous-early Eocene Laramide uplift, exhumation, and basin subsidence in Wyoming: Crustal responses to flat slab subduction. Tectonics 33:509–29.
Farlow JO, Hurlburt GR, Elsey RM, Britton ARC, Langston W. 2005. Femoral dimensions and body size of *Alligator mississippiensis*: Estimating the size of extinct mesoeucrocodylians. J Vertebr Paleontol 25:354–69.
Feldman A, Meiri S. 2014. Australian Snakes Do Not Follow Bergmann's Rule. Evol Biol 41:327–35.
Figueirido B, Pérez-Claros JA, Hunt RM, Palmqvist P. 2011. Body mass estimation in amphicyonid carnivoran mammals: A multiple regression approach from the skull and skeleton. Acta Palaeontol Pol 56:225–46.
Foreman BZ, Heller PL, Clementz MT. 2012. Fluvial response to abrupt global warming at the Palaeocene/Eocene boundary. Nature 491:92–95.
Fricke HC. 2003. Investigation of early Eocene water-vapor transport and paleoelevation using oxygen isotope data from geographically widespread mammal remains. Bull Geol Soc Am 115:1088–96.
Fricke HC, Wing SL. 2004. Oxygen isotope and paleobotanical estimates of temperature and d18O-latitude gradients over North America during the early Eocene. Am J Sci 304:612–35.
Frost DR, Etheridge R. 1989. A phylogenetic analysis and taxonomy of iguanian lizards. Univ Kansas Museum Nat Hist Misc Publ 81:1–65.
Fukuda Y, Saalfeld K, Lindner G, Nichols T. 2013. Estimation of total length from head length of saltwater crocodiles (*Crocodylus porosus*) in the Northern Territory, Australia. J Herpetol 47:34–40.
Gauthier JA. 1982. Fossil xenosaurid and anguid lizards from the early Eocene Wasatch Formation, southeast Wyoming, and a revision of the Anguioidea. Contrib to Geol Univ Wyoming 21:7–54.
Gauthier JA, Kearney M, Maisano JA, Rieppel O, Behlke ADB. 2012. Assembling the Squamate Tree of Life : Perspectives from the Phenotype and the Fossil Record Assembling the Squamate Tree of Life : Perspectives from the Phenotype and the Fossil Record. Bull Peabody Museum Nat Hist 53:3–308.
Gearty W, Payne JL. 2020. Physiological constraints on body size distributions in Crocodyliformes. Evolution (N Y) 74:245–55.
Gilbert EAB, Payne SL, Vickaryous MK. 2013. The anatomy and histology of caudal autotomy and regeneration in lizards. Physiol Biochem Zool 86:631–44.
Gilmore CW. 1928. Fossil Lizards of North America. Mem Natl Acad Sci 22:v–201.
Gingerich P. 1980. Early Cenozoic paleontology and stratigraphy of the Bighorn Basin, Wyoming. Pap Paleontol 24:1–156.
Gingerich PD. 1978. New Condylarthra (Mammalia) from the Paleocene and early Eocene of

North America. Contrib from Museum Paleontol Univ Michigan 25:1–9.
Godoy PL, Benson RBJ, Bronzati M, Butler RJ. 2019. The multi-peak adaptive landscape of crocodylomorph body size evolution. BMC Evol Biol 19:1–29.
Grande L. 2013. The Lost World of Fossil Lake Chicago: The University of Chicago Press.
Grant BW, Dunham AE. 1988. Thermally Imposed Time Constraints on the Activity of the Desert Lizard *Sceloporus Merriami*. Ecology 69:167–76.
Grant BW, Dunham AE. 1990. Elevational Covariation in Environmental Constraints and Life Histories of the Desert Lizard *Sceloporus Merriami*. Ecology 71:1765–76.
Greenwood DR, Wing SL. 1995. Eocene continental climates and latitudinal temperature gradients. Geology 23:1044–48.
Greer AE. 1974. On the Maximum Total Length of the Salt-Water Crocodile (*Crocodylus porosus*). J Herpetol 8:381–84.
Greer AE. 2001. Distribution of Maximum Snout-Vent Length among Species of Scincid Lizards. J Herpetol 35:383–95.
Gregory KM, McIntosh WC. 1996. Paleoclimate and paleoelevation of the Oligocene Pitch-Pinnacle flora, Sawatch Range, Colorado. Geol Soc Am Bull 108:545.
Gunnell GF, Gingerich PD. 1993. Skeleton of *Brachianodon westorum*, a new middle Eocene metacheiromyid (Mammalia, Palaeanodonta) from the early Bridgerian (Bridger A) of the southern Green River Basin, Wyoming. Contrib from Museum Paleontol Univ Michigan 28:365–92.
Halliday T, Adler K (Eds.). n.d. The New Encyclopedia of Reptiles and Amphibians. Second. ed Oxford University Press.
Hammer Ø, Harper DAT, Ryan PD. 2001. PAST: Palaeontological Statistics software package for education and data analysis. Palaeontol Electron 4:1–9.
Hampe A, Petit RJ. 2005. IDEAS AND PERSPECTIVES: Conserving biodiversity under climate change: the rear edge matters. Ecol Lett 8:461–67.
Head JJ, Bloch JI, Hastings AK, Bourque JR, Cadena EA, Herrera FA, David Polly P, Jaramillo CA. 2009. Giant boid snake from the Palaeocene neotropics reveals hotter past equatorial temperatures. Nature 457:715–18.
Head JJ, Gunnell GF, Holroyd PA, Howard Hutchison J, Ciochon RL. 2013. Giant lizards occupied herbivorous mammalian ecospace during the Paleogene greenhouse in Southeast Asia. Proc R Soc B Biol Sci 280.
Hecht M. 1975. The morphology and relationships of the largest known terrestrial lizard, *Megalania prisca* Owen, from the Pleistocene of Australia. Proc R Soc Victoria 87:239–50.
Herrera-Flores JA, Stubbs TL, Benton MJ. 2021. Ecomorphological diversification of squamates in the Cretaceous. R Soc Open Sci 8:1–11.
Hill R V., Lucas SG. 2006. New data on the anatomy and relationships of the Paleocene crocodylian *Akanthosuchus langstoni*. Acta Palaeontol Pol 51:455–64.
Hobbs K, Fawcett PJ. 2012. Paleocene climate change in the San Juan Basin, New Mexico: A paleosol perspective. In: American Geophysical Union, Fall Meeting 2012, abstract id. PP11B-2022 American Geophysical Union.
Hoffman A. 1979. Community paleoecology as an epiphenomenal science. Paleobiology1 5:357–79.
Hotton III N. 1955. A survey of adaptive relationships of dentition to the diet in the North American Iguanidae. Am Midl Nat 53:86–114.
Huang S, Eronen JT, Janis CM, Saarinen JJ, Silvestro D, Fritz SA. 2017. Mammal body size

evolution in North America and Europe over 20 Myr: Similar trends generated by different processes. Proc R Soc B Biol Sci 284:1–9.
Huber M, Caballero R. 2011. The early Eocene equable climate problem revisited. Clim Past 7:603–33.
Huey RB. 1974. Behavioral thermoregulation in lizards: Importance of associated costs. Science (80-) 184:1001–3.
Huey RB. 1991. Physiological Consequences of Habitat Selection. Am Nat 137:S91–115.
Huey RB, Hertz PE, Sinervo B. 2003. Behavioral drive versus behavioral inertia in evolution: A null model approach. Am Nat 161:357–66.
Huey RB, Kearney MR, Krockenberger A, Holtum JAM, Jess M, Williams SE. 2012. Predicting organismal vulnerability to climate warming: Roles of behaviour, physiology and adaptation. Philos Trans R Soc B Biol Sci 367:1665–79.
Huey RB, Kingsolver JG. 1989. Evolution of thermal sensitivity of ectotherm performance. Trends Ecol Evol 4:131–35.
Huey RB, Kingsolver JG. 1993. Evolution of Resistance to High Temperature in Ectotherms. Am Nat 142:S21–46.
Huey RB, Losos JB, Moritz C. 2010. Are Lizards toast? Science (80-) 328:832–33.
Huey RB, Slatkin M. 1976. Cost and benefits of lizard thermoregulation. Q Rev Biol 51:363–84.
Huey RB, Stevenson RD. 1979. Integrating Thermal Physiology and Ecology of Ectotherms : A Discussion of Approaches. Am Zool 19:357–66.
Hutchison JH. 1982. Turtle, crocodilian, and champsosaur diversity changes in the Cenozoic of the north-central region of Western United States. Palaeogeogr Palaeoclimatol Palaeoecol 37:149–64.
Hutchison JH. 1992. Western North American reptile and amphibian record across the Eocene-Oligocene boundary and its climatic implications. In: Prothero DR, Berggren WA, editors. Eocene-Oligocene Climatic and Biotic Evolution Princeton: Princeton University Press. p. 451–63.
Hyland EG, Huntington KW, Sheldon ND, Reichgelt T. 2018. Temperature seasonality in the North American continental interior during the Early Eocene Climatic Optimum. Clim Past 14:1391–1404.
Hyland EG, Sheldon ND. 2013. Coupled CO2-climate response during the Early Eocene Climatic Optimum. Palaeogeogr Palaeoclimatol Palaeoecol 369:125–35.
Hyland EG, Sheldon ND. 2016. Examining the spatial consistency of palaeosol proxies: Implications for palaeoclimatic and palaeoenvironmental reconstructions in terrestrial sedimentary basins. Sedimentology 63:959–71.
Janecke SU. 1994. Sedimentation and paleogeography of an Eocene to Oligocene rift zone, Idaho and Montana. Geol Soc Am Bull 106:1083–95.
Janzen DH. 1967. Why Mountain Passes are Higher in the Tropics. Am Nat 101:233–49.
Jardine P. 2011. The Paleocene-Eocene Thermal Maximum. Palaeontol Online 1:1–7.
John-Alder AB, Lowe CH, Bennett AF. 1983. Thermal dependence of locomotory energetics and aerobic capacity of the file monitor (Heloderma suspectum). J Comp Physiol 151:119–26.
Johnson KR, Ellis B. 2002. A Tropical Rainforest in Colorado 1.4 Million Years After the Cretaceous-Tertiary Boundary. Science (80-) 296:2379–83.
Johnson KR, Reynolds ML, Werth KW, Thomasson JR. 2003. Overview of the Late Cretaceous, early Paleocene, and early Eocene megafloras of the Denver Basin, Colorado. Rocky Mt Geol 38:101–20.

Keeling CD, Piper SC, Bacastow RB, Wahlen M, Whorf TP, Heimann M, Meijer HA. 2001. Exchanges of atmospheric CO2 and 13CO2 with the terrestrial biosphere and oceans from 1978 to 2000. I. Global aspects, SIO Reference Series, No. 01-06 San Diego, CA.
Keith DA, Akçakaya HR, Thuiller W, Midgley GF, Pearson RG, Phillips SJ, Regan HM, Araújo MB, Rebelo TG. 2008. Predicting extinction risks under climate change: Coupling stochastic population models with dynamic bioclimatic habitat models. Biol Lett 4:560–63.
Kemp ME, Hadly EA. 2015. Extinction biases in Quaternary Caribbean lizards. Glob Ecol Biogeogr 24:1281–89.
Kingsolver JG, Huey RB. 2008. Size, temperature, and fitness: Three rules. Evol Ecol Res 10:251–68.
Kowalski EA, Dilcher DL. 2003. Warmer paleotemperatures for terrestrial ecosystems. Proc Natl Acad Sci 100:167–70.
Kubisch E, Piantoni C, Williams J, Scolaro A, Navas CA, Ibargüengoytía NR. 2012. Do higher temperatures increase growth in the nocturnal gecko *Homonota darwini* (Gekkota: Phyllodactylidae)? A skeletochronological assessment analyzed at temporal and geographic scales. J Herpetol 46:587–95.
Lakin RJ, Barrett PM, Stevenson C, Thomas RJ, Wills MA. 2020. First evidence for a latitudinal body mass effect in extant Crocodylia and the relationships of their reproductive characters. Biol J Linn Soc 129:875–87.
Lang JW. 2008. Crocodilians. New Encycl Reptil Amphib.
Lavergne S, Mouquet N, Thuiller W, Ronce O. 2010. Biodiversity and climate change: Integrating evolutionary and ecological responses of species and communities. Annu Rev Ecol Evol Syst 41:321–50.
Lawler JJ, Ruesch AS, Olden JD, Mcrae BH. 2013. Projected climate-driven faunal movement routes. Ecol Lett 16:1014–22.
Longrich NR, Bhullar BAS, Gauthier JA. 2012. Mass extinction of lizards and snakes at the Cretaceous-Paleogene boundary. Proc Natl Acad Sci U S A 109:21396–401.
López-Victoria M, Herrón PA, Botello JC. 2011. Notes on the ecology of the lizards from Malpelo Island, Colombia. Bull Mar Coast Res 40:79–89.
Losos JB, Greene HW. 1988. Ecological and evolutionary implications of diet in monitor lizards. Biol J Linn Soc 35:379–407.
Lovegrove BG, Mowoe MO. 2013. The evolution of mammal body sizes: Responses to Cenozoic climate change in North American mammals. J Evol Biol 26:1317–29.
Lüthi D, Le Floch M, Bereiter B, Blunier T, Barnola JM, Siegenthaler U, Raynaud D, Jouzel J, Fischer H, Kawamura K, Stocker TF. 2008. High-resolution carbon dioxide concentration record 650,000-800,000 years before present. Nature 453:379–82.
MacFarling Meure C, Etheridge D, Trudinger C, Steele P, Langenfelds R, Van Ommen T, Smith A, Elkins J. 2006. Law Dome CO2, CH4 and N2O ice core records extended to 2000 years BP. Geophys Res Lett 33:2000–2003.
Makarieva AM, Gorshkov VG, Li BL. 2005a. Gigantism, temperature and metabolic rate in terrestrial poikilotherms. Proc R Soc B Biol Sci 272:2325–28.
Makarieva AM, Gorshkov VG, Li BL. 2005b. Temperature-associated upper limits to body size in terrestrial poikilotherms. Oikos 111:425–36.
Mannion PD, Benson RBJ, Carrano MT, Tennant JP, Judd J, Butler RJ. 2015. Climate constrains the evolutionary history and biodiversity of crocodylians. Nat Commun 6:1–9.
Markwick PJ. 1998a. Fossil crocodilians as indicators of Late Cretaceous and Cenozoic climates:

Implications for using palaeontological data in reconstructing palaeoclimate. Palaeogeogr Palaeoclimatol Palaeoecol 137:205–71.
Markwick PJ. 1998b. Fossil crocodilians as indicators of Late Cretaceous and Cenozoic climates: Implications for using palaeontological data in reconstructing palaeoclimate. Palaeogeogr Palaeoclimatol Palaeoecol 137:205–71.
Markwick PJ. 1998c. Crocodilian Diversity in Space and Time: The Role of Climate in Paleoecology and its Implication for Understanding K / T Extinctions. Paleobiology 24:470–97.
Marsh OC. 1871. Notice of some new fossil reptiles from the Cretaceous and Tertiary formations. Am J Sci 1:447–59.
Marsh OC. 1872. Preliminary description of new Tertiary reptiles, Parts I & II. Am J Sci 4:298–309.
Masson-Delmotte V, Zhai P, Pörtner H-O, Roberts D, Skea J, Shukla PR, Pirani A, Moufouma-Okia W, Péan C, Pidcock R, Connors S, Matthews JBR, Chen Y, Zhou X, Gomis MI, Lonnoy E, Maycock T, Tignor M, Waterfield T. 2018. IPCC, 2018: Summary for Policymakers. In: Global Warming of 1.5°C. An IPCC Special Report on the impacts of global warming of 1.5°C above pre-industrial levels and related global greenhouse gas emission pathways, in the context of strengthening the global Geneva, Switzerland.
McInerney FA, Wing SL. 2011. The Paleocene-Eocene Thermal Maximum: A Perturbation of Carbon Cycle, Climate, and Biosphere with Implications for the Future. Annu Rev Earth Planet Sci 39:489–516.
Meiri S. 2008. Evolution and ecology of lizard body sizes. Glob Ecol Biogeogr 17:724–34.
Meiri S. 2010. Length-weight allometries in lizards. J Zool 281:218–26.
Meiri S. 2018. Traits of lizards of the world: Variation around a successful evolutionary design. Glob Ecol Biogeogr 27:1168–72.
Melstrom KM. 2017. The relationship between diet and tooth complexity in living dentigerous saurians. J Morphol 278:500–522.
Meszoely CAM. 1970. North American fossil anguid lizards. Bull Museum Comp Zool 139:87–150.
Metzger KA, Herrel A. 2005. Correlations between lizard cranial shape and diet: A quantitative, phylogenetically informed analysis. Biol J Linn Soc 86:433–66.
Meyer HW. 1986. An evaluation of the methods for estimating paleoaltitudes using Tertiary floras from the Rio Grande Rift vicinity, New Mexico and Colorado.
Miles DB. 1994. Population Differentiation in Locomotor Performance and the Potential Response of a Terrestrial Organism to Global Environmental Change. Am Zool 34:422–36.
Miller-camp J. 2016. Patterns in Alligatorine Evolution.
Morgan ME, Badgley C, Gunnelp GF, Gingerich PD, Kappelman JW, Maas MC. 1995. Comparative paleoecology of Paleogene and Neogene mammalian faunas: Body-size structure. Palaeogeogr Palaeoclimatol Palaeoecol 115:287–317.
Moscato DA. 2013. A Glyptosaurine Lizard from the Eocene (late Uintan) of San Diego , California , and Implications for Glyptosaurine Evolution and Biogeography. .
Muñoz MM, Bodensteiner BL. 2019. Janzen's Hypothesis meets the Bogert Effect: Connecting climate variation, thermoregulatory behavior, and rates of physiological evolution. Integr Org Biol 1:1–12.
Muñoz MM, Losos JB. 2018. Thermoregulatory behavior simultaneously promotes and forestalls evolution in a tropical lizard. Am Nat 191:E15–26.

Muñoz MM, Stimola MA, Algar AC, Conover A, Rodriguez AJ, Landestoy MA, Bakken GS, Losos JB. 2014. Evolutionary stasis and lability in thermal physiology in a group of tropical lizards. Proc R Soc B Biol Sci 281:20132433.
Norris RD, Jones LS, Corfield RM, Cartlidge JE. 1996. Skiing in the Eocene Uinta mountains? Isotopic evidence in the Green River Formation for snow melt and large mountains. Geology 24:403–6.
O'Brien HD, Lynch LM, Vliet KA, Brueggen J, Erickson GM, Gignac PM. 2019. Crocodylian Head Width Allometry and Phylogenetic Prediction of Body Size in Extinct Crocodyliforms. Integr Org Biol 1.
Olalla-Tárraga MÁ, Rodríguez MÁ, Hawkins BA. 2006a. Broad-scale patterns of body size in squamate reptiles of Europe and North America. J Biogeogr 33:781–93.
Olalla-Tárraga MÁ, Rodríguez MÁ, Hawkins BA. 2006b. Broad-scale patterns of body size in squamate reptiles of Europe and North America. J Biogeogr 33:781–93.
Peppe DJ. 2010. Megafloral change in the early and middle Paleocene in the Williston Basin, North Dakota, USA. Palaeogeogr Palaeoclimatol Palaeoecol 298:224–34.
Peppe DJ, Royer DL, Cariglino B, Oliver SY, Newman S, Leight E, Enikolopov G, Fernandez-Burgos M, Herrera F, Adams JM, Correa E, Currano ED, Erickson JM, Hinojosa LF, Hoganson JW, Iglesias A, Jaramillo CA, Johnson KR, Jordan GJ, Kraft NJB, Lovelock EC, Lusk CH, Niinemets Ü, Peñuelas J, Rapson G, Wing SL, Wright IJ. 2011. Sensitivity of leaf size and shape to climate: Global patterns and paleoclimatic applications. New Phytol 190:724–39.
Peters RH. 1983. The Ecological Implications of Body Size. 1st ed New York, NY: Cambridge University Press.
Pianka ER. 1995. Evolution of body size: Varanid lizards as a model system. Am Nat 146:398–414.
Pianka ER, Vitt LJ. 2003. Lizards: Windows to the Evolution of Diversity Berkeley: University of California Press.
Pianka ER, Vitt LJ, Pelegrin N, Fitzgerald DB, Winemiller KO. 2017. Toward a Periodic Table of Niches, or Exploring the Lizard Niche Hypervolume. Am Nat 190:000–000.
Piantoni C, Navas CA, Ibargüengoytía NR. 2019. A real tale of Godzilla: Impact of climate warming on the growth of a lizard. Biol J Linn Soc 126:768–82.
Pincheira-Donoso D, Hodgson DJ, Tregenza T. 2008. The evolution of body size under environmental gradients in ectotherms: Why should Bergmann's rule apply to lizards? BMC Evol Biol 8:1–13.
Pincheira-Donoso D, Tregenza T, Hodgson DJ. 2007. Body size evolution in South American *Liolaemus* lizards of the *boulengeri* clade: A contrasting reassessment. J Evol Biol 20:2067–71.
Polly PD, Eronen JT, Fred M, Dietl GP, Mosbrugger V, Scheidegger C, Frank DC, Damuth J, Stenseth NC, Fortelius M. 2011. History matters: ecometrics and integrative climate change biology. Proc R Soc B Biol Sci 278:1131–40.
Pough FH. 1973. Lizard Energetics and Diet. Ecology 54:837–44.
Pough FH. 1980. The advantages of ectothermy for tetrapods. Am Nat 115:92–112.
Quintero I, Wiens JJ. 2013. Rates of projected climate change dramatically exceed past rates of climatic niche evolution among vertebrate species. Ecol Lett 16:1095–1103.
Rasmussen DL. 2003. Tertiary history of western Montana and east-central Idaho: A synopsis. In: Raynolds RG, Flores RM, editors. Cenozoic Systems of the Rocky Mountain Region

Denver, Colorado: Rocky Mountain Society of Economic Paleontologists and Mineralogists. p. 459–477.
Rasmussen DM, Foreman BZ. 2017. Provenance of lower Paleogene strata in the Huerfano basin: implications for uplift of the Wet Mountains, Colorado, U.S.A. J Sediment Res 87:579–93.
Retallack GJ. 2007. Cenozoic Paleoclimate on Land in North America. J Geol 115:271–94.
Ripple WJ, Wolf C, Newsome TM, Gregg JW, Lenton TM, Palomo I, Eikelboom JAJ, Law BE, Huq S, Duffy PB, Rockström J. 2021. World scientists' warning of a climate emergency 2021. Bioscience 71:894–98.
Robson SG, Banta ER. 1995. Arizona, Colorado, New Mexico, Utah HA 730-CUSGS Gr Water Atlas United States. (https://pubs.usgs.gov/ha/ha730/ch_c/C-text8.html).
Roehler HW. 1993. Eocene climates, depositional environments, and geography, greater Green River Basin, Wyoming, Utah, and Colorado. United States Geol Surv Prof Pap.
Roll U, Feldman A, Novosolov M, Allison A, Bauer AM, Bernard R, Böhm M, Castro-Herrera F, Chirio L, Collen B, Colli GR, Dabool L, Das I, Doan TM, Grismer LL, Hoogmoed M, Itescu Y, Kraus F, Lebreton M, Lewin A, Martins M, Maza E, Meirte D, Nagy ZT, Nogueira CDC, Pauwels OSG, Pincheira-Donoso D, Powney GD, Sindaco R, Tallowin OJS, Torres-Carvajal O, Trape JF, Vidan E, Uetz P, Wagner P, Wang Y, Orme CDL, Grenyer R, Meiri S. 2017a. The global distribution of tetrapods reveals a need for targeted reptile conservation. Nat Ecol Evol 1:1677–82.
Roll U, Feldman A, Novosolov M, Allison A, Bauer AM, Bernard R, Böhm M, Castro-Herrera F, Chirio L, Collen B, Colli GR, Dabool L, Das I, Doan TM, Grismer LL, Hoogmoed M, Itescu Y, Kraus F, Lebreton M, Lewin A, Martins M, Maza E, Meirte D, Nagy ZT, Nogueira CDC, Pauwels OSG, Pincheira-Donoso D, Powney GD, Sindaco R, Tallowin OJS, Torres-Carvajal O, Trape JF, Vidan E, Uetz P, Wagner P, Wang Y, Orme CDL, Grenyer R, Meiri S. 2017b. The global distribution of tetrapods reveals a need for targeted reptile conservation. Nat Ecol Evol 1:1677–82.
Rose KD. 1981. Composition and Species Diversity in Paleocene and Eocene Mammal Assemblages: An Empirical Study. J Vertebr Paleontol 1:367–88.
Rose KD. 2008. Palaeanodonta and pholidota. In: Janis CM, Gunnell GF, Uhen MD, editors. Evolution of Tertiary Mammals of North America: Volume 2, Small Mammals, Xenarthrans, and Marine Mammals Cambridge, UK: Cambridge University Press. p. 135–46.
Rose KD, Dunn RH, Grande L. 2014. A new skeleton of *Palaeosinopa didelphoides* (Mammalia, Pantolesta) from the early Eocene Fossil Butte Member, Green River Formation (Wyoming), and skeletal ontogeny in Pantolestidae. J Vertebr Paleontol 34:932–40.
Rose KD, Krishtalka L, Stucky RK. 1991. Revision of the Wind River faunas, early Eocene of central Wyoming. Part 11. Palaeanodonta (Mammalia). Ann Carnegie Museum 60:63–82.
Rose KD, Von Koenigswald W. 2005. An exceptionally complete skeleton of *Palaeosinopa* (Mammalia, Cimolesta, Pantolestidae) from the Green River formation, and other postcranial elements of the Pantolestidae from the Eocene of Wyoming (USA). Palaeontogr Abteilung A Palaozoologie - Stratigr 273:55–96.
Rothfuss JL, Lielke K, Weislogel AL. 2012. Application of detrital zircon provenance in paleogeographic reconstruction of an intermontane basin system, Paleogene Renova Formation, southwest Montana. In: Rasbury ET, Riggs NR, Hemming SR, editors. Mineralogical and Geochemical Approaches to Provenance: Geological Society of America

Special Paper 487 Denver, Colorado: Geological Society of America. p. 63–95.
Royer DL. 2012. Climate Reconstruction from Leaf Size and Shape: New Developments and Challenges. Paleontol Soc Pap 18:195–212.
Saarinen JJ, Boyer AG, Brown JH, Costa DP, Ernest M, Evans AR, Fortelius M, Gittleman JL, Marcus J, Harding LE, Lintulaakso K, Lyons SK, Okie JG, Sibly M, Stephens PR, Theodor J, Uhen MD, Smith FA. 2014. Patterns of maximum body size evolution in Cenozoic land mammals: eco-evolutionary processes and abiotic forcing. Proc R Soc B Biol Sci 281:1–10.
Sandau SD. 2005. The paleoclimate and paleoecology of a Uintan (Late Middle Eocene) flora and fauna from the Uinta Basin, Utah.
Sanggaard KW, Danielsen CC, Wogensen L, Vinding MS, Rydtoft LM, Mortensen MB, Karring H, Nielsen NC, Wang T, Thøgersen IB, Enghild JJ. 2012. Unique Structural Features Facilitate Lizard Tail Autotomy. PLoS One 7.
Scarpetta SG. 2019. *Peltosaurus granulosus* (Squamata, Anguidae) from the middle Oligocene of Sharps Corner, South Dakota, and the youngest known chronostratigraphic occurrence of Glyptosaurinae. J Vertebr Paleontol 39:e1622129.
Schmidt-Nielsen K. 1984. Scaling: Why is Animal Size So Important? Cambridge: Cambridge University Press.
Seebacher F, Franklin CE. 2012. Determining environmental causes of biological effects: The need for a mechanistic physiological dimension in conservation biology. Philos Trans R Soc B Biol Sci 367:1607–14.
Sereno PC, Larsson HCE, Sidor CA, Gado B. 2001. The giant crocodyliform *Sarcosuchus* from the cretaceous of Africa. Science (80-) 294:1516–19.
Sewall JO, Sloan LC. 2006. Come a little bit closer: A high-resolution climate study of the early Paleogene Laramide foreland. Geology 34:81–84.
Sheldon ND. 2018. Using Carbon Isotope Equilibrium to Screen Pedogenic Carbonate Oxygen Isotopes: Implications for Paleoaltimetry and Paleotectonic Studies. Geofluids 2018.
Sinervo B, Adolph SC. 1989. Thermal sensitivity of growth rate in hatchling *Scleroporus* lizards: Environmental, behavioural and genetic aspects. Oecologia 78:411–19.
Sinervo B, Méndez-de-la-Cruz F, Miles DB, Heulin B, Bastiaans E, Cruz MVS, Lara-Resendiz R, Martínez-Méndez N, Calderón-Espinosa ML, Meza-Lázaro RN, Gadsden H, Avila LJ, Morando M, De La Riva IJ, Sepúlveda PV, Rocha CFD, Ibargüengoytía N, Puntriano CA, Massot M, Lepetz V, Oksanen TA, Chappie DG, Bauer AM, Branch WR, Clobert J, Sites JW. 2010. Erosion of lizard diversity by climate change and altered thermal niches. Science (80-) 328:894–99.
Slavenko A, Feldman A, Allison A, Bauer AM, Böhm M, Chirio L, Colli GR, Das I, Doan TM, LeBreton M, Martins M, Meirte D, Nagy ZT, Nogueira C de C, Pauwels OSG, Pincheira-Donoso D, Roll U, Wagner P, Wang Y, Meiri S. 2019. Global patterns of body size evolution in squamate reptiles are not driven by climate. Glob Ecol Biogeogr 28:471–83.
Slavenko A, Tallowin OJS, Itescu Y, Raia P, Meiri S. 2016. Late Quaternary reptile extinctions: size matters, insularity dominates. Glob Ecol Biogeogr 25:1308–20.
Smith EN. 1979. Behavioral and physiological thermoregulation of crocodilians. Integr Comp Biol 19:239–47.
Smith KT. 2006. A diverse new assemblage of Late Eocene squamates (Reptilia) from the Chadron Formation of North Dakota, U.S.A. Palaeontol Electron 9:1–44.
Smith KT. 2009. A new lizard assemblage from the earliest Eocene (zone Wa0) of the Bighorn Basin, Wyoming, USA: Biogeography during the warmest interval of the Cenozoic, Journal

of Systematic Palaeontology.
Smith KT. 2011a. The evolution of mid-latitude faunas during the Eocene: Late Eocene lizards of the Medicine Pole Hills reconsidered. Bull Peabody Museum Nat Hist 52:3–105.
Smith KT. 2011b. The long-term history of dispersal among lizards in the early Eocene: New evidence from a microvertebrate assemblage in the Bighorn Basin of Wyoming, USA. Palaeontology 54:1243–70.
Smith KT, Gauthier JA. 2013. Early Eocene lizards of the Wasatch Formation near Bitter Creek, Wyoming: Diversity and paleoenvironment during an interval of global warming. Bull Peabody Museum Nat Hist 54:135–230.
Smith RJ. 2002. Estimation of body mass in paleontology. J Hum Evol 43:271–87.
Snell KE. 2011. Paleoclimate and paleoelevation of the western Cordillera in the United States.
Snell KE, Thrasher BL, Eiler JM, Koch PL, Sloan LC, Tabor NJ. 2013. Hot summers in the Bighorn Basin during the early Paleogene. Geology 41:55–58.
Snoke AW, Steidtmann JR, Roberts SM. 1993. Geology of Wyoming Laramie, WY.
Solórzano A, Núñez-Flores M, Inostroza-Michael O, Hernández CE. 2020. Biotic and abiotic factors driving the diversification dynamics of Crocodylia. Palaeontology 63:415–29.
Stamps JA. 1977. Rainfall, Moisture and Dry Season Growth Rates in *Anolis aeneus*. Copeia 1977:415–19.
Stein RA, Sheldon ND, Allen SE, Smith ME, Dzombak RM, Jicha BR. 2021. Climate and ecology in the Rocky Mountain Interior after the Early Eocene Climatic Optimum. Clim Past 17:2515–36.
Stout JB. 2012. New material of *Borealosuchus* from the Bridger Formation, with notes on the paleoecology of Wyoming's Eocene crocodylians. PalArch's J Vertebr Palaeontol 9:1–7.
Stucky RK. 1992. Mammalian faunas in North America of Bridgerian to Early Arikareean "Ages" (Eocene and Oligocene). In: Prothero DR, Berggren WA, editors. Eocene-Oligocene Climatic and Biotic Evolution Princeton, NJ: Princeton University Press. p. 464–93.
Sullivan RM. 1979. Revision of the Paleogene genus *Glyptosaurus* (Reptilia, Anguidae). Bull Am Museum Nat Hist 163.
Sullivan RM. 2019. The taxonomy, chronostratigraphy and paleobiogeography of glyptosaurine lizards (Glyptosaurinae, Anguidae). Comptes Rendus Palevol 18:747–63.
Swinehart JB, Souders VL, Degraw HM, Diffendal RF. 1985. Cenozoic paleogeography of western Nebraska. In: Flores RM, Kaplan SS, editors. Rocky Mountain Paleogeography Symposium 3: Cenozoic Paleogeography of the West-central United States Denver, Colorado: Rocky Mountain Section SEPM. p. 209–29.
The Paleobiology Database. n.d. . (www.paleobiodb.org).
Thomas Goodwin H, Bullock KM. 2012. Estimates of body mass for fossil giant ground squirrels, genus *Paenemarmota*. J Mammal 93:1169–77.
Thuiller W. 2004. Patterns and uncertainties of species' range shifts under climate change. Glob Chang Biol 10:2020–27.
Tomiya S, Zack SP, Spaulding M, Flynn JJ. 2021. Carnivorous mammals from the middle Eocene Washakie Formation, Wyoming, USA, and their diversity trajectory in a post-warming world. J Paleontol 95:1–115.
Townsend KEB, Rasmussen DT, Murphey PC, Evanoff E. 2010. Middle Eocene habitat shifts in the North American western interior: A case study. Palaeogeogr Palaeoclimatol Palaeoecol 297:144–58.

Toyama KS, Boccia CK. 2022. Bergmann's rule in *Microlophus* lizards: testing for latitudinal and climatic gradients of body size. bioRxiv 2022.01.18.476846.
Uetz P, Hallermann J. n.d. The Reptile Database.
Verdade LM. 2000. Regression equations between body and head measurements in the broad-snouted Caiman (*Caiman latirostris*). Rev Bras Biol 60:469–82.
Vidan E, Novosolov M, Bauer AM, Herrera FC, Chirio L, Campos Nogueira C, Doan TM, Lewin A, Meirte D, Nagy ZT, Pincheira-Donoso D, Tallowin OJS, Torres Carvajal O, Uetz P, Wagner P, Wang Y, Belmaker J, Meiri S. 2019. The global biogeography of lizard functional groups. J Biogeogr 00:1–12.
Villa A, Delfino M. 2019. A comparative atlas of the skull osteology of European lizards (Reptilia: Squamata). Zool J Linn Soc 1–100.
Vitt E.R. Pianka, W.E. Cooper, Jr., and K. Schwenk LJ. 2003. History and the global ecology of squamate reptiles. Am Nat 162:44–60.
Vitt LJ, Caldwell JP. 2009. Herpetology: An Introductory Biology of Amphibians and Reptiles. 3rd ed Burlington, MA: Elsevier.
Wassersug RJ, Hecht MK. 1967. The Status of the Crocodylid Genera *Procaimanoidea* and *Hassiacosuchus* in the New World. Herpetologica 23:30–34.
Webb GJW, Messel H, Crawford J, Yerbury MJ. 1978. Growth rates of *Crocodylus porosus* (Reptilia: Crocodilia) from Arnhem Land, Northern Australia. Wildl Res 5:385–99.
Whiting ET, Fox DL. 2021. Latitudinal and environmental patterns of species richness in lizards and snakes across continental North America. J Biogeogr 48:291–304.
Whiting ET, Hastings AK. 2015. First Fossil Alligator from the Late Eocene of Nebraska and the Late Paleogene Record of Alligators in the Great Plains. J Herpetol 49:560–69.
Wiens JJ, Hutter CR, Mulcahy DG, Noonan BP, Townsend TM, Sites JW, Reeder TW. 2012. Resolving the phylogeny of lizards and snakes (Squamata) with extensive sampling of genes and species. Biol Lett Lett 8:1043–46.
Wilf P. 2000. Late Paleocene-Early Eocene climate changes in Southwestern Wyoming: Paleobotanical analysis. Bull Geol Soc Am 112:292–307.
Wilf P, Beard KC, Davies-Vollum KS, Norejko JW. 1998. Portrait of a late Paleocene (early Clarkforkian) terrestrial ecosystem: Big Multi Quarry and associated strata, Washakie Basin, southwestern Wyoming. Palaios 13:514–32.
Wilf P, Wing SL, Greenwood DR, Greenwood CL. 1998. Using fossil leaves as paleoprecipitation indicators: An Eocene example. Geology 26:203–6.
Wing SL. 1987. Eocene and Oligocene floras and vegetation of the Rocky Mountains. Ann Missouri Bot Gard 74:748.
Wing SL. 1998. Tertiary vegetation of North America as a context for mammalian evolution. In: Janis CM, Scott KM, Jacobs LL, editors. Evolution of Tertiary Mammals of North America Cambridge University Press. p. 37–60.
Wing SL, Bao H, Koch PL. 2000. An early Eocene cool period? Evidence for continental cooling during the warmest part of the Cenozoic. In: Huber BT, Macleod KG, Wing SL, editors. Warm Climates in Earth History Cambridge, UK: Cambridge University Press. p. 197–237.
Wing SL, Bloch JI, Bowen GJ, Boyer DM, Chester S, Diefendorf AF, Harrington GJ, Kraus MJ, Secord R, Mcinerney FA. 2009. Coordinated sedimentary and biotic change during the Paleocene–Eocene Thermal Maximum in the Bighorn Basin, Wyoming, USA. In: Crouch EM, Strong CP, Hollis CJ, editors. Climatic and Biotic Events of the Paleogene (CBEP

2009), Extended Abstracts from an International Conference in Wellington, New Zealand, 12-15 January 2009 GNS Science Miscellaneous Series. p. 157–63.
Wing SL, Bown TM, Obradovich JD. 1991. Early Eocene biotic and climatic change in interior western North America. Geology 19:1189–92.
Wing SL, Greenwood DR. 1993. Fossils and fossil climate: The case for equable continental interiors in the Eocene. Philos Trans - R Soc London, B 341:243–52.
Wing SL, Harrington GJ, Smith FA, Bloch JI, Boyer DM, Freeman KH. 2005. Transient floral change and rapid global warming at the Paleocene-Eocene boundary. Science (80-) 310:993–96.
Wolfe JA. 1992. Climatic, floristic, and vegetational changes near the Eocene/Oligocene boundary in North America. In: Prothero DR, Berggren WA, editors. Eocene-Oligocene Climatic and Biotic Evolution Princeton, NJ: Princeton University Press. p. 421–36.
Wolfe JA, Forest CE, Molnar P. 1998. Paleobotanical evidence of Eocene and Oligocene paleoaltitudes in midlatitude western North America. Bull Geol Soc Am 110:664–78.
Woodburne MO (Ed.). 2004. Late Cretaceous and Cenozoic Mammals of North America: Biostratigraphy and Geochronology New York: Columbia University Press.
Woodward AR, White JH, Linda SB. 1995. Maximum Size of the Alligator (*Alligator mississippiensis*). J Herpetol 29:507–13.
Woolley CH, Thompson JR, Wu Y-H (Beckey), Bottjer DJ, Smith ND. 2020. Can a fragmented past be trusted? Assessing bias and phylogenetic signal in the squamate fossil record. J Vertebr Paleontol Progr Abstr 351–52.
Woolley CH, Thompson JR, Wu YH, Bottjer DJ, Smith ND. 2022. A biased fossil record can preserve reliable phylogenetic signal. Paleobiology 1–16.
Young MT, Bell MA, de Andrade MB, Brusatte SL. 2011. Body size estimation and evolution in metriorhynchid crocodylomorphs: Implications for species diversification and niche partitioning. Zool J Linn Soc 163:1199–1216.
Zachos J, Pagani M, Sloan L, Thomas E, Billups K. 2001. Trends, rhythms and aberrations in global climate 65 Ma to present. Science (80-) 292:686–93.
Zachos JC, Dickens GR, Zeebe RE. 2008. An early Cenozoic perspective on greenhouse warming and carbon-cycle dynamics. Nature 451:279–83.
Zamora-Camacho FJ, Reguera S, Moreno-Rueda G. 2014. Bergmann's Rule rules body size in an ectotherm: heat conservation in a lizard along a 2200-metre elevational gradient. J Evol Biol 27:2820–28.
Zanazzi A, Kohn MJ, MacFadden BJ, Terry DO. 2007. Large temperature drop across the Eocene-Oligocene transition in central North America. Nature 445:639–42.
Zani PA. 1996. Patterns of caudal-anatomy evolution in lizards. J Zool 240:201–30.
Zimmerman LC, Tracy CR. 1989. Interactions between the environment and ectothermy and herbivory in reptiles. Physiol Zool 62:374–409.
Zizka A, Silvestro D, Andermann T, Azevedo J, Duarte Ritter C, Edler D, Farooq H, Herdean A, Ariza M, Scharn R, Svantesson S, Wengström N, Zizka V, Antonelli A. 2019. CoordinateCleaner: Standardized cleaning of occurrence records from biological collection databases. Methods Ecol Evol 10:744–51.

BIBLIOGRAPHY

Adolph SC, Porter WP. 1993. Temperature, activity, and lizard life histories. Am Nat 142:273–95.

Allen SE. 2015. Fossil palm flowers from the Eocene of the Rocky Mountain Region with affinities to *Phoenix* L. (Arecaceae: Coryphoideae). Int J Plant Sci 176:586–96.

Allen SE. 2017a. The uppermost lower Eocene Blue Rim flora from the Bridger Formation of Southwestern Wyoming: Floristic composition, paleoclimate, and paleoecology.

Allen SE. 2017b. Reconstructing the local vegetation and seasonality of the lower Eocene Blue Rim site of Southwestern Wyoming using fossil wood. Int J Plant Sci 178:689–714.

Alroy J. 1998. Cope's Rule and the Dynamics of Body Mass Evolution in North American Fossil Mammals. Science (80-) 280:731–34.

Alroy J. 2000. New Methods for Quantifying Macroevolutionary Patterns and Processes. Paleobiology 26:707–33.

Anagnostou E, John EH, Edgar KM, Foster GL, Ridgwell A, Inglis GN, Pancost RD, Lunt DJ, Pearson PN. 2016. Changing atmospheric CO2 concentration was the primary driver of early Cenozoic climate. Nature 533:380–84.

Andreone F, Guarino FM. 2003. Giant and long-lived? Age structure in *Macroscincus coctei*, an extinct skink from Cape Verde. Amphib Reptil 24:459–70.

Angielczyk KD, Burroughs RW, Feldman CR. 2015. Do turtles follow the rules? Latitudinal gradients in species richness, body size, and geographic range area of the world's turtles. J Exp Zool Part B Mol Dev Evol 324:270–94.

Angilletta, Jr. MJ, Niewiarowski PH, Dunham AE, Leaché AD, Porter WP. 2004. Bergmann's Clines in Ectotherms: Illustrating a Life-History Perspective with Sceloporine Lizards. Am Nat 164:E168–83.

Angilletta MJ, Dunham AE. 2003. The Temperature-Size Rule in Ectotherms: Simple Evolutionary Explanations May Not Be General. Am Nat 162:332–42.

Angilletta MJ, Niewiarowski PH, Navas CA. 2002. The evolution of thermal physiology in ectotherms. 27:249–68.

Angilletta MJ, Steury TD, Sears MW. 2004. Temperature, growth rate, and body size in ectotherms: Fitting pieces of a life-history puzzle. Integr Comp Biol 44:498–509.

Araújo MB, Nogués-Bravo D, Diniz-Filho JAF, Haywood AM, Valdes PJ, Rahbek C. 2008. Quaternary climate changes explain diversity among reptiles and amphibians. Ecography (Cop) 31:8–15.

Arneth A, Shin YJ, Leadley P, Rondinini C, Bukvareva E, Kolb M, Midgley GF, Oberdorff T, Palomo I, Saito O. 2020. Post-2020 biodiversity targets need to embrace climate change. Proc Natl Acad Sci U S A 117:30882–91.

Arnold EN. 1984. Evolutionary aspects of tail shedding in lizards and their relatives. J Nat Hist 18:127–69.

Ashton KG, Feldman CR. 2003. Bergmann's Rule in Nonavian Reptiles : Turtles Follow It, Lizards and Snakes Reverse It. Evolution (N Y) 57:1151–63.

Aureliano T, Ghilardi AM, Guilherme E, Souza-Filho JP, Cavalcanti M, Riff D. 2015. Morphometry, bite-force, and paleobiology of the Late Miocene caiman *Purussaurus brasiliensis*. PLoS One 10:1–14.

Ballinger RE. 1983. Life-history variations. In: RB H, ER P, TW S, editors. Lizard Ecology: Studies of a Model Organism Cambridge and London: Harvard University Press. p. 241–

260.
Ballinger RE, Lemos-Espinal J, Sanoja-Sarabia S, Coady NR. 1995. Ecological observations of the Lizard, *Xenosaurus grandis* in Cuautlapan, Veracruz, Mexico. Biotropica 27:128–32.
Bansal U, Thaker M. 2021. Diet influences latitudinal gradients in life-history traits, but not reproductive output, in ectotherms. Glob Ecol Biogeogr 30:2431–41.
Barclay RS. 2003. Stratigraphy and megaflora of a K-T boundary section in the eastern Denver Basin, Colorado. Rocky Mt Geol 38:45–71.
Barnosky AD. 2015. Transforming the global energy system is required to avoid the sixth mass extinction. MRS Energy Sustain 2:1–13.
Barnosky AD, Bell CJ, Emslie SD, Goodwin HT, Mead JI, Repenning CA, Scott E, Shabel AB. 2004. Exceptional record of mid-Pleistocene vertebrates helps differentiate climatic from anthropogenic ecosystem perturbations. Proc Natl Acad Sci U S A 101:9297–9302.
Barnosky AD, Holmes M, Kirchholtes R, Lindsey E, Maguire KC, Poust AW, Allison Stegner M, Sunseri J, Swartz B, Swift J, Villavicencio NA, Wogan GOU. 2014. Prelude to the Anthropocene: Two new North American Land Mammal Ages (NALMAs). Anthr Rev 1:225–42.
Barnosky AD, Matzke N, Tomiya S, Wogan GOU, Swartz B, Quental TB, Marshall C, McGuire JL, Lindsey EL, Maguire KC, Mersey B, Ferrer EA. 2011. Has the Earth's sixth mass extinction already arrived? Nature 471:51–57.
Bartholomew GA, Tucker VA. 1964. Size, body temperature, thermal conductance, oxygen consumption, and heart rate in Australian varanid lizards. Physiol Zool 37:341–54.
Bateman PW, Fleming PA. 2009. To cut a long tail short: A review of lizard caudal autotomy studies carried out over the last 20 years. J Zool 277:1–14.
Beck DD. 2005. Biology of Gila Monsters and Beaded Lizards. 9th ed Berkeley: University of California Press.
Bennett AF. 1987. Evolution of the control of body temperature: Is warmer better? In: Dejours P, Bolis L, Taylor CR, Weibel ER, editors. Comparative Physiology: Life in Water and on Land Padova: IX-Liviana Press. p. 421–31.
Bergmann K. 1847. Über die Ver- hältnisse der wärmeokönomie der Thiere zu ihrer Grösse. Göttinger Stud 3:595–708.
Bertrand OC, Shelley SL, Wible JR, Williamson TE, Holbrook LT, Chester SGB, Butler IB, Brusatte SL. 2020. Virtual endocranial and inner ear endocasts of the Paleocene 'condylarth' *Chriacus*: new insight into the neurosensory system and evolution of early placental mammals. J Anat 236:21–49.
Bloch JI, Boyer DM, Strait SG, Wing SL. 2004. New Sections and Fossils From the Southern Bighorn Basin, Wyoming Document Faunal Turnover During the PETM. In: American Geophysical Union, Fall Meeting.
Boardman GS, Secord R. 2013. Stable isotope paleoecology of White River ungulates during the Eocene-Oligocene climate transition in northwestern Nebraska. Palaeogeogr Palaeoclimatol Palaeoecol 375:38–49.
Bochaton C, Kemp ME. 2017. Reconstructing the body sizes of Quaternary lizards using *Pholidoscelis Fitzinger*, 1843, and *Anolis* Daudin, 1802, as case studies. J Vertebr Paleontol 37:9 pp.
Bogert CM. 1949. Thermoregulation in reptiles, a factor in evolution. Evolution (N Y) 3:195–211.
Böhme M, Ilg A, Ossig A, Küchenhoff H. 2006. New method to estimate paleoprecipitation

using fossil amphibians and reptiles and the middle and late Miocene precipitation gradients in Europe. Geology 34:425–28.
Borths MR, Stevens NJ. 2017. The first hyaenodont from the late Oligocene Nsungwe Formation of Tanzania: Paleoecological insights into the Paleogene-Neogene carnivore transition. PLoS One 12:1–30.
Boyer DM, Georgi JA. 2007. Cranial morphology of a pantolestid eutherian mammal from the eocene bridger formation, Wyoming, USA: Implications for relationships and habitat. J Mamm Evol 14:239–80.
Brandt R, Navas CA. 2013. Body size variation across climatic gradients and sexual size dimorphism in Tropidurinae lizards. J Zool 290:192–98.
Brochu CA. 1997. A review of "*Leidyosuchus*" (Crocodyliformes, Eusuchia) from the Cretaceous through Eocene of North America. J Vertebr Paleontol 17:679–97.
Brochu CA. 1999. Phylogenetics, taxonomy, and historical biogeography of Alligatoroidea. J Vertebr Paleontol 19:9–100.
Brochu CA. 2000. Phylogenetic relationships and divergence timing of *Crocodylus* based on morphology and the fossil record. Copeia 2000:657–73.
Brochu CA. 2003. Phylogenetic approaches toward crocodylian history. Annu Rev Earth Planet Sci 31:357–97.
Brochu CA. 2004. Alligatorine phylogeny and the status of *Allognathosuchus mooki*, 1921. J Vertebr Paleontol 24:857–73.
Brochu CA. 2010. A new alligatorid from the lower Eocene Green River Formation of Wyoming and the origin of Caimans. J Vertebr Paleontol 30:1109–26.
Brochu CA. 2013. Phylogenetic relationships of Palaeogene ziphodont eusuchians and the status of *Pristichampsus* Gervais, 1853. Earth Environ Sci Trans R Soc Edinburgh 103:521–50.
Brochu CA, Adams A, Drumheller SK, Miller-Camp J, Rubin M. 2020. The interplay between regional and global climatic trends in crocodyliform faunal change. In: Journal of Vertebrate Paleontology The Society of Vertebrate Paleontology. p. 85–86.
Bronzati M, Montefeltro FC, Langer MC. 2012. A species-level supertree of Crocodyliformes. Hist Biol 24:598–606.
Bronzati M, Montefeltro FC, Langer MC. 2015. Diversification events and the effects of mass extinctions on Crocodyliformes evolutionary history. R Soc Open Sci 2:1–9.
Buckley LB, Nufio CR. 2014. Elevational clines in the temperature dependence of insect performance and implications for ecological responses to climate change. Conserv P 2:1–12.
Cadena EA, Ksepka DT, Jaramillo CA, Bloch JI. 2012. New pelomedusoid turtles from the late Palaeocene Cerrejón Formation of Colombia and their implications for phylogeny and body size evolution. J Syst Palaeontol 10:313–31.
Cadena EA, Scheyer TM, Carrillo-Briceño JD, Sánchez R, Aguilera-Socorro OA, Vanegas A, Pardo M, Hansen DM, Sánchez-Villagra MR. 2020. The anatomy, paleobiology, and evolutionary relationships of the largest extinct side-necked turtle. Sci Adv 6:1–13.
Campione NE, Evans DC. 2012. A universal scaling relationship between body mass and proximal limb bone dimensions in quadrupedal terrestrial tetrapods. BMC Biol 10.
Carlson CG, Anderson SB. 1965. Sedimentary and tectonic history of North Dakota part of Williston Basin. Bull Am Assoc Pet Geol 49:1833–46.
Castanet J, Baez M. 1991. Adaptation and evolution in *Gallotia* lizards from the Canary Islands: Age, growth, maturity and longevity. Amphibia-Reptilia 12:81–102.

Chamaillé-Jammes S, Massot M, Aragón P, Clobert J. 2006. Global warming and positive fitness response in mountain populations of common lizards *Lacerta vivipara*. Glob Chang Biol 12:392–402.
Chen IC, Hill JK, Ohlemüller R, Roy DB, Thomas CD. 2011. Rapid range shifts of species associated with high levels of climate warming. Science (80-) 333:1024–26.
Cherven VB, Jacob AF. 1985. Evolution of Paleogene Depositional Systems, Williston Basin, in Response to Global Sea Level Changes. In: Cenozoic Paleogeography of the West-Central United States AAPG Rocky Mountain Section (SEPM). p. 127–70.
Chester SGB, Bloch JI, Secord R, Boyer DM. 2010. A New Small-Bodied Species of *Palaeonictis* (Creodonta, Oxyaenidae) from the Paleocene-Eocene Thermal Maximum. J Mamm Evol 17:227–43.
Cicimurri DJ, Knight JL, Self-Trail JM, Ebersole SM. 2016. Late Paleocene glyptosaur (Reptilia: Anguidae) osteoderms from South Carolina, USA. J Paleontol 90:147–53.
Clarke A. 2003. Costs and consequences of evolutionary temperature adaptation. Trends Ecol Evol 18:573–81.
Clusella-Trullas S, Blackburn TM, Chown SL. 2011. Climatic Predictors of Temperature Performance Curve Parameters in Ectotherms Imply Complex Responses to Climate Change. Am Nat 177:738–51.
Conrad JL. 2006. An Eocene shinisaurid (Reptilia, Squamata) from Wyoming, U.S.A. J Vertebr Paleontol 26:113–26.
Cossette AP, Brochu CA. 2020. A systematic review of the giant alligatoroid *Deinosuchus* from the Campanian of North America and its implications for the relationships at the root of Crocodylia. J Vertebr Paleontol 40:e1767638.
Crowley TJ, Zachos JC. 2000. Comparison of zonal temperature profiles for past warm time periods. In: Huber BT, Macleod KG, Wing SL, editors. Warm Climates in Earth History Cambridge, UK: Cambridge University Press. p. 50–76.
Cruz FB, Fitzgerald LA, Espinoza RE, Schulte II JA. 2005. The importance of phylogenetic scale in tests of Bergmann's and Rapoport's rules: lessons from a clade of South American lizards. J Evol Biol 18:1559–74.
Damuth J. 1990. Problems in estimating body masses of archaic ungulates using dental measurements. Body Size Mamm Paleobiol Estim Biol Implic 229:tables 16.9-16.10.
Davies-Vollum KS. 1997. Early Palaeocene palaeoclimatic inferences from fossil floras of the western interior, USA. Palaeogeogr Palaeoclimatol Palaeoecol 136:145–64.
Davis J. 1967. Growth and Size of the Western Fence Lizard (*Sceloporus occidentalis*). Copeia 1967:721–31.
Davis MB, Shaw RG. 2001. Range shifts and adaptive responses to quaternary climate change. Science (80-) 292:673–79.
Dayan T, Simberloff D, Tchernov E, Yom-Tov Y. 1991. Calibrating the paleothermometer: climate, communities, and the evolution of size. Paleobiology 17:189–99.
Deconto RM, Thompson SL, Pollard D. 2000. Recent advances in paleoclimate modeling: Toward better simulations of warm paleoclimates. In: Huber BT, Macleod KG, Wing SL, editors. Warm Climates in Earth History Cambridge, UK: Cambridge University Press. p. 21–49.
Dettman DL, Lohmann KC. 2000. Oxygen isotope evidence for high-altitude snow in the Laramide Rocky Mountains of North America during the Late Cretaceous and Paleogene. Geology 28:243–46.

Deutsch CA, Tewksbury JJ, Huey RB, Sheldon KS, Ghalambor CK, Haak DC, Martin PR. 2008. Impacts of climate warming on terrestrial ectotherms across latitude. Proc Natl Acad Sci 105:6668–72.
Dickinson WR, Klute MA, Hayes MJ, Janecke SU, Lundin ER, Mckittrick MA, Olivares MD. 1988. Paleogeographic and paleotectonic setting of Laramide sedimentary basins in the central Rocky Mountain region: Reply. Geol Soc Am Bull 100:1023–39.
Douglass E. 1903. New vertebrates from the Montana Tertiary. Ann Carnegie Museum 2:145–99.
Dudgeon TW, Maddin HC, Evans DC, Mallon JC. 2020. The internal cranial anatomy of *Champsosaurus* (Choristodera: Champsosauridae): Implications for neurosensory function. Sci Rep 10:1–20.
Dunn RE, Strömberg CAE, Madden RH, Kohn MJ, Carlini AA. 2015. Linked canopy, climate, and faunal change in the Cenozoic of Patagonia. Science (80-) 347:258–61.
Dzombak RM, Midttun NC, Stein RA, Sheldon ND. 2021. Incorporating lateral variability and extent of paleosols into proxy uncertainty. Palaeogeogr Palaeoclimatol Palaeoecol 582:110641.
Egi N. 2001. Body mass estimates in extinct mammals from limb bone dimensions: The case of North American Hyaenodontids. Palaeontology 44:497–528.
Elder WP, Kirkland JI. 1994. Cretaceous paleogeography of the southern western interior region, Mesozoic Systems of the Rocky Mountain Region, USA.
ElShafie SJ. 2014. Body size and species richness changes in Glyptosaurinae (Squamata: Anguidae) through climatic transitions of the North American Cenozoic. Master's Thesis. Department of Earth & Atmospheric Sciences: University of Nebraska, Lincoln.
Elsworth PG, Seebacher F, Franklin CE. 2003. Sustained Swimming Performance in Crocodiles (*Crocodylus porosus*): Effects of Body Size and Temperature. J Herpetol 37:363–68.
Erickson BR. 1999. Fossil Lake Wannagan (Paleocene: Tiffanian) – Billings County, North Dakota. North Dakota Geol Surv MS:1–14.
Erickson GM, Gignac PM, Steppan SJ, Lappin AK, Vliet KA, Brueggen JD, Inouye BD, Kledzik D, Webb GJW. 2012. Insights into the ecology and evolutionary success of crocodilians revealed through bite-force and tooth-pressure experimentation. PLoS One 7:e31781.
Eronen JT, Janis CM, Chamberlain CP, Mulch A. 2015. Mountain uplift explains differences in palaeogene patterns of mammalian evolution and extinction between North America and Europe. Proc R Soc B Biol Sci 282:1–8.
Estes R, De Queiroz K, Gauthier J. 1988. Phylogenetic Relationships within Squamata. In: Estes R, Pregill G, editors. Phylogenetic Relationships of the Lizard Families Palo Alto, CA: Stanford University Press. p. 119–281.
Estes RA, Hutchison JH. 1980. Eocene lower vertebrates from Ellesmere Island, Canadian Arctic Archipelago. Palaeogeogr Palaeoclimatol Palaeoecol 30:325–47.
Evanoff E, Prothero DR, Lander RH. 1992. Eocene-Oligocene climatic change in North America: The White River Formation near Douglas, east-central Wyoming. In: Eocene-Oligocene Climatic and Biotic Evolution p. 116–30.
Evans SE. 2008. The Skull of Lizards and Tuatara. In: Gans C, Gaunt AS, Adler K, editors. The Skull of Lepidosauria. Volume 20,. ed Ithaca, NY: Society for the Study of Amphibians and Reptiles. p. 1–348.
Ezcurra MD. 2016. The phylogenetic relationships of basal archosauromorphs, with an emphasis on the systematics of proterosuchian archosauriforms. PeerJ 2016:e1778.

Fan M, Carrapa B. 2014. Late Cretaceous-early Eocene Laramide uplift, exhumation, and basin subsidence in Wyoming: Crustal responses to flat slab subduction. Tectonics 33:509–29.
Farlow JO, Hurlburt GR, Elsey RM, Britton ARC, Langston W. 2005. Femoral dimensions and body size of *Alligator mississippiensis*: Estimating the size of extinct mesoeucrocodylians. J Vertebr Paleontol 25:354–69.
Feldman A, Meiri S. 2014. Australian Snakes Do Not Follow Bergmann's Rule. Evol Biol 41:327–35.
Figueirido B, Pérez-Claros JA, Hunt RM, Palmqvist P. 2011. Body mass estimation in amphicyonid carnivoran mammals: A multiple regression approach from the skull and skeleton. Acta Palaeontol Pol 56:225–46.
Foreman BZ, Heller PL, Clementz MT. 2012. Fluvial response to abrupt global warming at the Palaeocene/Eocene boundary. Nature 491:92–95.
Fricke HC. 2003. Investigation of early Eocene water-vapor transport and paleoelevation using oxygen isotope data from geographically widespread mammal remains. Bull Geol Soc Am 115:1088–96.
Fricke HC, Wing SL. 2004. Oxygen isotope and paleobotanical estimates of temperature and d18O-latitude gradients over North America during the early Eocene. Am J Sci 304:612–35.
Frost DR, Etheridge R. 1989. A phylogenetic analysis and taxonomy of iguanian lizards. Univ Kansas Museum Nat Hist Misc Publ 81:1–65.
Fukuda Y, Saalfeld K, Lindner G, Nichols T. 2013. Estimation of total length from head length of saltwater crocodiles (*Crocodylus porosus*) in the Northern Territory, Australia. J Herpetol 47:34–40.
Gauthier JA. 1982. Fossil xenosaurid and anguid lizards from the early Eocene Wasatch Formation, southeast Wyoming, and a revision of the Anguioidea. Contrib to Geol Univ Wyoming 21:7–54.
Gauthier JA, Kearney M, Maisano JA, Rieppel O, Behlke ADB. 2012. Assembling the Squamate Tree of Life : Perspectives from the Phenotype and the Fossil Record Assembling the Squamate Tree of Life : Perspectives from the Phenotype and the Fossil Record. Bull Peabody Museum Nat Hist 53:3–308.
Gearty W, Payne JL. 2020. Physiological constraints on body size distributions in Crocodyliformes. Evolution (N Y) 74:245–55.
Gilbert EAB, Payne SL, Vickaryous MK. 2013. The anatomy and histology of caudal autotomy and regeneration in lizards. Physiol Biochem Zool 86:631–44.
Gilmore CW. 1928. Fossil Lizards of North America. Mem Natl Acad Sci 22:v–201.
Gingerich P. 1980. Early Cenozoic paleontology and stratigraphy of the Bighorn Basin, Wyoming. Pap Paleontol 24:1–156.
Gingerich PD. 1978. New Condylarthra (Mammalia) from the Paleocene and early Eocene of North America. Contrib from Museum Paleontol Univ Michigan 25:1–9.
Gingerich PD. 2006. Environment and evolution through the Paleocene-Eocene thermal maximum. Trends Ecol Evol 21:246–53.
Godoy PL, Benson RBJ, Bronzati M, Butler RJ. 2019. The multi-peak adaptive landscape of crocodylomorph body size evolution. BMC Evol Biol 19:1–29.
Grande L. 2013. The Lost World of Fossil Lake. Chicago: The University of Chicago Press.
Grant BW, Dunham AE. 1988. Thermally Imposed Time Constraints on the Activity of the Desert Lizard *Sceloporus Merriami*. Ecology 69:167–76.
Grant BW, Dunham AE. 1990. Elevational Covariation in Environmental Constraints and Life

Histories of the Desert Lizard *Sceloporus Merriami*. Ecology 71:1765–76.
Greenwood DR, Wing SL. 1995. Eocene continental climates and latitudinal temperature gradients. Geology 23:1044–48.
Greer AE. 1974. On the Maximum Total Length of the Salt-Water Crocodile (*Crocodylus porosus*). J Herpetol 8:381–84.
Greer AE. 2001. Distribution of Maximum Snout-Vent Length among Species of Scincid Lizards. J Herpetol 35:383–95.
Gregory KM, McIntosh WC. 1996. Paleoclimate and paleoelevation of the Oligocene Pitch-Pinnacle flora, Sawatch Range, Colorado. Geol Soc Am Bull 108:545.
Gunderson AR. 2013. Physiological Ecology and Vulnerability to Climate Warming in Anolis. 130.
Gunderson AR, Leal M. 2012. Geographic variation in vulnerability to climate warming in a tropical Caribbean lizard. Funct Ecol 26:783–93.
Gunderson AR, Stillman JH. 2015. Plasticity in thermal tolerance has limited potential to buffer ectotherms from global warming. Proc R Soc B Biol Sci 282.
Gunnell GF, Gingerich PD. 1993. Skeleton of *Brachianodon westorum*, a new middle Eocene metacheiromyid (Mammalia, Palaeanodonta) from the early Bridgerian (Bridger A) of the southern Green River Basin, Wyoming. Contrib from Museum Paleontol Univ Michigan 28:365–92.
Halliday T, Adler K (Eds.). n.d. The New Encyclopedia of Reptiles and Amphibians. Second. ed Oxford University Press.
Hammer Ø, Harper DAT, Ryan PD. 2001. PAST: Palaeontological Statistics software package for education and data analysis. Palaeontol Electron 4:1–9.
Hampe A, Petit RJ. 2005. Ideas and Perspectives: Conserving biodiversity under climate change: the rear edge matters. Ecol Lett 8:461–67.
Harley CDG. 2011. Climate change, keystone predation, and biodiversity loss. Science (80-) 334:1124–27.
Hastings AK, Hellmund M. 2017. Evidence for prey preference partitioning in the middle Eocene high-diversity crocodylian assemblage of the Geiseltal-Fossillagerstätte, Germany utilizing skull shape analysis. Geol Mag 154:119–46.
Head JJ, Bloch JI, Hastings AK, Bourque JR, Cadena EA, Herrera FA, David Polly P, Jaramillo CA. 2009. Giant boid snake from the Palaeocene neotropics reveals hotter past equatorial temperatures. Nature 457:715–18.
Head JJ, Gunnell GF, Holroyd PA, Howard Hutchison J, Ciochon RL. 2013. Giant lizards occupied herbivorous mammalian ecospace during the Paleogene greenhouse in Southeast Asia. Proc R Soc B Biol Sci 280.
Hecht M. 1975. The morphology and relationships of the largest known terrestrial lizard, *Megalania prisca* Owen, from the Pleistocene of Australia. Proc R Soc Victoria 87:239–50.
Herrera-Flores JA, Stubbs TL, Benton MJ. 2021. Ecomorphological diversification of squamates in the Cretaceous. R Soc Open Sci 8:1–11.
Hijmans RJ, Cameron SE, Parra JL, Jones PG, Jarvis A. 2005. Very high resolution interpolated climate surfaces for global land areas. Int J Climatol 25:1965–78.
Hill R V., Lucas SG. 2006. New data on the anatomy and relationships of the Paleocene crocodylian *Akanthosuchus langstoni*. Acta Palaeontol Pol 51:455–64.
Hobbs K, Fawcett PJ. 2012. Paleocene climate change in the San Juan Basin, New Mexico: A paleosol perspective. In: American Geophysical Union, Fall Meeting 2012, abstract id.

PP11B-2022 American Geophysical Union.
Hoffman A. 1979. Community paleoecology as an epiphenomenal science. Paleobiology1 5:357–79.
Hoffmann AA, Sgró CM. 2011. Climate change and evolutionary adaptation. Nature 470:479–85.
Hotton III N. 1955. A survey of adaptive relationships of dentition to the diet in the North American Iguanidae. Am Midl Nat 53:86–114.
Huang S, Eronen JT, Janis CM, Saarinen JJ, Silvestro D, Fritz SA. 2017. Mammal body size evolution in North America and Europe over 20 Myr: Similar trends generated by different processes. Proc R Soc B Biol Sci 284:1–9.
Huber M, Caballero R. 2011. The early Eocene equable climate problem revisited. Clim Past 7:603–33.
Huey RB. 1974. Behavioral thermoregulation in lizards: Importance of associated costs. Science (80-) 184:1001–3.
Huey RB. 1991. Physiological Consequences of Habitat Selection. Am Nat 137:S91–115.
Huey RB, Hertz PE, Sinervo B. 2003. Behavioral drive versus behavioral inertia in evolution: A null model approach. Am Nat 161:357–66.
Huey RB, Kearney MR, Krockenberger A, Holtum JAM, Jess M, Williams SE. 2012. Predicting organismal vulnerability to climate warming: Roles of behaviour, physiology and adaptation. Philos Trans R Soc B Biol Sci 367:1665–79.
Huey RB, Kingsolver JG. 1989. Evolution of thermal sensitivity of ectotherm performance. Trends Ecol Evol 4:131–35.
Huey RB, Kingsolver JG. 1993. Evolution of Resistance to High Temperature in Ectotherms. Am Nat 142:S21–46.
Huey RB, Losos JB, Moritz C. 2010. Are Lizards toast? Science (80-) 328:832–33.
Huey RB, Slatkin M. 1976. Cost and benefits of lizard thermoregulation. Q Rev Biol 51:363–84.
Huey RB, Stevenson RD. 1979. Integrating Thermal Physiology and Ecology of Ectotherms : A Discussion of Approaches. Am Zool 19:357–66.
Hutchison JH. 1982. Turtle, crocodilian, and champsosaur diversity changes in the Cenozoic of the north-central region of Western United States. Palaeogeogr Palaeoclimatol Palaeoecol 37:149–64.
Hutchison JH. 1992. Western North American reptile and amphibian record across the Eocene-Oligocene boundary and its climatic implications. In: Prothero DR, Berggren WA, editors. Eocene-Oligocene Climatic and Biotic Evolution Princeton: Princeton University Press. p. 451–63.
Hyland EG, Huntington KW, Sheldon ND, Reichgelt T. 2018. Temperature seasonality in the North American continental interior during the Early Eocene Climatic Optimum. Clim Past 14:1391–1404.
Hyland EG, Sheldon ND. 2013. Coupled CO2-climate response during the Early Eocene Climatic Optimum. Palaeogeogr Palaeoclimatol Palaeoecol 369:125–35.
Hyland EG, Sheldon ND. 2016. Examining the spatial consistency of palaeosol proxies: Implications for palaeoclimatic and palaeoenvironmental reconstructions in terrestrial sedimentary basins. Sedimentology 63:959–71.
Janecke SU. 1994. Sedimentation and paleogeography of an Eocene to Oligocene rift zone, Idaho and Montana. Geol Soc Am Bull 106:1083–95.
Janzen DH. 1967. Why Mountain Passes are Higher in the Tropics. Am Nat 101:233–49.

Jardine P. 2011. The Paleocene-Eocene Thermal Maximum. Palaeontol Online 1:1–7.
John-Alder AB, Lowe CH, Bennett AF. 1983. Thermal dependence of locomotory energetics and aerobic capacity of the file monitor (Heloderma suspectum). J Comp Physiol 151:119–26.
Johnson KR, Ellis B. 2002. A Tropical Rainforest in Colorado 1.4 Million Years After the Cretaceous-Tertiary Boundary. Science (80-) 296:2379–83.
Johnson KR, Reynolds ML, Werth KW, Thomasson JR. 2003. Overview of the Late Cretaceous, early Paleocene, and early Eocene megafloras of the Denver Basin, Colorado. Rocky Mt Geol 38:101–20.
Keeling CD, Piper SC, Bacastow RB, Wahlen M, Whorf TP, Heimann M, Meijer HA. 2001. Exchanges of atmospheric CO2 and 13CO2 with the terrestrial biosphere and oceans from 1978 to 2000. I. Global aspects, SIO Reference Series, No. 01-06 San Diego, CA.
Keith DA, Akçakaya HR, Thuiller W, Midgley GF, Pearson RG, Phillips SJ, Regan HM, Araújo MB, Rebelo TG. 2008. Predicting extinction risks under climate change: Coupling stochastic population models with dynamic bioclimatic habitat models. Biol Lett 4:560–63.
Kemp ME, Hadly EA. 2015. Extinction biases in Quaternary Caribbean lizards. Glob Ecol Biogeogr 24:1281–89.
Kingsolver JG. 2009. The Well-Temperatured Biologist. Am Nat 174:755–68.
Kingsolver JG, Huey RB. 2008. Size, temperature, and fitness: Three rules. Evol Ecol Res 10:251–68.
Koch PL. 1998. Isotopic Reconstruction of Past Continental Environments. Annu Rev Earth Planet Sci 26:573–613.
Kowalski EA, Dilcher DL. 2003. Warmer paleotemperatures for terrestrial ecosystems. Proc Natl Acad Sci 100:167–70.
Kozma R, Melsted P, Magnússon KP, Höglund J. 2016. Looking into the past - The reaction of three grouse species to climate change over the last million years using whole genome sequences. Mol Ecol 25:570–80.
Kubisch E, Piantoni C, Williams J, Scolaro A, Navas CA, Ibargüengoytía NR. 2012. Do higher temperatures increase growth in the nocturnal gecko *Homonota darwini* (Gekkota: Phyllodactylidae)? A skeletochronological assessment analyzed at temporal and geographic scales. J Herpetol 46:587–95.
Kump LR. 2011. The last great global warming. Sci Am 305:56–61.
Lakin RJ, Barrett PM, Stevenson C, Thomas RJ, Wills MA. 2020. First evidence for a latitudinal body mass effect in extant Crocodylia and the relationships of their reproductive characters. Biol J Linn Soc 129:875–87.
Lang JW. 2008. Crocodilians. New Encycl Reptil Amphib.
Lavergne S, Mouquet N, Thuiller W, Ronce O. 2010. Biodiversity and climate change: Integrating evolutionary and ecological responses of species and communities. Annu Rev Ecol Evol Syst 41:321–50.
Lawler JJ, Ruesch AS, Olden JD, Mcrae BH. 2013. Projected climate-driven faunal movement routes. Ecol Lett 16:1014–22.
Longrich NR, Bhullar BAS, Gauthier JA. 2012. Mass extinction of lizards and snakes at the Cretaceous-Paleogene boundary. Proc Natl Acad Sci U S A 109:21396–401.
López-Victoria M, Herrón PA, Botello JC. 2011. Notes on the ecology of the lizards from Malpelo Island, Colombia. Bull Mar Coast Res 40:79–89.
Losos JB, Greene HW. 1988. Ecological and evolutionary implications of diet in monitor lizards. Biol J Linn Soc 35:379–407.

Lovegrove BG, Mowoe MO. 2013. The evolution of mammal body sizes: Responses to Cenozoic climate change in North American mammals. J Evol Biol 26:1317–29.
Lüthi D, Le Floch M, Bereiter B, Blunier T, Barnola JM, Siegenthaler U, Raynaud D, Jouzel J, Fischer H, Kawamura K, Stocker TF. 2008. High-resolution carbon dioxide concentration record 650,000-800,000 years before present. Nature 453:379–82.
MacFarling Meure C, Etheridge D, Trudinger C, Steele P, Langenfelds R, Van Ommen T, Smith A, Elkins J. 2006. Law Dome CO2, CH4 and N2O ice core records extended to 2000 years BP. Geophys Res Lett 33:2000–2003.
Makarieva AM, Gorshkov VG, Li BL. 2005a. Gigantism, temperature and metabolic rate in terrestrial poikilotherms. Proc R Soc B Biol Sci 272:2325–28.
Makarieva AM, Gorshkov VG, Li BL. 2005b. Temperature-associated upper limits to body size in terrestrial poikilotherms. Oikos 111:425–36.
Mannion PD, Benson RBJ, Carrano MT, Tennant JP, Judd J, Butler RJ. 2015. Climate constrains the evolutionary history and biodiversity of crocodylians. Nat Commun 6:1–9.
Markwick PJ. 1994. "Equability," continentality, and Tertiary "climate": The crocodilian perspective. Geology 22:613–16.
Markwick PJ. 1998a. Fossil crocodilians as indicators of Late Cretaceous and Cenozoic climates: Implications for using palaeontological data in reconstructing palaeoclimate. Palaeogeogr Palaeoclimatol Palaeoecol 137:205–71.
Markwick PJ. 1998b. Fossil crocodilians as indicators of Late Cretaceous and Cenozoic climates: Implications for using palaeontological data in reconstructing palaeoclimate. Palaeogeogr Palaeoclimatol Palaeoecol 137:205–71.
Markwick PJ. 1998c. Crocodilian Diversity in Space and Time: The Role of Climate in Paleoecology and its Implication for Understanding K / T Extinctions. Paleobiology 24:470–97.
Marsh OC. 1871. Notice of some new fossil reptiles from the Cretaceous and Tertiary formations. Am J Sci 1:447–59.
Marsh OC. 1872. Preliminary description of new Tertiary reptiles, Parts I & II. Am J Sci 4:298–309.
Masson-Delmotte V, Zhai P, Pörtner H-O, Roberts D, Skea J, Shukla PR, Pirani A, Moufouma-Okia W, Péan C, Pidcock R, Connors S, Matthews JBR, Chen Y, Zhou X, Gomis MI, Lonnoy E, Maycock T, Tignor M, Waterfield T. 2018. IPCC, 2018: Summary for Policymakers. In: Global Warming of 1.5°C. An IPCC Special Report on the impacts of global warming of 1.5°C above pre-industrial levels and related global greenhouse gas emission pathways, in the context of strengthening the global Geneva, Switzerland.
Matson SD, Fox DL. 2008. Can Oxygen Isotopes From Turtle Bone Be Used To Reconstruct Paleoclimates? Palaios 23:24–34.
McInerney FA, Wing SL. 2011. The Paleocene-Eocene Thermal Maximum: A Perturbation of Carbon Cycle, Climate, and Biosphere with Implications for the Future. Annu Rev Earth Planet Sci 39:489–516.
Meiri S. 2008. Evolution and ecology of lizard body sizes. Glob Ecol Biogeogr 17:724–34.
Meiri S. 2010. Length-weight allometries in lizards. J Zool 281:218–26.
Meiri S. 2018. Traits of lizards of the world: Variation around a successful evolutionary design. Glob Ecol Biogeogr 27:1168–72.
Melstrom KM. 2017. The relationship between diet and tooth complexity in living dentigerous saurians. J Morphol 278:500–522.

Meszoely CAM. 1970. North American fossil anguid lizards. Bull Museum Comp Zool 139:87–150.
Metzger KA, Herrel A. 2005. Correlations between lizard cranial shape and diet: A quantitative, phylogenetically informed analysis. Biol J Linn Soc 86:433–66.
Meyer HW. 1986. An evaluation of the methods for estimating paleoaltitudes using Tertiary floras from the Rio Grande Rift vicinity, New Mexico and Colorado.
Midgley G, Hannah L. 2019. Extinction risk from climate change. Biodivers Clim Chang Transform Biosph 294–96.
Miles DB. 1994. Population Differentiation in Locomotor Performance and the Potential Response of a Terrestrial Organism to Global Environmental Change. Am Zool 34:422–36.
Miller-camp J. 2016. Patterns in Alligatorine Evolution.
Millien V, Kathleen Lyons S, Olson L, Smith FA, Wilson AB, Yom-Tov Y. 2006. Ecotypic variation in the context of global climate change: Revisiting the rules. Ecol Lett 9:853–69.
Morgan ME, Badgley C, Gunnelp GF, Gingerich PD, Kappelman JW, Maas MC. 1995. Comparative paleoecology of Paleogene and Neogene mammalian faunas: Body-size structure. Palaeogeogr Palaeoclimatol Palaeoecol 115:287–317.
Morin X, Thuiller W. 2009. Comparing niche- and process-based models to reduce prediction uncertainty in species range shifts under climate change. Ecology 90:1301–13.
Moscato DA. 2013. A Glyptosaurine Lizard from the Eocene (late Uintan) of San Diego , California , and Implications for Glyptosaurine Evolution and Biogeography. .
Muñoz MM, Bodensteiner BL. 2019. Janzen's Hypothesis meets the Bogert Effect: Connecting climate variation, thermoregulatory behavior, and rates of physiological evolution. Integr Org Biol 1:1–12.
Muñoz MM, Losos JB. 2018. Thermoregulatory behavior simultaneously promotes and forestalls evolution in a tropical lizard. Am Nat 191:E15–26.
Muñoz MM, Stimola MA, Algar AC, Conover A, Rodriguez AJ, Landestoy MA, Bakken GS, Losos JB. 2014. Evolutionary stasis and lability in thermal physiology in a group of tropical lizards. Proc R Soc B Biol Sci 281:20132433.
Norris RD, Jones LS, Corfield RM, Cartlidge JE. 1996. Skiing in the Eocene Uinta mountains? Isotopic evidence in the Green River Formation for snow melt and large mountains. Geology 24:403–6.
O'Brien HD, Lynch LM, Vliet KA, Brueggen J, Erickson GM, Gignac PM. 2019. Crocodylian Head Width Allometry and Phylogenetic Prediction of Body Size in Extinct Crocodyliforms. Integr Org Biol 1.
Olalla-Tárraga MÁ, Rodríguez MÁ, Hawkins BA. 2006a. Broad-scale patterns of body size in squamate reptiles of Europe and North America. J Biogeogr 33:781–93.
Olalla-Tárraga MÁ, Rodríguez MÁ, Hawkins BA. 2006b. Broad-scale patterns of body size in squamate reptiles of Europe and North America. J Biogeogr 33:781–93.
Peppe DJ. 2010. Megafloral change in the early and middle Paleocene in the Williston Basin, North Dakota, USA. Palaeogeogr Palaeoclimatol Palaeoecol 298:224–34.
Peppe DJ, Royer DL, Cariglino B, Oliver SY, Newman S, Leight E, Enikolopov G, Fernandez-Burgos M, Herrera F, Adams JM, Correa E, Currano ED, Erickson JM, Hinojosa LF, Hoganson JW, Iglesias A, Jaramillo CA, Johnson KR, Jordan GJ, Kraft NJB, Lovelock EC, Lusk CH, Niinemets Ü, Peñuelas J, Rapson G, Wing SL, Wright IJ. 2011. Sensitivity of leaf size and shape to climate: Global patterns and paleoclimatic applications. New Phytol 190:724–39.

Peters RH. 1983. The Ecological Implications of Body Size. 1st ed New York, NY: Cambridge University Press.
Pianka ER. 1973. The Structure of Lizard Communities. Annu Rev Ecol Syst 4:53–74.
Pianka ER. 1995. Evolution of body size: Varanid lizards as a model system. Am Nat 146:398–414.
Pianka ER, Vitt LJ. 2003. Lizards: Windows to the Evolution of Diversity Berkeley: University of California Press.
Pianka ER, Vitt LJ, Pelegrin N, Fitzgerald DB, Winemiller KO. 2017. Toward a Periodic Table of Niches, or Exploring the Lizard Niche Hypervolume. Am Nat 190:000–000.
Piantoni C, Navas CA, Ibargüengoytía NR. 2019. A real tale of Godzilla: Impact of climate warming on the growth of a lizard. Biol J Linn Soc 126:768–82.
Pincheira-Donoso D, Hodgson DJ, Tregenza T. 2008. The evolution of body size under environmental gradients in ectotherms: Why should Bergmann's rule apply to lizards? BMC Evol Biol 8:1–13.
Pincheira-Donoso D, Tregenza T, Hodgson DJ. 2007. Body size evolution in South American *Liolaemus* lizards of the *boulengeri* clade: A contrasting reassessment. J Evol Biol 20:2067–71.
Polly PD, Eronen JT, Fred M, Dietl GP, Mosbrugger V, Scheidegger C, Frank DC, Damuth J, Stenseth NC, Fortelius M. 2011. History matters: ecometrics and integrative climate change biology. Proc R Soc B Biol Sci 278:1131–40.
Pough FH. 1973. Lizard Energetics and Diet. Ecology 54:837–44.
Pough FH. 1980. The advantages of ectothermy for tetrapods. Am Nat 115:92–112.
Pound MJ, Haywood AM, Salzmann U, Riding JB, Lunt DJ, Hunter SJ. 2011. A Tortonian (Late Miocene, 11.61-7.25Ma) global vegetation reconstruction. Palaeogeogr Palaeoclimatol Palaeoecol 300:29–45.
Prothero DR, Berggren WA. 1992. Eocene-Oligocene climate and biotic evolution. Earth-Science Rev 34:568.
Quintero I, Wiens JJ. 2013. Rates of projected climate change dramatically exceed past rates of climatic niche evolution among vertebrate species. Ecol Lett 16:1095–1103.
Rasmussen DL. 2003. Tertiary history of western Montana and east-central Idaho: A synopsis. In: Raynolds RG, Flores RM, editors. Cenozoic Systems of the Rocky Mountain Region Denver, Colorado: Rocky Mountain Society of Economic Paleontologists and Mineralogists. p. 459–477.
Rasmussen DM, Foreman BZ. 2017. Provenance of lower Paleogene strata in the Huerfano basin: implications for uplift of the Wet Mountains, Colorado, U.S.A. J Sediment Res 87:579–93.
Retallack GJ. 2007. Cenozoic Paleoclimate on Land in North America. J Geol 115:271–94.
Ripple WJ, Wolf C, Newsome TM, Gregg JW, Lenton TM, Palomo I, Eikelboom JAJ, Law BE, Huq S, Duffy PB, Rockström J. 2021. World scientists' warning of a climate emergency 2021. Bioscience 71:894–98.
Robson SG, Banta ER. 1995. Arizona, Colorado, New Mexico, Utah HA 730-CUSGS Gr Water Atlas United States. (https://pubs.usgs.gov/ha/ha730/ch_c/C-text8.html).
Roehler HW. 1993. Eocene climates, depositional environments, and geography, greater Green River Basin, Wyoming, Utah, and Colorado. United States Geol Surv Prof Pap.
Roll U, Feldman A, Novosolov M, Allison A, Bauer AM, Bernard R, Böhm M, Castro-Herrera F, Chirio L, Collen B, Colli GR, Dabool L, Das I, Doan TM, Grismer LL, Hoogmoed M,

Itescu Y, Kraus F, Lebreton M, Lewin A, Martins M, Maza E, Meirte D, Nagy ZT, Nogueira CDC, Pauwels OSG, Pincheira-Donoso D, Powney GD, Sindaco R, Tallowin OJS, Torres-Carvajal O, Trape JF, Vidan E, Uetz P, Wagner P, Wang Y, Orme CDL, Grenyer R, Meiri S. 2017a. The global distribution of tetrapods reveals a need for targeted reptile conservation. Nat Ecol Evol 1:1677–82.

Roll U, Feldman A, Novosolov M, Allison A, Bauer AM, Bernard R, Böhm M, Castro-Herrera F, Chirio L, Collen B, Colli GR, Dabool L, Das I, Doan TM, Grismer LL, Hoogmoed M, Itescu Y, Kraus F, Lebreton M, Lewin A, Martins M, Maza E, Meirte D, Nagy ZT, Nogueira CDC, Pauwels OSG, Pincheira-Donoso D, Powney GD, Sindaco R, Tallowin OJS, Torres-Carvajal O, Trape JF, Vidan E, Uetz P, Wagner P, Wang Y, Orme CDL, Grenyer R, Meiri S. 2017b. The global distribution of tetrapods reveals a need for targeted reptile conservation. Nat Ecol Evol 1:1677–82.

Rose KD. 1981. Composition and Species Diversity in Paleocene and Eocene Mammal Assemblages: An Empirical Study. J Vertebr Paleontol 1:367–88.

Rose KD. 2008. Palaeanodonta and pholidota. In: Janis CM, Gunnell GF, Uhen MD, editors. Evolution of Tertiary Mammals of North America: Volume 2, Small Mammals, Xenarthrans, and Marine Mammals Cambridge, UK: Cambridge University Press. p. 135–46.

Rose KD, Chew AE, Dunn RH, Kraus MJ, Fricke HC, Zack SP. 2012. Earliest Eocene mammalian fauna from the Paleocene-Eocene Thermal Maximum at Sand Creek Divide, Southern Bighorn Basin, Wyoming. Univ Michigan Pap Paleontol 36:1–122.

Rose KD, Dunn RH, Grande L. 2014. A new skeleton of *Palaeosinopa didelphoides* (Mammalia, Pantolesta) from the early Eocene Fossil Butte Member, Green River Formation (Wyoming), and skeletal ontogeny in Pantolestidae. J Vertebr Paleontol 34:932–40.

Rose KD, Krishtalka L, Stucky RK. 1991. Revision of the Wind River faunas, early Eocene of central Wyoming. Part 11. Palaeanodonta (Mammalia). Ann Carnegie Museum 60:63–82.

Rose KD, Von Koenigswald W. 2005. An exceptionally complete skeleton of *Palaeosinopa* (Mammalia, Cimolesta, Pantolestidae) from the Green River formation, and other postcranial elements of the Pantolestidae from the Eocene of Wyoming (USA). Palaeontogr Abteilung A Palaozoologie - Stratigr 273:55–96.

Rothfuss JL, Lielke K, Weislogel AL. 2012. Application of detrital zircon provenance in paleogeographic reconstruction of an intermontane basin system, Paleogene Renova Formation, southwest Montana. In: Rasbury ET, Riggs NR, Hemming SR, editors. Mineralogical and Geochemical Approaches to Provenance: Geological Society of America Special Paper 487 Denver, Colorado: Geological Society of America. p. 63–95.

Royer DL. 2012. Climate Reconstruction from Leaf Size and Shape: New Developments and Challenges. Paleontol Soc Pap 18:195–212.

Saarinen JJ, Boyer AG, Brown JH, Costa DP, Ernest M, Evans AR, Fortelius M, Gittleman JL, Marcus J, Harding LE, Lintulaakso K, Lyons SK, Okie JG, Sibly M, Stephens PR, Theodor J, Uhen MD, Smith FA. 2014. Patterns of maximum body size evolution in Cenozoic land mammals: eco-evolutionary processes and abiotic forcing. Proc R Soc B Biol Sci 281:1–10.

Sandau SD. 2005. The paleoclimate and paleoecology of a Uintan (Late Middle Eocene) flora and fauna from the Uinta Basin, Utah.

Sanggaard KW, Danielsen CC, Wogensen L, Vinding MS, Rydtoft LM, Mortensen MB, Karring H, Nielsen NC, Wang T, Thøgersen IB, Enghild JJ. 2012. Unique Structural Features Facilitate Lizard Tail Autotomy. PLoS One 7.

Scarpetta SG. 2019. *Peltosaurus granulosus* (Squamata, Anguidae) from the middle Oligocene of Sharps Corner, South Dakota, and the youngest known chronostratigraphic occurrence of Glyptosaurinae. J Vertebr Paleontol 39:e1622129.
Scheibe JS. 1987. Climate , Competition , and the Structure of Temperate Zone Lizard Communities. Ecology 68:1424–36.
Schmidt-Nielsen K. 1984. Scaling: Why is Animal Size So Important? Cambridge: Cambridge University Press.
Secord R, Bloch JI, Chester SGB, Boyer DM, Wood AR, Wing SL, Kraus MJ, Mcinerney FA, Krigbaum J. 2012. Evolution of the Earliest Horses Paleocene-Eocene Thermal Maximum. 335:959–62.
Seebacher F, Franklin CE. 2012. Determining environmental causes of biological effects: The need for a mechanistic physiological dimension in conservation biology. Philos Trans R Soc B Biol Sci 367:1607–14.
Sereno PC, Larsson HCE, Sidor CA, Gado B. 2001. The giant crocodyliform *Sarcosuchus* from the cretaceous of Africa. Science (80-) 294:1516–19.
Sewall JO, Sloan LC. 2006. Come a little bit closer: A high-resolution climate study of the early Paleogene Laramide foreland. Geology 34:81–84.
Sheldon ND. 2018. Using Carbon Isotope Equilibrium to Screen Pedogenic Carbonate Oxygen Isotopes: Implications for Paleoaltimetry and Paleotectonic Studies. Geofluids 2018.
Sinervo B, Adolph SC. 1989. Thermal sensitivity of growth rate in hatchling *Scleroporus* lizards: Environmental, behavioural and genetic aspects. Oecologia 78:411–19.
Sinervo B, Adolph SC. 1994. Growth plasticity and thermal opportunity in *Sceloporus* lizards. Ecology 75:776–90.
Sinervo B, Méndez-de-la-Cruz F, Miles DB, Heulin B, Bastiaans E, Cruz MVS, Lara-Resendiz R, Martínez-Méndez N, Calderón-Espinosa ML, Meza-Lázaro RN, Gadsden H, Avila LJ, Morando M, De La Riva IJ, Sepúlveda PV, Rocha CFD, Ibargüengoytía N, Puntriano CA, Massot M, Lepetz V, Oksanen TA, Chappie DG, Bauer AM, Branch WR, Clobert J, Sites JW. 2010. Erosion of lizard diversity by climate change and altered thermal niches. Science (80-) 328:894–99.
Slavenko A, Feldman A, Allison A, Bauer AM, Böhm M, Chirio L, Colli GR, Das I, Doan TM, LeBreton M, Martins M, Meirte D, Nagy ZT, Nogueira C de C, Pauwels OSG, Pincheira-Donoso D, Roll U, Wagner P, Wang Y, Meiri S. 2019. Global patterns of body size evolution in squamate reptiles are not driven by climate. Glob Ecol Biogeogr 28:471–83.
Slavenko A, Tallowin OJS, Itescu Y, Raia P, Meiri S. 2016. Late Quaternary reptile extinctions: size matters, insularity dominates. Glob Ecol Biogeogr 25:1308–20.
Smith EN. 1979. Behavioral and physiological thermoregulation of crocodilians. Integr Comp Biol 19:239–47.
Smith GR, Ballinger RE, Nietfeldt JW. 1994. Elevational Variation of Growth Rates in Neonate *Sceloporus jarrovi*: An Experimental Evaluation. Funct Ecol 8:215.
Smith KT. 2006. A diverse new assemblage of Late Eocene squamates (Reptilia) from the Chadron Formation of North Dakota, U.S.A. Palaeontol Electron 9:1–44.
Smith KT. 2009. A new lizard assemblage from the earliest Eocene (zone Wa0) of the Bighorn Basin, Wyoming, USA: Biogeography during the warmest interval of the Cenozoic, Journal of Systematic Palaeontology.
Smith KT. 2011a. The evolution of mid-latitude faunas during the Eocene: Late Eocene lizards of the Medicine Pole Hills reconsidered. Bull Peabody Museum Nat Hist 52:3–105.

Smith KT. 2011b. The long-term history of dispersal among lizards in the early Eocene: New evidence from a microvertebrate assemblage in the Bighorn Basin of Wyoming, USA. Palaeontology 54:1243–70.
Smith KT, Gauthier JA. 2013. Early Eocene lizards of the Wasatch Formation near Bitter Creek, Wyoming: Diversity and paleoenvironment during an interval of global warming. Bull Peabody Museum Nat Hist 54:135–230.
Smith RJ. 2002. Estimation of body mass in paleontology. J Hum Evol 43:271–87.
Snell KE. 2011. Paleoclimate and paleoelevation of the western Cordillera in the United States.
Snell KE, Thrasher BL, Eiler JM, Koch PL, Sloan LC, Tabor NJ. 2013. Hot summers in the Bighorn Basin during the early Paleogene. Geology 41:55–58.
Snoke AW, Steidtmann JR, Roberts SM. 1993. Geology of Wyoming Laramie, WY.
Solórzano A, Núñez-Flores M, Inostroza-Michael O, Hernández CE. 2020. Biotic and abiotic factors driving the diversification dynamics of Crocodylia. Palaeontology 63:415–29.
Stamps JA. 1977. Rainfall, Moisture and Dry Season Growth Rates in *Anolis aeneus*. Copeia 1977:415–19.
Stein RA, Sheldon ND, Allen SE, Smith ME, Dzombak RM, Jicha BR. 2021. Climate and ecology in the Rocky Mountain Interior after the Early Eocene Climatic Optimum. Clim Past 17:2515–36.
Stout JB. 2012. New material of *Borealosuchus* from the Bridger Formation, with notes on the paleoecology of Wyoming's Eocene crocodylians. PalArch's J Vertebr Palaeontol 9:1–7.
Strömberg CAE. 2011. Evolution of grasses and grassland ecosystems. Annu Rev Earth Planet Sci 39:517–44.
Stucky RK. 1992. Mammalian faunas in North America of Bridgerian to Early Arikareean "Ages" (Eocene and Oligocene). In: Prothero DR, Berggren WA, editors. Eocene-Oligocene Climatic and Biotic Evolution Princeton, NJ: Princeton University Press. p. 464–93.
Sullivan RM. 1979. Revision of the Paleogene genus *Glyptosaurus* (Reptilia, Anguidae). Bull Am Museum Nat Hist 163.
Sullivan RM. 2019. The taxonomy, chronostratigraphy and paleobiogeography of glyptosaurine lizards (Glyptosaurinae, Anguidae). Comptes Rendus Palevol 18:747–63.
Sunday JM, Bates AE, Kearney MR, Colwell RK, Dulvy NK, Longino JT, Huey RB. 2014. Thermal-safety margins and the necessity of thermoregulatory behavior across latitude and elevation. Proc Natl Acad Sci 111:5610–15.
Swinehart JB, Souders VL, Degraw HM, Diffendal RF. 1985. Cenozoic paleogeography of western Nebraska. In: Flores RM, Kaplan SS, editors. Rocky Mountain Paleogeography Symposium 3: Cenozoic Paleogeography of the West-central United States Denver, Colorado: Rocky Mountain Section SEPM. p. 209–29.
Terry DO. 2001. Paleopedology of the Chadron Formation of northwestern Nebraska: Implications for paleoclimatic change in the North American midcontinent across the Eocene-Oligocene boundary. Palaeogeogr Palaeoclimatol Palaeoecol 168:1–38.
The Paleobiology Database. n.d. . (www.paleobiodb.org).
Thomas Goodwin H, Bullock KM. 2012. Estimates of body mass for fossil giant ground squirrels, genus *Paenemarmota*. J Mammal 93:1169–77.
Thuiller W. 2004. Patterns and uncertainties of species' range shifts under climate change. Glob Chang Biol 10:2020–27.
Tobin TS, Wilson GP, Eiler JM, Hartman JH. 2014. Environmental change across a terrestrial

Cretaceous-Paleogene boundary section in eastern Montana, USA, constrained by carbonate clumped isotope paleothermometry. Geology 42:351–54.
Tomiya S, Zack SP, Spaulding M, Flynn JJ. 2021. Carnivorous mammals from the middle Eocene Washakie Formation, Wyoming, USA, and their diversity trajectory in a post-warming world. J Paleontol 95:1–115.
Townsend KEB, Rasmussen DT, Murphey PC, Evanoff E. 2010. Middle Eocene habitat shifts in the North American western interior: A case study. Palaeogeogr Palaeoclimatol Palaeoecol 297:144–58.
Toyama KS, Boccia CK. 2022. Bergmann's rule in *Microlophus* lizards: testing for latitudinal and climatic gradients of body size. bioRxiv 2022.01.18.476846.
Uetz P, Hallermann J. n.d. The Reptile Database.
Valdes PJ. 2000. Warm climate forcing mechanisms. In: Huber BT, Macleod KG, Wing SL, editors. Warm Climates in Earth History2 Cambridge, UK: Cambridge University Press. p. 3–20.
Verdade LM. 2000. Regression equations between body and head measurements in the broad-snouted Caiman (*Caiman latirostris*). Rev Bras Biol 60:469–82.
Vidan E, Novosolov M, Bauer AM, Herrera FC, Chirio L, Campos Nogueira C, Doan TM, Lewin A, Meirte D, Nagy ZT, Pincheira-Donoso D, Tallowin OJS, Torres Carvajal O, Uetz P, Wagner P, Wang Y, Belmaker J, Meiri S. 2019. The global biogeography of lizard functional groups. J Biogeogr 00:1–12.
Villa A, Delfino M. 2019. A comparative atlas of the skull osteology of European lizards (Reptilia: Squamata). Zool J Linn Soc 1–100.
Villamarín F, Jardine TD, Bunn SE, Marioni B, Magnusson WE. 2018. Body size is more important than diet in determining stable-isotope estimates of trophic position in crocodilians. Sci Rep 8:1–11.
Vitt E.R. Pianka, W.E. Cooper, Jr., and K. Schwenk LJ. 2003. History and the global ecology of squamate reptiles. Am Nat 162:44–60.
Vitt LJ, Caldwell JP. 2009. Herpetology: An Introductory Biology of Amphibians and Reptiles. 3rd ed Burlington, MA: Elsevier.
Wang IJ, Glor RE, Losos JB. 2013. Quantifying the roles of ecology and geography in spatial genetic divergence. Ecol Lett 16:175–82.
Wassersug RJ, Hecht MK. 1967. The Status of the Crocodylid Genera *Procaimanoidea* and *Hassiacosuchus* in the New World. Herpetologica 23:30–34.
Webb GJW, Messel H, Crawford J, Yerbury MJ. 1978. Growth rates of *Crocodylus porosus* (Reptilia: Crocodilia) from Arnhem Land, Northern Australia. Wildl Res 5:385–99.
Whiting ET, Fox DL. 2021. Latitudinal and environmental patterns of species richness in lizards and snakes across continental North America. J Biogeogr 48:291–304.
Whiting ET, Hastings AK. 2015. First Fossil Alligator from the Late Eocene of Nebraska and the Late Paleogene Record of Alligators in the Great Plains. J Herpetol 49:560–69.
Wiens JJ, Brandley MC, Reeder TW. 2006. Why Does a Trait Evolve Multiple Times Within a Clade? Repeated Evolution of Snakelike Body Form in Squamate Reptiles. Evolution (N Y) 60:123.
Wiens JJ, Hutter CR, Mulcahy DG, Noonan BP, Townsend TM, Sites JW, Reeder TW. 2012. Resolving the phylogeny of lizards and snakes (Squamata) with extensive sampling of genes and species. Biol Lett Lett 8:1043–46.
Wilberg EW, Turner AH, Brochu CA. 2019. Evolutionary structure and timing of major habitat

shifts in Crocodylomorpha. Sci Rep 9:1–10.
Wilf P. 2000. Late Paleocene-Early Eocene climate changes in Southwestern Wyoming: Paleobotanical analysis. Bull Geol Soc Am 112:292–307.
Wilf P, Beard KC, Davies-Vollum KS, Norejko JW. 1998. Portrait of a late Paleocene (early Clarkforkian) terrestrial ecosystem: Big Multi Quarry and associated strata, Washakie Basin, southwestern Wyoming. Palaios 13:514–32.
Wilf P, Johnson KR, Huber BT. 2003. Correlated terrestrial and marine evidence for global climate changes before mass extinction at the Cretaceous-Paleogene boundary. Proc Natl Acad Sci 100:599–604.
Wilf P, Wing SL, Greenwood DR, Greenwood CL. 1998. Using fossil leaves as paleoprecipitation indicators: An Eocene example. Geology 26:203–6.
Williams SE, Shoo LP, Isaac JL, Hoffmann AA, Langham G. 2008. Towards an integrated framework for assessing the vulnerability of species to climate change. PLoS Biol 6.
Wing SL. 1987. Eocene and Oligocene floras and vegetation of the Rocky Mountains. Ann Missouri Bot Gard 74:748.
Wing SL. 1998. Tertiary vegetation of North America as a context for mammalian evolution. In: Janis CM, Scott KM, Jacobs LL, editors. Evolution of Tertiary Mammals of North America Cambridge University Press. p. 37–60.
Wing SL, Bao H, Koch PL. 2000. An early Eocene cool period? Evidence for continental cooling during the warmest part of the Cenozoic. In: Huber BT, Macleod KG, Wing SL, editors. Warm Climates in Earth History Cambridge, UK: Cambridge University Press. p. 197–237.
Wing SL, Bloch JI, Bowen GJ, Boyer DM, Chester S, Diefendorf AF, Harrington GJ, Kraus MJ, Secord R, Mcinerney FA. 2009. Coordinated sedimentary and biotic change during the Paleocene–Eocene Thermal Maximum in the Bighorn Basin, Wyoming, USA. In: Crouch EM, Strong CP, Hollis CJ, editors. Climatic and Biotic Events of the Paleogene (CBEP 2009), Extended Abstracts from an International Conference in Wellington, New Zealand, 12-15 January 2009 GNS Science Miscellaneous Series. p. 157–63.
Wing SL, Bown TM, Obradovich JD. 1991. Early Eocene biotic and climatic change in interior western North America. Geology 19:1189–92.
Wing SL, Greenwood DR. 1993. Fossils and fossil climate: The case for equable continental interiors in the Eocene. Philos Trans - R Soc London, B 341:243–52.
Wing SL, Harrington GJ, Smith FA, Bloch JI, Boyer DM, Freeman KH. 2005. Transient floral change and rapid global warming at the Paleocene-Eocene boundary. Science (80-) 310:993–96.
Wolfe JA. 1979. Temperature parameters of humid to mesic forests of eastern Asia and relation to forests of other regions of the Northern Hemisphere and Australasia. US Geol Surv Prof Pap 1106:1–37.
Wolfe JA. 1980. Tertiary climates and floristic relationships at high latitudes in the Northern Hemisphere. Palaeogeogr Palaeoclimatol Palaeoecol 30:313–23.
Wolfe JA. 1992. Climatic, floristic, and vegetational changes near the Eocene/Oligocene boundary in North America. In: Prothero DR, Berggren WA, editors. Eocene-Oligocene Climatic and Biotic Evolution Princeton, NJ: Princeton University Press. p. 421–36.
Wolfe JA. 1994. Tertiary climatic changes at middle latitudes of western North America. Palaeogeogr Palaeoclimatol Palaeoecol 103:195–205.
Wolfe JA, Forest CE, Molnar P. 1998. Paleobotanical evidence of Eocene and Oligocene

paleoaltitudes in midlatitude western North America. Bull Geol Soc Am 110:664–78.
Woodburne MO (Ed.). 2004. Late Cretaceous and Cenozoic Mammals of North America: Biostratigraphy and Geochronology New York: Columbia University Press.
Woodward AR, White JH, Linda SB. 1995. Maximum Size of the Alligator (*Alligator mississippiensis*). J Herpetol 29:507–13.
Woodward HN, Horner JR, Farlow JO. 2011. Osteohistological Evidence for Determinate Growth in the American Alligator. J Herpetol 45:339–42.
Woolley CH, Thompson JR, Wu Y-H (Beckey), Bottjer DJ, Smith ND. 2020. Can a fragmented past be trusted? Assessing bias and phylogenetic signal in the squamate fossil record. J Vertebr Paleontol Progr Abstr 351–52.
Woolley CH, Thompson JR, Wu YH, Bottjer DJ, Smith ND. 2022. A biased fossil record can preserve reliable phylogenetic signal. Paleobiology 1–16.
Young MT, Bell MA, de Andrade MB, Brusatte SL. 2011. Body size estimation and evolution in metriorhynchid crocodylomorphs: Implications for species diversification and niche partitioning. Zool J Linn Soc 163:1199–1216.
Zachos J, Pagani M, Sloan L, Thomas E, Billups K. 2001. Trends, rhythms and aberrations in global climate 65 Ma to present. Science (80-) 292:686–93.
Zachos JC, Dickens GR, Zeebe RE. 2008. An early Cenozoic perspective on greenhouse warming and carbon-cycle dynamics. Nature 451:279–83.
Zamora-Camacho FJ, Reguera S, Moreno-Rueda G. 2014. Bergmann's Rule rules body size in an ectotherm: heat conservation in a lizard along a 2200-metre elevational gradient. J Evol Biol 27:2820–28.
Zanazzi A, Kohn MJ, MacFadden BJ, Terry DO. 2007. Large temperature drop across the Eocene-Oligocene transition in central North America. Nature 445:639–42.
Zani PA. 1996. Patterns of caudal-anatomy evolution in lizards. J Zool 240:201–30.
Zimmerman LC, Tracy CR. 1989. Interactions between the environment and ectothermy and herbivory in reptiles. Physiol Zool 62:374–409.
Zizka A, Silvestro D, Andermann T, Azevedo J, Duarte Ritter C, Edler D, Farooq H, Herdean A, Ariza M, Scharn R, Svantesson S, Wengström N, Zizka V, Antonelli A. 2019. CoordinateCleaner: Standardized cleaning of occurrence records from biological collection databases. Methods Ecol Evol 10:744–51.

APPENDICES

DATA AVAILABILITY STATEMENT

All data are available to qualified researchers upon request. Captions for supporting information are given below.

CHAPTER 1 SUPPORTING INFORMATION

Chapter 1 Supplementary Table Captions

S1.1 Table. Anguidae regression equations and tests. Sample sizes indicate number of extant anguid specimens that included the element used in the given regression. If a regression did not pass the Homoskedasticity Test, I did not proceed to test the residuals of that regression for normal distribution. The remaining details are only provided for regressions that passed both tests. In some cases, both the untransformed and natural log transformed regressions for a given element passed both tests. In these instances, I chose a preferred regression based on other criteria, which are listed in the "Notes" column.

S1.2 Table. Varanidae regression equations and tests. Sample sizes indicate number of extant varanid specimens that included the element used in the given regression. If a regression did not pass the Homoskedasticity Test, I did not proceed to test the residuals of that regression for normal distribution. The remaining details are only provided for regressions that passed both tests. In some cases, both the untransformed and natural log transformed regressions for a given element passed both tests. In these instances, I chose a preferred regression based on other criteria, which are listed in the "Notes" column.

S1.3 Table. Xenosauridae regression equations and tests. Sample sizes indicate number of extant xenosaurid specimens that included the element used in the given regression. For each xenosaurid anatomical element used, both the untransformed and natural log transformed regressions for the given element passed the tests for homoskedasticity and normal distribution of residuals. I chose the untransformed regressions because they had much smaller ranges of error.

S1.4 Table. Teiidae regression equations and tests. Sample sizes indicate number of extant teiid specimens that included the element used in the given regression. If a regression did not pass the Homoskedasticity Test, I did not proceed to test the residuals of that regression for normal distribution. The remaining details are only provided for regression that passed both tests.

S1.5 Table. Scincidae regression equations and tests. Sample sizes indicate number of extant scincid specimens that included the element used in the given regression. If a regression did not pass the Homoskedasticity Test, I did not proceed to test the residuals of that regression for normal distribution. The remaining details are only provided for regressions that passed both tests.

S1.6 Table. Xantusiidae regression equations and tests. Sample sizes indicate number of extant xantusiid specimens that included the element used in the given regression. I only used regressions that passed tests for homoskedasticity and normal distribution of residuals. In one case, both the untransformed and natural log transformed regressions for the given element passed both tests, but I chose the untransformed regression because it had a smaller range of error.

S1.7 Table. Iguania regression equations and tests. Sample sizes indicate number of extant iguanian specimens that included the element used in the given regression. If a regression did not pass the Homoskedasticity Test, I did not proceed to test the residuals of that regression for normal distribution. The remaining details are only provided for regressions that passed both tests.

S1.8 Table. Helodermatidae regression equations and tests. Sample sizes indicate number of extant helodermatid specimens that included the element used in the given regression. Here, both the untransformed and natural log transformed regressions for the given element passed the tests for homoskedasticity and normal distribution of residuals, but I chose the untransformed regression because it had a much smaller range of error.

S1.9 Table. Anatomical ratios for fossil anguids, extant anguids, and extant helodermatid lizards. For fossil anguid lizards, ratios for several key genera are listed first, followed by the mean ratios for all fossil anguids in that size class (large vs. small-to-medium). The rows labeled "ALL" contain ratios for the entire fossil anguid or extant anguid datasets as indicated. Numbers in **bold** font indicate ratios calculated from a single specimen (listed in **bold** in the "Group" column). Abbreviations: DL = Dentary Length, FeL = Femur Length, FrL = Frontal Length, HL = Head Length, HuL = Humerus Length, MnL = Mandible Length, MxL = Maxilla Length, PaL = Parietal Length, SVL = Snout-Vent Length, TiL = Tibia Length.

S1.10 Table. Anguidae reference specimens. These fossil anguid specimens have complete or nearly complete skulls. I used anatomical ratios from these specimens to estimate needed measurements for other fossil anguid specimens referred to the same or closely related genera.

Chapter 1 Supplementary Dataset Captions

S1.1 Dataset. Fossil lizard data. Measurements, locality information, and body size estimates for all fossil lizard specimens sampled.

S1.2 Dataset. Extant lizard data. Data for all extant lizard specimens measured. Measurements taken from photographs are indicated in bold font.

CHAPTER 2 SUPPORTING INFORMATION

Chapter 2 Supplementary Table Captions

S2.1 Table. Crocodyliform regression equations and tests. Sample sizes indicate number of extant crocodylian specimens that included the element used in the given regression. If a regression did not pass the Homoskedasticity Test, I did not proceed to test the residuals of that regression for normal distribution. The remaining details are only provided for regressions that passed both tests. In some cases, both the untransformed and natural log transformed regressions for a given element passed both tests. In these instances, I chose a preferred regression based on other criteria, which are listed in the "Notes" column.

Chapter 2 Supplementary Dataset Captions

S2.1 Dataset. Fossil crocodyliform data. Measurements, locality information, and body size estimates for all fossil crocodyliform specimens sampled.

S2.2 Dataset. Extant crocodylian data. Data for all extant crocodylian specimens measured.

CHAPTER 3 SUPPORTING INFORMATION

Chapter 3 Supplementary Table Captions

S3.1 Table. Climate vs. body size correlation results. Values in each cell indicate (R^2, p(uncorr.)). Numbers in bold font indicate regressions that are included in the figures.

Chapter 3 Supplementary Dataset Captions

S3.1 Dataset. Mean annual paleotemperature (MAPT) data. Values, locality coordinates, and references for all MAPT data sampled.

S3.2 Dataset. Mean annual paleoprecipitation (MAPP) data. Values, locality coordinates, and references for all MAPP data sampled.